Acta Pharmacologica Sinica (2012) 33: 289–290

www.nature.com/aps

Editorial

A new era for GPCR research: structures, biology and drug discovery

H Eric XU[1, 2, *], Rui-ping XIAO[3, 4, *]

[1]VARI-SIMM Center, Center for Structure and Function of Drug Targets, State Key Laboratory of Drug Research, Shanghai Institute of Materia Medica, Chinese Academy of Sciences, Shanghai 201203, China; [2]Laboratory of Structural Sciences, Van Andel Research Institute, 333 Bostwick Ave, NE, Grand Rapids, MI 49503, USA; [3]Institute of Molecular Medicine, Center for Life Sciences, Peking University, Beijing 100871, China; [4]Drug Discovery Center, School of Chemical Biology and Biotechnology, Peking University Shenzhen Graduate School, Shenzhen 518055, China

Acta Pharmacologica Sinica (2012) 33: 289–290; doi: 10.1038/aps.2012.16

Cells in a living organism must communicate with each other through continuously sending and receiving messages. G-protein coupled receptors (GPCRs) are the largest family of communicating molecules at the cell surface. They transmit diverse extracellular signals, ranging from light and small chemical hormones to large peptide and protein hormones, and as such they play crucial roles in numerous physiological and pathological processes. More importantly, GPCRs are the most successful class of drug targets that are relevant to many major diseases, including cancer, heart failure, and inflammatory diseases. Over 50% of currently used drugs are targeted to GPCRs. However, these drugs target only 50–60 GPCRs, leaving the majority of human GPCRs, exceeding 800, unexplored for drug discovery. Given the prominent roles of GPCRs in biology and their successful track records as drug targets, GPCRs have become a hot frontier in basic research of life science and therapeutic discovery of translational medicines.

In this special issue, there are nine exciting reviews that cover a broad scope of GPCR structures, biology, diseases, and drug discovery. Among them, four reviews are dedicated to GPCR structures. Over the last few years, we have witnessed a revolution in Class A GPCR structural biology. Rhodopsin is the founding member of the GPCR family and its signaling mechanism is a paradigm for many other GPCRs. The crystal structure of bovine rhodopsin was first solved in 2000 and since then structures of rhodopsin have been solved in several functional states, including the inactivated dark state, partially active opsin, and the fully active state that is bound with a Gαt peptide. ZHOU, MELCHER, and XU review the signaling mechanisms gained from rhodopsin structures and compare these mechanisms to other members of Class A GPCRs, most notably β2-adrenergic receptor (β2AR)[1]. Class B and C GPCRs distinguished themselves from Class A GPCRs by having a large extracellular domain for binding of ligands. Compared to Class A GPCRs, structure determination for the full-length receptors of other families of GPCRs is lagging behind. However, structures for a half dozen of Class B and C GPCR extracellular domains (ECDs) in complex with their respective ligands have been determined. The structures and ligand binding mechanisms of Class B and Class C GPCRs will be reviewed by the XU and LIU groups, respectively[2, 3]. The rapid explosion of Class A GPCR structures is owed to technology development in various stages of structure determination; including protein expression, purification, crystallization, and X-ray diffraction, for which a thorough review is provided by ZHAO and WU[4].

Following the reviews of GPCR structures, five reviews are focused on GPCR biology, diseases, and drug discovery. β2AR is a prototype of GPCRs, and in parallel to rhodopsin, it has been serving as a model for studying other GPCRs. WOO and XIAO review the signaling mechanisms by β-adrenergic receptor subtypes that provide a basis for developing selective biased β2 agonists for the treatment of heart failure[5]. Moving from heart to immune systems, YE and SUN review the role of GPCRs in inflammation processes from chemotaxisis to transcriptional regulation of inflammation programs[6]. Lappano and Maggiolini provide a systematic review on the relationship of cancers with various subfamilies of GPCRs, which may serve as the basis for developing novel pharmacological interventions for cancers[7]. A large number of GPCRs are orphan

* To whom correspondence should be addressed.
E-mail eric.xu@vai.org (H Eric XU);
xiaor@pku.edu.cn (Rui-ping XIAO)
Received 2012-01-27 Accepted 2012-02-06

receptors whose ligand remains unknown. Despite missing cognate ligands, many orphan GPCRs are known to play important physiological functions, mostly from genetic knockout studies. LIU and colleagues provide a thorough review on different class of orphan nuclear receptors, their functions, and possible strategies for identification of endogenous ligands[8]. Finally, as one of the most important drug targets, GPCRs are widely pursued by both academic and industrial research for drug discovery. ZHANG and XIE provide a comprehensive review on methods of GPCR drug discovery, including various ligand binding and cell-based functional assays, many of which are tool kits for basic research as well as drug discovery for GPCRs[9].

Followed the waves of technological advances and interdisciplinary approaches in modern biological research, the field of GPCRs is evolving rapidly into a new phase of exciting progresses. With a rich history of biology and drug discovery, GPCR research is expected to continue to be a dominant source of innovative medicines for the 21st Century. We hope that the collection of these nine exciting reviews will provide a window into this new era of GPCR research and drug discovery.

References

1 Zhou XE, Melcher K, Xu HE. Structure and activation of rhodopsin. Acta Pharmacol Sin 2012; 33: 291–9.
2 Pal K, Melcher K, Xu HE. Structure and mechanism for recognition of peptide hormones by Class B G-protein-coupled receptors. Acta Pharmacol Sin 2012; 33: 300–11.
3 Chun L, Zhang WH, Liu JF. Structure and ligand recognition of Class C GPCRs. Acta Pharmacol Sin 2012; 33: 312–23.
4 Zhao Q, Wu BL. Ice breaking in GPCR structural biology. Acta Pharmacol Sin 2012; 33: 324–34.
5 Woo AY, Xiao RP. β-Adrenergic receptor subtype signaling in heart: From bench to bedside. Acta Pharmacol Sin 2012; 33: 335–41.
6 Sun L, Ye RD. Role of G protein-coupled receptors in inflammation. Acta Pharmacol Sin 2012; 33: 342–50.
7 Lappano R, Maggiolini M. GPCRs and cancer. Acta Pharmacol Sin 2012; 33: 351–62.
8 Tang XL, Wang Y, Li DL, Luo J, Liu MY. Orphan G protein-coupled receptors (GPCRs): biological functions and potential drug targets. Acta Pharmacol Sin 2012; 33: 363–71.
9 Zhang R, Xie X. Tools for GPCR drug discovery. Acta Pharmacol Sin 2012; 33: 372–84.

Acta Pharmacologica Sinica (2012) 33: 291–299
 1671-4083/12 $32.00
www.nature.com/aps

Review

Structure and activation of rhodopsin

X Edward ZHOU[1, *], Karsten MELCHER[1], H Eric XU[1, 2, *]

[1]*Laboratory of Structural Sciences, Van Andel Research Institute, NE, Grand Rapids, MI 49503, USA;* [2]*VARI-SIMM Center, Center for Structure and Function of Drug Targets, State Key Laboratory of Drug Research, Shanghai Institute of Materia Medica, Chinese Academy of Sciences, Shanghai 201203, China*

Rhodopsin is the first G-protein-coupled receptor (GPCR) with its three-dimensional structure solved by X-ray crystallography. The crystal structure of rhodopsin has revealed the molecular mechanism of photoreception and signal transduction in the visual system. Although several other GPCR crystal structures have been reported over the past few years, the rhodopsin structure remains an important model for understanding the structural and functional characteristics of other GPCRs. This review summarizes the structural features, the photoactivation, and the G protein signal transduction of rhodopsin.

Keywords: G-protein-coupled receptor (GPCR); rhodopsin; crystal structure; photoactivation; transduction

Acta Pharmacologica Sinica (2012) 33: 291–299; doi: 10.1038/aps.2011.171; published online 23 Jan 2012

Introduction

Rhodopsin, a visual pigment found in the rod photoreceptor cells of the retina, is responsible for converting photons into chemical signals that stimulate biological processes in the nervous systems of humans and other vertebrate animals, allowing them to sense light[1]. Rhodopsin is a member of class A of the GPCR superfamily[2], which is a large group of cell surface signaling receptors that transduce extracellular signals into intracellular pathways through the activation of heterotrimeric G proteins. The human GPCR superfamily, comprised of about 900 members, is involved in many aspects of human physiology and diseases, and it represents the most important protein targets for pharmaceutical drug discovery[2].

The crystal structure of ground-state bovine rhodopsin containing the reverse agonist 11-*cis*-retinal was the first high-resolution GPCR structure solved by X-ray crystallography[3–6]. Recently, crystal structures have been published for both opsin and rhodopsin in active conformations, with or without the binding of a peptide derived from the C-terminal helix α5 of the α subunit of G protein transducin[7–11]. The crystal structures of rhodopsin and the results of related biochemical and biophysical studies[12] have revealed the molecular mechanisms of photoactivation and visual signal transduction, leading to a significant progress in understanding the signaling pathways of the entire GPCR superfamily[13].

As the first solved GPCR crystal structure, bovine rhodopsin has been used as a structural template in many efforts of molecular modeling and in designing therapeutic drugs for human diseases related to GPCR signaling pathways[14]. More recently, crystal structures have been published for β1-adrenergic receptor[15], A_{2A} adenosine receptor[16], β2-adrenergic receptor[17–21], and the complex of β2-adrenergic receptor with a trimeric G protein[21]. These results have further enriched our understanding of ligand-induced activation and downstream signal transduction by GPCRs.

In this review we summarize the structural features, the photoactivation, and the G protein signal transduction of rhodopsin.

Overall structure of bovine rhodopsin

The crystal structure of inactive, 11-*cis*-retinal-bound bovine rhodopsin was first determined by Palczewski *et al* in 2000[3] and later by a few other groups[4–6]. The bovine rhodopsin structure features a seven-transmembrane (7TM) helix core architecture with three loop regions on both the extracellular and the cytoplasmic side of the membrane (Figure 1A and 1B). The N-terminus of rhodopsin, located on the extracellular side, consists of a two-stranded β sheet stretching from Gly4 to Pro11, followed by a loop region of about 24 amino acid residues (Figure 1A and 1B). The residues Asn2 and Asn15 are glycosylation sites for the receptor, and mutations that replace these residues with alanine lower the receptor's light-sensing activity[22]. The Thr4, Asn5, Thr17, Pro23, and Asn28 residues

* To whom correspondence should be addressed.
E-mail edward.zhou@vai.org (X Edward ZHOU);
eric.xu@vai.org (H Eric XU)
Received 2011-09-23 Accepted 2011-11-12

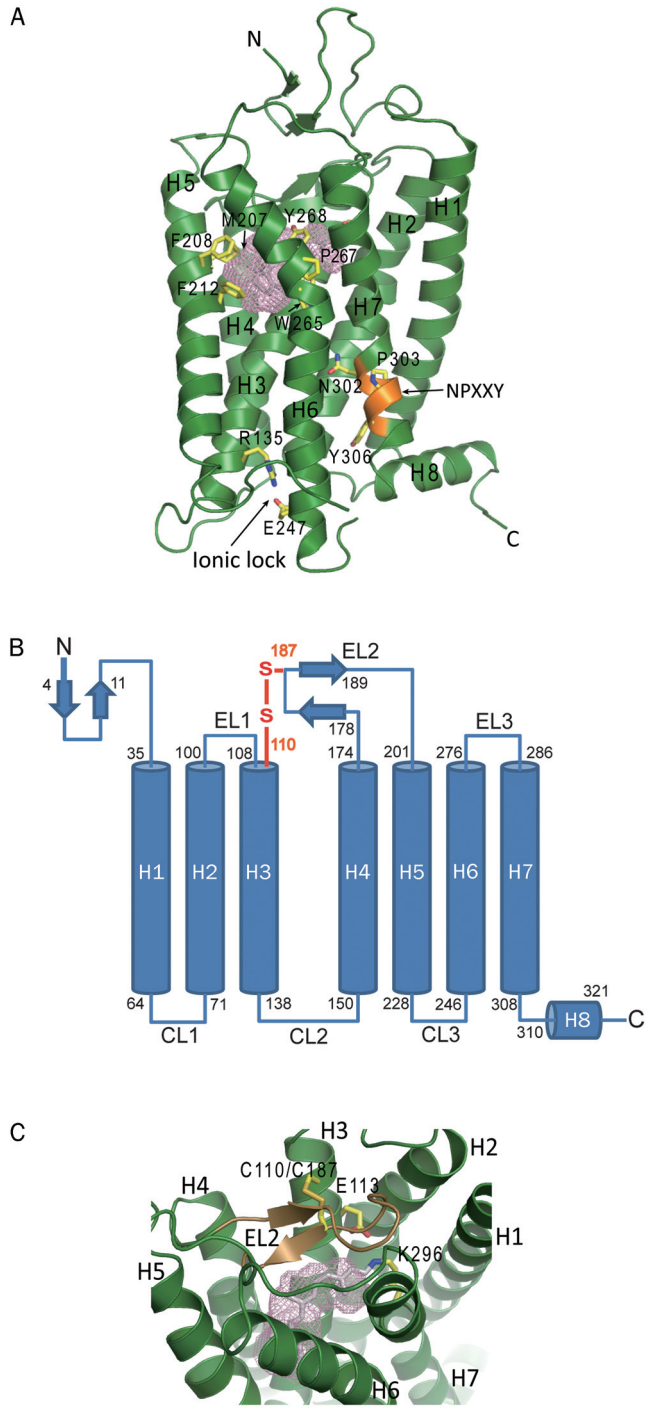

Figure 1. Overall structure of ground sate bovine rhodopsin and its key features (PDB: 1F88). (A) The seven-transmembrane helix domain with the retinal in gray stick and the ligand binding pocket shown as a pink mesh. Major ligand binding residues around the ligand binding pocket are shown as yellow sticks and are labeled. Other features include the ionic lock (yellow sticks) and the NPXXY motif (orange). (B) Two-dimensional sequence of bovine rhodopsin with the starting and ending residues of secondary structural elements indicated. The disulfide bond connecting EL2 to helix 3 is shown in orange. N, amino terminus; C, carboxyl terminus; EL, extracellular loop; CL, cytoplasmic loop. (C) The ligand binding pocket (pink mesh) of rhodopsin with EL2 (the lid of the pocket) shown in dark brown. The disulfide bond between C110 and C187 is labeled.

in this region have been proved to be crucial for the correct folding of the receptor, and mutations in these residues can lead to autosomal dominant retinitis pigmentosa (ADRP)[23, 24].

The second extracellular loop region (EL2), between helix 4 and helix 5 or from Gly175 to Asn200, is the longest among three extracellular loop regions, and it is essential for ligand binding of the receptor (Figure 1C). Biochemical data have shown that the interaction of EL2 with the helix bundle is important for the correct folding and biological function of the receptor[25]. The majority of this loop region, from Tyr178 to Ile189, forms a twisted two-stranded β sheet that is positioned at the opening of the ligand binding pocket, serving as a "lid" to block rapid exit of the ligand from the pocket (Figure 1C). The position of this β sheet is stabilized by hydrophobic interactions between residues Tyr178, Pro180, Met183 (Leu in humans), Cys185, and Cys187 of EL2, and surrounding residues of the helix bundle, especially those from helices 1, 2, 3, and 7. It is also stabilized by a disulfide bond between Cys187 of the β sheet and Cys110 of helix 3, and by a hydrogen bonding network among Glu181 and Tyr192 of EL2, Tyr268 of helix6 and a few water molecules. Between the two strands of this β sheet is a salt bridge formed by Asp190 and Arg177, which is a key interaction for maintaining the functional conformation of this lid over the retinal binding site (Figure 1C)[26].

The architecture of the 7TM domain is a common feature across the GPCR superfamily with many conserved residues[16–20]. Among the seven helices, helix 6, from Lys246 to His276 in the ground-state model, bends about 36° at Pro267, with both ends facing away from the core of the 7TM domain (Figure 1A)[3]. Upon photoactivation, the cytoplasmic end of this helix shifts further away from the 7TM core, and this shift creates a crevice in the cytoplasmic side of the receptor for binding the α subunit of G protein transducin[8, 11].

The ligand binding site of rhodopsin is a pocket on the extracellular side of the transmembrane bundle. It is surrounded by hydrophobic residues that stabilize the polyene backbone of the retinal, among which are Met207, Phe208, and Phe212 from helix 5, and Trp265 and Tyr268 from helix 6 (Figure 1A and 1C)[3, 4, 6]. The positions and the conformations of those hydrophobic residues undergo dynamic changes during the photoactivation of the retinal and the conformational changes in the receptor[7, 8, 11].

Another important feature of this receptor is the "ionic lock", a salt bridge between Arg135 of helix 3 and Glu247 of helix 6 (Figure 1A)[3, 4, 6]. This salt bridge blocks the G protein binding site of the receptor in its inactive conformation. Upon photoactivation, the transmembrane bundle undergoes a conformational change: the cytoplasmic side of helix 6 bends further away from the 7TM core and the ionic lock breaks, resulting in an opening on the cytoplasmic side of the receptor for G protein interaction[7, 8, 11].

A conserved NPXXY motif on helix 7 is also common to all the GPCR family members based on sequence alignment and crystal structures[3, 16–18]. It has an important role in receptor activation: this motif shifts toward helix 6 and the key residue Tyr306 on this motif flips toward helix 6, helping breaking the

ionic lock and pushing helix 6 away from the transmembrane bundle (Figure 1A).

The C-terminus of rhodopsin is on the cytoplasmic side of the membrane, extending from residue Met309 at the C-terminal end of helix 7 to the last residue of the receptor, and featuring a short amphipathic helix (helix 8) perpendicular to helix 7 (Figure 1A and 1B)[3, 4, 6]. It forms hydrophobic interactions by its residues Phe313, Cys316, and Met317 with residues Leu57, Val61 of helix 1 and His65 in the loop following helix 1, and is covalently anchored to the membrane by palmitoylation of residues Cys322 and Cys323 in the loop following helix 8. The C-terminal loop following residue Asn326 is disordered in all the crystal structures. In this region there are serine residues Ser334, Ser338, and Ser343, whose phosphorylation is important for arrestin binding to terminate the cycle of G protein activation[27].

The loop region CL3 between helices 5 and 6 on the cytoplasmic side is flexible and largely disordered in ground-state rhodopsin crystal structures, but is structured in most activated rhodopsin models[8–11] (Figure 1A and 1B) . Upon activation, the majority of this loop region becomes part of the elongated helix 5 that provides more interface for G protein interaction.

Ligand-induced conformational change and activation of rhodopsin

Retinal is one of the vitamin A compounds derived from carotenoids (Figure 2A). It is the photoactive moiety of rhodopsin that captures light and converts photons into chemical signals. Vision starts with the absorption of photons, and the photon-triggered isomerization of the retinal from the 11-*cis* to the all-*trans* state, followed by conformational changes in the 7TM domain of rhodopsin to accommodate the binding of G proteins, leading to the downstream signal transduction[28].

The ligand binding pocket of rhodopsin, with a volume of about 352 Å^3, is located on the luminal side of the receptor

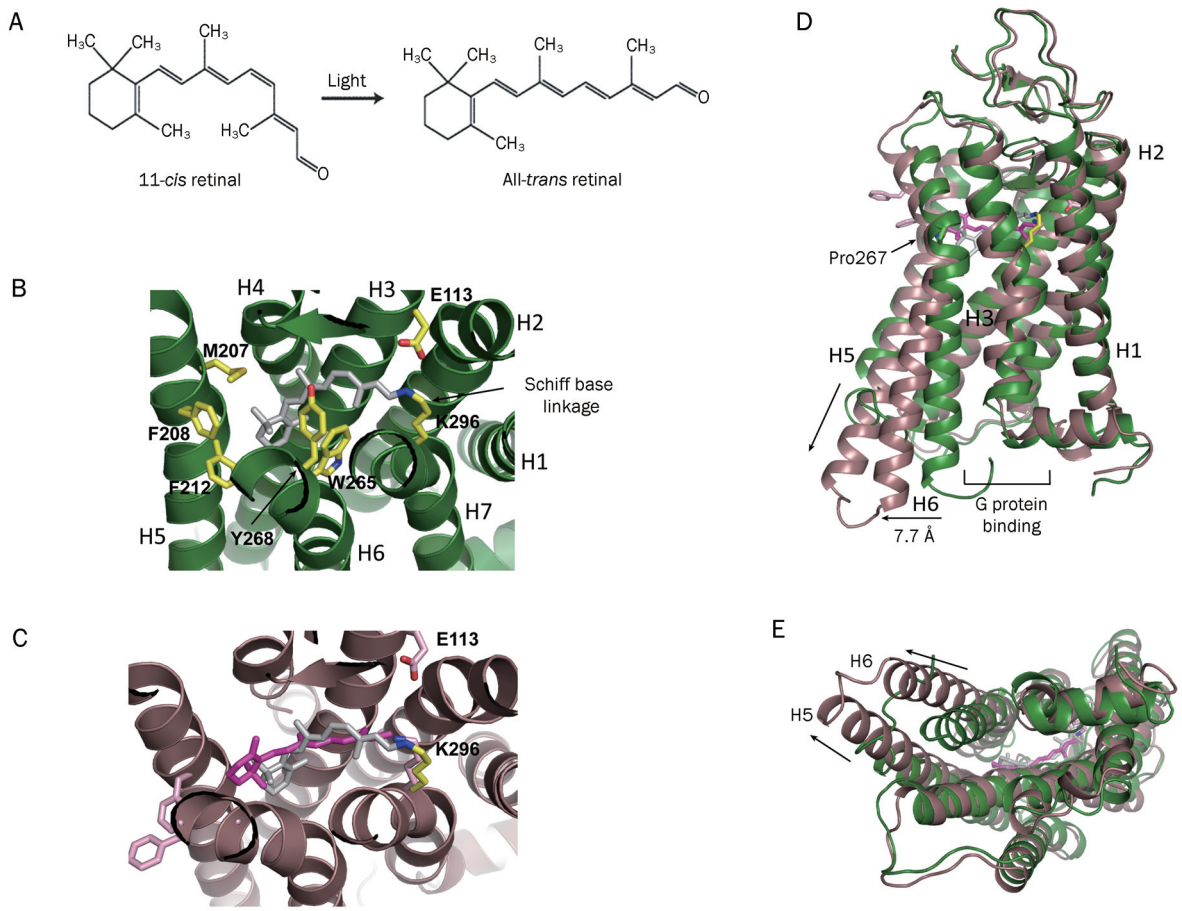

Figure 2. Ligand binding and conformational changes in rhodopsin. (A) Chemical structures of 11-*cis*- and all-*trans*-retinal. (B) 11-*cis*-retinal (in gray) in the ligand binding pocket is associated with the surrounding residues of the protein moiety (green, PDB: 1F88). (C) Conformational changes in retinal and the protein moiety of rhodopsin upon photoactivation. The photoactivated all-*trans*-retinal (PDB: 3PQR) is magenta and the ground-state 11-*cis*-retinal (PDB: 1F88, gray) is superposed on the activated all-*trans*-retinal for comparison. The protein moiety of activated rhodopsin (PDB: 3PQR) is dark brown. (D) The key conformational changes in rhodopsin upon photoactivation are the outward tilting of the cytoplasmic end of helix 6 (indicated by the horizontal arrow), creating a crevice for G-protein binding, and the elongation of the cytoplasmic end of helix 5 (indicated by the vertical arrow) that provides more interface for G-protein interaction. Green shows the ground-state conformation (PDB: 1F88), and brown shows the activated conformation (PDB: 3PQR). (E) Bottom view of panel D.

(Figure 1A, 1C, and 2B). Prior to photoactivation, 11-*cis*-retinal in the ligand binding pocket is covalently bound to Lys296 of helix 7 through a Schiff base linkage. The Schiff base is protonated and the linkage is stabilized by charge delocalization over the π-electron system of the polyene backbone of the retinal chromophore, and by an electrostatic interaction with the carboxyl group of Glu113 of helix 3 (Figure 2B)[3, 4, 6]. The retinal in the ligand binding pocket is also stabilized by the surrounding hydrophobic residues including Met207, Phe208 and Phe212 from helix 5 and Trp265 and Tyr268 from helix 6 (Figure 2B). The Schiff base linkage and its electrostatic interaction are essential for maintaining the ground-state conformation of rhodopsin, and a mutation that alters either Lys296 or Glu113 results in constitutive activation of the receptor[29].

Upon light absorption, the π-electron system of the retinal chromophore undergoes a π→π* transition that lowers the potential energy barrier for *cis-trans* isomerization. The isomerization changes the retinal from a bending *cis* configuration to a straight *trans* configuration. It flips the aldehyde group and the C_{20} methyl group about 180° around the C_{11}=C_{12} double bond, and tilts the β-ionone group toward the space between helices 5 and 6 (Figure 2C). The photon-induced *cis-trans* transition in the retinal leads to a sterically strained excited-state rhodopsin that thermally decays through a series of intermediates, photorhodopsin, bathorhodopsin, lumirhodopsin, and metarhodopsin I, and forms the active-state metarhodopsin II[7, 8, 11, 30–32]. During the thermal relaxation, the protein moiety of rhodopsin undergoes a series of conformational changes that lead to the formation of a G protein binding site on the cytoplasmic side of the 7TM bundle[7–11] (Figure 2D and 2E). The major conformational changes are the bending of helix 6 at Pro267, and the eight-residue elongation of the C-terminus of helix 5, the addition coming from the CL3 loop (Figure 2D and 2E). The bending of helix 6 results in the cytoplasmic end of this helix tilting away from the transmembrane core, and creates an opening with a diameter of about 14 Å[8, 10, 11]. The cytoplasmic end of helix 6 in all-*trans*-retinal bound rhodopsin is about 7.7 Å away from that of the *cis*-retinal bound conformation. The Pro267 residue of helix 6 is highly conserved among GPCR family members, and it is believed that it serves as a hinge for the bending because it has no hydrogen bond between its backbone nitrogen atom and the carbonyl group of the residue one helical turn upstream. The elongation of the cytoplasmic side of helix 5 expands the interface for G protein interaction, and thus contributes the binding affinity of rhodopsin for the G protein transducin (Figure 2D and 2E).

Rhodopsin-G protein interaction

The binding of the C-terminus of the α subunit of transducin to rhodopsin was defined by the crystal structure of rhodopsin in complex with a synthetic peptide, GαCT (Gα C-terminus), derived from the C-terminus of helix α5 of the Gα subunit[8, 10, 11] (Figure 3A). The outward movement of helix 6 of rhodopsin breaks the ionic lock between Arg135 on helix 3 and Glu247 on helix 6, thus creating an opening that accommodates the C-terminal helix of the α subunit of transducin. The binding of the Gα peptide on the cytoplasmic side of rhodopsin is largely facilitated by two sets of interactions: a) hydrophobic interactions between the peptide residues Leu341, Leu344, Val347, Leu349, and Phe350, and the receptor residues Ala246, Val250, and Met253 on helix 6, Val138 and Val139, and the backbone of Arg135 on helix 3, and Leu72 and Leu76 on helix 2, and 6) polar interactions between the carbonyl groups of residues Gly348 and Lys345 of the peptide, and the residues Asn310 and Q312 of helix 8 (Figure 3A). The binding of the α subunit of transducin to rhodopsin induces the exchange of GDP for GTP on the α subunit, and this exchange triggers the dissociation of the GTP-bound Gα subunit from the Gβγ dimer and the receptor. Both the dissociated GTP-bound α subunit and the βγ dimer of transducin then activate downstream signaling pathways[33].

Comparison of the rhodopsin-Gα peptide structure with the recently published crystal structure of the β2-adrenergic receptor in complex with its trimeric G protein[21] revealed noteworthy differences. Helix α5 of the intact Gα subunit binds to the receptor in a position tilted about 38° toward helix 6 and 2 Å away from the bottom of the crevice relative to the position of the Gα peptide in the active rhodopsin-peptide complex (Figure 3B and 3C). The intact G protein α subunit does not fit deeply in the crevice of the receptor as the peptide does, probably because the whole Gα subunit is much larger, and therefore is not able to fit in the deep crevice in the transmembrane bundle of the receptor. Also in the β2-AR-G protein complex, helix 6 is bent outward about 26° more than that in the activated rhodopsin structure, and the opening of the crevice is larger than that of rhodopsin, to accommodate the intact C-terminal helix of the Gα subunit in the β2-AR-G protein complex (Figure 3B and 3C). Because the crystal structure of a rhodopsin-full length G protein complex is not available, we still do not have the whole picture of the interface of rhodopsin with the Gα subunit as a full length protein in the context of intact trimeric transducin.

Structural understanding of disease-related rhodopsin mutations

Rhodopsin is central to the process of vision. Mutations in rhodopsin are major causes of vision diseases or disorders. More than 120 point mutations have been identified in human gene of rhodopsin, many of which lead to vision diseases such as ADRP and congenital stationary night blindness (see http://www.retina-international.org/sci-news/rhomut.htm for most disease-linked mutations). Crystal structures have provided us molecular basis for understanding how mutations in rhodopsin influence the protein folding, stability and/or biological functions of the receptor.

Retinal is the photoactive chromophore in rhodopsin, and is the key to the entire light signal transduction. Crystal structures have revealed that 11-*cis*-retinal is covalently bound by Lys296 of helix 7 in ground state rhodopsin (Figure 2A and 2B). Mutations of this retinal binding residue, K296M and K296E, cause severe ADRP[34]. These mutants have been

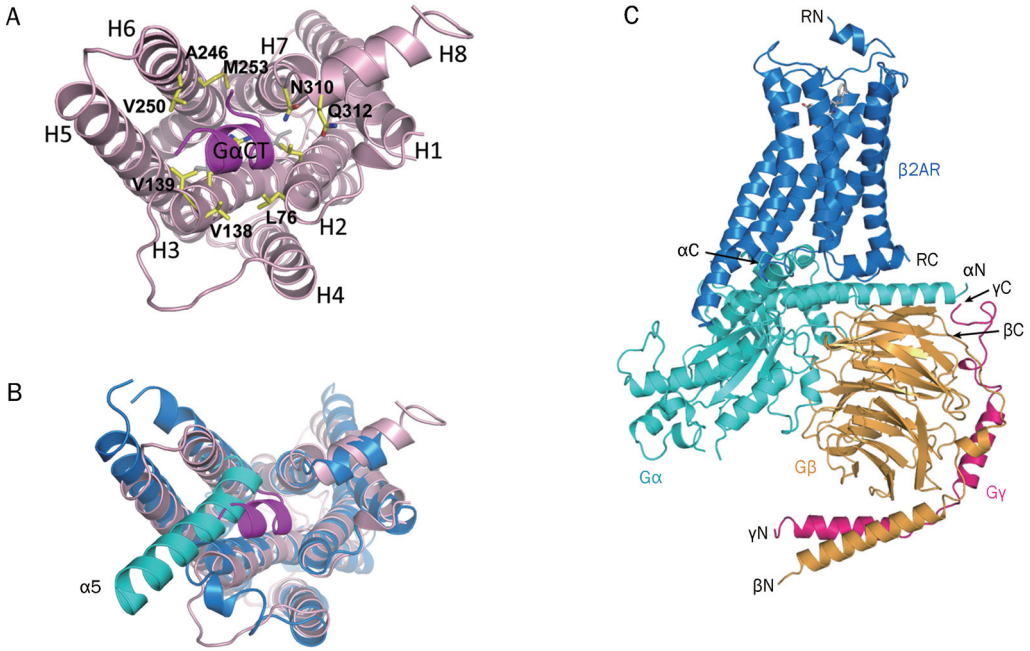

Figure 3. Rhodopsin-G protein interface. (A) Rhodopsin in complex with a synthetic peptide derived from helix α5 of the Gα subunit of transducin (PDB: 3PQR). The rhodopsin residues interacting with the Gα peptide are labeled. (B) Comparison of the binding mode of rhodopsin with the synthetic peptide and that of the β2-adrenergic receptor with intact G protein (PDB: 3SN6). The β2-adrenergic receptor is blue and the Gα subunit is cyan. For clarity, only helix α5 of the Gα subunit is shown. (C) The whole-complex model of the β2-adrenergic receptor with intact G protein (PDB: 3SN6). The β2-adrenergic receptor is blue, the Gα subunit is cyan, the Gβ subunit is brown, and the Gγ subunit is pink. RN, N-terminus of the receptor; RC, C-terminus of the receptor; αN, N-terminus of the Gα subunit; αC, C-terminus of the Gα subunit; βN, N-terminus of the Gβ subunit; βC, C-terminus of the Gβ subunit; γN, N-terminus of the Gγ subunit; γC, C-terminus of the Gγ subunit.

found to be folded properly, but constitutively activated[35]. Substitutions of other residues interacting with or at proximity of retinal can change retinal binding affinity of the receptor. It has been identified that mutations of those residues M44T[36], G114D[37], G114V[38], L125R[39], C167R[40], Y178N[41], Y178C[42], E181K[40], S186P[40], S186W[43], G188R[44], G188E[45], M207R[46], M216R[47], and M216K[48] (Lue216 in bovine), cause different levels of ADRP disease. Mutations of G90D[49] and A292E[50], two other retinal binding residues, have been found in patients with congenital stationary night blindness.

The conserved residue Pro267 is at the kink in helix 6 and serves as a hinge for the bending of helix 6 to create the G protein binding site at cytoplasmic side of rhodopsin. Replacement of this residue with other non-proline residues affects the conformation of the G protein binding site of rhodopsin and the kinetics of transducin activation[51, 52]. Mutations of P267L and P267R have been reported to cause ADRP[41, 52, 53].

Based on the crystal structure of rhodopsin in complex with peptide GαCT[8, 10, 11], the binding of the α subunit of transducin to rhodopsin is facilitated by hydrophobic residues at the interface of the two proteins. Cys140 in CL2 is an important residue at rhodopsin side for G protein binding[54]. Mutation C140S that lowers the hydrophobicity of the residue has been found associated with ADRP[45].

Mutations of residue Cys110 to Arg, Phe, or Tyr[37, 55], or Cys187 to Tyr[56], have been identified in ADRP patients. The conserved residues Cys110 and Cys187 forms a disulfide bond that constrains EL2, the lid of the ligand binding pocket, and is required for the biological function of the receptor (Figure 1B)[57]. Mutations of those residues break the disulfide bond, thus affect the folding and biological function of the receptor.

GPCRs are membrane proteins and their interactions with the phospholipid bilayer membrane have great influence on their physiological functions[58]. Mutations at the membrane interaction interface of rhodopsin can change the affinity of rhodopsin to the phospholipid bilayers and influence the functions of the receptor. Lue46 is a hydrophobic residue at the membrane interaction interface of rhodopsin, and mutation of L46R largely affects the membrane-receptor interaction and causes severe ADRP[59]. Other disease-linked mutations at the receptor-membrane interface are F45L[60], P53R[61], and V209M[45].

Some disease-causing mutations in rhodopsin occur at post-translational modification residues including glycosylation or phosphorylation sites. Glycosylation is important for correct folding and stability of most eukaryotic proteins. N-terminal glycosylation sites of rhodopsin are located at Asn2, Thr4, Asn15 and Thr17, and mutations of those residues, T4K[62], N15S[63], and T17M[60], are responsible for ADRP. Rhodopsin phosphorylation is a key step of the regulatory mechanism of light signal transduction. Activated rhodopsin is phosphorylated by rhodopsin kinase at multiple sites in its C-terminal

region, and the phosphorylation facilitates the association of arrestin that completely terminates light signal transduction. Mutations of a rhodopsin kinase binding residue Arg135 to Gly[45], Trp[60], Pro[64], or Leu[60], and the mutation of a phosphorylation site Thr342 to Met, which affect phosphorylation and rhodopsin-arrestin interaction, lead to ADRP[65].

Comparison of the activation of GPCRs and nuclear hormone receptors

Nuclear hormone receptors (NRs) and GPCRs are two different groups of protein receptors that sense extracellular signals and transduce those signals to the inside of cells. GPCRs transmit signals by coupling ligand-receptor interactions to G protein activation. Activated G proteins then trigger the downstream signaling cascades in the cytoplasm to regulate various biological events in the cells. In contrast, ligand binding converts NRs into transcriptional activators that directly bind target genes and stimulate their expression. A typical nuclear receptor ligand binding domain forms a conserved helical sandwich fold that harbors a ligand binding pocket adjacent to its C-terminal activation function helix AF2. Ligand binding does not change the helical sandwich scaffold but induces the rearrangement of the receptor's AF2 helix and the formation of a coactivator binding cleft for the recruitment of transcriptional coactivators, which further facilitate the formation of transcription complexes and subsequent gene expression[66] (Figure 4A). In the cascade of NR activation, the conformation of the receptor core structure remains unchanged. That is a major difference from the activation of a GPCR, in which the core 7TM domain is rearranged upon ligand binding and receptor activation and the core domain rearrangement creates a crevice at the cytoplasmic side of the receptor for G protein interaction and signal transduction (Figure 4B)[10, 11, 21].

While GPCRs and NRs are functionally comparable, the GPCR group has many more members than the NR family, and senses a wide variety of environmental signals. It is interesting that the GPCR group members, in spite of their highly diverse ligands, share a highly conserved 7TM core architecture for ligand binding and G protein interaction, whereas the NRs share a conserved three-layered helix bundle for ligand binding and coactivator recruitment. In summary, ligand

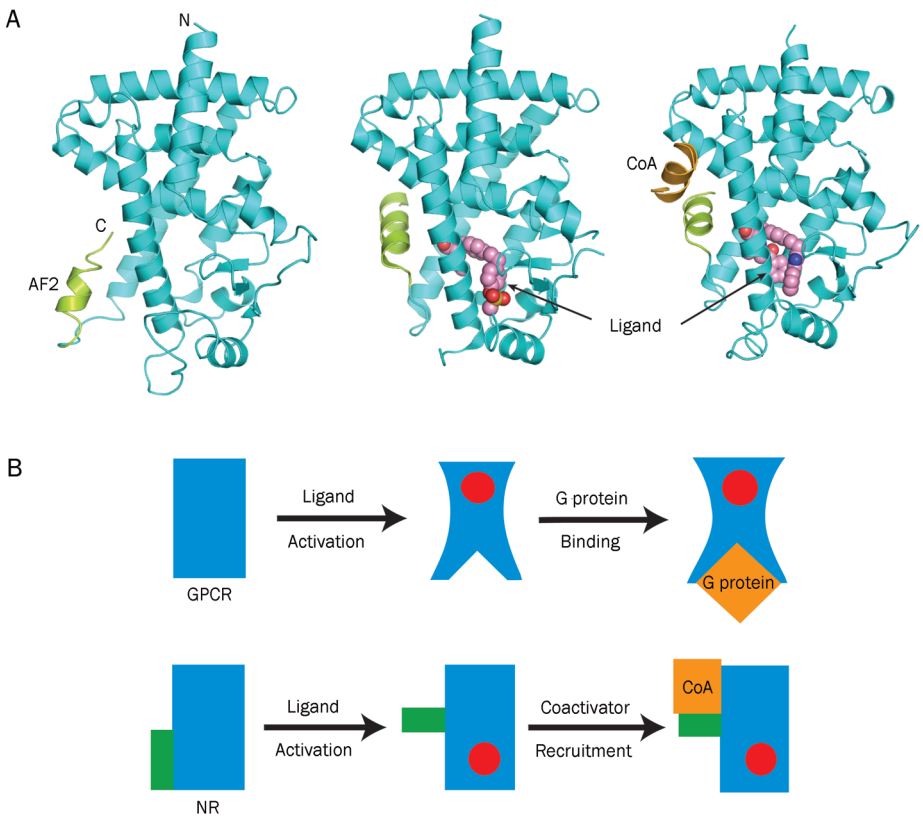

Figure 4. A comparison of the ligand-induced activation modes of GPCRs and nuclear receptors. (A) Ligand-induced rearrangement of the C-terminal AF2 helix and coactivator recruitment of a peroxisome proliferator-activated receptor ligand binding domain (PPAR LBD). At left is an apo PPAR LBD (PDB: 1PRG)[69]; middle, the LBD upon the ligand binding-induced conformational change in the AF2 helix and the formation of the coactivator binding site (PDB: 1I7G)[70]; at right, the LBD upon the subsequent coactivator recruitment (PDB: 1K7L)[71]. The LBD core structure is cyan; the AF2 helix, green; and the coactivator motif, brown. (B) Cartoon presentation showing that ligand activation induces conformational changes in the core domain of GPCRs but not in that of NRs. Blue are the core domains of both receptors; Red are the ligands; Orange are the G protein binding to the GPCR and the coactivator binding to the NR.

binding and activation in GPCRs involve a much more extensive rearrangement of the 7TM helical core than the helical sandwich of NRs.

Rhodopsin as a molecular model for GPCR studies

During the long period before the second GPCR crystal structure was published in 2007[17, 18] , rhodopsin was the only GPCR crystal structure available, and it has been used extensively as a model for understanding the structural and functional characteristics of other GPCRs[67, 68]. Whereas more GPCR crystal structures have been published and the importance of the rhodopsin structure as a molecular template for modeling other GPCRs has been correspondingly diminished, rhodopsin still remains a prototype of the GPCR superfamily and a model system for all 7TM domain proteins.

All GPCR structures have a conserved transmembrane core domain followed by helix 8 on the cytoplasmic side. The root mean square deviation (RMSD) of the residues of the 7TM core structures between rhodopsin and other GPCRs whose structures have been solved are among 1.2 to 1.4 Å, indicating a close similarity and high level of conservation. The most significant structural differences between rhodopsin and other GPCRs are in the ligand binding pocket and the lid covering the pocket, the EL2 loop region. The EL2 of rhodopsin adopts a β-sheet fold, which tightly plugs into the entrance of the pocket, while the EL2 regions of other solved GPCR structures are loosely positioned above the ligand binding pocket and can be more easily opened for ligands to move in or out. This is consistent with the observation that rhodopsin is activated by the photon-triggered isomerization of retinal in the ligand binding pocket, which requires the ligand not only being bound but also being tightly hold in the pocket, while most other GPCRs are activated by simply binding to the ligands. Although the mechanism of activation differs, rhodopsin and other solved GPCR structures share conserved core residues that define the conformation of the seven transmembrane domain and the molecular basis of the conformational change upon ligand activation, G protein interaction, and downstream signal transduction.

Acknowledgements

We thank D NADZIEJKA for editing the manuscript. This work was supported in part by the Jay and Betty Van Andel Foundation, and National Institute of Health grant GM087413 (H Eric XU).

References

1 Hubbard R, Kropf A. The action of light on rhodopsin. Proc Natl Acad Sci U S A 1958; 44: 130–9.
2 Fredriksson R, Lagerström MC, Lundin LG, Schiöth HB. The G-protein-coupled receptors in the human genome form five main families. Phylogenetic analysis, paralogon groups, and fingerprints. Mol Pharmacol 2003; 63: 17.
3 Palczewski K, Kumasaka T, Hori T, Behnke CA, Motoshima H, Fox BA, *et al*. Crystal structure of rhodopsin: A G protein-coupled receptor. Science 2000; 289: 739–45.
4 Li J, Edwards PC, Burghammer M, Villa C, Schertler GF. Structure of bovine rhodopsin in a trigonal crystal form. J Mol Biol 2004; 343: 1409–38.
5 Standfuss J, Xie G, Edwards PC, Burghammer M, Oprian DD, Schertler GF. Crystal structure of a thermally stable rhodopsin mutant. J Mol Biol 2007; 372: 1179–88.
6 Okada T, Sugihara M, Bondar AN, Elstner M, Entel P, Buss V. The retinal conformation and its environment in rhodopsin in light of a new 2.2 Å crystal structure. J Mol Biol 2004; 342: 571–83.
7 Salom D, Lodowski DT, Stenkamp RE, Le Trong I, Golczak M, Jastrzebska B, *et al*. Crystal structure of a photoactivated deprotonated intermediate of rhodopsin. Proc Natl Acad Sci U S A 2006; 103: 16123–8.
8 Standfuss J, Edwards PC, D'Antona A, Fransen M, Xie G, Oprian DD, *et al*. The structural basis of agonist-induced activation in constitutively active rhodopsin. Nature 2011; 471: 656–60.
9 Park JH, Scheerer P, Hofmann KP, Choe HW, Ernst OP. Crystal structure of the ligand-free G-protein-coupled receptor opsin. Nature 2008; 454: 183–7.
10 Scheerer P, Park JH, Hildebrand PW, Kim YJ, Krauss N, Choe HW, *et al*. Crystal structure of opsin in its G-protein-interacting conformation. Nature 2008; 455: 497–502.
11 Choe HW, Kim YJ, Park JH, Morizumi T, Pai EF, Krauss N, *et al*. Crystal structure of metarhodopsin II. Nature 2011; 471: 651–5.
12 Brown MF, Martinez-Mayorga K, Nakanishi K, Salgado GF, Struts AV. Retinal conformation and dynamics in activation of rhodopsin illuminated by solid-state H NMR spectroscopy. Photochem Photobiol 2009; 85: 442–53.
13 Jastrzebska B, Tsybovsky Y, Palczewski K. Complexes between photoactivated rhodopsin and transducin: progress and questions. Biochem J 2010; 428: 1–10.
14 Bosch L, Iarriccio L, Garriga P. New prospects for drug discovery from structural studies of rhodopsin. Curr Pharm Des 2005; 11: 2243–56.
15 Warne T, Serrano-Vega MJ, Baker JG, Moukhametzianov R, Edwards PC, Henderson R, *et al*. Structure of a beta1-adrenergic G-protein-coupled receptor. Nature 2008; 454: 486–91.
16 Jaakola VP, Griffith MT, Hanson MA, Cherezov V, Chien EY, Lane JR, *et al*. The 2.6 angstrom crystal structure of a human A2A adenosine receptor bound to an antagonist. Science 2008; 322: 1211–7.
17 Rasmussen SG, Choi HJ, Rosenbaum DM, Kobilka TS, Thian FS, Edwards PC, *et al*. Crystal structure of the human beta2 adrenergic G-protein-coupled receptor. Nature 2007; 450: 383–7.
18 Cherezov V, Rosenbaum DM, Hanson MA, Rasmussen SG, Thian FS, Kobilka TS, *et al*. High-resolution crystal structure of an engineered human beta2-adrenergic G protein-coupled receptor. Science 2007; 318: 1258–65.
19 Rasmussen SG, Choi HJ, Fung JJ, Pardon E, Casarosa P, Chae PS, *et al*. Structure of a nanobody-stabilized active state of the beta(2) adrenoceptor. Nature 2011; 469: 175–80.
20 Rosenbaum DM, Zhang C, Lyons JA, Holl R, Aragao D, Arlow DH, *et al*. Structure and function of an irreversible agonist: beta(2) adrenoceptor complex. Nature 2011; 469: 236–40.
21 Rasmussen SG, Devree BT, Zou Y, Kruse AC, Chung KY, Kobilka TS, *et al*. Crystal structure of the beta(2) adrenergic receptor–Gs protein complex. Nature 2011; 477: 549–55.
22 Kaushal S, Ridge KD, Khorana HG. Structure and function in rhodopsin: the role of asparagine-linked glycosylation. Proc Natl Acad Sci U S A 1994; 91: 4024–8.
23 Sung CH, Davenport CM, Hennessey JC, Maumenee IH, Jacobson SG, Heckenlively JR, *et al*. Rhodopsin mutations in autosomal dominant retinitis pigmentosa. Proc Natl Acad Sci U S A 1991; 88: 6481–5.
24 Al-Maghtheh M, Gregory C, Inglehearn C, Hardcastle A, Bhattacharya

S. Rhodopsin mutations in autosomal dominant retinitis pigmentosa. Hum Mutat 1993; 2: 249–55.
25 Karnik SS, Khorana HG. Assembly of functional rhodopsin requires a disulfide bond between cysteine residues 110 and 187. J Biol Chem 1990; 265: 17520–4.
26 Janz JM, Fay JF, Farrens DL. Stability of dark state rhodopsin is mediated by a conserved ion pair in intradiscal loop E-2. J Biol Chem 2003; 278: 16982–91.
27 Ohguro H, Rudnicka-Nawrot M, Buczylko J, Zhao X, Taylor JA, Walsh KA, *et al*. Structural and enzymatic aspects of rhodopsin phosphorylation. J Biol Chem 1996; 271: 5215–24.
28 Chabre M. Trigger and amplification mechanisms in visual phototransduction. Annu Rev Biophys Biophys Chem 1985; 14: 331–60.
29 Rao VR, Oprian DD. Activating mutations of rhodopsin and other G protein-coupled receptors. Annu Rev Biophys Biomol Struct 1996; 25: 287–314.
30 Nakamichi H, Okada T. Crystallographic analysis of primary visual photochemistry. Angew Chem Int Ed Engl 2006; 45: 4270–3.
31 Nakamichi H, Okada T. Local peptide movement in the photoreaction intermediate of rhodopsin. Proc Natl Acad Sci U S A 2006; 103: 12729–34.
32 Ruprecht JJ, Mielke T, Vogel R, Villa C, Schertler GF. Electron crystallography reveals the structure of metarhodopsin I. EMBO J 2004; 23: 3609–20.
33 Ridge KD, Palczewski K. Visual rhodopsin sees the light: structure and mechanism of G protein signaling. J Biol Chem 2007; 282: 9297–301.
34 Yang T, Snider BB, Oprian DD. Synthesis and characterization of a novel retinylamine analog inhibitor of constitutively active rhodopsin mutants found in patients with autosomal dominant retinitis pigmentosa. Proc Natl Acad Sci U S A 1997; 94: 13559–64.
35 Keen TJ, Inglehearn CF, Lester DH, Bashir R, Jay M, Bird AC, *et al*. Autosomal dominant retinitis pigmentosa: four new mutations in rhodopsin, one of them in the retinal attachment site. Genomics 1991; 11: 199–205.
36 Reig C, Antich J, Gean E, Garcia-Sandoval B, Ramos C, Ayuso C, *et al*. Identification of a novel rhodopsin mutation (Met-44-Thr) in a simplex case of retinitis pigmentosa. Hum Genet 1994; 94: 283–6.
37 Vaithinathan R, Berson EL, Dryja TP. Further screening of the rhodopsin gene in patients with autosomal dominant retinitis pigmentosa. Genomics 1994; 21: 461–3.
38 Dryja TP, McEvoy JA, McGee TL, Berson EL. Novel rhodopsin mutations Gly114Val and Gln184Pro in dominant retinitis pigmentosa. Invest Ophthalmol Vis Sci 2000; 41: 3124–7.
39 Dryja TP. Doyne Lecture. Rhodopsin and autosomal dominant retinitis pigmentosa. Eye (Lond) 1992; 6: 1–10.
40 Dryja TP, Hahn LB, Cowley GS, McGee TL, Berson EL. Mutation spectrum of the rhodopsin gene among patients with autosomal dominant retinitis pigmentosa. Proc Natl Acad Sci U S A 1991; 88: 9370–4.
41 Souied E, Gerber S, Rozet JM, Bonneau D, Dufier JL, Ghazi I, *et al*. Five novel missense mutations of the rhodopsin gene in autosomal dominant retinitis pigmentosa. Hum Mol Genet 1994; 3: 1433–4.
42 Farrar GJ, Kenna P, Redmond R, Shiels D, McWilliam P, Humphries MM, *et al*. Autosomal dominant retinitis pigmentosa: a mutation in codon 178 of the rhodopsin gene in two families of Celtic origin. Genomics 1991; 11: 1170–1.
43 Matias-Florentino M, Ayala-Ramirez R, Graue-Wiechers F, Zenteno JC. Molecular screening of rhodopsin and peripherin/RDS genes in Mexican families with autosomal dominant retinitis pigmentosa. Curr Eye Res 2009; 34: 1050–6.
44 Liu X, Garriga P, Khorana HG. Structure and function in rhodopsin: correct folding and misfolding in two point mutants in the intradiscal domain of rhodopsin identified in retinitis pigmentosa. Proc Natl Acad Sci U S A 1996; 93: 4554–9.
45 Macke JP, Davenport CM, Jacobson SG, Hennessey JC, Gonzalez-Fernandez F, Conway BP, *et al*. Identification of novel rhodopsin mutations responsible for retinitis pigmentosa: implications for the structure and function of rhodopsin. Am J Hum Genet 1993; 53: 80–9.
46 Farrar GJ, Findlay JB, Kumar–Singh R, Kenna P, Humphries MM, Sharpe E, *et al*. Autosomal dominant retinitis pigmentosa: a novel mutation in the rhodopsin gene in the original 3q linked family. Hum Mol Genet 1992; 1: 769–71.
47 Haim M, Grundmann K, Gal A, Rosenberg T. Novel rhodopsin mutation (M216R) in a Danish family with autosomal dominant retinitis pigmentosa. Ophthalmic Genet 1996; 17: 193–7.
48 Al-Maghtheh M, Inglehearn C, Lunt P, Jay M, Bird A, Bhattacharya S. Two new rhodopsin transversion mutations (L40R; M216K) in families with autosomal dominant retinitis pigmentosa. Hum Mutat 1994; 3: 409–10.
49 Sieving PA, Richards JE, Naarendorp F, Bingham EL, Scott K, Alpern M. Dark-light: model for nightblindness from the human rhodopsin Gly-90 → Asp mutation. Proc Natl Acad Sci U S A 1995; 92: 880–4.
50 Dryja TP, Berson EL, Rao VR, Oprian DD. Heterozygous missense mutation in the rhodopsin gene as a cause of congenital stationary night blindness. Nat Genet 1993; 4: 280–3.
51 Nakayama TA, Khorana HG. Mapping of the amino acids in membrane-embedded helices that interact with the retinal chromophore in bovine rhodopsin. J Biol Chem 1991; 266: 4269–75.
52 Hwa J, Garriga P, Liu X, Khorana HG. Structure and function in rhodopsin: packing of the helices in the transmembrane domain and folding to a tertiary structure in the intradiscal domain are coupled. Proc Natl Acad Sci U S A 1997; 94: 10571–6.
53 Sheffield VC, Fishman GA, Beck JS, Kimura AE, Stone EM. Identification of novel rhodopsin mutations associated with retinitis pigmentosa by GC-clamped denaturing gradient gel electrophoresis. Am J Hum Genet 1991; 49: 699–706.
54 Natochin M, Gasimov KG, Moussaif M, Artemyev NO. Rhodopsin determinants for transducin activation: a gain-of-function approach. J Biol Chem2003; 278: 37574–81.
55 Fuchs S, Kranich H, Denton MJ, Zrenner E, Bhattacharya SS, Humphries P, *et al*. Three novel rhodopsin mutations (C110F, L131P, A164V) in patients with autosomal dominant retinitis pigmentosa. Hum Mol Genet 1994; 3: 1203.
56 Richards JE, Scott KM, Sieving PA. Disruption of conserved rhodopsin disulfide bond by Cys187Tyr mutation causes early and severe autosomal dominant retinitis pigmentosa. Ophthalmology 1995; 102: 669–77.
57 Hwa J, Klein-Seetharaman J, Khorana HG. Structure and function in rhodopsin: Mass spectrometric identification of the abnormal intradiscal disulfide bond in misfolded retinitis pigmentosa mutants. Proc Natl Acad Sci U S A 2001; 98: 4872–6.
58 Huber T, Botelho AV, Beyer K, Brown MF. Membrane model for the G-protein-coupled receptor rhodopsin: hydrophobic interface and dynamical structure. Biophys J 2004; 86: 2078–100.
59 Rodriguez JA, Herrera CA, Birch DG, Daiger SP. A leucine to arginine amino acid substitution at codon 46 of rhodopsin is responsible for a severe form of autosomal dominant retinitis pigmentosa. Hum Mutat 1993; 2: 205–13.
60 Sung CH, Schneider BG, Agarwal N, Papermaster DS, Nathans J. Functional heterogeneity of mutant rhodopsins responsible for auto-

somal dominant retinitis pigmentosa. Proc Natl Acad Sci U S A 1991; 88: 8840–4.

61 Inglehearn CF, Keen TJ, Bashir R, Jay M, Fitzke F, Bird AC, *et al*. A completed screen for mutations of the rhodopsin gene in a panel of patients with autosomal dominant retinitis pigmentosa. Hum Mol Genet 1992; 1: 41–5.

62 Bunge S, Wedemann H, David D, Terwilliger DJ, van den Born LI, Aulehla-Scholz C, *et al*. Molecular analysis and genetic mapping of the rhodopsin gene in families with autosomal dominant retinitis pigmentosa. Genomics 1993; 17: 230–3.

63 Kranich H, Bartkowski S, Denton MJ, Krey S, Dickinson P, Duvigneau C, *et al*. Autosomal dominant 'sector' retinitis pigmentosa due to a point mutation predicting an Asn-15-Ser substitution of rhodopsin. Hum Mol Genet 1993; 2: 813–4.

64 Chuang JZ, Vega C, Jun W, Sung CH. Structural and functional impairment of endocytic pathways by retinitis pigmentosa mutant rhodopsin-arrestin complexes. J Clin Invest 2004; 114: 131–40.

65 Scott KM, Sieving PA, Bingham E, Bhagat VJ, Sullivan J, Alpern M, *et al*. Rhodopsin mutations associated with autosomal dominant retinitis pigmentosa. Am J Hum Genet 1993; 53: 147.

66 Li Y, Lambert MH, Xu HE. Activation of nuclear receptors: a perspective from structural genomics. Structure 2003; 11: 741–6.

67 Jacobson KA, Gao ZG, Liang BT. Neoceptors: reengineering GPCRs to recognize tailored ligands. Trends Pharmacol Sci 2007; 28: 111–6.

68 Costanzi S. On the applicability of GPCR homology models to computer-aided drug discovery: a comparison between in silico and crystal structures of the beta2-adrenergic receptor. J Med Chem 2008; 51: 2907–14.

69 Nolte RT, Wisely GB, Westin S, Cobb JE, Lambert MH, Kurokawa R, *et al*. Ligand binding and co-activator assembly of the peroxisome proliferator-activated receptor-gamma. Nature 1998; 395: 137–43.

70 Cronet P, Petersen JF, Folmer R, Blomberg N, Sjoblom K, Karlsson U, *et al*. Structure of the PPARalpha and -gamma ligand binding domain in complex with AZ 242; ligand selectivity and agonist activation in the PPAR family. Structure 2001; 9: 699–706.

71 Xu HE, Lambert MH, Montana VG, Plunket KD, Moore LB, Collins JL, *et al*. Structural determinants of ligand binding selectivity between the peroxisome proliferator-activated receptors. Proc Natl Acad Sci U S A 2001; 98: 13919–24.

Acta Pharmacologica Sinica (2012) 33: 300–311
 1671-4083/12 $32.00
www.nature.com/aps

Review

Structure and mechanism for recognition of peptide hormones by Class B G-protein-coupled receptors

Kuntal PAL[1], Karsten MELCHER[1, *], H Eric XU[1, 2, *]

[1]*Laboratory of Structural Sciences, Van Andel Research Institute, Grand Rapids, MI 49503, USA;* [2]*VARI-SIMM Center, Center for Structure and Function of Drug Targets, State Key Laboratory of Drug Research, Shanghai Institute of Materia Medica, Chinese Academy of Sciences, Shanghai 201203, China*

Class B G-protein-coupled receptors (GPCRs) are receptors for peptide hormones that include glucagon, parathyroid hormone, and calcitonin. These receptors are involved in a wide spectrum of physiological activities, from metabolic regulation and stress control to development and maintenance of the skeletal system. As such, they are important drug targets for the treatment of diabetes, osteoporosis, and stress related disorders. Class B GPCRs are organized into two modular domains: an extracellular domain (ECD) and a helical bundle that contains seven transmembrane helices (TM domain). The ECD is responsible for the high affinity and specificity of hormone binding, and the TM domain is required for receptor activation and signal coupling to downstream G-proteins. Although the structure of the full-length receptor remains unknown, the ECD structures have been well characterized for a number of Class B GPCRs, revealing a common fold for ligand recognition. This review summarizes the general structural principles that guide hormone binding by Class B ECDs and their implications in the design of peptide hormone analogs for therapeutic purposes.

Keywords: G-protein-coupled receptor (GPCR); parathyroid hormone; glucagon; calcitonin; crystal structure

Acta Pharmacologica Sinica (2012) 33: 300–311; doi: 10.1038/aps.2011.170; published online 23 Jan 2012

Introduction

GPCRs are cell-surface receptors that share a common molecular architecture consisting of a seven transmembrane (7TM)/heptahelical domain (HD) with an extracellular N-terminus and an intracellular C-terminus. The seven transmembrane helices are interconnected by three extracellular and three intracellular loops (Figure 1A). All GPCRs share a common signaling mechanism mediated by heterotrimeric G proteins that stimulate the synthesis of intracellular second messengers, including cyclic AMP, inositol phosphate, and Ca^{2+} ions. GPCRs constitute a large family whose members are involved in numerous physiological functions and represent more than 30% of all pharmaceutical drug targets. Based on sequence homology of their transmembrane domains, G-protein coupled receptors are further classified into five subfamilies[1]. The Class A or rhodopsin family constitutes the largest group with more than 700 receptors and is characterized by high sequence identity. The Class B or secretin receptor family is a small subgroup with only 15 peptide-binding receptors in humans (Table 1) that are the focus of this review. The other classes are the glutamate (Class C), adhesion (Class D), and frizzled/smoothened (Class E) receptor families[2, 3]. While all GPCRS share the same core structure to transduce exogenous signals across the membrane, they differ largely in their ligand recognition mechanism due to structural differences in their extracellular domains. Class B GPCRs are characterized by the presence of large extracellular domains of 100 to 160 residues that are the main determinants for ligand binding specificity and play crucial roles in receptor activation[4].

Although full length GPCR structures have been solved only for Class A receptors, the structures of several Class B extracellular domains (ECDs), both in apo and hormone-bound form, have been determined by X-ray crystallography and NMR[5–16]. These structures have provided substantial information about the conformation of Class B ECDs and the structural mechanisms of ligand binding and selectivity. Table 1 provides a list of the currently solved 16 ECD structures that collectively cover eight of the fifteen receptors.

Class B GPCR ligands are related peptide hormones

In contrast to the wide variety of Class A GPCR ligands, all Class B ligands are peptide hormones that share significant degrees of homology with each other (Figure 1B). All of them

* To whom correspondence should be addressed.
E-mail eric.xu@vai.org (H Eric XU);
Karsten.Melcher@vai.org (Karsten MELCHER)
Received 2011-09-22 Accepted 2011-11-12

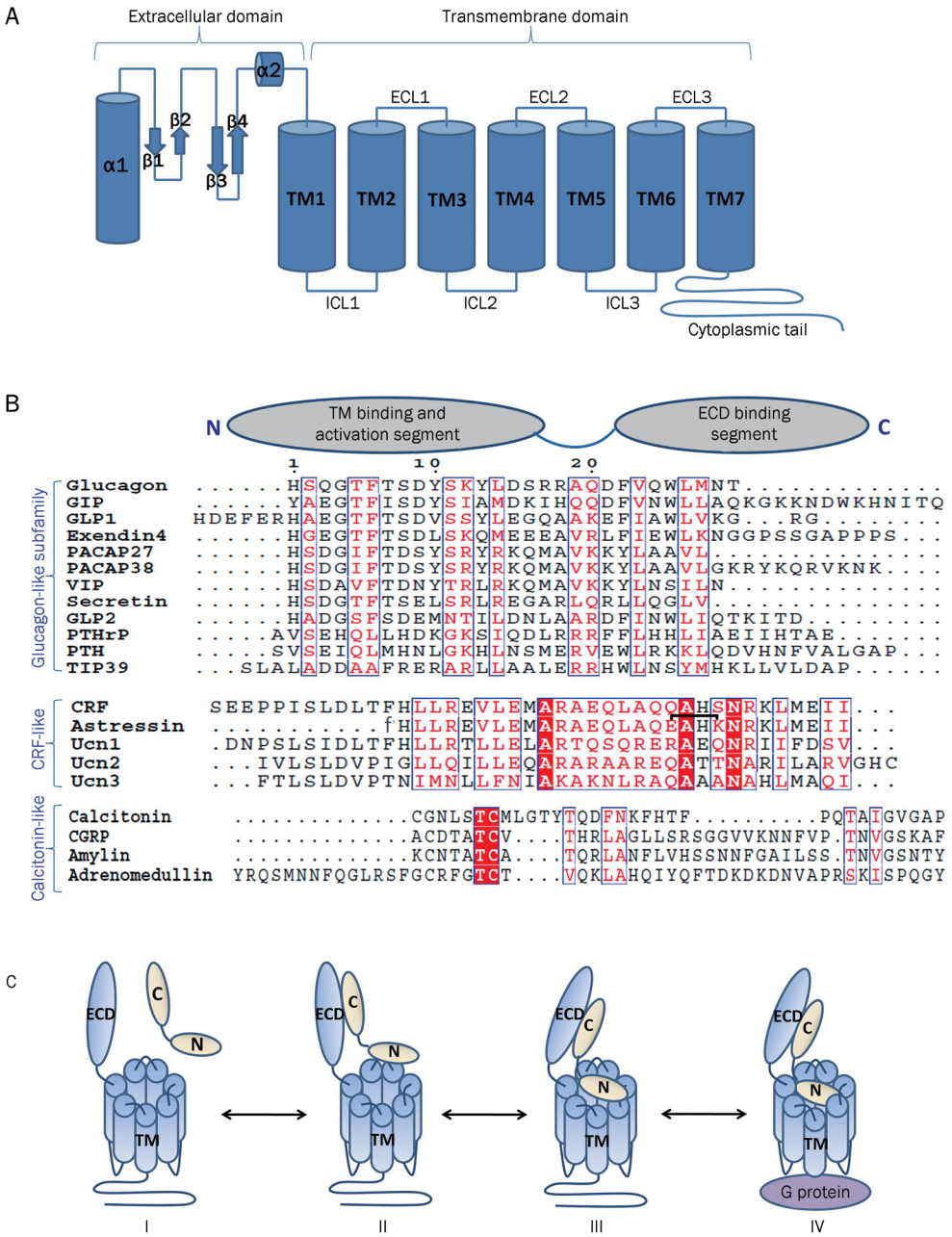

Figure 1. (A) Cartoon presentation of the general architecture of Class B GPCRs consisting of a N-terminal extracellular domain (ECD) and a C-terminal transmembrane domain (7TM). The ECD forms a three layer α-β-β/α fold and the 7TM domain seven membrane-spanning helices connected by three extracellular loops (ECLs) and three intracellular loops (ICLs). (B) Sequence alignment of Class B GPCR ligands with cartoon presentation of their N- and C-terminal domains on top. Based on sequence similarity, ligands can be grouped into glucagon-like, CRF-like, and calcitonin-like subfamilies. Identical residues are shown as white letters on red background. Partially conserved residues are shown as red letters. The residue numbering on top corresponds to that of glucagon. The lactam bridge in astressin is indicated by a black bracket, "f" in the astressin sequence indicates D-phenylalanine. (C) Two domain binding model for class B GPCRs. (I) Peptide hormone and receptor are orientated for initial receptor ligand binding. (II) The initial complex forms between the C-terminus of the peptide and the ECD of the receptor. (III) This interaction facilitates the binding of the free N-terminus of the peptide to the juxtamembrane region of the 7TM domain of the receptor. (IV) This binding induces a conformational change in the 7TM and cytoplasmic domain of the receptor, which mediates its interaction with a heterotrimeric G protein.

have great potential as therapeutic targets for neuronal and endocrinal disorders.

Secretin is the sole ligand of the secretin receptor. It stimulates secretion of acid-neutralizing fluids in pancreas and duodenum. The expression of the secretin receptor in different parts of the CNS imply that secretin also plays important roles in the brain[17].

Growth hormone releasing hormone (GHRH) is the sole

Table 1. An overview of secretin receptor family members and their ligands, with structural details and therapeutic applications.

Secretin family receptor	Cognate ligands	ECD-PDB	Physiological relevance	Disorders	Therapeutic drugs
CRFR1	CRF, Urocortin1	3EHS, 3EHU[11], 2L27[13],	Stress related pathway	Depression/Anxiety	Corticorelin/ Acthrel (approved)
CRFR2α	CRF, Urocortin1, Urocortin2, Urocortin3	1U34[5], 2JND[6], 3N96, 3N95, 3N93[14]	Stress related pathway, Cardiac contractility, Angiogenesis	Depression/Anxiety, Heart failure, Cancer	
PTH1R	PTH, PTHrP	3L2J [39], 3C4M[10], 3H3G[12]	Ca^{2+} homeostasis Hyperparathyroidism	Osteoporosis	Forteo (approved) Preotact (approved in Europe)
PTH2R	PTH, Tip39	–	Hypothalamic secretion, Nociception		
GHRH receptor	GHRH	–	Growth hormone secretion	Dwarfism	Tesamorelin (approved)
Glucagon receptor	Glucagon	–	Glucose homeostasis	Type 2 diabetes	
GLP1 receptor	GLP-1, Exendin4	3I0L[76], 3C59[9]	Insulin secretion	Type 2 diabetes	Byetta/Exenatide, Liraglutide (both approved)
GLP-2 receptor	GLP-2		Glucagon secretion, Gut mucosal growth	Short bowel syndrome	Teduglutide (Phase III)
GIP receptor	GIP	2QKH[7]	Insulin secretion Lipid metabolism	Type 2 diabetes	–
PAC1R	PACAP, VIP	3N94[16], 2JOD[8]	Neurotransmitter, Neuromodulator, Neuroprotection	Schizophrenia, Medulloblastoma	–
VPAC1R	VIP, PACAP	–	Vasodilation, Digestion, Neuroprotection	Crohn's disease, rheumatoid arthritis	–
VPAC2R	VIP, PACAP	2X57	Vasodilation, Digestion, Neuroprotection	Schizophrenia	–
Secretin receptor	Secretin	–	Pancreatic secretin H_2O homeostasis		–
Calcitonin receptor	Calcitonin	-	Ca^{2+} homeostasis	Osteoporosis	Miacalcin, Cibacalcin (approved)
AMY receptor (CTR /RAMP1,2,3)	Amylin		Glucose homeostasis	Diabetes	Pramlintide/Smylin (approved)
CGRP receptor (CLR/RAMP1)	CGRP	3N7S[15]	Vasodilation	Migraine	Telcagepant (Phase III fail)
AM_1 receptor (CLR/RAMP2)	Andromedulin	2XVT (RAMP2)	Circulatory system, Vasodilation	Cardiovascular disease	
AM_2 receptor (CLR/RAMP3)	CGRP, Andromedulin		Vasodilation, Cellular tolerance for oxidative stress	Cardiovascular diseases	–

hormone of the GHRH receptor and stimulates growth hormone secretion.

Corticotrophin release factor (CRF) and urocortins are ligands for CRF receptors 1 and 2 (CRFRs) and function predominantly as mediators of stress responses[18]. Urocortin 2 also has antiangiogenic activity important for tumor suppression function[19].

Parathyroid hormone (PTH), parathyroid hormone related peptides (PTHrPs), and tuberoinfundibular peptide Tip39 are ligands for PTH receptors (PTH1R and PTH2R) that control calcium and phosphate homeostasis[20] and can function as neuromodulators[21].

Glucagon, glucagon like peptides (GLPs), and glucose dependent insulinotropic polypeptide (GIP) are ligands for glucagon receptor (GLPRs and GIPR), respectively, and are important regulators of glucose homeostasis[22, 23].

Pituitary adenylate cyclase activating polypeptide (PACAP) and vasoactive intestinal peptide (VIP) are shared ligands of three receptors, PAC1R, VPAC1R, and VPAC2R. PAC1R is preferentially activated by PACAP, a neuroprotective modulator and stimulator of nerve cell regeneration, while VPACR is efficiently activated by both the vasodilation-stimulating VIP and PACAP. VIP also performs neuroprotective function with VPAC2R. Both hormones also have neurotransmitter function and affect secretion or production of other hormones[24].

Calcitonin (CT), calcitonin-gene-related peptide (CGRP), amylin (AMY), and andromedullin (AM) form a separate subclass of Class B hormones with roles in Ca^{2+}- and glucose-homeostasis as well as vasodilation. Their receptors, calcitonin receptor (CTR) and calcitonin-like receptor (CLR), associate with three members of receptor activity-modifying proteins (RAMP1 to RAMP3) that modulate their hormone selectivity[25].

In addition, two non-human peptide ligands, Exendin-4 and Astressin, have pharmacological roles in treating type-2 diabetes and stress related disorders. Exendin-4 is derived from the saliva of Gila monster. As an analog of GLP-1, it activates GLP1R and stimulates glucose-dependent insulin secretion[26]. Astressin is a synthetically designed high affinity antagonist for CRFR, in which *D*-Phe replaces *L*-Phe at the 12th position of CRF (12–41). In addition, lactam cyclization between astressin Glu30 and Lys33 stabilizes helix formation and strongly increases the affinity of the peptide.

Crystal structures of Class B GPCR ligands[7, 27] revealed single continuous amphipathic α-helices, while NMR solution structures[28, 29] indicated that the free peptide hormones are disordered or only partially α-helical, but adopt amphipathic α-helices upon receptor binding. Binding studies employing truncated and chimeric peptide ligands demonstrated separate contributions by the peptide N- and C-termini. N terminal truncations turn the peptide ligands into potent antagonists[24, 30], suggesting that the N-termini play critical roles in receptor activation, but are not essential for receptor binding. In contrast, C-terminally deleted peptides are still capable of receptor activation, but bind the receptors with markedly lower affinities[31]. Finally, peptides consisting of the C-terminus of PTH and the N-terminus of calcitonin were unable to activate either PTHR or CTR, but efficiently activated a chimeric receptor consisting of the N-terminal ECD from PTH1R and the membrane embedded C-terminus from CTR[32]. Several other similar hybrid experiments with glucagon, GLP1R, calcitonin, VIP, and PACAP confirmed the distinct roles of the N- and C-termini of the peptide hormones in receptor interaction and activation[30, 31, 33–35]. These data provided the basis of the "two domain model", which proposes that Class B hormone C-termini form initial complexes with their receptor ECDs, which in turn allows their N-termini to interact with the 7TM domains to activate the receptors (Figure 1C). This model was further supported for CRF by NMR chemical shift perturbation data in combination with the charge distribution in CRF ECD and its antagonist astressin[5]. Finally, the first high resolution structure of the complex between a Class B GPCR ECD and its ligand, the crystal structure of the GIPR ECD–GIP (1–42) complex, directly illustrated that the C-terminus of the ligand formed the main ECD interaction while the N-terminus of the peptide remained free[7].

The peptide hormone N- and C-termini expressed as separate peptides are biologically inactive, implying that their linkage is required for hormone activity[36]. The residues that connect the termini appear to function as α-helical linkers, whose length and orientation, but not sequence, are required for full receptor activation[36].

The extracellular domains of Class B GPCRs share a common fold

While the 7TM domains of Class B GPCRs are highly homologous, their ECDs share exceptionally low levels of sequence identity (Figure 2B). Therefore, structural studies of ECDs are crucial to understand ligand specificity and selectivity. Table 1 provides an overview of the 15 human Class B receptors and their ECD structures and functions.

The basic fold of the extracellular domain is a three-layer α-β-β/α structure

The first structures of the extracellular domain of a Class B GPCR were the NMR structures of the ECD of murine CRFR2β in apo form[5] and as complex with the synthetic antagonist astressin[6]. These structures revealed the core region of the ECD, which is comprised of two pairs of antiparallel β-sheets interconnected by hairpin loops. This fold is stabilized by three interlayer disulfide bonds and by hydrophobic interactions and resembles the short consensus repeat fold of complement control protein[37]. However, the N-terminus of the ECD was not resolved in these structures. The ligand-bound ECD crystal structures of hGIPR–GIP (1–42) and hPTH1R–PTH (15–34) (Figure 2E&2C) demonstrated that the N-termini of their ECDs form long single α-helices that are connected by a disulfide bond with the first β strand and whose residues contribute to the ECD-ligand binding pocket[7, 10]. Overall, the ECDs share a three-layer α-β-β/α architecture, in which the N-terminal α-helix forms the first outer layer, the β1-β2 sheet and adjacent loops the middle layer, and the β3-β4 and the

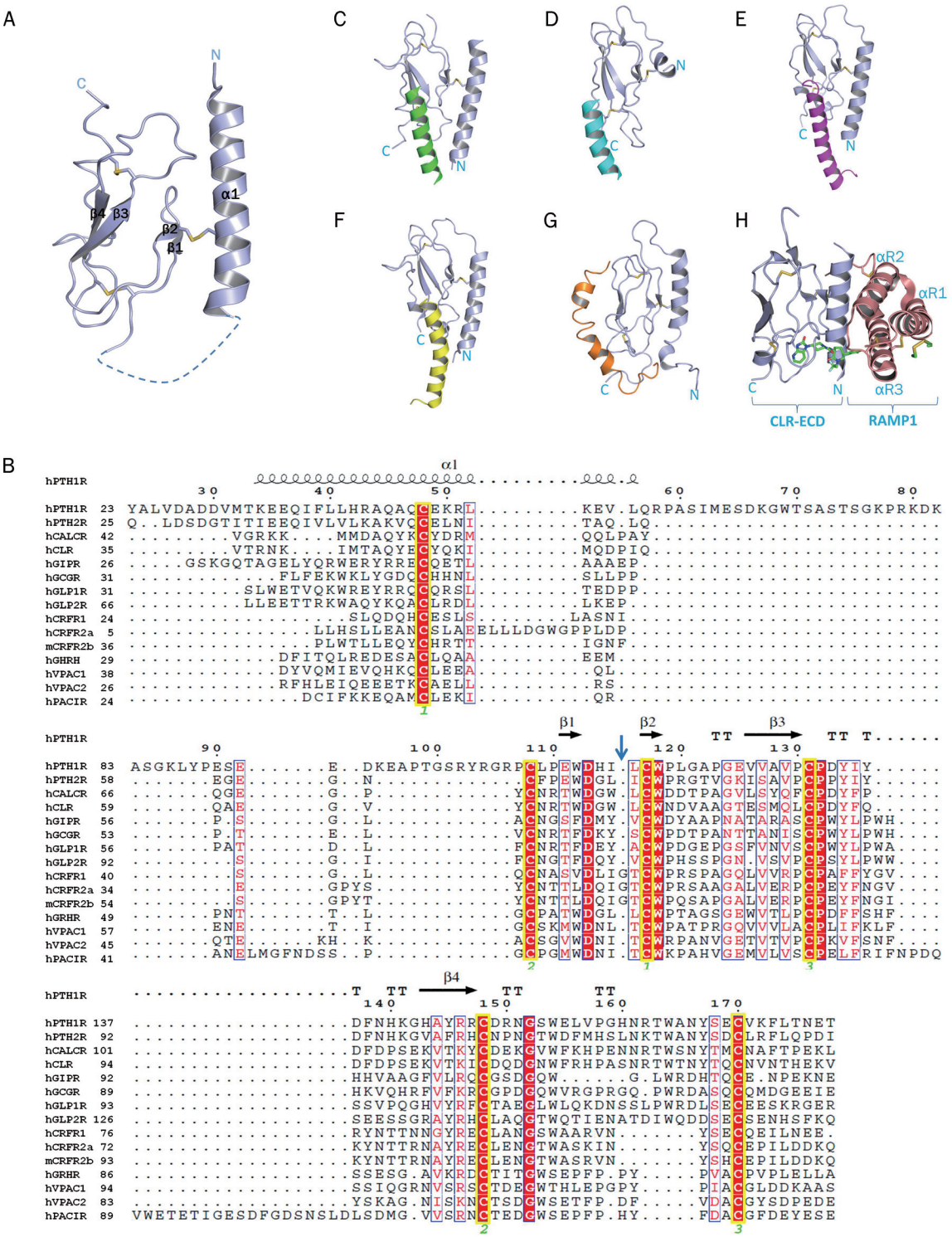

Figure 2. (A) A ribbon diagram of the basic architecture of the "secretin family recognition fold" of the extracellular domain of class B GPCRs. The structure is mainly divided into three layers consisting of an N terminal α helix and two pairs of antiparallel β sheets. The conserved disulfide bonds connecting the three layers are depicted as sticks. (B) Sequence alignment of the extracellular domains of human Class B GPCRs with secondary structure elements for PTH1R indicated on top (PDB: 3C4M). Invariant and conserved residues are highlighted. The glycine residues specific for the CRFR subfamily are marked by a blue arrow. Invariant cysteine residues are indicated by a yellow box. Identical residues are shown as white letters on red background. Partially conserved residues are shown as red letters on white background. The residue numbering on top corresponds to that of hPTH1R. Cysteine pairs forming disulfide bonds are indicated by yellow outlines and by green numbers at the bottom. TT=tight turns. (C) Structure of the hPTH1R-PTH ECD complex with the ECD shown in light blue and PTH in green. (D) Structure of the hCRFR1-CRF complex with the ECD shown in light blue and CRF in cyan. (E) Structure of the hGIPR-GIP complex with the ECD in light blue and GIP in magenta. (F) Structure of the hGLP1R-Glp1 complex with the ECD in light blue and Glp1 in yellow. (G) Structure of the PAC1R-PACAP complex with the ECD in light blue and PACAP in orange. (H) Structure of the CLR-Telcagepant (a small molecule drug for the treatment of migraine) with the CLR-ECD in light blue and RAMP1 in salmon.

C-terminus, which for some ECDs includes a short (one-to-two turns) α-helix, the second outer layer (Figure 2A and 2C–2H). This organization, together with the principal hormone recognition mechanism, has also been found in the hGIPR–GIP, hPTH1R–PTH, hGLP1R–GLP1, and hCRFR1–CRF (Figure 2C–2G). This conserved α-β-β/α fold has also been named 'secretin family recognition fold' that serves as the consensus mechanism of Class B GPCR ligand binding[16].

The sequence homology of the ECDs is very low and limited to the six disulfide-forming cysteines and only about a dozen other conserved residues (Figure 2B). Four of the residues are identical in all receptor ECDs and have been shown to play important roles in tertiary structure stabilization (D113, W118, P132, and W154 with respect to PTH1R in the alignment shown Figure 2B)[10]. The first disulfide bond links the N terminal helix to the middle layer β-sheet, the second one links the middle layer to the outer β-sheet, and the third one links the middle layer to the C-terminus of the ECD. While the position of the disulfide bonds and secondary structure elements is highly conserved, the loops connecting the structure motifs vary considerably and therefore likely provide the basis for ligand binding specificities.

Glucagon-like and CRF-like hormones adopt different positions in their ligand-binding pockets

The overall binding pattern of Class B GPCR peptide ligands to their cognate receptors shows a high level of similarity. In all complex crystal structures, the peptide binds in amphipathic α-helical conformation to the same face of the ECD. With the exception of the PAC1R-PACAP[8] NMR structure, whose accuracy remains in doubt[16, 38], the C-terminus of the peptide forms hydrophobic and hydrogen bond interactions with the ligand binding pocket of the ECD while the N-terminus of the peptide remains free and shows a high level of flexibility. The glucagon-like and the CRF-like subfamilies differ from each other both by their amino acid sequence signature (Figure 1B) and by their relative position in the ligand binding pocket. As illustrated in Figure 3A, the position of the CRF C-terminal helix is translationally shifted by 5–8 Å relative to the location of PTH, GIP, and GLP. These differences can be explained by two features. First, the CRFR ECDs are characterized by one invariant glycine (Gly52 for CRFR1; blue arrow in Figure 2B) in the loop connecting β1 and β2 that is missing in peptide hormones of the glucagon-like subfamily and that causes a further extension of the loop. Second, the CRFR N-terminal helices of the ECD are much shorter than those of PTHR, GIPR, and GLPR (Figures 2D–2F) and that can therefore not mediate ligand interactions[11]. It should be noted, that differences in ligand position could also be induced by experimental approaches.

Based upon the ligand-bound ECD structures, we illustrate possible models for the binding of these two hormone subclasses to a full length receptor (Figure 3B) to provide the relative dimensions of ligands and receptors and to illustrate the burial of the ligands. In the GIP model, the N-terminus of the ligand forms a straight helical extension of the C-terminus to fit into the pocket formed between the 7TM helices. The CRF model accounts for the *L*-shaped conformation with a bend after the 23rd residue seen in the recent NMR structure of hCRFR1-CRF (PDB: 2L27)[13]. Thus, ligands may adopt dif-

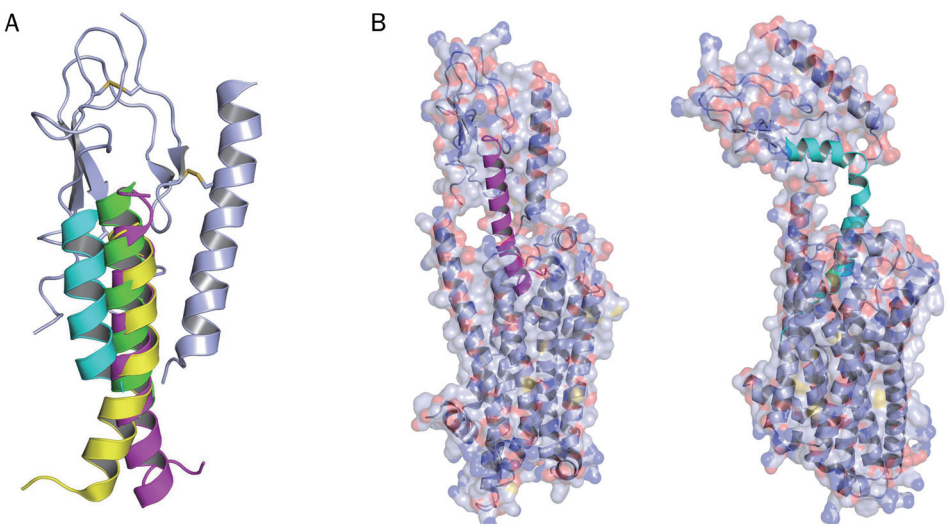

Figure 3. (A) Structural alignment of ECD-bound Class B GPCR ligands. The ligands form helical conformations with their C termini interacting with the ECD. The N termini remain free and show a high level of flexibility. The ligands shown are PTH(15–34) in green, GIP(1–42) in magenta, GLP1(7–37) in yellow, and CRF(22–41) in cyan. (B) Models displaying possible hormone positions in the context of full length receptors. Models of ECD-bound GIP(1–42) (magenta) [PDB: 2QKH] and a modified CRF (cyan) [PDB: 2L27] were superpositioned on a model of the transmembrane domain of turkey β1-adrenergic receptor [PDB: 2Y03]. The ECD was adjusted manually with distance constraints using COOT. The different binding positions between CRF-like and glucagon-like subfamily peptides suggest that the ECDs may also adopt two different conformations in the context of full length receptors. Note that these models just illustrate relative dimensions of receptors and ligands as well as predictions of ligand binding sites. Only structures of the complexes between full length receptors and their ligands can provide accurate position and conformation of receptor-bound ligands.

ferent positions in spite of a common structural interaction mechanism. The exact nature of complete ligand binding can only be determined by structural analyses of full length receptors.

Ligand-binding induces conformational changes in some ECDs

Most ECD structures have only been obtained in complex with ligand, indicating that ligand binding stabilizes these proteins and therefore favors crystallization of ECD-ligand complexes[14]. Hormone-induced conformational changes in the ECD have been clearly shown for CRFR1[11], where superposition of apo (3EHS) and CRF-bound structures (3EHU) revealed a major rearrangement of the ECD secondary structure. Ligand binding shifted the loop connecting the β3 and β4 strands by approximately 5–7 Å towards the peptide hormone. Phe72 in that loop shifted in the ligand bound structure by 7.2 Å and its side chain rotated towards the C terminus of the peptide to allow formation of a hydrophobic interaction. These changes illustrate the dynamic plasticity of the CRFR1 ECD. It will be interesting to see, if similar conformational rearrangements also occur in other ECDs of this class.

In contrast to CRFR1, no major conformational change was detectable between the apo and PTH-bound structure of PTH1R, a representative of the glucagon-like subclass of hormones[39]. Instead, the long second (C terminal) α-helix of the apo PTH1R ECD mimicked the structure of the peptide hormone in the complex structure.

Peptide ligands can modulate the monomer–dimer equilibrium of Class B GPCRs

Receptor oligomerization has been demonstrated for different classes of GPCRs[40]. In the case of Class C GPCRs, homo- or hetero-dimerization mediates receptor activation[41]. Dimerization has also been demonstrated for Class A GPCRs[42, 43], including the real-time imaging of muscarinic acetylcholine receptor dimerization in live CHO-cells by total internal reflection fluorescence microscopy (TIRFM)[44]. Based upon several functional studies, Class B GPCRs can dimerize/oligomerize via their heptahelical domains. In particular, the lipid-exposed hydrophobic surface of their TM4 helices appears to mediate receptor homo-dimerization[45, 46]. The functional significance of Class B GPCR oligomerization is poorly understood. In the case of the secretin receptor, disruption of the interaction between tagged receptors in cells had no effect on ligand binding, but did reduce receptor signaling by an unknown mechanism[45]. In addition to homo-oligomerization, hetero-oligomer formation has also been observed between VIP receptors VIP1R/VPAC2 and the secretin receptor[47] as well as for calcitonin receptor[48], CRFR[49], and PAC1R[50].

The ligand-bound structures of Class B GPCR ECDs mostly presented monomeric conformations. The exception is the PTH1 receptor, whose ECD adopted a dimeric conformation in the absence, but not the presence, of ligand. This result is consistent with bioluminescence resonance energy transfer (BRET) analysis of full length PTH1R, which demonstrated that addition of ligand leads to disruption of receptor dimers[39]. The dimeric arrangement of protomers in the apo ECD was mediated by the C-terminal α2 helix, which occupied the peptide binding groove of the other monomer. In the absence of ligand, the C-terminal helix thus structurally mimics the ligand which leads to the dimer formation. Dimer formation was validated by BRET experiments with receptors in which the α2-helical region of the ECD was mutated. While these experiments provided a structural basis for ECD-mediated receptor dimerization for PTH1R, this feature may not be shared among other members of secretin family receptors.

Class B peptide ligands adopt α-helical conformations upon receptor binding

In complex with their receptor ECDs, peptide hormones are α-helical in both crystal and solution structures. In most cases, the helices were amphipathic, especially at the C terminus, which is the main determinant for ECD binding. In contrast, the free peptides appear to be unstructured in water and adopt their helical structure upon complex formation. The thermodynamic and spectroscopic analysis of GIP peptide upon binding to GIPR revealed the burial of a solvent accessible region and an increase in α helical structure, which contributes to an increase in receptor affinity and the formation of a tight hormone-receptor complex[7]. Using NMR techniques, a transition from an unstructured to an α-helical conformation was also observed for the binding of CRF to its ECD in an analysis of the minimum peptide length requirement for ECD binding[51]. These results agree with a comparative NMR analysis of the conformational changes in PACAP (1–27) upon association with its full length receptor in micelles[52].

The helix-capping residues at the N termini of Class B hormone ligands play a crucial role in initiating the transition to an α-helical conformation[53]. Functional studies using α-aminoisobutyrate analogs of PTH have also shown that the N terminal region forms a helical conformation when complexed with the extracellular loops and TM domains of PTH1R[54].

Many ECDs can interact with different ligands

Selectivity within the glucagon-like and CRF-like subfamilies is determined by non-conserved amino acids

Most Class B GPCR can bind to more than one ligand. For example, PAC1R has a very high affinity for PACAP [both PACAP(1–38) and (1–27)], but can also interact with VIP. Early demonstration of glucagon/GLP1 selectivity was achieved by the use of chimeric GLP1 and glucagon receptors[30, 31].

The family of CRF/Ucn peptides signals through two different receptors, CRFR1 and CRFR2. Although these two receptors share 68% sequence identity, they differ markedly in ligand selectivity. CRFR1 is selective for CRF and Ucn1 while CRFR2 binds all four ligands CRF, Ucn1, Ucn2, and Ucn3 with affinities that range from high to moderate. Structural and biochemical analysis of the binding of the CRFR ECDs to the C termini of CRF, Ucn1, Ucn2, and Ucn3 identified the selectivity determinants that distinguish between the highly similar

peptide hormones. The importance of these critical residues responsible for selectivity was confirmed by swapping experiments. Ucn1 and CRF contain an arginine at position 35 that is missing in Ucn2 and Ucn3 and that may determine selectivity to CRFR1 by binding to a CRFR1-specific negatively charged pocket consisting of Gln103 and Glu104[14]. Importantly, the affinity and selectivity patterns of the ECDs closely match those of the full length receptors[55]. Thermodynamic and CD analyses of CRF and urocortins may help to evaluate whether an inherent high helical propensity is responsible for the high affinity binding of Ucn1 (relative to CRF and Ucn2/3) to both CRFRs.

The structural determinants of the selectivity of PTHRs are still unclear. The three ligands PTH, PTHrP, and TIP39 mediate their biological functions through two receptors, PTH1R and PTH2R. PTH can bind both receptors, while PTHrP is selective for PTH1R and TIP 39 is selective for PTH2R[56]. Radioligand binding studies with wildtype and chimeric PTH2R/PTH1R receptors have pointed to the N terminal six residues of the ligand and to the extracellular loops of the TM domains as important selectivity determinants[57]. In addition, the presence of Trp23[58], a residue that is invariant in both PTH and TIP39, is probably responsible for selective binding of these two ligands to PTH2R.

Importantly, binding of different ligands can induce highly distinct pharmacological receptor responses. This was first shown for CRFR, where different physiological ligands and CRF receptor subtypes can differentially stimulate signaling pathways in human myometrial cells[59], effects that could only partially be confirmed in other cell types[60]. Many GPCRs can signals through β-arrestins in addition to the classical G protein pathways[61] and certain PTH analogs have been shown to function as "biased agonists" that preferentially signal either through G proteins or through β-arrestins[62, 63].

Radioligand dissociation experiments with full length PTH1R and G proteins have shown that PTH (1-34) has a higher affinity than PTHrP (1–36) for PTH1R in its G protein-uncoupled conformation (R^0 state), while both peptides bind PTH1R with equal affinities in its G protein-coupled state (R^G). Since the ECD adopts the same conformation when bound to either PTH or PTHrP, it is likely that this selectivity is due to ligand-selective rearrangements in the heptahelical domain of the receptor. Therefore, full length structures of PTH1R with PTH and PTHrP will be required to provide a structural basis for the ligand selectivity of the R^0 and R^G states of the receptor. Analysis of differential ligand binding to different states of receptor may significantly contribute to the development of specific peptide analogs for therapeutic purposes[64] (see below).

Selectivity of the calcitonin subfamily of receptors is modulated by RAMPs

At a different level of selectivity, the calcitonin receptor CTR and the calcitonin-like receptor CLR form heterodimeric complexes with transmembrane protein partners called receptor activity modifying proteins (RAMPs). The complex between CLR and RAMP1 is selectively bound and activated by the calcitonin gene-related peptide (CGRP), while CLR in complex with RAMP2 and RAMP3 form adrenomedullin AM_1 and AM_2 receptors, respectively. In the absence of RAMPs, CTR is preferentially activated by calcitonin, whereas it functions predominatly through amylin (AMY) in combination with RAMP1, 2, and 3[65]. The functional association of several other Class B members with RAMPs has been reported previously, but the functional role of these complexes remains unknown[25].

The first crystal structure of RAMP1 (PDB: 2YX8) revealed a triangular arrangement of a three helix bundle that is stabilized by three interconnecting disulfide bonds formed between six invariant cysteine residues (Figure 4A)[66]. The subsequent crystal structure of RAMP1 in complex with the extracellular domain of CLR (PDB: 3N7P, 3N7R, SN7S) identified both hydrophobic and electrostatic interactions between the R2 and R3 helices of RAMP1 and the N terminal helix of the CLR ECD[15]. The main RAMP residues that form hydrophobic interactions with CLR are the conserved Tyr66, Phe93, His97 and Phe101 (numbering refers to RAMP1, see alignment in Figure 4A). Based upon the high sequence and structural conservation (root mean square deviation of 1.24 Å) between RAMP1 and RAMP2, similar interactions are predicted for the CLR-RAMP2 complex. However, structural alignment of the CLR-RAMP1 complex (PDB: 3N7S) with apo RAMP2 (PDB: 2XVT) reveals a sterical clash between the side chain of Arg97 in the second helix of RAMP2 (RAMP1 has an alanine at the corresponding position) and the side chain of CLR Gln45 (Figure 4B), suggesting that RAMP2 may structurally rearrange when forming the ternary CLR-RAMP2-AM complex.

Structure-based chemical modification of peptide ligands is important for therapeutic applications

The potential for therapeutic applications of Class B GPCRs and their peptide binding partners is enormous. However, direct application of these peptides as therapeutic drugs is hampered by their low efficacy due to poor bioavailability and rapid degradation. Therefore, a substantial amount of research is dedicated to the design of stable, chemically modified analogs of these peptides[67]. Modifications used to increase peptide stability include (i) N-terminal fatty acid acylation (GLP1) or hexonylation (VIP), (ii) generation of chimeric hormones (Glp1/PACAP fusions), (iii) midchain modifications by mercaptopropionic acid derivatization of Cys14 in andromedulin and by replacing *L*-Phe12 in CRF with *D*-Phe, as well as (iv) alteration at the C-terminus by PEGylation (GIP)[68–72]. The resulting agonists and antagonists have increased metabolic stability, biological activity, and bioavailability. For example, the energy metabolism-regulating hormone Glp1 is highly unstable with a bioavailability of only 1–2 min due to its rapid enzymatic degradation by dipeptidyl peptidase 4. In contrast, the N-acylated Glp1 analog Liraglutide has a half life of 14 h, which makes it suitable for the treatment of type 2 diabetes[73]. Exenatide, an analog of the naturally occurring Glp1 agonist Exendin-4, in which the second alanine

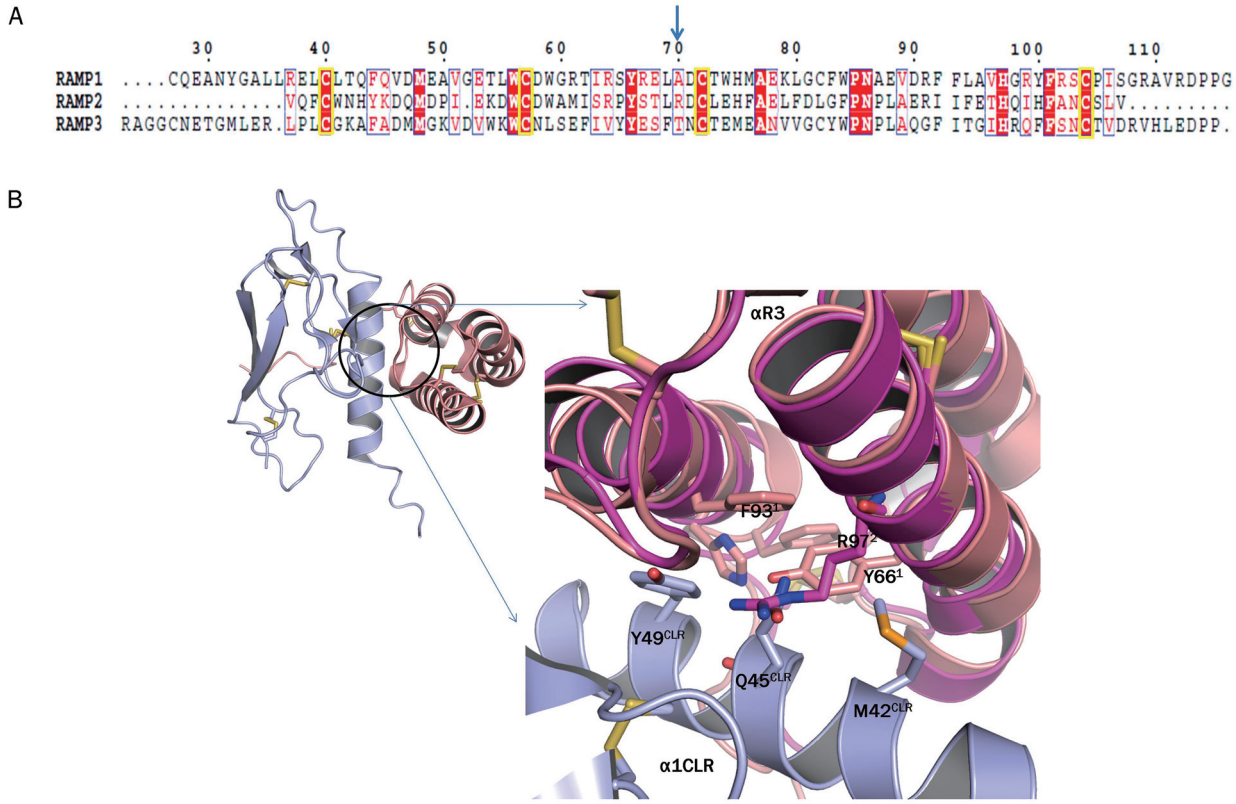

Figure 4. (A) Sequence alignment of RAMP 1, 2, and 3. The important non-conserved residue in the RAMP1-CLR interaction pocket has been highlighted by a blue arrow. Invariant cysteine residues have been shown in yellow box. Identical residues are shown as white letters on red background. Partially conserved residues are shown as red letters. The residue numbering on top corresponds to that of RAMP1. (B) Structural representation of the CGRP receptor with the CLR-ECD in light blue and RAMP1 in salmon. Structural alignment of the binding interface of the RAMP1-CLR complex (salmon-lightblue; PDB: 3N7S) with apo RAMP2 (magenta; PDB: 2XVT). The helices 2 and 3 of RAMP have been marked. The side chains of RAMP2 R97 and CLR Q45^{CLR} in the binding interface sterically clash.

is substituted by serine, improves both stability and activity[73]. Exenatide increases insulin secretion in response to high blood sugar levels and suppresses the pancreatic release of glucagon. Similarly, a tetra-substituted analog of GHRH (1–29) circumvents proteolytic cleavage by associating with serum albumin[74]. Introduction of two proline residues at the very N-terminus of PTH (1–34) generated an analog that is resistant against degradation by dipeptidase and that is currently in use for the treatment of osteoporosis[75].

Conclusions

The structures of the ECDs of Class B GPCRs in apo and hormone-bound forms have identified the main determinants of receptor-peptide specificity and have established the unique fold of the extracellular receptor domains and the conserved conformation of their bound peptide ligands. The structural data are consistent with various previous *in vivo* functional studies. Therefore, in the absence of full length receptor structures, ECD-hormone complexes provide the best model for rational drug design and further studies. There remains an ongoing need for structural interrogations of ligand-receptor specificities and selectivities for the design of more precise, specific, and stable peptides as therapeutic drugs to treat the many diseases impacted by Class B hormones.

Crystallization of full length Class B GPCRs may provide an even more formidable challenge than crystallization of Class A GPCRs due to the presence of the Class B-specific long flexible N terminal extracellular-domains. The main bottleneck for crystallization of GPCRs has been their conformational flexibility. This bottleneck could be overcome for several Class A GPCRs by protein engineering approaches, including the introduction of stability-enhancing mutations, replacement of flexible surface loops with stable proteins like T4 lysozyme, and stabilization by complex formation with nanobodies. In addition, improvements in the lipidic cubic phase method of membrane protein crystallization and in data collection using micro beam technology have further stretched the boundaries of membrane protein crystallization. Given these technical advances, we look optimistically into the future of Class B GPCR crystallography.

Acknowledgements

This work was supported in part by the Jay and Betty Van Andel Foundation, and National Institute of Health grant

GM087413 (H Eric XU).

References

1 Fredriksson R, Lagerstrom MC, Lundin LG, Schioth HB. The G-protein-coupled receptors in the human genome form five main families. Phylogenetic analysis, paralogon groups, and fingerprints. Mol Pharmacol 2003; 63: 1256–72.
2 Foord SM, Bonner TI, Neubig RR, Rosser EM, Pin JP, Davenport AP, *et al*. International Union of Pharmacology. XLVI. G protein-coupled receptor list. Pharmacol Rev 2005; 57: 279–88.
3 Harmar AJ. Family-B G-protein-coupled receptors. Genome Biol 2001; 2; REVIEWS3013.
4 Lagerstrom MC, Schioth HB. Structural diversity of G protein-coupled receptors and significance for drug discovery. Nat Rev Drug Discov 2008; 7: 339–57.
5 Grace CR, Perrin MH, DiGruccio MR, Miller CL, Rivier JE, Vale WW, *et al*. NMR structure and peptide hormone binding site of the first extracellular domain of a type B1 G protein-coupled receptor. Proc Natl Acad Sci U S A 2004; 101: 12836–41.
6 Grace CR, Perrin MH, Gulyas J, Digruccio MR, Cantle JP, Rivier JE, *et al*. Structure of the N-terminal domain of a type B1 G protein-coupled receptor in complex with a peptide ligand. Proc Natl Acad Sci U S A 2007; 104: 4858–63.
7 Parthier C, Kleinschmidt M, Neumann P, Rudolph R, Manhart S, Schlenzig D, *et al*. Crystal structure of the incretin-bound extracellular domain of a G protein-coupled receptor. Proc Natl Acad Sci U S A 2007; 104: 13942–7.
8 Sun C, Song D, Davis-Taber RA, Barrett LW, Scott VE, Richardson PL, *et al*. Solution structure and mutational analysis of pituitary adenylate cyclase-activating polypeptide binding to the extracellular domain of PAC1-RS. Proc Natl Acad Sci U S A 2007; 104: 7875–80.
9 Runge S, Thogersen H, Madsen K, Lau J, Rudolph R. Crystal structure of the ligand-bound glucagon-like peptide-1 receptor extracellular domain. J Biol Chem 2008; 283: 11340–7.
10 Pioszak AA, Xu HE. Molecular recognition of parathyroid hormone by its G protein-coupled receptor. Proc Natl Acad Sci U S A 2008; 105: 5034–9.
11 Pioszak AA, Parker NR, Suino-Powell K, Xu HE. Molecular recognition of corticotropin-releasing factor by its G-protein-coupled receptor CRFR1. J Biol Chem 2008; 283: 32900–12.
12 Pioszak AA, Parker NR, Gardella TJ, Xu HE. Structural basis for parathyroid hormone-related protein binding to the parathyroid hormone receptor and design of conformation-selective peptides. J Biol Chem 2009; 284: 28382–91.
13 Grace CR, Perrin MH, Gulyas J, Rivier JE, Vale WW, Riek R. NMR structure of the first extracellular domain of corticotropin-releasing factor receptor 1 (ECD1-CRF-R1) complexed with a high affinity agonist. J Biol Chem 2010; 285: 38580–9.
14 Pal K, Swaminathan K, Xu HE, Pioszak AA. Structural basis for hormone recognition by the Human CRFR2{alpha} G protein-coupled receptor. J Biol Chem 2010; 285: 40351–61.
15 ter Haar E, Koth CM, Abdul-Manan N, Swenson L, Coll JT, Lippke JA, *et al*. Crystal structure of the ectodomain complex of the CGRP receptor, a class-B GPCR, reveals the site of drug antagonism. Structure 2010; 18: 1083–93.
16 Kumar S, Pioszak A, Zhang C, Swaminathan K, Xu HE. Crystal structure of the PAC1R extracellular domain unifies a consensus fold for hormone recognition by class B G-protein coupled receptors. PLoS One 2011; 6: e19682.
17 Horvath K, Stefanatos G, Sokolski KN, Wachtel R, Nabors L, Tildon JT. Improved social and language skills after secretin administration in patients with autistic spectrum disorders. J Assoc Acad Minor Phys 1998; 9: 9–15.
18 Bale TL, Vale WW. CRF and CRF receptors: role in stress responsivity and other behaviors. Annu Rev Pharmacol Toxicol 2004; 44: 525–57.
19 Hao Z, Huang Y, Cleman J, Jovin IS, Vale WW, Bale TL, *et al*. Urocortin2 inhibits tumor growth via effects on vascularization and cell proliferation. Proc Natl Acad Sci U S A 2008; 105: 3939–44.
20 Poole KE, Reeve J. Parathyroid hormone — a bone anabolic and catabolic agent. Curr Opin Pharmacol 2005; 5: 612–7.
21 Dobolyi A, Palkovits M, Usdin TB. The TIP39-PTH2 receptor system: unique peptidergic cell groups in the brainstem and their interactions with central regulatory mechanisms. Prog Neurobiol 2010; 90: 29–59.
22 Yamada Y. Gastric inhibitory polypeptide (GIP) receptor. Nippon Rinsho 1997; 55: 512–6.
23 Nauck MA, Baller B, Meier JJ. Gastric inhibitory polypeptide and glucagon-like peptide-1 in the pathogenesis of type 2 diabetes. Diabetes 2004; 53: S190–6.
24 Vaudry D, Gonzalez BJ, Basille M, Yon L, Fournier A, Vaudry H. Pituitary adenylate cyclase-activating polypeptide and its receptors: from structure to functions. Pharmacol Rev 2000; 52: 269–324.
25 Sexton PM, Morfis M, Tilakaratne N, Hay DL, Udawela M, Christopoulos G, *et al*. Complexing receptor pharmacology: modulation of family B G protein-coupled receptor function by RAMPs. Ann N Y Acad Sci 2006; 1070: 90–104.
26 Xu G, Stoffers DA, Habener JF, Bonner-Weir S. Exendin-4 stimulates both beta-cell replication and neogenesis, resulting in increased beta-cell mass and improved glucose tolerance in diabetic rats. Diabetes 1999; 48: 2270–6.
27 Sasaki K, Dockerill S, Adamiak DA, Tickle IJ, Blundell T. X-ray analysis of glucagon and its relationship to receptor binding. Nature 1975; 257: 751–7.
28 Grace CR, Perrin MH, Cantle JP, Vale WW, Rivier JE, Riek R. Common and divergent structural features of a series of corticotropin releasing factor-related peptides. J Am Chem Soc 2007; 129: 16102–14.
29 Venneti KC, Hewage CM. Conformational and molecular interaction studies of glucagon-like peptide-2 with its N-terminal extracellular receptor domain. FEBS Lett 2011; 585: 346–52.
30 Runge S, Gram C, Brauner-Osborne H, Madsen K, Knudsen LB, Wulff BS. Three distinct epitopes on the extracellular face of the glucagon receptor determine specificity for the glucagon amino terminus. J Biol Chem 2003; 278: 28005–10.
31 Runge S, Wulff BS, Madsen K, Brauner-Osborne H, Knudsen LB. Different domains of the glucagon and glucagon-like peptide-1 receptors provide the critical determinants of ligand selectivity. Br J Pharmacol 2003; 138: 787–94.
32 Bergwitz C, Gardella TJ, Flannery MR, Potts JT Jr, Kronenberg HM, Goldring SR, *et al*. Full activation of chimeric receptors by hybrids between parathyroid hormone and calcitonin. Evidence for a common pattern of ligand-receptor interaction. J Biol Chem 1996; 271: 26469–72.
33 Stroop SD, Kuestner RE, Serwold TF, Chen L, Moore EE. Chimeric human calcitonin and glucagon receptors reveal two dissociable calcitonin interaction sites. Biochemistry 1995; 34: 1050–7.
34 Holtmann MH, Hadac EM, Miller LJ. Critical contributions of amino-terminal extracellular domains in agonist binding and activation of secretin and vasoactive intestinal polypeptide receptors. Studies of chimeric receptors. J Biol Chem 1995; 270: 14394–8.
35 Laburthe M, Couvineau A, Marie JC. VPAC receptors for VIP and PACAP. Receptors Channels 2002; 8: 137–53.
36 Beyermann M, Rothemund S, Heinrich N, Fechner K, Furkert J, Dathe

M, *et al*. A role for a helical connector between two receptor binding sites of a long-chain peptide hormone. J Biol Chem 2000; 275: 5702–9.
37 Norman DG, Barlow PN, Baron M, Day AJ, Sim RB, Campbell ID. Three-dimensional structure of a complement control protein module in solution. J Mol Biol 1991; 219: 717–25.
38 Parthier C, Reedtz-Runge S, Rudolph R, Stubbs MT. Passing the baton in class B GPCRs: peptide hormone activation via helix induction? Trends Biochem Sci 2009; 34: 303–10.
39 Pioszak AA, Harikumar KG, Parker NR, Miller LJ, Xu HE. Dimeric arrangement of the parathyroid hormone receptor and a structural mechanism for ligand-induced dissociation. J Biol Chem 2010; 285: 12435–44.
40 Gurevich VV, Gurevich EV. How and why do GPCRs dimerize? Trends Pharmacol Sci 2008; 29: 234–40.
41 Pin JP, Kniazeff J, Liu J, Binet V, Goudet C, Rondard P, *et al*. Allosteric functioning of dimeric class C G-protein-coupled receptors. FEBS J 2005; 272: 2947–55.
42 Fotiadis D, Jastrzebska B, Philippsen A, Muller DJ, Palczewski K, Engel A. Structure of the rhodopsin dimer: a working model for G-protein-coupled receptors. Curr Opin Struct Biol 2006; 16: 252–9.
43 Fung JJ, Deupi X, Pardo L, Yao XJ, Velez-Ruiz GA, Devree BT, *et al*. Ligand-regulated oligomerization of beta(2)-adrenoceptors in a model lipid bilayer. EMBO J 2009; 28: 3315–28.
44 Hern JA, Baig AH, Mashanov GI, Birdsall B, Corrie JE, Lazareno S, *et al*. Formation and dissociation of M1 muscarinic receptor dimers seen by total internal reflection fluorescence imaging of single molecules. Proc Natl Acad Sci U S A 2010; 107: 2693–8.
45 Harikumar KG, Pinon DI, Miller LJ. Transmembrane segment IV contributes a functionally important interface for oligomerization of the Class II G protein-coupled secretin receptor. J Biol Chem 2007; 282: 30363–72.
46 Harikumar KG, Morfis MM, Sexton PM, Miller LJ. Pattern of intra-family hetero-oligomerization involving the G-protein-coupled secretin receptor. J Mol Neurosci 2008; 36: 279–85.
47 Harikumar KG, Morfis MM, Lisenbee CS, Sexton PM, Miller LJ. Constitutive formation of oligomeric complexes between family B G protein-coupled vasoactive intestinal polypeptide and secretin receptors. Mol Pharmacol 2006; 69: 363–73.
48 Seck T, Baron R, Horne WC. The alternatively spliced deltae13 transcript of the rabbit calcitonin receptor dimerizes with the C1a isoform and inhibits its surface expression. J Biol Chem 2003; 278: 23085–93.
49 Kraetke O, Wiesner B, Eichhorst J, Furkert J, Bienert M, Beyermann M. Dimerization of corticotropin-releasing factor receptor type 1 is not coupled to ligand binding. J Recept Signal Transduct Res 2005; 25: 251–76.
50 Maurel D, Comps-Agrar L, Brock C, Rives ML, Bourrier E, Ayoub MA, *et al*. Cell-surface protein-protein interaction analysis with time-resolved FRET and snap-tag technologies: application to GPCR oligomerization. Nat Methods 2008; 5: 561–7.
51 Mesleh MF, Shirley WA, Heise CE, Ling N, Maki RA, Laura RP. NMR structural characterization of a minimal peptide antagonist bound to the extracellular domain of the corticotropin-releasing factor1 receptor. J Biol Chem 2007; 282: 6338–46.
52 Inooka H, Ohtaki T, Kitahara O, Ikegami T, Endo S, Kitada C, *et al*. Conformation of a peptide ligand bound to its G-protein coupled receptor. Nat Struct Biol 2001; 8: 161–5.
53 Neumann JM, Couvineau A, Murail S, Lacapere JJ, Jamin N, Laburthe M. Class-B GPCR activation: is ligand helix-capping the key? Trends Biochem Sci 2008; 33: 314–9.
54 Shimizu N, Guo J, Gardella TJ. Parathyroid hormone (PTH)-(1–14) and -(1–11) analogs conformationally constrained by alpha-aminoisobutyric acid mediate full agonist responses via the juxtamembrane region of the PTH-1 receptor. J Biol Chem 2001; 276: 49003–12.
55 Lewis K, Li C, Perrin MH, Blount A, Kunitake K, Donaldson C, *et al*. Identification of urocortin III, an additional member of the corticotropin-releasing factor (CRF) family with high affinity for the CRF2 receptor. Proc Natl Acad Sci U S A 2001; 98: 7570–5.
56 Usdin TB, Hoare SR, Wang T, Mezey E, Kowalak JA. TIP39: a new neuropeptide and PTH2-receptor agonist from hypothalamus. Nat Neurosci 1999; 2: 941–3.
57 Hoare SR, Clark JA, Usdin TB. Molecular determinants of tuberoinfundibular peptide of 39 residues (TIP39) selectivity for the parathyroid hormone-2 (PTH2) receptor. N-terminal truncation of TIP39 reverses PTH2 receptor/PTH1 receptor binding selectivity. J Biol Chem 2000; 275: 27274–83.
58 Abraham-Nordling M, Persson B, Nordling E. Model of the complex of Parathyroid hormone-2 receptor and Tuberoinfundibular peptide of 39 residues. BMC Res Notes 2010; 3: 270.
59 Grammatopoulos DK, Randeva HS, Levine MA, Katsanou ES, Hillhouse EW. Urocortin, but not corticotropin-releasing hormone (CRH), activates the mitogen-activated protein kinase signal transduction pathway in human pregnant myometrium: an effect mediated via R1alpha and R2beta CRH receptor subtypes and stimulation of Gq-proteins. Mol Endocrinol 2000; 14: 2076–91.
60 Brar BK, Chen A, Perrin MH, Vale W. Specificity and regulation of extracellularly regulated kinase1/2 phosphorylation through corticotropin-releasing factor (CRF) receptors 1 and 2beta by the CRF/urocortin family of peptides. Endocrinology 2004; 145: 1718–29.
61 Lefkowitz RJ, Shenoy SK. Transduction of receptor signals by beta-arrestins. Science 2005; 308: 512–7.
62 Gesty-Palmer D, Chen M, Reiter E, Ahn S, Nelson CD, Wang S, *et al*. Distinct beta-arrestin- and G protein-dependent pathways for parathyroid hormone receptor-stimulated ERK1/2 activation. J Biol Chem 2006; 281: 10856–64.
63 Gesty-Palmer D, Flannery P, Yuan L, Corsino L, Spurney R, Lefkowitz RJ, *et al*. A beta-arrestin-biased agonist of the parathyroid hormone receptor (PTH1R) promotes bone formation independent of G protein activation. Sci Transl Med 2009; 1: 1ra1.
64 Hoare SR. Mechanisms of peptide and nonpeptide ligand binding to Class B G-protein-coupled receptors. Drug Discov Today 2005; 10: 417–27.
65 Poyner DR, Sexton PM, Marshall I, Smith DM, Quirion R, Born W, *et al*. International Union of Pharmacology. XXXII. The mammalian calcitonin gene-related peptides, adrenomedullin, amylin, and calcitonin receptors. Pharmacol Rev 2002; 54: 233–46.
66 Kusano S, Kukimoto-Niino M, Akasaka R, Toyama M, Terada T, Shirouzu M, *et al*. Crystal structure of the human receptor activity-modifying protein 1 extracellular domain. Protein Sci 2008; 17: 1907–14.
67 Dangoor D, Biondi B, Gobbo M, Vachutinski Y, Fridkin M, Gozes I, *et al*. Novel glycosylated VIP analogs: synthesis, biological activity, and metabolic stability. J Pept Sci 2008; 14: 321–8.
68 Knudsen LB, Nielsen PF, Huusfeldt PO, Johansen NL, Madsen K, Pedersen FZ, *et al*. Potent derivatives of glucagon-like peptide-1 with pharmacokinetic properties suitable for once daily administration. J Med Chem 2000; 43: 1664–9.
69 Langer I, Gregoire F, Nachtergael I, De Neef P, Vertongen P, Robberecht P. Hexanoylation of a VPAC2 receptor-preferring ligand markedly increased its selectivity and potency. Peptides 2004; 25:

275–8.

70 Xiao Q, Giguere J, Parisien M, Jeng W, St-Pierre SA, Brubaker PL, *et al*. Biological activities of glucagon-like peptide-1 analogues *in vitro* and *in vivo*. Biochemistry 2001; 40: 2860–9.

71 Spyroulias GA, Papazacharias S, Pairas G, Cordopatis P. Monitoring the structural consequences of Phe12 → D-Phe and Leu15 → Aib substitution in human/rat corticotropin releasing hormone. Implications for design of CRH antagonists. Eur J Biochem 2002; 269: 6009–19.

72 Gault VA, Kerr BD, Irwin N, Flatt PR. C-terminal mini-PEGylation of glucose-dependent insulinotropic polypeptide exhibits metabolic stability and improved glucose homeostasis in dietary-induced diabetes. Biochem Pharmacol 2008; 75: 2325–33.

73 Gallwitz B. The evolving place of incretin–based therapies in type 2 diabetes. Pediatr Nephrol 2010; 25: 1207–17.

74 Teichman SL, Neale A, Lawrence B, Gagnon C, Castaigne JP, Frohman LA. Prolonged stimulation of growth hormone (GH) and insulin-like growth factor I secretion by CJC-1295, a long-acting analog of GH-releasing hormone, in healthy adults. J Clin Endocrinol Metab 2006; 91: 799–805.

75 Chunxiao W, Jingjing L, Yire X, Min D, Zhaohui W, Gaofu Q, *et al*. Study on preparation and activity of a novel recombinant human parathyroid hormone(1–34) analog with N-terminal Pro-Pro extension. Regul Pept 2007; 141: 35–43.

76 Underwood CR, Garibay P, Knudsen LB, Hastrup S, Peters GH, Rudolph R, *et al*. Crystal structure of glucagon-like peptide-1 in complex with the extracellular domain of the glucagon-like peptide-1 receptor. J Biol Chem 2010; 285: 723–30.

Acta Pharmacologica Sinica (2012) 33: 312–323
 1671-4083/12 $32.00
www.nature.com/aps

Review

Structure and ligand recognition of class C GPCRs

Lei CHUN, Wen-hua ZHANG, Jian-feng LIU*

Sino-France Laboratory for Drug Screening, Key Laboratory of Molecular Biophysics of Ministry of Education, College of Life Science and Technology, Huazhong University of Science and Technology, Wuhan 430074, China

The G-protein-coupled receptors (GPCRs) are one of the largest super families of cell-surface receptors and play crucial roles in virtually every organ system. One particular family of GPCRs, the class C GPCRs, is distinguished by a characteristically large extracellular domain and constitutive dimerization. The structure and activation mechanism of this family result in potentially unique ligand recognition sites, thereby offering a variety of possibilities by which receptor activity might be modulated using novel compounds. In the present article, we aim to provide an overview of the exact sites and structural features involved in ligand recognition of the class C GPCRs. Furthermore, we demonstrate the precise steps that occur during the receptor activation process, which underlie the possibilities by which receptor function may be altered by different approaches. Finally, we use four typical family members to illustrate orthosteric and allosteric sites with representative ligands and their corresponding therapeutic potential.

Keywords: structure; ligands; G-protein-coupled receptors (GPCRs); orthosteric sites; allosteric sites; allosteric modulators

Acta Pharmacologica Sinica (2012) 33: 312–323; doi: 10.1038/aps.2011.186; published online 30 Jan 2012

Introduction

The G-protein-coupled receptors (GPCRs) form the largest class of cell surface receptors and play a major role in cellular perception of the environment[1]. GPCRs are sensitive to a diverse range of ligands that include light (photons), ions, amino acids and large proteins, and they represent an important market for pharmaceutical companies. Approximately 50 GPCRs are estimated to be targeted by nearly half of the currently marketed drugs, and at least 300 GPCRs remain to be exploited[2]. Intense efforts have been devoted to screening new GPCR ligands that display high potential as drug leads. However, for many GPCRs, such efforts have failed to yield viable drug candidates. Numerous issues prohibit traditional GPCR-targeted drug discovery. For instance, ligands screened by traditional techniques usually act on GPCR orthosteric sites. The conserved characteristics of the orthosteric sites make it difficult to achieve high selectivity for specific GPCR subtypes. Furthermore, the persistent treatment regime of orthosteric ligands often leads to potent side effects and tolerance to the drugs. In addition, for some GPCRs, such as peptide or protein receptors, it is inherently difficult to design synthetic orthosteric ligands. Therefore, the pharmaceutical industry is searching for alternative approaches to identify new modulators of GPCRs. The determination of GPCR structures, mechanisms and ways in which to modulate these properties are therefore of critical importance.

The GPCRs can be classified into five families based on the sequence phylogeny of a conserved heptahelical transmembrane domain (7TM)[3]. Among these families, class C GPCRs are defined by two unique structural features: first, they possess a large extracellular domain that is distal to the 7TM and contains the orthosteric sites; second, they form constitutive dimers with unique activation modes compared with other classes of GPCRs[4]. Class C GPCRs are composed of metabotropic glutamate receptors (mGlu receptors), γ-aminobutyric acid$_B$ receptors (GABA$_B$ receptors), Ca^{2+}-sensing receptors (CaS receptors), sweet and amino acid taste receptors, pheromone receptors, odorant receptors in fish and several orphan receptors[3]. mGlu, GABA$_B$, and CaS receptors represent an important new class of therapeutic targets that are integral to disorders that affect the central neural system (CNS) and calcium homeostasis[4, 5]. The taste receptors, on the other hand, attract significant attention from food companies because the taste additives that target these receptors represent a key feature of the large food industry market[5].

The recently identified class C GPCRs have been targeted by only two therapeutic drugs currently on the market[6]. By contrast, in recent years there have been tremendous advances in the discovery of allosteric modulators of class C GPCRs, most likely as a result of the existence of multiple modula-

* To whom correspondence should be addressed.
E-mail jfliu@mail.hust.edu.cnn
Received 2011-10-07 Accepted 2011-12-09

tion sites for various ligands[7]. Cinacalcet, one of the first two allosteric modulators of GPCRs on the market, targets the CaS receptor[5]. This review focuses on the structural features that are involved in ligand recognition by class C GPCRs. The possibilities of modulating receptor function through different types of ligands are then discussed. Finally, representative ligands and the associated sites of four typical family members that contain therapeutic potential are reviewed in detail. The ligands described in this review are small chemical molecules. Peptide ligands, such as antibodies, are not discussed.

Representative family members

L-Glutamate serves as the neurotransmitter at the majority of excitatory synapses in the mammalian CNS. As the metabotropic receptors for glutamate, mGlu receptors participate in the modulation of synaptic transmission and neuronal excitability throughout the CNS[8, 9]. The mGlu receptors are sub-classified into three groups based on sequence homology, G-protein coupling, and ligand selectivity[9]. Group I (mGlu1 and 5) couple to Gq/G11 and activate phospholipase Cβ, resulting in the hydrolysis of phosphoinositides and the generation of inositol 1,4,5-trisphosphate (IP3) and diacylglycerol, whereas Group II (mGlu 2 and 3) and Group III (mGlu 4, 6, 7, and 8) couple predominantly to Gi/o, which inhibits adenylyl cyclase and directly regulates ion channels and other downstream signaling partners via the liberation of Gβγ subunits[10]. The widespread expression of mGlu receptors makes these receptors particularly attractive drug targets, and recent studies continue to validate the therapeutic utility of mGlu receptor ligands in neurological and psychiatric disorders, such as Parkinson's disease[11], Fragile X syndrome[12], Alzheimer's disease[13], anxiety, and schizophrenia[14].

GABA is a major inhibitory neurotransmitter in the mammalian CNS. As the metabotropic receptor for GABA, $GABA_B$ receptor mediates slow and prolonged synaptic inhibition[15]. The $GABA_B$ receptor functions as an obligate heterodimer of two subtypes, $GABA_{B1}$ and $GABA_{B2}$[16, 17]. $GABA_{B1}$ contains the GABA binding site[18], while $GABA_{B2}$ is responsible for Gi/o protein activation[19]. In addition to a role in neuronal excitability and plasticity, $GABA_B$ receptor may promote neuron survival under conditions of metabolic stress[20], ischemia[21], or apoptosis[22]. This receptor is a promising target for the treatment of many diseases, including spasticity, neuropathic pain[23], drug addiction, schizophrenia, anxiety, depression and epilepsy[24, 25].

The CaS receptor is a unique class C GPCR that can be activated by ions without the cooperation of other ligands[4]. This receptor is highly sensitive to a very slight change in extracellular Ca^{2+} concentrations, which ensures its significant role in regulating calcium homeostasis[26]. The CaS receptor is involved in several disorders, including hyperparathyroidism, osteoporosis and different forms of hypocalcemia[26–28]. The clinical success of Cinacalcet indicates that more efforts should be devoted to the discovery of novel ligands that modulate CaS receptor activation.

The class C GPCRs contain three taste receptor subunits (T1R1, T1R2, and T1R3) that form two heterodimers, the sweet receptor (T1R2/T1R3) and the umami receptor (T1R1/T1R3)[29, 30]. Only *cis* activation occurs within the sweet and umami taste receptors, which means T1R2 in the sweet receptor or T1R1 in the umami receptor are involved in both orthosteric ligand recognition and in G protein activation, whereas the common subunit T1R3 loses the corresponding function[31]. In addition to natural sugars, the sweet taste receptor is also sensitive to artificial sweeteners, sweet proteins and some *D*-amino acids. In most mammals, the umami receptor can be activated by *L*-amino acids, whereas the human orthologue is only sensitive to monosodium glutamate and *L*-aspartate. Flavor enhancers, such as purine nucleotides, have the ability to potentiate umami receptor function. These artificial sweeteners and flavor enhancers represent a large food sector market[6].

Structural features of class C GPCRs

Class C GPCRs are composed of an exceptionally large extracellular domain, a heptahelical transmembrane domain and an intracellular carboxyl-terminal (C-terminal) domain (Figure 1A). One distinct structural feature of class C GPCRs is the extracellular domain that contains a Venus flytrap (VFT) module and a cysteine rich domain (CRD, except in the $GABA_B$ receptor). The 7TM domain is conserved among all GPCRs with the exception that class C GPCR 7TMs contain only the allosteric sites. The orthosteric sites are contained within the VFT. The C-terminal tail of class C GPCRs is a highly variable domain and plays a role in scaffolding and signaling protein coupling[3]. All the domains except for the intracellular C-terminal domain provide plentiful ligand action sites. The other unique characteristic of class C GPCRs is their mandatory dimerization, either as homodimers (mGlu and CaS receptors) or heterodimers ($GABA_B$ receptor and T1Rs) (Figure 1B). The allosteric interaction between different dimer domains results in a particularly complicated activation process.

Extracellular domain

Venus flytrap module

The VFTs of class C GPCRs share sequence and structural similarity with bacterial periplasmic binding proteins (PBPs)[31]. A generally accepted hypothesis is that the fusion of an ancestral rhodopsin-like receptor and a PBP formed the common ancestor of the class C GPCRs[3]. Additional detailed phylogenetic analysis of VFTs from four typical groups of class C GPCRs reveals that functional divergence involved positive selection and is partially responsible for the evolutionary patterns of the VFTs (Figure 2)[32]. The functionally divergent sites could represent potential drug targets that participate in ligand recognition.

Among class C GPCRs, the VFT of the mGlu1 receptor is the first for which a crystal structure was solved, both in the absence and presence of its orthosteric ligands (Figure 1C)[33]. The crystal structure of VFT revealed a bilobate domain with two lobes being separated by a cleft in which endogenous

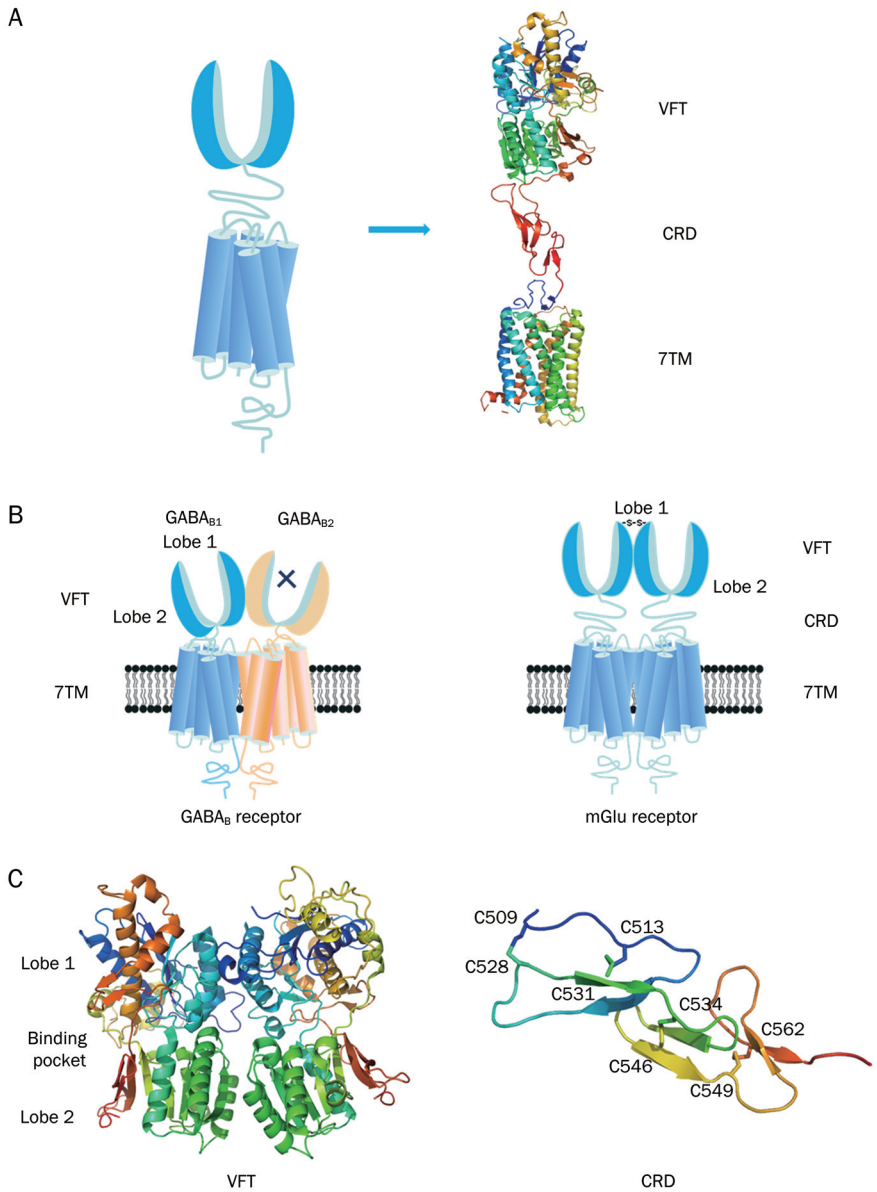

Figure 1. Schematic structure of class C GPCRs. (A) Structural organization of class C GPCRs. Class C GPCRs have a common structure consisting of a VFT with two lobes (lobe 1 and lobe 2) separating by a cleft as orthosteric site, a 7TM and a CRD for all but $GABA_B$ receptor. The crystal structure of mGlu3 receptor (PDB ID 2E4W) was used for the VFT and CRD. The bovine rhodopsin crystal structure (PDB ID 1GZM) was used for the 7TM. (B) Schematic representation of two prototypical class C GPCRs as heterodimer ($GABA_B$ receptor), or homodimer (mGlu receptor).For $GABA_B$ receptor, the VFT is directly linked to the 7TM. Two subunits, $GABA_{B1}$ and $GABA_{B2}$, form an obligatory heterodimer. $GABA_{B1}$ is responsible for endogenous ligands binding, while $GABA_{B2}$ is responsible for G protein activating. For mGlu receptors, the VFT connects to the 7TM via CRD. mGlu receptors form homodimers which could offer two orthosteric sites per dimer. (C) The determined cystal structure for the VFT and CRD. The first solved structure is the VFT of mGlu1 receptor (PDB ID 1EWK), which shows that the VFT oscillates between an open and a closed conformation. The crystal structure of whole extracellular domain including the VFT and CRD (PDB ID 2E4W) has been solved firstly in mGlu3 receptor.

ligands bind[33, 34]. The VFT oscillates between an open and closed conformation in the absence of bound ligand. In the presence of ligand, glutamate interacts with lobe 1 in the open form of the VFT and then stabilizes a closed form through additional contacts with lobe 2. Competitive antagonists inhibit receptor activation by preventing VFT closure[35], whereas locking the VFT in a closed conformation with an artificial disulfide bond results in a constitutively active receptor[36].

VFTs form constitutive dimers. Based on the crystal structure and mutational analysis of mGlu1 VFTs, the hydrophobic interaction between lobe 1 of each monomer is the main driving force for VFT dimerization[37, 38]. Additionally, a disulfide bond linking the two VFTs was demonstrated to stabilize this dimer[37, 39, 40]. Similar to mGlu receptors, lobe 1 from each of the two hetero-subunits of the $GABA_B$ receptor, $GABA_{B1}$ and $GABA_{B2}$, mediates subunit interaction[41, 42]. The lobe 1 N-glycan, which is located at the interface of either $GABA_{B1}$ or $GABA_{B2}$, prevents receptor heterodimerization and cell surface trafficking[42].

Cysteine rich domain (CRD)

For most class C GPCRs (except for the $GABA_B$ receptor), the VFT and 7TM are connected by the CRD. The CRD is a roughly 80 amino acid segment that contains nine completely conserved cysteines[3]. The crystal structure of the complete extracellular domain of the mGlu3 receptor was solved in 2007 (Figure 1C)[43]. Based on this structure, the CRD forms an independent domain with a length of 40 Å, which physically separates the VFT and the 7TM. The CRD plays an important role in receptor activation of the mGlu receptors, CaS receptors and sweet taste receptors with subunit T1R3[44, 45]. In mGlu-like receptors, a conserved disulfide bridge between the VFT and the CRD is required for the allosteric interaction between

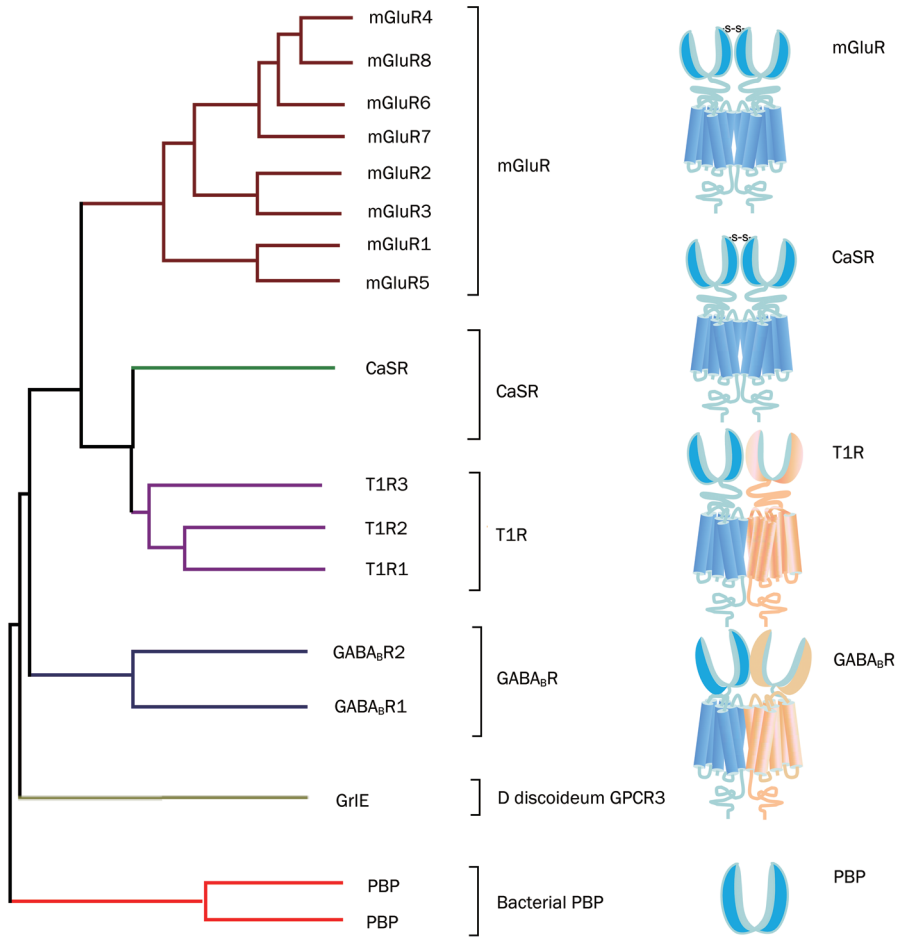

Figure 2. The bootstrap tree of the prototypical members from human class C GPCRs. The sequence of the VFT were aligned using the default parameters and the homologous bacterial PBPs were used as an outgroup to root the trees. Class C GPCRs form obligatory dimers. Homodimers (mGluR and CaSR) linked by a disulfide bond between their VFTs, while heterodimers (GABA$_B$R and T1R) are not covalently linked.

the VFT and the 7TM. Mutation of this disulfide bond abolished agonist-induced activation of the mGlu receptors[46].

Heptahelical transmembrane domain (7TM)

Similar to other GPCRs, class C GPCRs possess heptahelical transmembrane helices that are linked by three short intra- (iloops) and extracellular loops, which are always smaller than 30 residues. Despite the low primary sequence similarity, several similar 3D structural features of the 7TM exist between the class C GPCRs and the rhodopsin-like receptors, including the conserved disulfide bond that connects the top of TM3 and the second extracellular loop, the central position of TM3, the 8th helix following the 7TM that is related to G-protein coupling as well as several conserved residues[3].

In contrast to rhodopsin-like GPCRs, the 7TM of class C GPCRs does not participate in ligand recognition or binding. However, this domain in class C GPCRs still contains a conserved binding pocket that corresponds to the orthosteric sites of rhodopsin-like GPCRs[47]. This binding pocket represents a site where many synthetic molecules could potentially bind and modulate receptor activity.

Activation mechanism and approaches for modulating activity

Binding of competitive agonist to the VFT induces a series of conformational changes in all of the domains and activates the G-protein. This activation mechanism is particularly complicated as a result of the constitutive dimerization of this family. The dimeric receptor contains four or six independent domains in which allosteric interactions occur between each neighboring pair such that a conformational change in one domain will facilitate changes in others. For a long time, how the different domains work together to activate the coupled effectors remained poorly understood. The main hindrance in investigating this issue stems from difficulties in solving the receptor structure in the presence and absence of agonist. In 2000, the first crystal structures of the mGlu1 receptor broke this barrier. These structures revealed the dynamics of the VFT and mechanism of modulation by glutamate. A subsequent study in 2002 reported the structure of the mGlu1 receptor in the presence of an antagonist (MCPG) or an allosteric modulator (Gd^{3+}). However, the structure of the 7TM domain remains unsolved, and details of the conformational change of the complete receptor in response to stimulation remain elusive. Our current knowledge regarding the activation process relies mainly on bioinformatic analyses, mutation constructs and advanced functional techniques. In general, the activation progress of class C GPCRs includes the following three sequential events: 1) a competitive agonist binds to one VFT in the dimer and stabilizes the closed conformation; 2) the VFT in

the closed conformation transduces the activation signal to the 7TM directly or via the CRD; 3) the rearranged 7TM activates the G protein.

Ligand recognition by VFT

Crystal structure analysis of the mGlu1 receptor revealed that agonist binding induces rearrangement of the dimeric VFTs[33, 34]. In the resting state (R), lobes 2 of each monomer are far away from one another and the dimeric VFTs are in an open conformation. In the active state (A), lobe 2 from each monomer moves close enough to contact each other, while the dimeric VFTs are stabilized in a closed conformation in response to binding of a competitive agonist. Consistent with the above model, N-glycan wedge scanning in the $GABA_B$ receptor revealed that the interaction and relative movement of lobe 2 from each monomer is important for agonist affinity and receptor activation[42].

Constitutive dimerization ensures that each receptor dimer contains two orthosteric sites in most cases. However, according to mutational analysis in mGlu receptors, one ligand is sufficient to activate the receptor dimer[48]. That is, a ligand binding to one subunit leads to the closure of one VFT and Aco (Active/closed open) conformation is sufficient to stabilize the active conformation of the receptor. Although the Acc (Active/close close) conformation with two bound agonists has higher activation efficacy, a cation such as Gd^{3+} is needed to stabilize this conformation. In the absence of a cation, electrostatic repulsion between lobe 2 from each monomer would make this conformation drastically unstable[34].

Activating signal transduction from the VFT to the 7TM

Because the VFT and the 7TM of class C GPCRs are relatively independent domains, transduction of the activating signal from the VFT to the 7TM is a crucial step in receptor activation, despite the fact that many details remain to be defined. For mGlu-like receptors, the CRD plays a central role in transmitting the activating signal from the VFT to the 7TM. A conserved disulfide bond between the VFT and the CRD is indispensable for the allosteric interaction between the two domains[46]. Furthermore, a recent observation showed that ligand binding to the VFT triggers the relative movement of two CRDs during receptor activation. The introduction of an inter-subunit disulfide bond between the two CRDs in the receptor dimer stabilized the active conformation[49]. For the $GABA_B$ receptor, which lacks the CRD, it is most likely that the VFT directly interacts with the 7TM, independent of the short linker between them[19].

The model that one VFT is capable of activating one receptor dimer raises the question of whether the closed VFT domain activates the 7TM domain in the same subunit (*cis*-activation) or the closed VFT activates the 7TM of the other subunit (*trans*-activation). Recently, it has been demonstrated that the 7TM of the obligatory heterodimeric $GABA_B$ receptor can be directly *trans*-activated either by the $GABA_{B1}$ VFT and 7TM or by the dimeric VFTs formed by $GABA_{B1}$ and $GABA_{B2}$[50]. In contrast, only *cis*-activation occurs in the T1R receptor[31]. The activation mechanism of homodimeric receptors with two orthosteric sites is difficult to study. The results for mGlu-like receptors showed that both *cis*- and *trans*-activation occur in the mGlu receptor activation mechanism[51].

G-protein activation by 7TM

Due to the difficulties in transmembrane protein research, no crystal structures of the 7TM domain of any class C GPCR have been determined. There is no direct data to indicate that a conformational change in the 7TM occurs during receptor activation. Bioinformatic and mutational analyses suggest that the 7TM oscillates between various active and inactive conformations[46, 47]. FRET detection of the conformational change in the iloops of the mGlu1 receptor demonstrated that agonist binding induces iloop2 from each monomer in the dimeric 7TMs to move apart from each other, implying that the dimeric 7TMs rotate away from the interface during the activation process[52-54].

Chimeric constructs and mutational analyses indicate that the C-terminal end of the Gα subunit lies within a cavity formed by iloop 2 and 3 in class C GPCRs[55]. In addition, the 8th helix also plays a role in G-protein coupling[55, 56]. Finally, it is important to mention that the highly conserved and unusually short iloop 3 of class C GPCRs plays an equivalent role to that of iloop 2 in rhodopsin-like receptors[57].

Ligand recognition sites

Class C GPCRs contain multiple ligand interaction sites as a result of their particularly complicated structure and activation mechanism. These ligand binding sites are divided into two groups: orthosteric and allosteric binding sites. The endogenous ligand binding sites, or orthosteric sites, reside in the VFT domain. Both competitive agonists and antagonists interact with this site and induce significant conformational changes in the VFT: binding of a full agonist stabilizes a closed conformation[35], whereas binding of competitive antagonists stabilizes an open conformation[33, 34, 43]. Binding of partial agonists results in a partial or a complete, yet unstable, closure of the VFT domain[35, 58]. In contrast, the allosteric sites are topographically distinct from the orthosteric sites in any given receptor. The binding of allosteric modulators changes the receptor conformation and, thereby, the affinities and/or efficacies of orthosteric ligands. In general, the positive allosteric modulators (PAMs) facilitate the action of the orthosteric agonists, whereas the negative allosteric modulators (NAMs) block the activation of orthosteric agonists by stabilizing the 7TM in an inactive conformation. The large extracellular domain and constitutive dimerization of class C GPCRs provide more potential allosteric sites compared with other GPCRs. To date, there are three groups of allosteric sites in class C GPCRs that have been reported (Figure 3).

7TM allosteric sites

Due to the existence of the large extracellular domain, the 7TM of class C GPCRs lacks an orthosteric site, which instead is located within the VFT. However, the binding pocket

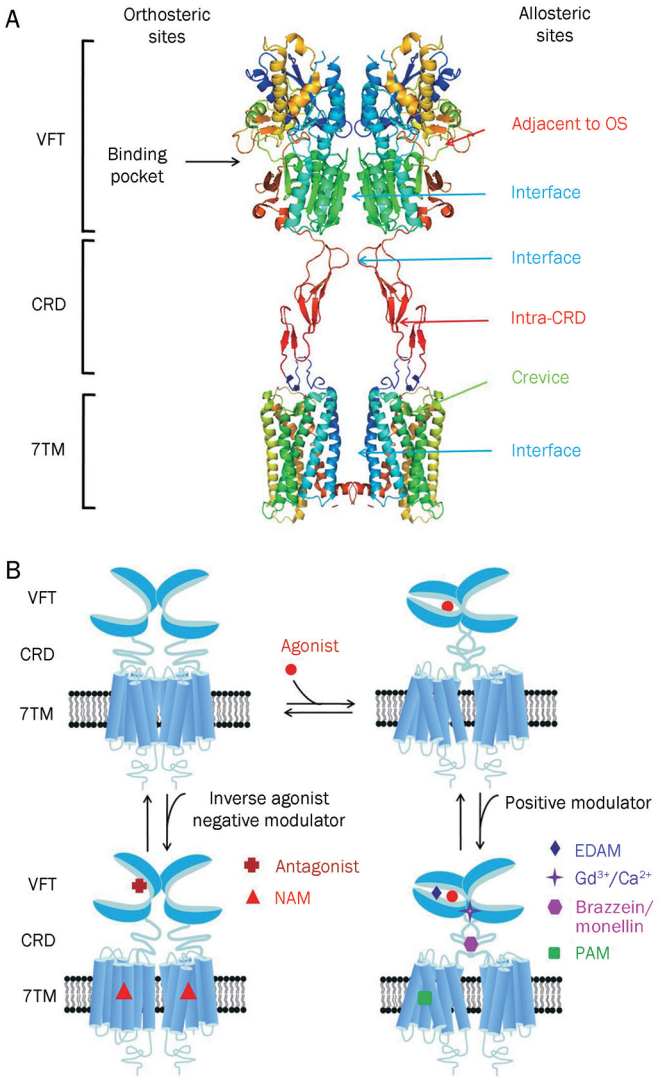

Figure 3. Great variety of ligands to modulate class C GPCRs function. (A) Schematic model of orthosteric sites and allosteric sites in mGlu-like receptor. There are four groups of allosteric sites in class C GPCR: sites in the 7TM, which have been studied extensively; sites in the extracellular domain including VFT and CRD and sites in the interface between VFT, CRD and 7TM, the latter two open the new possibilities to modulate activity of mGlu receptors. The structure model was built according to the crystal structure of mGlu3 VFT and CRD (PDB ID 2E4W) and the crystal structure of bovine rhodopsin 7TM (PDB ID 1GZM). (B) Modulation mechanism of various ligands on the function of homodimeric class C GPCRs. The orthosteric agonists promote the VFT closure while the antagonists prevent it. The extracellular domain allosteric modulators (EDAM) bind to a site adjacent to the orthosteric site and increase the agonist effect. The Gd^{3+} ion binds to the interface of the lobe 2 of the VFTs and stabilizes the full active conformation when both VFTs are closed. The sweet proteins brazzein or monellin interact on the CRD of human T1R3 and increase the agonist effect. The typical PAMs or NAMs bind to the 7TM and stabilize the active or inactive conformation of 7TM, respectively.

is conserved and is formed by residues in TM3, 5, 6, and 7, which correspond to orthosteric sites within the 7TM of rhodopsin-like receptors[3, 59]. Many allosteric modulators for class C GPCRs have been demonstrated to bind in this pocket. Homology modeling, docking analysis and mutagenesis studies have shown that nine conserved amino acid residues in the 7TM of T1R3 are involved in allosteric modulator binding. The corresponding residues have also been found in the 7TM of CaS[60-63] and mGlu receptors[64–66]. This implies that class C GPCRs share a common binding site for allosteric modulators. Distinct from this common binding pocket, there are several other allosteric sites located in the 7TM of class C GPCRs. Taken together, the main group of allosteric sites in class C GPCRs resides in the 7TM. Most allosteric modulators that have been described for class C GPCRs interact with this domain.

VFT allosteric sites adjacent to orthosteric sites

Recently, the VFT binding pocket was shown to be large enough to accommodate both orthosteric and allosteric sites, which are adjacent to each other but do not overlap. Small molecules binding to this allosteric site could cooperate with endogenous ligand to stabilize the closed conformation of the VFT. These small molecules are new allosteric modulators and are called extracellular domain allosteric modulators (EDAM). To date, there are three groups of EDAMs and their corresponding sites have been identified: IMP to the T1R1 VFT of the umami taste receptor[31], SE-2/SE-3 to the T1R2 VFT of the sweet taste receptor[67] and the (R)-PCEP derivatives with long alkyl chains to the VFT of the mGlu4 receptor[68, 69].

Allosteric sites located at the interfaces between the VFT, CRD and 7TM

Constitutive dimerization plays a crucial role in the activation of class C GPCRs so the sites involved in dimerization represent another group of allosteric sites. In the Acc conformation of the mGlu1 receptor, electrostatic repulsion from the four adjacent negatively charged residues Glu233 and Glu238 (and the analogous residues in the dimeric VFTs) makes the active conformation unstable. The introduction of a cation, such as Gd^{3+} or Ca^{2+}, can neutralize this electrostatic repulsion and stabilize the active conformation. It was shown that the Gd^{3+} ion binds at the interface between lobe 2 of the VFTs[34]. Therefore, the interface of the dimeric VFT constitutes a group of allosteric sites.

Recent data show that the relative movement of dimeric CRDs is potentially involved in the mGlu receptor activation process[49], so this region could represent another allosteric site. In support of this hypothesis, Jiang *et al* identified 10 residues in the CRD of human T1R3 and the hinge region of T1R2 that play an important role in the effect of sweet proteins, such as brazzein[45].

Ligand binding sites of four typical class C GPCR family members

So far, there are only two therapeutic drugs that target class C GPCRs on the market: Baclofen, an agonist targeting the $GABA_B$ receptor, and Cinacalcet, an allosteric modulator tar-

geting the CaS receptor. The former represents a conventional orthosteric drug, while the latter represents a novel allosteric modulator. Allosteric modulators currently attract significant attention because they offer important advantages over orthosteric drugs. First, they often have no effect on their own and act in concert with physiological receptor activation, which results in fewer side effects and a decreased propensity for desensitization; second, their binding sites do not undergo selective pressure so they display a higher subtype selectivity; third, multiple allosteric sites make it easy to synthesize novel molecules that exhibit increased bioavailability and desirable pharmacokinetic properties. Diverse allosteric modulators have been identified for class C GPCRs as a result of their plentiful allosteric sites and the numerous possibilities to modulate their function by acting on multiple steps during the activation process (Table 1).

Taste receptors — multiplicity of various ligand-binding sites

A unique characteristic of taste receptors is their diversity of ligand-binding sites. Aside from the orthosteric sites, there are at least eight allosteric sites that have been identified in taste receptors: the EDAM sites for IMP in T1R1-VFT[31] and for SE-2/SE-3 in T1R2-VFT[67]; the allosteric agonist sites for sweet proteins in T1R3-CRD[45], cyclamate in sweet receptor T1R3 7TM[70], S807 in T1R1 7TM[31] and S819 in T1R2-7TM[31]; the PAM site for cyclamate in the umami receptor T1R3-7TM[70]; and the NAM site for lactisole in both the sweet and umami receptor T1R3-7TM[71]. These sites might represent potential targets for health-related products or drugs to treat diseases, such as hypertension or diabetes.

mGlu receptors — the most promising candidates for clinical applications

The orthosteric sites of mGlu receptor subtypes are the most highly conserved throughout evolution, such that there are almost no orthosteric ligands that display higher selectivity for a given subtype. Moreover, the glutamate-binding pocket strictly selects for agonists with amino acid-like structures, which are notoriously difficult to synthesize and display undesirable pharmacokinetics. By contrast, most of the allosteric modulators for mGlu receptors possess better subtype selectivity as a result of less conserved allosteric sites and better pharmacological properties due to their structural diversity and more extensive lipophilic nature[72].

The first allosteric modulator that was discovered for class C GPCRs is CPCCOEt, which functions as a NAM for the mGlu1 receptor. Numerous allosteric modulators of group I mGlu receptors have since been identified. It has been proposed that the movement of Trp798 in TM6 of mGlu1 (Trp784 at the homologous position in mGlu5) is essential for receptor activation[66]. The PAMs stabilize the active conformation of this group by facilitating the movement of a conserved Trp in TM6, whereas the NAMs prevent the relative movement between TM6 and TM3[66]. For the mGlu5 receptor, most PAMs and NAMs share an overlapping binding pocket that is composed of TM3, 5, 6, and 7[73], except for a small number of distinct sites[74]. For the mGlu1 receptor, however, the PAMs and NAMs bind to distinct sites in the 7TM[64, 65, 75–77], except for a shared site that consists of Val757 in TM3[65, 77]. Removed from the conserved binding pocket, there is a distinct allosteric site located in TM1. An unique PAM for both the mGlu1 and mGlu5 receptors, CPPHA, was shown to bind to this site. Phe585 in TM1 of mGlu5 (Phe599 at the corresponding position in mGlu1) is essential for the recognition of CPPHA[74].

The allosteric modulators of the mGlu5 receptor are leading with regard to the development of pharmaceuticals that target class C GPCRs. Convincing preclinical data have shown a significant effect of several PAMs in schizophrenia[14]. Furthermore, positive clinical results have also been obtained for NAMs in *L*-DOPA-induced tardive dyskinesia in Parkinson's disease[11].

Most allosteric modulators for group II mGlu receptors are PAMs. These modulators provide greater subtype selectivity compared with the agonists, especially in the case of the mGlu2 receptor. Ser688 and/or Gly689 in TM4 and Asn735 in TM5 have been shown to be involved in PAM binding to the mGlu2 receptor[78]. The competitive agonists for group II mGlu receptors display potent activity against anxiety[79] disorders and schizophrenia[80] in clinical trials; however, they are unable to discriminate between the group II subtypes. PAMs with selectivity for the mGlu2 receptor have displayed similar effects as agonists in an animal model[81], which suggests that there is a high possibility for success in clinical trials.

Compared with the modulators that have been described for group I and II mGlu receptors, notably fewer allosteric modulators have been identified that target group III mGlu receptors. It also important to note that some allosteric modulators that target group I mGlu receptors have the opposite effect on group III mGlu receptors. Recently, the mGlu4 receptor has been the focus of significant attention because the corresponding PAMs that target this receptor represent promising novel drugs with which to treat Parkinson's disease[11].

$GABA_B$ receptors — the unique PAM CGP7930

Currently there is only one drug on the market, baclofen, that functions as a competitive agonist towards the $GABA_B$ receptor. Clinical applications over the course of several decades have shown that baclofen is an undesirable antispastic agent due to its potent side effects, unfavorable pharmacokinetic properties and a tendency for patients to develop tolerance to the drug. The newly described allosteric modulators provide opportunities to develop new therapeutic agents for several $GABA_B$ receptor related disorders.

CGP7930 is a typical PAM that was the first to be identified that targets the $GABA_B$ receptor[82]. This PAM can both enhance the potency and the maximal response that is induced by GABA[82]. Radioligand binding experiments suggest that CGP7930 not only promotes agonist affinity to the orthosteric sites but also strengthens the interaction between the $GABA_B$ receptor and the preferred $G\alpha_o$[83]. A growing body of evidence has shown that CGP7930 interacts with the $GABA_{B2}$ 7TM[82]. According to a recently proposed model in which

Table 1. Mapping the prototypical ligands to various sites in class C GPCRs.

Ligand binding sites		Taste receptor		Metabotropic glutamate receptors			$GABA_B$ receptor	CaS receptor
		Sweet receptor	Umami receptor	Group I	Group II	Group III		
VFT	Orthosteric sites	Sucrose or other sugars, sweetners such as aspartame, neotame and saccharides	*L*-amino acids	*L*-glutamate, 3,5-DHPG, Quisqualate	*L*-glutamate, LY354740, LY404039, DCG-IV	*L*-glutamate, ACPT-I, L-SOP, L-AP4 (mGlu4), PPG (mGlu8), DCPG (mGlu8)	GABA, baclofen CGP54626	Ca^{2+}
	Sites for EDAM	SE2, SE3 for T1R2 subunit; Sweet proteins (brazzein or monelllin) for T1R2 subunit	IMP for T1R1 subunit			(R)-PCEP with long alkyl chain for mGlu4	Ca^{2+} binding site ajacetnt to orthosteric site in $GABA_{B1}$ subunit	*L*-amino acids including *L*-phenylalaine and *L*-tryptophan
	Interface			Gd^{3+} ion at the interface of lobe 2				
CRD		Sweet proteins (brazzein or monelllin) for T1R3 subunit						
7TM	Conserved binding pocket	Cyclamate and Lactisole for T1R3 subunit	Cyclamate and Lactisole for T1R3 subunit	EM-TBPC as NAM for mGlu1; CPCCOEt as NAM for mGlu1; Ro-67-7476 as PAM for mGlu1; DFB as PAM for mGlu5; MPEP, fenobam as NAM for mGlu5	LY487379 and BINA as two prototypical PAMs for mGlu2	CPPHA, DFB as NAMs for mGlu4; MPEP, SIB-1893, PHCCC as PAM for mGlu4; AMN082 as allosteric agonist for mGlu7; MDIP, MMPIP as NAMs for mGlu7		Structurally related phenylalkylamine calcimimetics (Cinacalcet in market) and calcilytics
	Other sites within 7TM	S819 for T1R2 subunit	S807 for T1R1 subunit	CPPHA as PAM for mGlu5 or mGlu1 (high concentration)			GS39783 as PAM (within $GABA_{B2}$ 7TM, exact binding site not identified)	Structurally distinct calcilytics
	Interface						CGP7930 as PAM possibly binding the interface in $GABA_{B2}$ subunit	

VFT, Venus Flytrap; CRD, cysteine rich domain; 7TM, heptahelical transmembrane domain; PAM, positive allosteric modulator; NAM, negative allosteric modulator.

agonist binding induces the widening of the cleft between the two 7TMs without changing the helical configuration of each subunit, it is possible that CGP7930 binds at the interface to enhance the separation of the two 7TMs[84]. Interestingly, CGP7930 has been found to function as an independent partial agonist in cAMP assays[85]. We reported for the first time that CGP7930 itself could induce ERK1/2 phosphorylation in cultured cerebellar granule neurons (CGNs)[86]. Furthermore, we found that CGP7930 alone could protect CGNs from apoptosis via transactivation of the insulin-like growth factor 1 (IGF-1) receptor[22]. There is no obvious difference between CGP7930 and GABA or baclofen to explain the function described above[22]. So far, CGP7930 is a unique PAM in that it is the only such modulator that has been reported to exert an independent physiological effect. In addition to CGP7930, a number of PAMs that target the $GABA_B$ receptor have been reported, such as GS39783[87]. Several allosteric agonists have also been synthesized, including rac-BHFF and its analogs[88]. However, no NAMs that target the $GABA_B$ receptor have been described.

It has been reported recently that several amino acids[89, 90] and Ca^{2+} [91, 92] can modulate $GABA_B$ receptor function via a conserved pocket that is located near the orthosteric sites, which is reminiscent of the modulation that has been observed for mGlu-like receptors. Unfortunately, animal models suggest that the existing allosteric modulators for the $GABA_B$ receptor are not suitable for clinical use due to their low potency and unfavorable pharmacokinetic properties[5]. Therefore, it is necessary to identify new allosteric sites on the $GABA_B$ receptor that may lead to the discovery of new types of therapeutic ligands.

CaS receptors — first clinical success

To date, four groups of ligands have been identified for the CaS receptor: the endogenous cations[93], the *L*-amino acids (such as *L*-phenylalanine and *L*-tryptophan[94]), the calcimimetics and the calcilytics[95]. Except for the cations, the latter three groups are all allosteric modulators. Both the orthosteric site for Ca^{2+} and the allosteric site for *L*-amino acids reside in the VFT. The amino acid sites are adjacent to the orthosteric site, which corresponds to the amino acid binding pocket in the mGlu or $GABA_B$ receptors[96]. The calcimimetic and calcilytic sites are located in the 7TM. Structurally similar calcimimetics and calcilytics share a common allosteric binding pocket, whereas structurally distinct calcilytics recognize distinct sites[97].

Among these ligands, the orthosteric agonists are inorganic ions, so it is difficult to mimic them with synthetic molecules. The *L*-amino acid type modulators are also not suitable for therapeutic development due to their poor bioavailability and blood-brain barrier permeability. The calcimimetics and the calcilytics, however, have successfully circumvented these problems. The calcimimetic drug Cinacalcet has already been approved to treat hyperparathyroidism clinically; meanwhile, several calcilytics have shown potent effects in animal models of osteoporosis[27] and hypocalcemia[26]. Although one calcilytic drug, ronacaleret, did not display positive effects in a phase II clinical trial[98], a second generation of calcilytics with optimized characteristics is awaiting clinical validation.

Conclusion

Class C GPCRs distinguish themselves from other GPCRs by two distinct structural features: first, they possess an unusually large extracellular domain that is responsible for orthosteric ligand recognition, while the 7TM (which normally contains the orthosteric ligand-binding site) has gained many allosteric sites; second, the functional class C GPCR molecules are obligatory dimers, so the interface between the VFT, CRD, and 7TM constitutes another important allosteric site. Furthermore, it was recently demonstrated that the VFT is large enough to accommodate allosteric modulatory sites adjacent to the orthosteric sites. The unique structure and complicated activation mechanism of class C GPCRs makes it possible to modulate their function by many new approaches. In recent years, allosteric modulation has become the most attractive approach because of the decreased side effects and development of patient tolerance, improved subtype selectivity and increased chemical accessibility. The development of allosteric modulators for class C GPCRs has progressed fast. Among them, Cinacalcet was the first clinical success. Following Cinacalcet, group I and II mGlu receptor modulators are expected to enter the market in the near future as the next generation of drugs that target class C GPCRs. By contrast, allosteric drugs that modulate the group III mGlu and $GABA_B$ receptors might represent a drug generation for the more distant future. To promote the application of allosteric modulation therapeutics that target class C GPCRs, future efforts should focus on investigating the precise structural dynamics and allosteric modulation mechanisms. Determination of the receptor structures is a direct way to address such issues. Traditional mutational analysis and chimeric constructs are also powerful tools that report on related information in the absence of a crystal structure for a particular receptor. Advanced functional assays, such as BRET (bioluminescence resonance energy transfer) or FRET (fluorescence resonance energy transfer), are widely used to reveal conformational changes and dimer or oligomer formation. Additionally, computational approaches, such as ligand- or structure-based homology modeling and docking, are gaining importance as valuable complements to experimental structure-function studies. These techniques, in combination with modern drug screening assays, make it possible to identify molecules targeting class C GPCRs through sites and mechanisms other then traditional orthosteric small molecules.

Acknowledgements

This work was supported by grants from the Key Project of National Natural Science Foundation of China (NSFC) (No 31130028) and the National Basic Research Program of China (973 Program) (No 2012CB518006).

References

1 George SR, O'Dowd BF, Lee SP. G-protein-coupled receptor oligomerization and its potential for drug discovery. Nat Rev Drug Discov 2002; 1: 808–20.
2 Lagerstrom MC, Schioth HB. Structural diversity of G protein-coupled receptors and significance for drug discovery. Nat Rev Drug Discov 2008; 7: 339–57.
3 Pin JP, Galvez T, Prezeau L. Evolution, structure, and activation mechanism of family 3/C G-protein-coupled receptors. Pharmacol Ther 2003; 98: 325–54.
4 Rondard P, Goudet C, Kniazeff J, Pin JP, Prezeau L. The complexity of their activation mechanism opens new possiblities for the modulation of mGlu and $GABA_B$ class C G protein-coupled receptors. Neuropharmacology 2011; 60: 82–92.
5 Urwyler S. Allosteric modulation of family C G-protein-coupled receptors: from molecular insights to therapeutic perspectives. Pharmacol Rev 2011; 63: 59–126.
6 Kniazeff J, Prezeau L, Rondard P, Pin JP, Goudet C. Dimers and beyond: The functional puzzles of class C GPCRs. Pharmacol Ther 2011; 130: 9–25.
7 Conn PJ, Christopoulos A, Lindsley CW. Allosteric modulators of GPCRs: a novel approach for the treatment of CNS disorders. Nat Rev Drug Discov 2009; 8: 41–54.
8 Conn PJ, Pin J-P. Pharmacology and functions of metabotropic glutamate receptors. Annue Rev Pharmacol Toxicol 1997; 37: 205–37.
9 Niswender CM, Conn PJ. Metabotropic glutamate receptors: physiology, pharmacology, and disease. Annue Rev Pharmacol Toxicol 2010; 50: 295–322.
10 Pin JP, Acher F. The metabotropic glutamate receptors: structure, activation mechanism and pharmacology. Curr Drug Targets CNS Neurol Disord 2002; 1: 297–317.
11 Johnson KA, Conn PJ, Niswender CM. Glutamate receptors as therapeutic targets for Parkinson's disease. CNS Neurol Disord Drug Targets 2009; 8: 475–91.
12 Dolen G, Carpenter RL, Ocain TD, Bear MF. Mechanism-based approaches to treating fragile X. Pharmacol Ther 2010; 127: 78–93.
13 Marino MJ, Williams DL Jr, O'Brien JA, Valenti O, McDonald TP, Clements MK, *et al*. Allosteric modulation of group III metabotropic glutamate receptor 4: a potential approach to parkinson's disease treatment. Proc Natl Acad Sci U S A 2003; 100: 13668–73.
14 Conn PJ, Lindsley CW, Jones CK. Activation of metabotropic gluatamate receptors as a novel approach for the treatment of schizophrenia. Trends Pharmacol Sci 2009; 30: 25–31.
15 Bettler B, Tiao JY. Molecular diversity, trafficking and subcellular localization of $GABA_B$ receptors. Pharmacol Ther 2006; 110: 533–43.
16 Jones KA, Borowsky B, Tamm JA, Craig DA, Durkin MM, Dai M, *et al*. $GABA_B$ receptors function as heteromeric assembly of the subunits $GABA_BR1$ and $GABA_BR2$. Nature 1998; 396: 674–79.
17 Kaupmann K, Malitschek B, Schuler V, Heid J, Froestl W, Beck P, *et al*. $GABA_B$-receptor subtypes assemble into functional heteromeric complexes. Nature 1998; 396: 683–7.
18 Galvez T, Parmentier ML, Joly C, Malitschek B, Kaupmann K, Kuhn R, *et al*. Mutagenesis and modeling of the $GABA_B$ receptor extracellular domain support a Venus flytrap mechanism for ligand binding. J Biol Chem 1999; 274: 13362–9.
19 Margeta-Mitrovic M, Jan YN, Jan LY. Function of GB1 and GB2 subunits in G protein coupling of $GABA_B$ receptors. Proc Natl Acad Sci U S A 2001; 98: 14649–54.
20 Kuramoto N, Wilkins ME, Fairfax BP, Revilla-Sanchez R, Terunuma M, Tamaki K, *et al*. Phospho-dependent functional modulation of $GABA_B$ receptors by the metabolic sensor AMP-dependent protein kinase. Neuron 2007; 53: 233–47.
21 Dave KR, Lange-Asschenfeldt C, Raval AP, Prado R, Busto R, Saul I, *et al*. Ischemic preconditioning ameliorates excitotoxicity by shifting glutamate/gamma-aminobutyric acid release and biosynthesis. J Neurosci Res 2005; 82: 665–73.
22 Tu H, Xu C, Zhang W, Liu Q, Rondard P, Pin JP, *et al*. $GABA_B$ receptor activation protects neurons from apoptosis via IGF-1 receptor transactivation. J Neurosci 2010; 30: 749–59.
23 Goudet C, Magnaghi V, Landry M, Nagy F, Gereau RW 4th, Pin JP. Metabotropic receptors for glutamate and GABA in pain. Brain Res Rev 2009; 60: 43–56.
24 Cryan JF, Kaupmann K. Don't worry 'B' happy!: a role for $GABA_B$ receptors in anxiety and depression. Trends Pharmacol Sci 2005; 26: 36–43.
25 Bowery NG. $GABA_B$ receptor: a site of therapeutic benefit. Curr Opin Pharmacol 2006; 6: 37–43.
26 Brown EM. Clinical lessons from the calcium-sensing receptor. Nat Clin Pract Endocrinol Metab 2007; 3: 122–33.
27 Deal C. Future therapeutic targets in osteoporosis. Curr Opin Rheumatol 2009; 21: 380–5.
28 Brown EM. Anti-parathyroid and anti-calcium sensing receptor antibodies in autoimmune hypoparathyroidism. Endocrinol Metab Clin North Am 2009; 38: 437–45.
29 Montmayeur JP, Liberles SD, Matsunami H, Buck LB. A candidate taste receptor gene near a sweet taste locus. Nat Neurosci 2001; 4: 492–8.
30 Nelson G, Hoon MA, Chandrashekar J, Zhang Y, Ryba NJ, Zuker CS. Mammalian sweet taste receptors. Cell 2001; 106: 381–90.
31 Zhang F, Klebansky B, Fine RM, Xu H, Pronin A, Liu H, *et al*. Molecular mechanism for the umami taste synergism. Proc Natl Acad Sci U S A 2008; 105: 20930–4.
32 Cao J, Huang S, Qian J, Huang J, Jin L, Su Z, *et al*. Evolution of the class C GPCR Venus flytrap modules involved positive selected functional divergence. BMC Evol Biol 2009; 9: 67.
33 Kunishima N, Shimada Y, Tsuji Y, Sato T, Yamamoto M, Kumasaka T, *et al*. Structural basis of glutamate recognition by a dimeric metabotropic glutamate receptor. Nature 2000; 407: 971–7.
34 Tsuchiya D, Kunishima N, Kamiya N, Jingami H, Morikawa K. Structural views of the ligand-binding cores of a metabotropic glutamate receptor complexed with an antagonist and both glutamate and Gd^{3+}. Proc Natl Acad Sci U S A 2002; 99: 2660–5.
35 Bessis AS, Rondard P, Gaven F, Brabet I, Triballeau N, Prezeau L, *et al*. Closure of the Venus flytrap module of mGlu8 receptor and the activation process: Insights from mutations converting antagonists into agonists. Proc Natl Acad Sci U S A 2002; 99: 11097–102.
36 Kniazeff J, Saintot PP, Goudet C, Liu J, Charnet A, Guillon G, *et al*. Locking the dimeric $GABA_B$ G-protein-coupled receptor in its active state. J Neurosci 2004; 24: 370–7.
37 Tsuji Y, Shimada Y, Takeshita T, Kajimura N, Nomura S, Sekiyama N, *et al*. Cryptic dimer interface and domain organization of the extracellular region of metabotropic glutamate receptor subtype 1. J Biol Chem 2000; 275: 28144–51.
38 Romano C, Miller JK, Hyrc K, Dikranian S, Mennerick S, Takeuchi Y, *et al*. Covalent and noncovalent interactions mediate metabotropic glutamate receptor mGlu5 dimerization. Mol Pharmacol 2001; 59: 46–53.
39 Ray K, Hauschild BC, Steinbach PJ, Goldsmith PK, Hauache O, Spiegel AM. Identification of the cysteine residues in the amino-terminal extracellular domain of the human Ca^{2+} receptor critical for dimerization. Implications for function of monomeric Ca^{2+} receptor. J Biol

Chem 1999; 274: 27642–50.
40 Ray K, Hauschild BC. Cys-140 is critical for metabotropic glutamate receptor-1 dimerization. J Biol Chem 2000; 275: 34245–51.
41 Liu J, Maurel D, Etzol S, Brabet I, Ansanay H, Pin JP, *et al*. Molecular determinants involved in the allosteric control of agonist affinity in the $GABA_B$ receptor by the $GABA_{B2}$ subunit. J Biol Chem 2004; 279: 15824–30.
42 Rondard P, Huang S, Monnier C, Tu H, Blanchard B, Oueslati N, *et al*. Functioning of the dimeric $GABA_B$ receptor extracellular domain revealed by glycan wedge scanning. EMBO J 2008; 27: 1321–32.
43 Muto T, Tsuchiya D, Morikawa K, Jingami H. Structures of the extracellular regions of the group II/III metabotropic glutamate receptors. Proc Natl Acad Sci U S A 2007; 104: 3759–64.
44 Hu J, Hauache O, Spiegel AM. Human Ca^{2+} receptor cysteine-rich domain. Analysis of function of mutant and chimeric receptors. J Biol Chem 2000; 275: 16382–9.
45 Jiang P, Ji Q, Liu Z, Snyder LA, Benard LM, Margolskee RF, *et al*. The cysteine-rich region of T1R3 determines responses to intensely sweet proteins. J Biol Chem 2004; 279: 45068–75.
46 Rondard P, Liu J, Huang S, Malhaire F, Vol C, Pinault A, *et al*. Coupling of agonist binding to effector domain activation in metabotropic glutamate-like receptors. J Biol Chem 2006; 281: 24653–61.
47 Goudet C, Gaven F, Kniazeff J, Vol C, Liu J, Cohen-Gonsaud M, *et al*. Heptahelical domain of metabotropic glutamate receptor 5 behaves like rhodopsin-like receptors. Proc Natl Acad Sci U S A 2004; 101: 378–83.
48 Kniazeff J, Bessis AS, Maurel D, Ansanay H, Prezeau L, Pin JP. Closed state of both binding domains of homodimeric mGlu receptors is required for full activity. Nat Struct Mol Biol 2004; 11: 706–13.
49 Huang S, Cao J, Jiang M, Labesse G, Liu J, Pin JP, *et al*. Interdomain movements in metabotropic glutamate receptor activation. Proc Natl Acad Sci U S A 2011; 108: 15480–5.
50 Monnier C, Tu H, Bourrier E, Vol C, Lamarque L, Trinquet E, *et al*. Trans-activation between 7TM domains: implication in heterodimeric $GABA_B$ receptor activation. EMBO J 2011; 30: 32–42.
51 Brock C, Oueslati N, Soler S, Boudier L, Rondard P, Pin JP. Activation of a dimeric metabotropic glutamate receptor by intersubunit rearrangement. J Biol Chem 2007; 282: 33000–8.
52 Tateyama M, Abe H, Nakata H, Saito O, Kubo Y. Ligand-induced rearrangement of the dimeric metabotropic glutamate receptor 1alpha. Nat Struct Mol Biol 2004; 11: 637–42.
53 Tateyama M, Kubo Y. Dual signaling is differentially activated by different active states of the metabotropic glutamate receptor 1alpha. Proc Natl Acad Sci U S A 2006; 103: 1124–8.
54 Marcaggi P, Mutoh H, Dimitrov D, Beato M, Knopfel T. Optical measurement of mGluR1 conformational changes reveals fast activation, slow deactivation, and sensitization. Proc Natl Acad Sci U S A 2009; 106: 11388–93.
55 Pin JP, Joly C, Heinemann SF, Bockaert J. Domains involved in the specificity of G protein activation in phospholipase C-coupled metabotropic glutamate receptors. EMBO J 1994; 13: 342–8.
56 Bai M, Trivedi S, Brown EM. Dimerization of the extracellular calcium-sensing receptor (CaR) on the cell surface of CaR-transfected HEK293 cells. J Biol Chem 1998; 273: 23605–10.
57 Yamashita T, Terakita A, Shichida Y. The second cytoplasmic loop of metabotropic glutamate receptor functions at the third loop position of rhodopsin. J Biochem 2001; 130: 149–55.
58 Frauli M, Hubert N, Schann S, Triballeau N, Bertrand HO, Acher F, *et al*. Amino-pyrrolidine tricarboxylic acids give new insight into group III metabotropic glutamate receptor activation mechanism. Mol Pharmacol 2007; 71: 704–12.
59 Brauner-Osborne H, Wellendorph P, Jensen AA. Structure, pharmacology and therapeutic prospects of family C G-protein coupled receptors. Curr Drug Targets 2007; 8: 169–84.
60 Hu J, Reyes-Cruz G, Chen W, Jacobson KA, Spiegel AM. Identification of acidic residues in the extracellular loops of the seven-transmembrane domain of the human Ca^{2+} receptor critical for response to Ca^{2+} and a positive allosteric modulator. J Biol Chem 2002; 277: 46622–31.
61 Petrel C, Kessler A, Maslah F, Dauban P, Dodd RH, Rognan D, *et al*. Modeling and mutagenesis of the binding site of Calhex 231, a novel negative allosteric modulator of the extracellular Ca^{2+}-sensing receptor. J Biol Chem 2003; 278: 49487–94.
62 Petrel C, Kessler A, Dauban P, Dodd RH, Rognan D, Ruat M. Positive and negative allosteric modulators of the Ca^{2+}-sensing receptor interact within overlapping but not identical binding sites in the transmembrane domain. J Biol Chem 2004; 279: 18990–7.
63 Hu J, McLarnon SJ, Mora S, Jiang J, Thomas C, Jacobson KA, *et al*. A region in the seven-transmembrane domain of the human Ca^{2+} receptor critical for response to Ca^{2+}. J Biol Chem 2005; 280: 5113–20.
64 Pagano A, Ruegg D, Litschig S, Stoehr N, Stierlin C, Heinrich M, *et al*. The non-competitive antagonists 2-methyl-6-(phenylethynyl)pyridine and 7-hydroxyiminocyclopropan[b]chromen-1a-carboxylic acid ethyl ester interact with overlapping binding pockets in the transmembrane region of group I metabotropic glutamate receptors. J Biol Chem 2000; 275: 33750–8.
65 Malherbe P, Kratochwil N, Knoflach F, Zenner MT, Kew JN, Kratzeisen C, *et al*. Mutational analysis and molecular modeling of the allosteric binding site of a novel, selective, noncompetitive antagonist of the metabotropic glutamate 1 receptor. J Biol Chem 2003; 278: 8340–7.
66 Malherbe P, Kratochwil N, Zenner MT, Piussi J, Diener C, Kratzeisen C, *et al*. Mutational analysis and molecular modeling of the binding pocket of the metabotropic glutamate 5 receptor negative modulator 2-methyl-6-(phenylethynyl)-pyridine. Mol Pharmacol 2003; 64: 823–32.
67 Zhang F, Klebansky B, Fine RM, Liu H, Xu H, Servant G, *et al*. Molecular mechanism of the sweet taste enhancers. Proc Natl Acad Sci U S A 2010; 107: 4752–7.
68 Triballeau N, Acher F, Brabet I, Pin JP, Bertrand HO. Virtual screening workflow development guided by the "receiver operating characteristic" curve approach. Application to high-throughput docking on metabotropic glutamate receptor subtype 4. J Med Chem 2005; 48: 2534–47.
69 Selvam C, Oueslati N, Lemasson IA, Brabet I, Rigault D, Courtiol T, *et al*. A virtual screening hit reveals new possibilities for developing group III metabotropic glutamate receptor agonists. J Med Chem 2010; 53: 2797–813.
70 Jiang P, Cui M, Zhao B, Snyder LA, Benard LM, Osman R, *et al*. Identification of the cyclamate interaction site within the transmembrane domain of the human sweet taste receptor subunit T1R3. J Biol Chem 2005; 280: 34296–305.
71 Jiang P, Cui M, Zhao B, Liu Z, Snyder LA, Benard LM, *et al*. Lactisole interacts with the transmembrane domains of human T1R3 to inhibit sweet taste. J Biol Chem 2005; 280: 15238–46.
72 Gregory KJ, Dong EN, Meiler J, Conn PJ. Allosteric modulation of metabotropic glutamate receptors: structural insights and therapeutic potential. Neuropharmacology 2011; 60: 66–81.
73 Muhlemann A, Ward NA, Kratochwil N, Diener C, Fischer C, Stucki A, *et al*. Determination of key amino acids implicated in the actions of allosteric modulation by 3,3'-difluorobenzaldazine on rat mGlu5 receptors. Eur J Pharmacol 2006; 529: 95–104.

74 Chen Y, Goudet C, Pin JP, Conn PJ. N-{4-Chloro-2-[(1,3-dioxo-1,3-dihydro-2H-isoindol-2-yl)methyl]phenyl}-2-hy droxybenzamide (CPPHA) acts through a novel site as a positive allosteric modulator of group 1 metabotropic glutamate receptors. Mol Pharmacol 2008; 73: 909–18.

75 Litschig S, Gasparini F, Rueegg D, Stoehr N, Flor PJ, Vranesic I, *et al*. CPCCOEt, a noncompetitive metabotropic glutamate receptor 1 antagonist, inhibits receptor signaling without affecting glutamate binding. Mol Pharmacol 1999; 55: 453–61.

76 Knoflach F, Mutel V, Jolidon S, Kew JN, Malherbe P, Vieira E, *et al*. Positive allosteric modulators of metabotropic glutamate 1 receptor: characterization, mechanism of action, and binding site. Proc Natl Acad Sci U S A 2001; 98: 13402–7.

77 Hemstapat K, de Paulis T, Chen Y, Brady AE, Grover VK, Alagille D, *et al*. A novel class of positive allosteric modulators of metabotropic glutamate receptor subtype 1 interact with a site distinct from that of negative allosteric modulators. Mol Pharmacol 2006; 70: 616–26.

78 Rowe BA, Schaffhauser H, Morales S, Lubbers LS, Bonnefous C, Kamenecka TM, *et al*. Transposition of three amino acids transforms the human metabotropic glutamate receptor (mGluR)-3-positive allosteric modulation site to mGluR2, and additional characterization of the mGluR2-positive allosteric modulation site. J Pharmacol Exp Ther 2008; 326: 240–51.

79 Grillon C, Cordova J, Levine LR, Morgan CA 3rd. Anxiolytic effects of a novel group II metabotropic glutamate receptor agonist (LY354740) in the fear-potentiated startle paradigm in humans. Psychopharmacology (Berl) 2003; 168: 446–54.

80 Patil ST, Zhang L, Martenyi F, Lowe SL, Jackson KA, Andreev BV, *et al*. Activation of mGlu2/3 receptors as a new approach to treat schizophrenia: a randomized Phase 2 clinical trial. Nat Med 2007; 13: 1102–7.

81 Swanson CJ, Bures M, Johnson MP, Linden AM, Monn JA, Schoepp DD. Metabotropic glutamate receptors as novel targets for anxiety and stress disorders. Nat Rev Drug Discov 2005; 4: 131–44.

82 Urwyler S, Mosbacher J, Lingenhoehl K, Heid J, Hofstetter K, Froestl W, *et al*. Positive allosteric modulation of native and recombinant gamma-aminobutyric acid(B) receptors by 2,6-Di-tert-butyl-4-(3-hydroxy-2,2-dimethyl-propyl)-phenol (CGP7930) and its aldehyde analog CGP13501. Mol Pharmacol 2001; 60: 963–71.

83 DeLapp NW. The antibody-capture [^{35}S]GTPgammaS scintillation proximity assay: a powerful emerging technique for analysis of GPCR pharmacology. Trends Pharmacol Sci 2004; 25: 400–1.

84 Matsushita S, Nakata H, Kubo Y, Tateyama M. Ligand-induced rearrangements of the $GABA_B$ receptor revealed by fluorescence resonance energy transfer. J Biol Chem 2010; 285: 10291–9.

85 Binet V, Brajon C, Le Corre L, Acher F, Pin JP, Prezeau L. The heptahelical domain of $GABA_{B2}$ is activated directly by CGP7930, a positive allosteric modulator of the $GABA_B$ receptor. J Biol Chem 2004; 279: 29085–91.

86 Tu H, Rondard P, Xu C, Bertaso F, Cao F, Zhang X, *et al*. Dominant role of $GABA_{B2}$ and Gbetagamma for $GABA_B$ receptor-mediated-ERK1/2/CREB pathway in cerebellar neurons. Cell Signal 2007; 19: 1996–2002.

87 Urwyler S, Pozza MF, Lingenhoehl K, Mosbacher J, Lampert C, Froestl W, *et al*. N,N′-Dicyclopentyl-2-methylsulfanyl-5-nitro-pyrimidine-4,6-diamine (GS39783) and structurally related compounds: novel allosteric enhancers of gamma-aminobutyric acidB receptor function. J Pharmacol Exp Ther 2003; 307: 322–30.

88 Malherbe P, Masciadri R, Norcross RD, Knoflach F, Kratzeisen C, Zenner MT, *et al*. Characterization of (*R,S*)-5,7-di-*tert*-butyl-3-hydroxy-3-trifluoromethyl-3*H*-benzofuran-2-one as a positive allosteric modulator of $GABA_B$ receptors. Br J Pharmacol 2008; 154: 797–811.

89 Kerr DI, Ong J, Puspawati NM, Prager RH. Arylalkylamines are a novel class of positive allosteric modulators at $GABA_B$ receptors in rat neocortex. Eur J Pharmacol 2002; 451: 69–77.

90 Kerr DI, Ong J. Potentiation of metabotropic $GABA_B$ receptors by *L*-amino acids and dipeptides in rat neocortex. Eur J Pharmacol 2003; 468: 103–8.

91 Wise A, Green A, Main MJ, Wilson R, Fraser N, Marshall FH. Calcium sensing properties of the $GABA_B$ receptor. Neuropharmacology 1999; 38: 1647–56.

92 Galvez T, Urwyler S, Prezeau L, Mosbacher J, Joly C, Malitschek B, *et al*. Ca^{2+} requirement for high-affinity gamma-aminobutyric acid (GABA) binding at $GABA_B$ receptors: involvement of serine 269 of the $GABA_B$R1 subunit. Mol Pharmacol 2000; 57: 419–26.

93 Brauner-Osborne H, Jensen AA, Sheppard PO, O'Hara P, Krogsgaard-Larsen P. The agonist-binding domain of the calcium-sensing receptor is located at the amino-terminal domain. J Biol Chem 1999; 274: 18382–6.

94 Zhang Z, Qiu W, Quinn SJ, Conigrave AD, Brown EM, Bai M. Three adjacent serines in the extracellular domains of the CaR are required for *L*-amino acid-mediated potentiation of receptor function. J Biol Chem 2002; 277: 33727–35.

95 Saidak Z, Brazier M, Kamel S, Mentaverri R. Agonists and allosteric modulators of the calcium-sensing receptor and their therapeutic applications. Mol Pharmacol 2009; 76: 1131–44.

96 Silve C, Petrel C, Leroy C, Bruel H, Mallet E, Rognan D, *et al*. Delineating a Ca^{2+} binding pocket within the Venus flytrap module of the human calcium-sensing receptor. J Biol Chem 2005; 280: 37917–23.

97 Arey BJ, Seethala R, Ma Z, Fura A, Morin J, Swartz J, *et al*. A novel calcium-sensing receptor antagonist transiently stimulates parathyroid hormone secretion *in vivo*. Endocrinology 2005; 146: 2015–22.

98 Fitzpatrick LA, Smith PL, McBride TA, Fries MA, Hossain M, Dabrowski CE, *et al*. Ronacaleret, a calcium-sensing receptor antagonist, has no significant effect on radial fracture healing time: Results of a randomized, double-blinded, placebo-controlled Phase II clinical trial. Bone 2011; 49: 845–52.

Acta Pharmacologica Sinica (2012) 33: 324–334
 1671-4083/12 $32.00
www.nature.com/aps

Review

Ice breaking in GPCR structural biology

Qiang ZHAO*, Bei-li WU

The Joint Laboratories of GPCR Research, Center of Structures and Functions of Drug Targets, Shanghai Institute of Materia Medica, Chinese Academy of Sciences, Shanghai 201203, China

G-protein-coupled receptors (GPCRs) are one of the most challenging targets in structural biology. To successfully solve a high-resolution GPCR structure, several experimental obstacles must be overcome, including expression, extraction, purification, and crystallization. As a result, there are only a handful of unique structures reported from this protein superfamily, which consists of over 800 members. In the past few years, however, there has been an increase in the amount of solved GPCR structures, and a few high-impact structures have been determined: the peptide receptor CXCR4, the agonist bound receptors, and the GPCR-G protein complex. The dramatic progress in GPCR structural studies is not due to the development of any single technique, but a combination of new techniques, new tools and new concepts. Here, we summarize the progress made for GPCR expression, purification, and crystallization, and we highlight the technical advances that will facilitate the future determination of GPCR structures.

Keywords: G-protein-coupled receptors (GPCRs); expression study; mutagenesis; surfactant; crystallization; bicelle; lipidic cubic phase

Acta Pharmacologica Sinica (2012) 33: 324–334; doi: 10.1038/aps.2011.187; published online 30 Jan 2012

Introduction

Membrane proteins comprise approximately 30% of organism proteomes; however, they comprise only 1.1% of the total protein data bank (PDB) entries (862 coordinate files in a total of 75 694 depositions). Among which, the GPCRs are greatly under-represented in the PDB when compared to the other general protein families. These receptors are involved in every physiological activity, including sight, taste, and hormone regulation, *etc*. They function as signal transmitters that can sense a huge variety of signals and amplify them inside the cells, leading to different cell responses, and are involved in almost all human diseases. Among the approximately 400 non-olfactory receptors, 50–60 receptors are the targets of approximately 40% of the drugs on the market, while the other 350 are yet to be explored. As the largest protein family of drug targets in the human body, there are only 45 deposited structure files representing 7 unique receptors[1–7]. Moreover, this set is somewhat redundant, as the β1 and β2 adrenergic receptors are closely related. Given that over 800 receptors are found in the human genome and that a large variety of ligands specifically bind to this protein family, the mechanisms of ligand recognition and signal transduction are largely uncharacterized.

To successfully solve a GPCR structure, one needs to overcome multiple bottlenecks, including expression, extraction, and the formation of crystal contacts. In addition to these general difficulties that have been long known in crystallizing membrane proteins, the flexibility of the receptor poses a major obstacle[8, 9]. It has been observed repeatedly for multiple receptors that the transmembrane helix bundle rearranges during activation. The distances between the helices differ by up to 10–14 Å during this process[10–12]. It has also been reported that between the active and inactive states, these receptors have multiple intermediate states that are induced by different types of ligands, and each state might correlate to its own structural features. Because GPCRs are so flexible, they are generally in a mixture of different conformations, and the field tends to use a concept of "energy landscape" instead of "conformation" to describe the dynamics of GPCRs[13]. It is not uncommon to observe that exchanging the ligand or mutating one amino acid of the GPCR can dramatically reduce the diffraction resolution or even abolish crystallization altogether. This is probably one of the key reasons why it took researchers an additional 15 years after the first high-resolution membrane protein structure was reported in 1985[1] to obtain the first GPCR structure. Despite the current low success rates for achieving high-resolution structures, years of technology developments and studies of this protein family have shed light on this challenging project. Recent breakthroughs include the structures of novel GPCRs[7], discovery of new activity states of GPCRs[10, 14–16] and a structure of GPCR in complex with other proteins[11]. This review will focus on new

* To whom correspondence should be addressed.
E-mail zhaoq@mail.shcnc.ac.cn
Received 2011-10-08 Accepted 2011-12-06

clues and the latest progress on the structure determination of GPCRs.

The experimental procedure for obtaining a membrane protein crystal structure typically involves three steps: the protein has to be functionally expressed, purified in detergent micelles and crystallized. We will summarize the recent technological developments accordingly.

Protein expression

With few exceptions, GPCRs are often found in very small amounts in native tissue, which makes it nearly impossible to purify the amounts of material necessary for crystallographic studies from natural sources. It is therefore necessary to set up a robust recombinant expression system. To achieve high yields of recombinant GPCR proteins, gaining a better understanding of the host organisms is an emerging strategy compared to standard techniques such as the screening of promoters, development of fusion adducts, and adjusting the culture process parameters. Conventionally, there are 4 types of expression host systems used in protein X-ray structural studies: *E coli*, yeast, insect cells and mammalian cells, and each system has its own limitations that restrict its use in GPCR overexpression studies.

Mammalian cells and insect cells

Among the four systems, the mammalian cell expression system is the closest to the natural environment of GPCRs, and thus serves as an expression host for many GPCRs. The yield of some receptors in this system is as high as 10 mg/L of media[17]; however, most of the receptors are designed for functional studies so far, and only a few of those were applied to overexpression. High cost, difficulty in scaling up and long experimental cycles are barriers that limit the use of mammalian cell expression systems.

On the contrary, insect cells, which shares similar disadvantages as mammalian systems, are a more successful host. Six out of seven unique receptors were expressed in either sf9 cells or high5 cells[18]. After careful optimization, the baculovirus expression system often has increased protein yields over that of mammalian cells such as HEK cells[19].

Yeast

Yeast is an attractive expression system because it can be engineered as a microorganism while possessing eukaryotic machinery[20]. Yeast has a short generation time (approximately 2 h), requires relatively simple media and is easy to work with. Years of characterization have also provided numerous plasmids and experience in scale-up fermentation. As a eukaryotic expression system, yeast can post-translationally modify the receptor; therefore, it was one of the earliest expression systems used for GPCR. However, the yeast system has its own drawbacks. The composition/quantity of N-glycans and the membrane composition of yeast are different from those of mammalian systems. This may cause problems when a correct modification or lipid environment is necessary for the functional expression of some receptors, such as rhodopsin or opioid receptors[21, 22]. In addition, yeast cells are surrounded by a cell wall that is notoriously hard to handle when trying to extract membrane and intracellular proteins.

Initial attempts were made in yeast systems, such as *S cerevisiae*, *S pombe* and *P pichia*, to express the β_2 adrenergic receptor, the M1 muscarinic receptor and the opioid receptors[23–25]. Multiple factors including supplementation of a ligand, histidine and DMSO were evaluated and optimized[26, 27], and quite a few receptors were reported with expression levels of >1 mg/L of media[28, 29], which is sufficient for structural studies. Recently, Iwata's group solved the crystal structure of the human Histamine H1 receptor, which was expressed in *P pichia*[7]. To avoid the complication of saccharide modification in the yeast system, the N-terminal portion comprising 19 amino acids which includes two glycosylation sites (Asn5 and Asn18) were truncated. The receptor sequence was also optimized according to the codon usage for *P pichia* to achieve a higher expression level[30]. The structure had very high similarity to the structure of β_2 adrenergic receptor and the D3 dopamine receptor, which were obtained using higher eukaryotic expression systems[7]. These results indicate that yeast has the ability to correctly fold mammalian GPCRs and has the potential for applications in protein crystallographic research.

Despite this tremendous success, we do not completely understand this expression system yet. Research from different groups raises our concern about the homogeneity of yeast-expressed material[8, 31–33]. Their results indicate that the expressed product is a mixture of functional and nonfunctional receptors, because during optimization the expression of the functional GPCR will dramatically increase but the overall expression level is somewhat constant. In addition, the expression of GPCRs is case-sensitive. Although multiple receptors showed a relatively high expression of 1–10 mg/L of culture, the ratio of functional expression is extremely low. O'MALLEY *et al* investigated 12 GPCRs expressed in *S cerevisiae*, and only the A_{2A} adenosine receptor retained its ligand binding activity. Other receptors, despite being processed and expressed in the same conditions, failed to localize in the plasma membrane and had no detectable ligand binding[31]. A more detailed study using N-terminal sequencing and N-glycosylation detection demonstrated that most of these nonfunctional receptors were not properly processed. In addition to *S cerevisiae*, *P pichia* had similar problems in processing signal sequences[34], indicating that there are still some fundamental differences within the higher eukaryotic systems. Currently, little is known regarding the factors that govern the folding and cellular trafficking of heterologously expressed GPCRs in yeast, and more efforts are needed in the future to make this system more robust and desirable.

E coli

Although it is known that eukaryotic membrane proteins, especially GPCRs, are impossible to express efficiently in prokaryotic systems, the low-cost and easy-to-handle nature of *E coli* encouraged the exploration of this system for the

expression of GPCRs. Initially, researchers managed to make some progress by successfully obtaining GPCRs such as the β_2 adrenergic receptor and the 5-hydroxtryptamine receptor (5HT1α) with functional ligand-binding activity[35]. The key was to use a maltose-binding protein (MBP) as an N-terminal fusion tag, which helped the receptor to be expressed and folded in the periplasm. Grisshammer *et al* also found that addition of thioredoxin A to the C-terminus of GPCR further increased their stability and yield[36].

However, even if all of the expression parameters are optimized, the GPCRs expressed in *E coli* may not be sufficient for direct use in crystallographic studies yet. To date, most crystallization studies are focused on indirect uses, such as expression or stability screening, to facilitate higher throughput in a short period of time. The best example of this was provided by the Tate group in solving the crystal structures of the β1 adrenergic receptor and the A_{2A} adenosine receptor in the active state[16, 37]. All of the mutants were expressed in *E coli* using a procedure that is similar to Grisshammer's, and the construct optimization was performed accordingly, before the final transfer to insect cells for large-scale preparations. The work of PLÜCKTHUN *et al* pushes these approaches to a new level. They developed a fluorescence-activated cell sorting (FACS) method that could enhance both the expression level and stability of GPCRs while retaining function and tailoring ligand selectivity[38]. Using this approach, the expression levels of multiple GPCRs were increased several folds, and a receptor analog that more prone to bind agonists *vs* antagonists was obtained, similar to results from the Tate group when they solved the active state A_{2A} adenosine receptor structure[39]. Moreover, data from both the Tate and Plückthun groups indicate that all the results from prokaryotic systems can be successfully transferred to eukaryotic expression systems. This is truly exciting because one can take advantage of the reduced cost, the lower demand for experience and the dramatically shorter experimental cycles of prokaryotic systems. However, although this approach is very promising now, the application of prokaryotic expression systems for structural studies requires further development.

Because certain GPCRs are currently produced at sufficient levels for X-ray crystallographic trials, it is speculated that heterologous expression of GPCRs may no longer be a bottleneck in obtaining crystal structures. However, there remain many unknown factors that are important for optimizing GPCR expression. It is not surprising to see >100 fold differences in yield among various GPCRs within each of the expression systems. While milligram quantities of certain GPCRs are attainable, the majority of GPCRs are still either produced at very low levels or not at all. Developing reliable expression techniques for GPCRs is still a major priority for the structural characterization of GPCRs.

It's all about stability

Once acceptable expression is achieved, the issue of extracting the receptor out of the lipid bilayer starts to limit the downstream processes toward crystallization. Most of the GPCRs are intrinsically unstable and quickly lose their native fold when solubilized[9]. It is generally known that protein stability is correlated to the chances of protein crystal formation, and this point has been repeatedly demonstrated by the Tate and Stevens groups. Multiple methods have been carried out to engineer the receptor for higher stability.

T4 lysozyme fusion

The most successful attempt at engineering a GPCR to solve its structure is the generation of a T4 lysozyme fused protein. This was first developed during solving the high-resolution structure of the β_2 adrenergic receptor[2, 40]. It has long been known that the third intracellular loop is very flexible, and is believed preventing the formation of crystals. Replacing of this loops with the T4 lysozyme moiety will not only provide an additional surface for crystal contact, but also restrain the movement of the GPCR helix bundle and thus provides higher thermal stability[40]. Research also revealed that this replacement does not alter either the GPCR's ligand binding or signal transduction ability. Subsequent research showed that this T4 lysozyme (T4L) fusion method is applicable to different GPCRs, even though the junction sites are slightly different and must be carefully screened[5, 6].

Different methods are used to determine the best T4L fusion. Initially, the insertion site was decided by receptor surface expression screening. Together with determination of more GPCR structures, a more systematic screening method combining ligand-binding affinity, protein homogeneity and stability was developed[5, 6, 41]. Guided by this method, several structures were successfully solved including the chemokine receptor CXCR4 and the dopamine receptor D3.

Antibodies/nanobodies

The application of antibodies is a traditional method for dealing with flexible/instable proteins. So far, two GPCR structures have been solved in the presence of antibodies that recognizing the receptor[10, 42], both of which are β_2 adrenergic receptor structures. Similar with the use of the T4 lysozyme fusion, these antibodies target the cytoplasmic side of the receptor, especially the unstructured intracellular loop 3 (ICL3) region. In the β_2AR-Fab5 complex structure, the Fab5 recognizes both the junction of the helix V to ICL3 (I233-V242) and the junction of ICL3 to helix VI (L266 and K270)[42], which will restrain the movement of these two helices. Furthermore, in the β_2AR-Nb80 complex, the nanobody Nb80 also specifically recognizes both helix V and helix VI in the cytoplasmic end. In addition, its CDR3 loop inserted into the hydrophobic pocket between helices V/VI and helices III/VII[10]. These antibodies do help with the formation of crystal contacts, but their role in restricting the receptor dynamics is equally important. It looks like the helices V and VI are the key element to be stabilized before the receptor is actually crystalized.

This method do improve our chances of getting crystals, however, the application of antibodies for GPCRs is not straightforward. One major obstacle is the existence of very high concentration of detergents. These receptors generally

require higher protein concentrations for crystallization (30–50 mg/mL or higher), which typically requires at least a 100-fold concentration. As a result, the detergent concentration in the final crystallization samples is strikingly high (approximately 2% in the case of DDM), and some of these antibodies will dissociate from the receptor molecules under such conditions. The fact that only the β_2 adrenergic receptor has been crystallized with the help of antibodies indicates that this method is equally challenging, and extensive work is needed before practical use.

Mutations

Besides the lysozyme fusion and antibodies, additional mutations are generally needed to facilitate crystallization. The most common is a E3.41W mutation, which was first introduced in the β_2 adrenergic receptor (the amino acid is represented using the Ballesteros-Weinstein numbering-system[43]). In the sequence alignment of β_2 adrenergic receptor with other GPCRs, there is an hydrophilic glutamate residue in the middle of helix III that is buried in the hydrophobic helix bundle[44] (Figure 1B), which might reduce the stability to the whole receptor. Mutation of this residue to an aromatic residue dramatically increases the yield of the purified material and greatly improves the receptor's melting temperature. Additional research showed that similar to the T4 lysozyme fusion, this mutation could also be applied to other receptors, even if their corresponding positions are already hydrophobic residues[5, 6] (Figure 1).

In some cases, although the mutations themselves make the receptor stable enough to be crystalized, it remains difficult to explain the rationale for these mutants. Tate and Schertler have mapped almost every residue in the receptor and measured the thermal stability of the corresponding mutants. The most promising mutations were then combined and further screened for the highest stability to tolerate the harsh environment during extraction, purification and crystallization[38, 45]. Guided by this method, they solved the crystal structures of the β1 adrenergic receptor with different ligands and the A_{2A} adenosine receptor structure in an active state[4, 16]. Similarly, PLÜCKTHUN *et al* used error-prone PCR (epPCR) to construct a library of mutations of target gene which were expressed and sorted by flow cytometry to screen for higher expression or stability. The sorted cells were kept and then epPCR and pooled for 4 rounds before they were analyzed for sequence diversity. The most consistent mutations were selected and successfully applied to higher expression systems such as

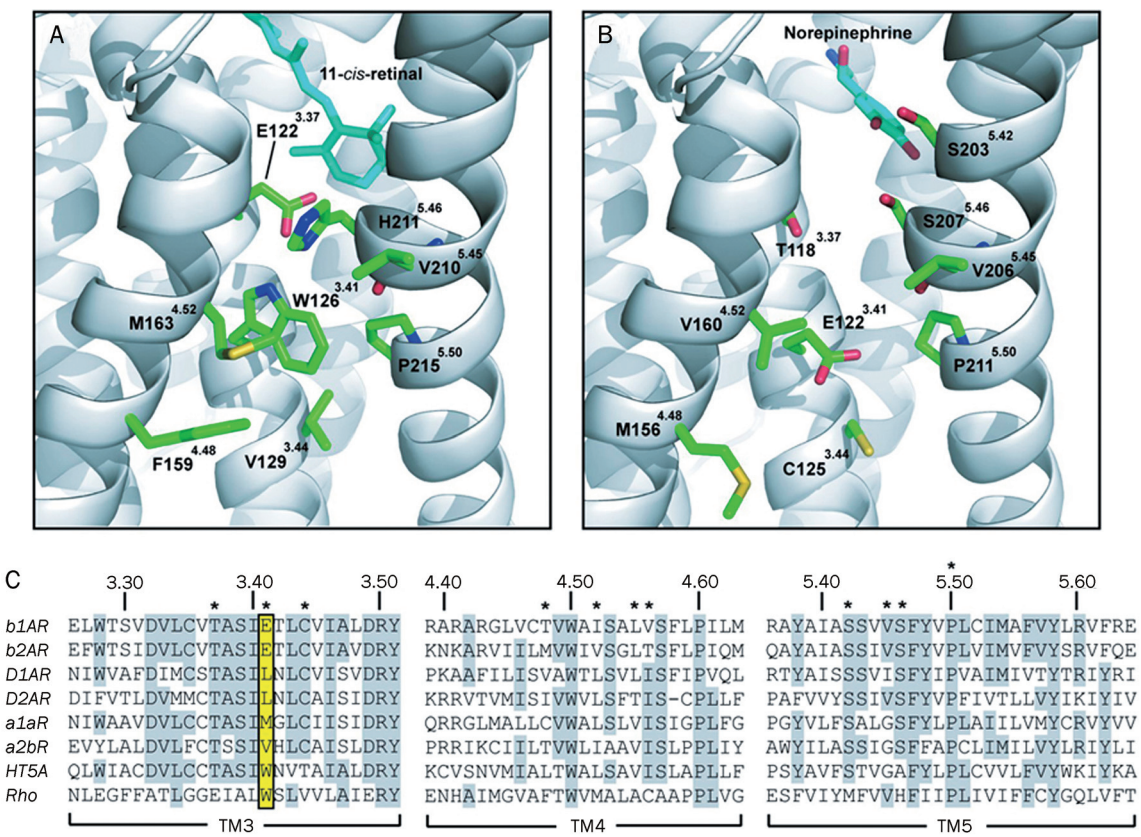

Figure 1. Structural models of the TM4-3-5 interface, indicating the most frequent 3.41 (Ballesteros and Weinstein System) mutation in GPCR structures. (A, B) Rhodopsin inactive state structure (PDB ID code 1U19) and β_2AR structure showing residues proximal to 3.41. TM helices are colored grey and side-chains carbon atoms are colored green. (C) Clustal W sequence alignment illustrating the residue conservation in TM3, TM4, and TM5 for the βARs, rhodopsin and several members of the biogenic amine family. Identical residues are highlighted in grey. Key residues mentioned in the text are marked with asterisks. Position 3.41 is highlighted in yellow[44].

insect cells, and by this, higher expression and stability were then achieved[38, 39].

These three groups tested stabilization mutant using 5 GPCRs independently and found some very interesting consistencies[37–39, 45, 46]. Each of the five receptor genes contained 5.6±1.1 mutants to maximize the protein stability compared to the wild type, with a total 28 mutants. The majority of these mutations are located in the helix bundle (26 out of 28 mutations), and they are not spread evenly on all the seven transmembrane helices (Figure 2). Nearly half of the mutations are distributed from helix V through helix VII, where there was significant movement upon activation. Surprisingly, helix II is also one frequently mutated region. More than 30% of the stabilizing mutations occurred on this helix (9 out of 28 mutations) for no obvious reason. The other helices, especially helix IV, are barely touched which is probably due to it is nowhere near helix V, VI, or VII in the spatial helix bundle. Although only a few mutations appeared on identical positions, the majority of the mutations lie only in several specific pockets. These pockets are located in the intracellular end of the receptor, and only a few mutations are located in the extracellular half that facilitates the binding of certain ligands. This is not completely unexpected, as research showed that the intracellular portion displayed more structural dynamics in different active state. In contrast, the extracellular half, despite having significant diversity within the gene superfamily, has only very minor changes when different ligands are bound.

GPCRs have enormous conformational diversity, which is believed to be one of the key obstacles to crystallization. To date, all the receptor analogs achieved from mutation screening had a modified binding preference depending on the type of ligands used[4, 16]. For example, in the structure of the A_{2A} adenosine receptor bound to agonists adenosine and NECA, four mutations in the receptor greatly reduced the affinity with the antagonists, while the agonist binding was unaltered[16]. The shift in binding affinity indicates that the receptor could only adopt restrained conformations, thus its stability and homogeneity were improved, which would further allow crystallization. Because most of these conformational restraining mutations are located in the intracellular portion of the GPCR where they are more conserved in both structure and sequence than the other regions, further studies could potentially reveal a general rule that could apply to the other GPCRs and guide our future studies.

Surfactants

Traditionally, short-chain detergents form smaller micelles around membrane proteins than the long alkyl ones, which would leave larger surface areas exposed to form crystal contacts. However, these short-chain detergents are also far more denaturing than the long-chain detergents that are normally used to purify GPCRs in a functional form. It is very challenging to choose a detergent that can balance the hydrophobicity and hydrophilicity for each target protein, and as a result, the crystals are often of low quality and difficult to improve. Based on the understanding achieved from previous X-ray crystallographic work, several new amphiphiles and detergents have been developed by modifications of known surfac-

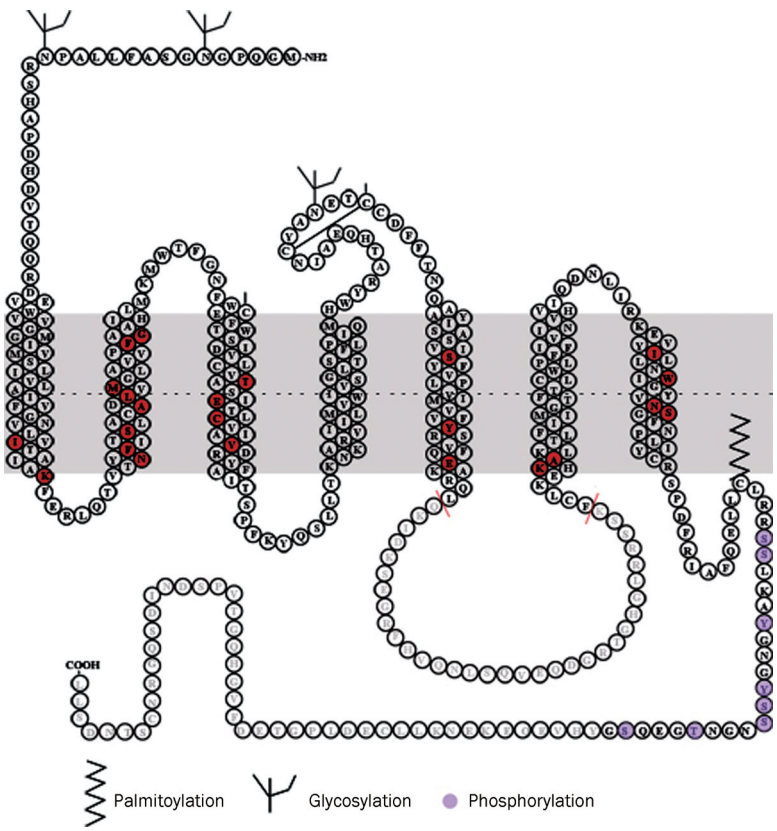

Figure 2. A snake β_2AR plot to brief summary of the mutagenesis studies aiming higher GPCR stability[37, 38, 44–46, 91]. The mutations on different receptors are applied to β_2AR receptor based on the Ballesteros and Weinstein Number System[43] and labeled in red on the Figure. The post translational modifications such as glycosylation and phosphorylation are labeled as indicated.

tants or *de novo* design. Some of these novel amphiphiles (*eg*, nanodiscs and amphipols) have found broad application in membrane protein biochemistry and are used for solubilization and stabilization of GPCRs for functional studies.

One example of these modified detergents is branch-chained detergent which contains a short, branched alkyl chain at the interface between the polar head and the apolar tail. This type of detergent mimics a lipid molecule with a second aliphatic chain, reducing the water penetration. Hong *et al* showed that even one carbon branch could have dramatic effects and these detergents could be successfully applied to solubilization, stabilization and crystallization of membrane proteins[47]. Another example of such detergents is maltose-neopentyl glycol (MNG) amphiphiles that are built around a central quaternary carbon atom[48] (Figure 3A and 3B). This carbon atom enables the incorporation of two hydrophilic and two hydrophobic subunits and restrains their conformational flexibility. Some of these MNG detergents have been tested on both GPCRs and other membrane proteins, and proved to enhance structural stability and the chances of successful crystallization. The authors also claimed that these detergents improved the crystal size and quality of membrane proteins with less stability, such as β_2AR-T4L bound to agonists. In short, these modified detergents displayed distinct properties from their conventional analogs and have promising use in the maintenance of native GPCR folding and function[48].

The *de novo* synthesis of detergents includes protein-based nanodiscs[49, 50], amphiphilic polymers (amphipols)[51–53], peptide-based amphiphiles[54–56], fluorinated detergents[53, 57] and tripod detergents[58, 59]. One good example is the so-called "facial amphiphile", which is a new detergent concept created by several groups. These detergents make the protein-detergent complexes (PDC) as small as possible by creating a flat and rigid hydrophobic surface. McGregor *et al* have reported that lipopeptides (LPDs) are self-assembled into a cylindrical micelle with a width similar to that of a lipid bilayer, and further form a rigid sheath around the protein surface[55]. Zhang *et al* have developed cholate-based amphiphiles that project hydrophilic maltose units from one side of the steroidal skeleton, which is then further developed by the design of "tandem facial amphiphiles (TFAs)"[60, 61]. The TFAs contain a pair of maltose-functionalized deoxycholate units, making it long enough to match the bilayer width. These facial amphiphiles are very successful in reducing the micelle size. Both Zhang *et al* and Chae *et al* showed that the facial amphiphiles are only approximately 1/6 of the micelle size compared to the traditional detergents such as DDM, with an aggregation number of approximately 37 for FAs and only approximately 6 for the TFAs per PDC[60, 61]. Although there is yet to be a direct application of these facial amphiphiles in

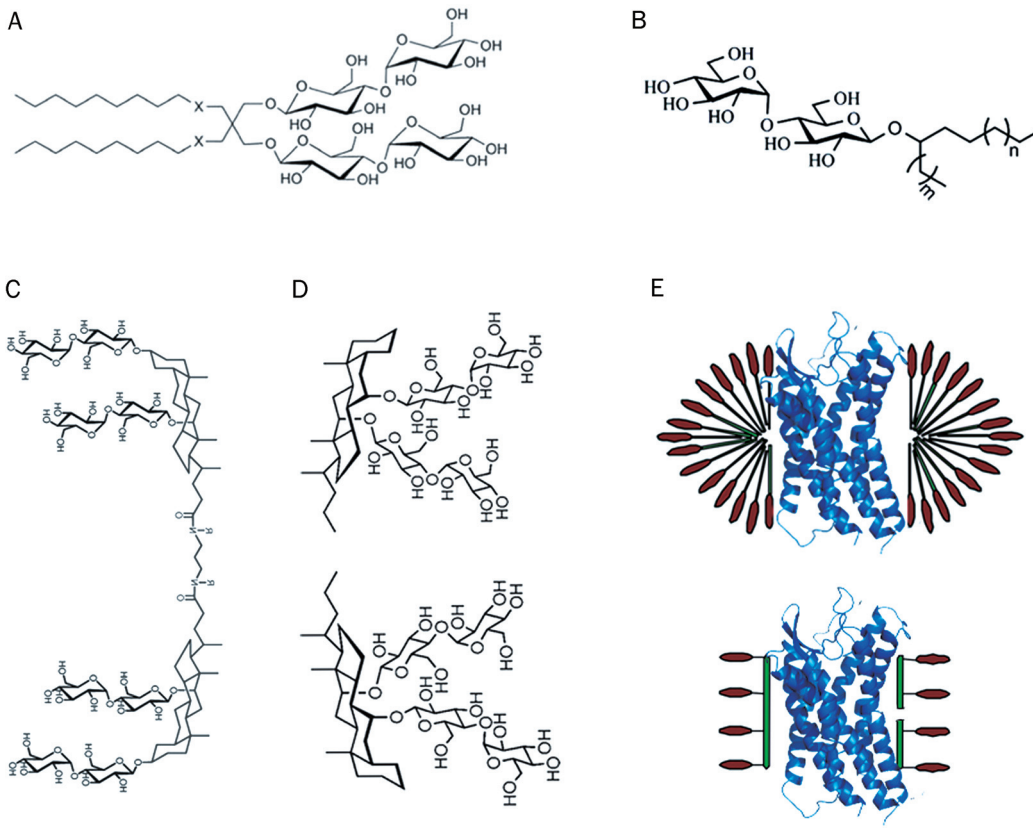

Figure 3. A brief summary of the new detergents to facilitate the GPCR structure study. (A) MNG[48]; (B) branched detergent[47]; (C) tandem facial amphiphiles (TFA)[61]; (D) facial amphiphiles[60]; (E) a cartoon about the working hypothesis of facial amphiphiles and tandem facial amphiphiles in compare with conventional detergents[60].

crystallization trials, their biophysical properties exhibit significant potential in the structural study of this challenging protein family (Figure 3C, 3D, and 3E).

Recently, systematic screening of the branched detergents, MNGs and the facial amphiphiles for protein thermal stability was carried out using multiple GPCRs. More than half of these new detergents provided equal or higher thermal stability than the best conventional detergents (unpublished data). However, different GPCRs still have different preferences for different surfactants, and it seems very unlikely that one single amphiphile is ideal for all of the receptors due to their sequence variety. A deeper understanding of the interaction between membrane proteins and detergents is still required for further development of detergents.

Crystallization and data collection

To solve the structures of GPCRs, high-quality crystals must be obtained, which represents a major challenge. Several techniques are employed to crystallize GPCRs, including the traditional direct use of solubilized protein-surfactant complexes, or the so-called *in surfo* method[4, 16], the bicelle method[10, 15], and the lipidic cubic phase, or in meso method.

In surfo method

Although the *in surfo* method remains one of the most efficient in membrane protein crystallography, it exhibits dramatic limitations in GPCR structural studies. Research has shown that GPCRs tend to reserve more conformations in detergent micelles than in lipid bilayers, and as a direct result, very few GPCRs could crystallize directly in detergent micelles. Most of the current GPCR structures obtained using the *in surfo* method are modified by mutation to reduce their chances of adopting other conformations[4, 16] as mentioned above.

Bicelle method

The other methods, such as the newly developed bicelles, nanodiscs or lipidic cubic phase (LCP), seek to trap each membrane protein molecule within a lipid bilayer before crystallization and take advantage of a native-like environment to preserve their integrity[62]. Compared to the *in surfo* method, the bicelle method uses a lipid bilayer of finite size and maintains the ability to diffuse in three dimensions in the process of forming a three-dimensional lattice (Figure 4A). Bicelles are typically made of two lipids, one of which forms a lipid bilayer, while the other forms an amphipathic, micelle-like cover for the bilayer and shields it from the solvent[63]. The important interactions between lipids and proteins have been preserved within bicelles, as clear density for a CHAPSO molecule inserted between protein subunits is observed in the structure of bacteriorhodopsin. The bicelles have displayed broad utilities in every aspect of GPCR study[64]. The ability to grow crystals at room temperature significantly expands the applicability of bicelle crystallization[42, 65]. Nanodiscs, on the other hand, use an amphipathic protein coat to encapsulate the bilayer segment instead of detergent, which makes nanodiscs more stable than bicelles at low concentrations[49, 66]. The nanodisc is constrained by two molecules of a membrane scaffold protein that wraps around the edges of the discoidal structure in a belt-like arrangement. These constructs maintain a very well-defined size depending on the type of protein coat[67]. Because the smallest nanodiscs are approximately 10 nm, their application in crystallography is still quite limited, and more work needs to be performed to remove the 3-D packing restraints before successful crystallization. To date, these bilayer-based, diffusible structures have been most useful for NMR methods or for assessing the ligand binding of GPCRs[67–69].

In meso method

Crystallization in lipidic phases has only recently been developed but has already become an essential tool in the arsenal of membrane protein crystallization, especially for GPCRs[70, 71]. The cubic phase is a bicontinuous lipidic meso phase formed spontaneously by mixing monoacylglycerols (MAGs) and water at a given ratio[72] (Figure 4B). It consists of a curved bicontinuous lipid bilayer in three dimensions, separating two congruent networks of water channels. When protein samples are used as an aqueous solution, the high concentration of lipid molecules will replace the detergent molecules around the protein, and thus, the receptor is reconstituted to the lipid bilayer. When a certain precipitant is added, the receptor will start to nucleate, and a temporary phase transition will be formed, ensuring crystal growth (Figure 4C).

Monoolein is a default lipid for crystallogenesis studies. However, some other lipids such as monomyristolein (C14:1c9) and monopentadecenoin (C15:1c10) could also be used for crystallization studies. The different host MAGs, or MAGs with different additives (usually cholesterol or phospholipids), come with varying properties including hydrophobic thickness, intrinsic curvature, and lateral pressure profile[73, 74]. These lipids have shown a profound effect upon nucleation, crystal shape and diffraction in different targets[73]. This method originated from Ehud Landau and Jürg Rosenbusch in 1996 and was soon followed by application to bacteriorhodopsin[75, 76], the β2 adrenergic receptor[2], the chemokine receptor CXCR4[5], and the dopamine receptor D3[6].

It should be safe to assume that during the conditions of crystallogenesis, receptor molecules have to retain a certain level of freedom to diffuse so that nucleation and crystal growth can occur. As mentioned above, we learned that the lipidic cubic phase is composed of highly curved lipid bilayers and is connected by a water channel of a certain size[77]. As proteins diffuse through the cubic phase, they encounter horse saddles of high Gaussian curvature[78]. In some cases, one could find their protein stuck inside the lipid bilayers, either due to the energy barrier of crossing the horse saddle and the monkey saddle, or due to the limited size of the water channel. Several groups have tried to build a computational model, but they had little success[78, 79]. The reason for failure might be that there are several components in the crystallization trials, quite a few of which, such as salt, PEGs and trace amounts of detergent, could alter the dimensions or even the phase behav-

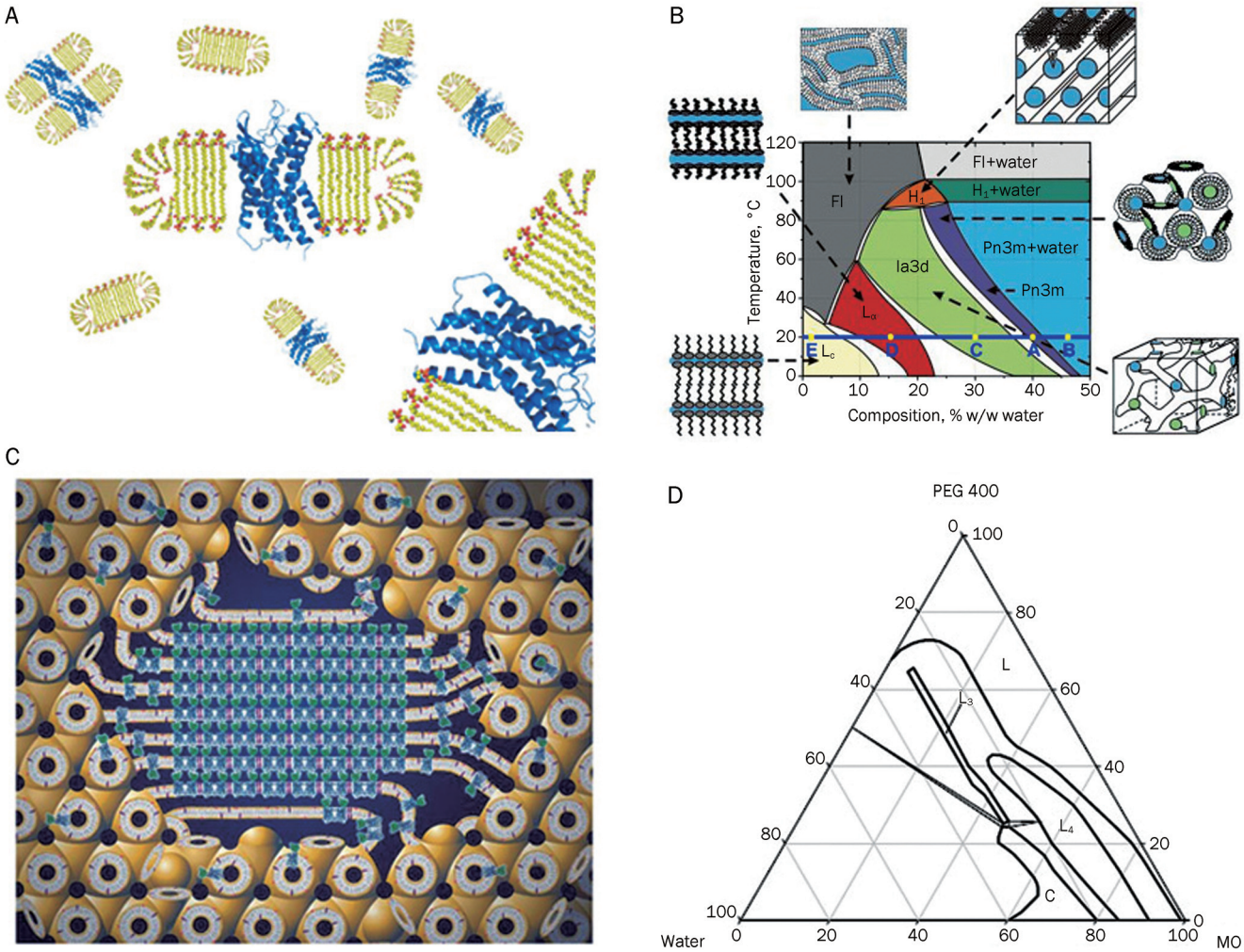

Figure 4. Phase diagram of lipidic cubic phase use Monoolein. A) A representative figure of GPCR in bicelle. The receptor is surrounded by a DMPC lipid bilayer, which is further covered by detergents. The receptor-lipid-detergent is afloat in the solution. D) the phase-temp diagram of Monoolein and water system[72], the phase will transit as lipid:water ratio or temperature change; C) crystallization of GPCRs in cubic phase, the receptor is in cartoon, the bicontinuous lipid bilayer is drawn in yellow and white and the dark blue represents the water channel and aqueous solution; D) Phase behavior of lipid-water-PEG400 system, representing the influences of additives and lipids on the phase[81].

ior of the whole system[80, 81] (Figure 4D).

Unlike the theoretical analysis, progress was made by experimental studies of the lipidic cubic phase guiding the crystallization studies. One powerful approach, fluorescence recovery after photobleaching (FRAP), seeks to assess the ability that GPCRs have while in the lipidic bilayer-based meso phase and identify conditions that favor diffusion in two dimensions as freely as possible to find other protein partners with which to build the two-dimensional array[82]. A major advance is the application of fluorescence to assay the diffusion rates, seeking conditions that maximize the diffusibility. Based on the FRAP method, high throughput FRAP (HT-FRAP), which combines traditional FRAP with an automation technique, was further developed and showed a dramatic advance in reducing the work load[83]. Instead of measuring the full recovery curve, the precise motion control allows it to scan a 96-well plate and compare exact spots at different time points, which increases the measurement efficiency by approximately 50 fold. This is a key element for the application of this technique to practical research. Using this method, one can now pre-screen host lipids, precipitant conditions, and identities of ligands with microgram quantities of material to magnify the chances of crystallogenesis and rule out conditions that are not conducive to diffusion, nucleation, and crystal growth[83]. LCP-Tm, another LCP tool to measure the stability of the receptor in the host's lipids without the use of labels, will also facilitate the screening of better constructs and ligands[84]. Assisted by different LCP tools, the variables of the multi-dimensional crystallization space are notably reduced, and thus, the bottleneck in obtaining initial crystal leads is substantially overcome.

Of course, like any other crystallization technique, the in meso method has its own drawbacks: it is relatively hard to handle, incompatible with some of the precipitants, rather small that are general invisible under cryo conditions. To

make things worse, to generate crystals of sufficient quality so that their structure may be obtained, the lipidic cubic phase generally requires a higher receptor concentration (>50 mg/mL)[2, 5, 6, 14], which challenges the already troubled expression and purification protocols of GPCRs. Most of the above obstacles are diminished by the development of robotic systems and microfocus beams. Robotic crystallization technologies, which can dispense subnanoliter-scale drops in 96-well plates within minutes, have expended the use of the lipidic cubic phase by substantially increasing the number of crystallization conditions that can be explored with limited amounts of sample[72, 85]. Another recent innovation is the microfocus beamline at synchrotrons[86], which makes data collection from the undersized GPCR crystals possible. Smaller X-ray beams, reduction of the diffraction background, and an increase in the beam intensity remarkably improve the resolution and the data statistics compared to the general synchrotron beams, and allow useful diffraction data to be extracted from smaller crystals[2, 86]. Although tighter focus comes at the cost of greater radiation damage to the crystal, it can be overcome by merging data from several or even tens of crystals[2, 6] (hundreds in some cases, data unpublished) and newer detectors[87]. Some other techniques, although not as essential as microfocus beams or crystallization robots, significantly improve research efficiency. Sample-exchange robots that allow crystals to be replaced without entering the experimental hutch are showing more and more impact on X-ray diffraction data collection. Rapid crystal alignment and raster tools will further accelerate the systematic screening of invisible crystals in the cryo loops, and more crystals could be tested in a shorter amount of time[88–90]. With the combination of the benefits from all the above techniques, the lipidic cubic phase is becoming the most popular method in determining the structures of GPCRs.

Future prospects

Structure-based drug design targeting of G-protein coupled receptors has long been limited by the availability of high-resolution receptor structures. However, this limitation is decreasing, as multiple GPCR structures have been determined. The year 2011 could be considered a new landmark for understanding this largest drug target family. In this year, not only have new GPCR structures been obtained, but also structures of activated receptors and even the magnificent structure of the GPCR-G protein complex. These structures, and the purified membrane proteins that are produced before the structures are resolved, will enable us to develop a rational approach to the treatment of cancer, autoimmune diseases, and infectious diseases that endanger human health. This new progress also indicates that we are starting to understand how GPCRs function in response to the binding of a natural ligand or a drug. This is also a direct result of the unremitting development of techniques during the last few years. The introduction of effective new tools for the membrane structural biologist reflects the ingenuity of the current researchers and lays the groundwork for applications to numerous diseases. It is safe to expect more structures in the near future as newer techniques, tools, chemicals and protocols will be applied to research that will further shorten the timeline and reduce the resources needed for solving a GPCR structure.

References

1 Palczewski K, Kumasaka T, Hori T, Behnke CA, Motoshima H, Fox BA, *et al*. Crystal structure of rhodopsin: A G protein-coupled receptor. Science 2000; 289: 739–45.
2 Cherezov V, Rosenbaum DM, Hanson MA, Rasmussen SG, Thian FS, Kobilka TS, *et al*. High-resolution crystal structure of an engineered human beta2-adrenergic G protein-coupled receptor. Science 2007; 318: 1258–65.
3 Jaakola VP, Griffith MT, Hanson MA, Cherezov V, Chien EY, Lane JR, *et al*. The 2.6 angstrom crystal structure of a human A_{2A} adenosine receptor bound to an antagonist. Science 2008; 322: 1211–7.
4 Warne T, Serrano-Vega MJ, Baker JG, Moukhametzianov R, Edwards PC, Henderson R, *et al*. Structure of a beta1-adrenergic G-protein-coupled receptor. Nature 2008; 454: 486–91.
5 Wu B, Chien EY, Mol CD, Fenalti G, Liu W, Katritch V, *et al*. Structures of the CXCR4 chemokine GPCR with small-molecule and cyclic peptide antagonists. Science 2010; 330: 1066–71.
6 Chien EY, Liu W, Zhao Q, Katritch V, Han GW, Hanson MA, *et al*. Structure of the human dopamine D3 receptor in complex with a D2/D3 selective antagonist. Science 2010; 330: 1091–5.
7 Shimamura T, Shiroishi M, Weyand S, Tsujimoto H, Winter G, Katritch V, *et al*. Structure of the human histamine H1 receptor complex with doxepin. Nature 2011; 475: 65–70.
8 Lundstrom K. Structural genomics of GPCRs. Trends Biotechnol 2005; 23: 103–8.
9 Bockenhauer S, Furstenberg A, Yao XJ, Kobilka B, Moerner WE. Conformational dynamics of single G protein-coupled receptors in solution. J Phys Chem B 2011; 115: 13328–38.
10 Rasmussen SG, Choi HJ, Fung JJ, Pardon E, Casarosa P, Chae PS, *et al*. Structure of a nanobody-stabilized active state of the $beta_2$ adrenoceptor. Nature 2011; 469: 175–80.
11 Rasmussen SG, DeVree BT, Zou Y, Kruse AC, Chung KY, Kobilka TS, *et al*. Crystal structure of the $beta_2$ adrenergic receptor-Gs protein complex. Nature 2011; 477: 549–55.
12 Park JH, Scheerer P, Hofmann KP, Choe HW, Ernst OP. Crystal structure of the ligand-free G-protein-coupled receptor opsin. Nature 2008; 454: 183–7.
13 Deupi X, Kobilka BK. Energy landscapes as a tool to integrate GPCR structure, dynamics, and function. Physiology (Bethesda) 2010; 25: 293–303.
14 Xu F, Wu H, Katritch V, Han GW, Jacobson KA, Gao ZG, *et al*. Structure of an agonist-bound human A_{2A} adenosine receptor. Science 2011; 332: 322–7.
15 Rosenbaum DM, Zhang C, Lyons JA, Holl R, Aragao D, Arlow DH, *et al*. Structure and function of an irreversible agonist-beta(2) adrenoceptor complex. Nature 2011; 469: 236–40.
16 Dore AS, Robertson N, Errey JC, Ng I, Hollenstein K, Tehan B, *et al*. Structure of the adenosine A_{2A} receptor in complex with ZM241385 and the xanthines XAC and caffeine. Structure 2011; 19: 1283–93.
17 Reeves PJ, Kim JM, Khorana HG. Structure and function in rhodopsin: a tetracycline-inducible system in stable mammalian cell lines for high-level expression of opsin mutants. Proc Natl Acad Sci U S A 2002; 99: 13413–8.
18 Kempf J, Snook LA, Vonesch JL, Dahms TE, Pattus F, Massotte D. Expression of the human mu opioid receptor in a stable Sf9 cell line. J Biotechnol 2002; 95: 181–7.

19 Hanson MA, Brooun A, Baker KA, Jaakola VP, Roth C, Chien EY, *et al*. Profiling of membrane protein variants in a baculovirus system by coupling cell-surface detection with small-scale parallel expression. Protein Expr Purif 2007; 56: 85–92.
20 Reilander H, Weiss HM. Production of G-protein-coupled receptors in yeast. Curr Opin Biotechnol 1998; 9: 510–7.
21 Kaushal S, Ridge KD, Khorana HG. Structure and function in rhodopsin: the role of asparagine-linked glycosylation. Proc Natl Acad Sci U S A 1994; 91: 4024–8.
22 Lagane B, Gaibelet G, Meilhoc E, Masson JM, Cezanne L, Lopez A. Role of sterols in modulating the human mu-opioid receptor function in *Saccharomyces cerevisiae*. J Biol Chem 2000; 275: 33197–200.
23 King K, Dohlman HG, Thorner J, Caron MG, Lefkowitz RJ. Control of yeast mating signal transduction by a mammalian beta 2-adrenergic receptor and Gs alpha subunit. Science 1990; 250: 121–3.
24 Payette P, Gossard F, Whiteway M, Dennis M. Expression and pharmacological characterization of the human M1 muscarinic receptor in *Saccharomyces cerevisiae*. FEBS Lett 1990; 266: 21–5.
25 Talmont F, Sidobre S, Demange P, Milon A, Emorine LJ. Expression and pharmacological characterization of the human mu-opioid receptor in the methylotrophic yeast *Pichia pastoris*. FEBS Lett 1996; 394: 268–72.
26 Beukers MW, Klaassen CH, De Grip WJ, Verzijl D, Timmerman H, Leurs R. Heterologous expression of rat epitope-tagged histamine H2 receptors in insect Sf9 cells. Br J Pharmacol 1997; 122: 867–74.
27 Weiss HM, Haase W, Reilander H. Expression of an integral membrane protein, the $5HT_{5A}$ receptor. Methods Mol Biol 1998; 103: 227–39.
28 Sarramegna V, Talmont F, Seree de Roch M, Milon A, Demange P. Green fluorescent protein as a reporter of human mu-opioid receptor overexpression and localization in the methylotrophic yeast *Pichia pastoris*. J Biotechnol 2002; 99: 23–39.
29 Mollaaghababa R, Davidson FF, Kaiser C, Khorana HG. Structure and function in rhodopsin: expression of functional mammalian opsin in *Saccharomyces cerevisiae*. Proc Natl Acad Sci U S A 1996; 93: 11482–6.
30 Asada H, Uemura T, Yurugi-Kobayashi T, Shiroishi M, Shimamura T, Tsujimoto H, *et al*. Evaluation of the pichia pastoris expression system for the production of GPCRs for structural analysis. Microb Cell Fact 2011; 10: 24.
31 O'Malley MA, Mancini JD, Young CL, McCusker EC, Raden D, Robinson AS. Progress toward heterologous expression of active G-protein-coupled receptors in *Saccharomyces cerevisiae*: Linking cellular stress response with translocation and trafficking. Protein Sci 2009; 18: 2356–70.
32 Shukla AK, Haase W, Reinhart C, Michel H. Heterologous expression and comparative characterization of the human neuromedin U subtype II receptor using the methylotrophic yeast *Pichia pastoris* and mammalian cells. Int J Biochem Cell Biol 2007; 39: 931–42.
33 Butz JA, Niebauer RT, Robinson AS. Co-expression of molecular chaperones does not improve the heterologous expression of mammalian G-protein coupled receptor expression in yeast. Biotechnol Bioeng 2003; 84: 292–304.
34 Zhang R, Kim TK, Qiao ZH, Cai J, Pierce WM Jr, Song ZH. Biochemical and mass spectrometric characterization of the human CB2 cannabinoid receptor expressed in *Pichia pastoris* — importance of correct processing of the N-terminus. Protein Expr Purif 2007; 55: 225–35.
35 Bertin B, Freissmuth M, Breyer RM, Schutz W, Strosberg AD, Marullo S. Functional expression of the human serotonin $5\text{-}HT_{1A}$ receptor in *Escherichia coli*. Ligand binding properties and interaction with recombinant G protein alpha-subunits. J Biol Chem 1992; 267: 8200–6.
36 Grisshammer R, Duckworth R, Henderson R. Expression of a rat neurotensin receptor in *Escherichia coli*. Biochem J 1993; 295: 571–6.
37 Serrano-Vega MJ, Magnani F, Shibata Y, Tate CG. Conformational thermostabilization of the beta1-adrenergic receptor in a detergent-resistant form. Proc Natl Acad Sci U S A 2008; 105: 877–82.
38 Sarkar CA, Dodevski I, Kenig M, Dudli S, Mohr A, Hermans E, *et al*. Directed evolution of a G protein-coupled receptor for expression, stability, and binding selectivity. Proc Natl Acad Sci U S A 2008; 105: 14808–13.
39 Dodevski I, Pluckthun A. Evolution of three human GPCRs for higher expression and stability. J Mol Biol 2011; 408: 599–615.
40 Rosenbaum DM, Cherezov V, Hanson MA, Rasmussen SG, Thian FS, Kobilka TS, *et al*. GPCR engineering yields high-resolution structural insights into beta2-adrenergic receptor function. Science 2007; 318: 1266–73.
41 Alexandrov AI, Mileni M, Chien EY, Hanson MA, Stevens RC. Microscale fluorescent thermal stability assay for membrane proteins. Structure 2008; 16: 351–9.
42 Rasmussen SG, Choi HJ, Rosenbaum DM, Kobilka TS, Thian FS, Edwards PC, *et al*. Crystal structure of the human beta2 adrenergic G-protein-coupled receptor. Nature 2007; 450: 383–7.
43 Ballesteros J, Weinstein H. Integrated methods for the construction of three-dimensional models and computational probing of structure-function relations in G protein-coupled receptors. Methods Neurosci 1995; 25: 366–428.
44 Roth CB, Hanson MA, Stevens RC. Stabilization of the human beta2-adrenergic receptor TM4-TM3-TM5 helix interface by mutagenesis of Glu122(3.41), a critical residue in GPCR structure. J Mol Biol 2008; 376: 1305–19.
45 Lebon G, Bennett K, Jazayeri A, Tate CG. Thermostabilisation of an agonist-bound conformation of the human adenosine A_{2A} receptor. J Mol Biol 2011; 409: 298–310.
46 Shibata Y, White JF, Serrano-Vega MJ, Magnani F, Aloia AL, Grisshammer R, *et al*. Thermostabilization of the neurotensin receptor NTS1. J Mol Biol 2009; 390: 262–77.
47 Hong WX, Baker KA, Ma X, Stevens RC, Yeager M, Zhang Q. Design, synthesis, and properties of branch-chained maltoside detergents for stabilization and crystallization of integral membrane proteins: human connexin 26. Langmuir 2010; 26: 8690–6.
48 Chae PS, Rasmussen SG, Rana RR, Gotfryd K, Chandra R, Goren MA, *et al*. Maltose-neopentyl glycol (MNG) amphiphiles for solubilization, stabilization and crystallization of membrane proteins. Nat Methods 2010; 7: 1003–8.
49 Bayburt TH, Sligar SG. Self-assembly of single integral membrane proteins into soluble nanoscale phospholipid bilayers. Protein Sci 2003; 12: 2476–81.
50 Nath A, Atkins WM, Sligar SG. Applications of phospholipid bilayer nanodiscs in the study of membranes and membrane proteins. Biochemistry 2007; 46: 2059–69.
51 Tribet C, Audebert R, Popot JL. Amphipols: polymers that keep membrane proteins soluble in aqueous solutions. Proc Natl Acad Sci U S A 1996; 93: 15047–50.
52 Gorzelle BM, Hoffman AK, Keyes MH, Gray DN, Ray DG, Sanders CR. Amphipols can support the activity of a membrane enzyme. J Am Chem Soc 2002; 124: 11594–5.
53 Breyton C, Pucci B, Popot JL. Amphipols and fluorinated surfactants: Two alternatives to detergents for studying membrane proteins *in vitro*. Methods Mol Biol 2010; 601: 219–45.

54 Schafmeister CE, Miercke LJ, Stroud RM. Structure at 2.5 A of a designed peptide that maintains solubility of membrane proteins. Science 1993; 262: 734–8.
55 McGregor CL, Chen L, Pomroy NC, Hwang P, Go S, Chakrabartty A, *et al*. Lipopeptide detergents designed for the structural study of membrane proteins. Nat Biotechnol 2003; 21: 171–6.
56 Kiley P, Zhao X, Vaughn M, Baldo MA, Bruce BD, Zhang S. Self-assembling peptide detergents stabilize isolated photosystem I on a dry surface for an extended time. PLoS Biol 2005; 3: e230.
57 Barthelemy P, Ameduri B, Chabaud E, Popot JL, Pucci B. Synthesis and preliminary assessments of ethyl-terminated perfluoroalkyl nonionic surfactants derived from tris(hydroxymethyl)acrylamidomethane. Org Lett 1999; 1: 1689–92.
58 McQuade DT, Quinn MA, Yu SM, Polans AS, Krebs MP, Gellman SH. Rigid amphiphiles for membrane protein manipulation. Angew Chem Int Ed Engl 2000; 39: 758–61.
59 Chae PS, Wander MJ, Bowling AP, Laible PD, Gellman SH. Glycotripod amphiphiles for solubilization and stabilization of a membrane-protein superassembly: importance of branching in the hydrophilic portion. Chembiochem 2008; 9: 1706–9.
60 Zhang Q, Ma X, Ward A, Hong WX, Jaakola VP, Stevens RC, *et al*. Designing facial amphiphiles for the stabilization of integral membrane proteins. Angew Chem Int Ed Engl 2007; 46: 7023–5.
61 Chae PS, Gotfryd K, Pacyna J, Miercke LJ, Rasmussen SG, Robbins RA, *et al*. Tandem facial amphiphiles for membrane protein stabilization. J Am Chem Soc 2010; 132: 16750–2.
62 Wu H, Su K, Guan X, Sublette ME, Stark RE. Assessing the size, stability, and utility of isotropically tumbling bicelle systems for structural biology. Biochim Biophys Acta 2010; 1798: 482–8.
63 Faham S, Bowie JU. Bicelle crystallization: a new method for crystallizing membrane proteins yields a monomeric bacteriorhodopsin structure. J Mol Biol 2002; 316: 1–6.
64 Arnold A, Labrot T, Oda R, Dufourc EJ. Cation modulation of bicelle size and magnetic alignment as revealed by solid-state NMR and electron microscopy. Biophys J 2002; 83: 2667–80.
65 Faham S, Boulting GL, Massey EA, Yohannan S, Yang D, Bowie JU. Crystallization of bacteriorhodopsin from bicelle formulations at room temperature. Protein Sci 2005; 14: 836–40.
66 Bayburt TH, Sligar SG. Membrane protein assembly into Nanodiscs. FEBS Lett 2010; 584: 1721–7.
67 Borch J, Hamann T. The nanodisc: a novel tool for membrane protein studies. Biol Chem 2009; 390: 805–14.
68 Leitz AJ, Bayburt TH, Barnakov AN, Springer BA, Sligar SG. Functional reconstitution of beta2-adrenergic receptors utilizing self-assembling Nanodisc technology. Biotechniques 2006; 40: 601–2.
69 Borch J, Roepstorff P, Moller-Jensen J. Nanodisc-based co-immunoprecipitation for mass spectrometric identification of membrane-interacting proteins. Mol Cell Proteomics 2011; 10: 0110.006775.
70 Wohri AB, Johansson LC, Wadsten-Hindrichsen P, Wahlgren WY, Fischer G, Horsefield R, *et al*. A lipidic-sponge phase screen for membrane protein crystallization. Structure 2008; 16: 1003–9.
71 Caffrey M. Crystallizing membrane proteins for structure determination: use of lipidic mesophases. Annu Rev Biophys 2009; 38: 29–51.
72 Caffrey M, Cherezov V. Crystallizing membrane proteins using lipidic mesophases. Nat Protoc 2009; 4: 706–31.
73 Li D, Lee J, Caffrey M. Crystallizing membrane proteins in lipidic mesophases. A host lipid screen. Cryst Growth Des 2011; 11: 530–7.
74 Qiu H, Caffrey M. Lyotropic and thermotropic phase behavior of hydrated monoacylglycerols: structure characterization of monovaccenin. J Phys Chem B 1998; 102: 4819–29.
75 Landau EM, Rosenbusch JP. Lipidic cubic phases: a novel concept for the crystallization of membrane proteins. Proc Natl Acad Sci U S A 1996; 93: 14532–5.
76 Pebay-Peyroula E, Rummel G, Rosenbusch JP, Landau EM. X-ray structure of bacteriorhodopsin at 2.5 angstroms from microcrystals grown in lipidic cubic phases. Science 1997; 277: 1676–81.
77 Cherezov V, Clogston J, Papiz MZ, Caffrey M. Room to move: crystallizing membrane proteins in swollen lipidic mesophases. J Mol Biol 2006; 357: 1605–18.
78 Grabe M, Neu J, Oster G, Nollert P. Protein interactions and membrane geometry. Biophys J 2003; 84: 854–68.
79 Templer RH, Seddon JM, Duesing PM. Modeling the phase behavior of the inverse hexagonal and inverse bicontinuous cubic phases in 2:1 fatty acid/phosphatidylcholine mixtures. J Phys Chem B 1998; 102: 7262–71.
80 Misquitta Y, Caffrey M. Detergents destabilize the cubic phase of monoolein: implications for membrane protein crystallization. Biophys J 2003; 85: 3084–96.
81 Wadsten-Hindrichsen P, Bender J, Unga J, Engstrom S. Aqueous self-assembly of phytantriol in ternary systems: effect of monoolein, distearoylphosphatidylglycerol and three water-miscible solvents. J Colloid Interface Sci 2007; 315: 701–13.
82 Cherezov V, Liu J, Griffith M, Hanson MA, Stevens RC. LCP-FRAP assay for pre-screening membrane proteins for in meso crystallization. Cryst Growth Des 2008; 8: 4307–15.
83 Xu F, Liu W, Hanson MA, Stevens RC, Cherezov V. Development of an automated high throughput LCP-FRAP assay to guide membrane protein crystallization in lipid mesophases. Cryst Growth Des 2011; 11: 1193–201.
84 Liu W, Hanson MA, Stevens RC, Cherezov V. LCP-Tm: an assay to measure and understand stability of membrane proteins in a membrane environment. Biophys J 2010; 98: 1539–48.
85 Cherezov V, Peddi A, Muthusubramaniam L, Zheng YF, Caffrey M. A robotic system for crystallizing membrane and soluble proteins in lipidic mesophases. Acta Crystallogr D Biol Crystallogr 2004; 60: 1795–807.
86 Bowler MW, Guijarro M, Petitdemange S, Baker I, Svensson O, Burghammer M, *et al*. Diffraction cartography: applying microbeams to macromolecular crystallography sample evaluation and data collection. Acta Crystallogr D Biol Crystallogr 2010; 66: 855–64.
87 Kraft P, Bergamaschi A, Broennimann C, Dinapoli R, Eikenberry EF, Henrich B, *et al*. Performance of single-photon-counting PILATUS detector modules. J Synchrotron Radiat 2009; 16: 368–75.
88 Cherezov V, Hanson MA, Griffith MT, Hilgart MC, Sanishvili R, Nagarajan V, *et al*. Rastering strategy for screening and centring of microcrystal samples of human membrane proteins with a sub-10 microm size X-ray synchrotron beam. J R Soc Interface 2009; 6: S587–97.
89 Mader K, Marone F, Hintermuller C, Mikuljan G, Isenegger A, Stampanoni M. High-throughput full-automatic synchrotron-based tomographic microscopy. J Synchrotron Radiat 2011; 18: 117–24.
90 Joachimiak A. High-throughput crystallography for structural genomics. Curr Opin Struct Biol 2009; 19: 573–84.

Acta Pharmacologica Sinica (2012) 33: 335–341
 1671-4083/12 $32.00
www.nature.com/aps

Review

β-Adrenergic receptor subtype signaling in heart: From bench to bedside

Anthony Yiu Ho WOO[1, 2], Rui-ping XIAO[1, 2, *]

[1]*Institute of Molecular Medicine, Center for Life Sciences, Peking University, Beijing 100871, China;* [2]*Drug Discovery Center, School of Chemical Biology and Biotechnology, Peking University Shenzhen Graduate School, Shenzhen 518055, China*

β-Adrenergic receptor (βAR) stimulation by the sympathetic nervous system or circulating catecholamines is broadly involved in peripheral blood circulation, metabolic regulation, muscle contraction, and central neural activities. In the heart, acute βAR stimulation serves as the most powerful means to regulate cardiac output in response to a fight-or-flight situation, whereas chronic βAR stimulation plays an important role in physiological and pathological cardiac remodeling.

There are three βAR subtypes, β_1AR, β_2AR and β_3AR, in cardiac myocytes. Over the past two decades, we systematically investigated the molecular and cellular mechanisms underlying the different even opposite functional roles of β_1AR and β_2AR subtypes in regulating cardiac structure and function, with keen interest in the development of novel therapies based on our discoveries. We have made three major discoveries, including (1) dual coupling of β_2AR to G_s and G_i proteins in cardiomyocytes, (2) cardioprotection by β_2AR signaling in improving cardiac function and myocyte viability, and (3) PKA-independent, CaMKII-mediated β_1AR apoptotic and maladaptive remodeling signaling in the heart. Based on these discoveries and salutary effects of β_1AR blockade on patients with heart failure, we envision that activation of β_2AR in combination with clinically used β_1AR blockade should provide a safer and more effective therapy for the treatment of heart failure.

Keywords: β-adrenergic receptor; heart failure; signal transduction; cardiovascular system

Acta Pharmacologica Sinica (2012) 33: 335–341; doi: 10.1038/aps.2011.201; published online 30 Jan 2012

Introduction

Heart failure (HF) is a syndrome characterized by the insufficient pumping of blood to meet the need of the body. It is a chronic and severely debilitating disease with people older than 65 composed more than 75% of all cases[1]. Regardless of the cause, the failing heart usually ends up in a viscous cycle of progressive functional decline. Owing to its high prevalence, morbidity, mortality and significant health-care costs, HF represents a major current health problem in China and its prevalence is in an upward trend as atherothrombotic diseases, which often lead to HF, will be the first cause of death in the world by 2020[2].

In congestive HF, both the activities of the sympathetic nervous system and the renin-angiotensin system (RAS) are increased[3]. Initially, the increased activity of these neurohormonal systems serves to compensate for the reduced blood pressure and cardiac output. But long term exposure to high levels of circulating catecholamines and angiotensin increases the workload of the heart, and causes maladaptive cardiac remodeling and myocyte death[4–6]. Many of these effects appear to be mediated by the signal transduction cascades of the receptors involved.

β-Adrenergic receptor (βAR) and angiotensin receptor belong to the superfamily of G protein-coupled receptors (GPCRs) or seven transmembrane receptors. GPCRs constitute the most ubiquitous of plasma membrane receptors. They are involved in the regulation of many important physiological functions and also serve as the most important drug targets[7]. Over the past 25 years, βAR antagonists (β-blockers), angiotensin converting enzyme inhibitors (ACEIs) and angiotensin II receptor blockers (ARBs), alone or in combination, have been used to treat HF conditions. Their use ameliorates the deterioration of left ventricular function, improves symptoms and hemodynamics, and decreases the mortality rate and the need for hospitalization[8–11]. However, these therapeutic agents have limited effectiveness in some patient populations and they also have some adverse effects. Therefore, there is a compelling need to develop new treatments that can improve clinical outcomes.

* To whom correspondence should be addressed.
E-mail xiaor@pku.edu.cn
Received 2011-11-16 Accepted 2011-12-19

Subtype-specific βAR signaling in the heart

βARs exist as three subtypes, β_1, β_2, and β_3, and the former two are important in the regulation of excitation-contraction coupling of myocardium. β_1AR is the predominant receptor subtype expressed in the heart. Its stimulation results in the activation of the G_s-adenylyl cyclase (AC)-cAMP-protein kinase A (PKA) signaling cascade. In ventricular myocytes, the phosphorylation of PKA substrates including phospholamben, *L*-type calcium channel, ryanodine receptor, cardiac troponin I, and cardiac myosin-binding protein C results in the increase in calcium transient and contractility. In pacemaker cells, PKA-mediated phosphorylation of membrane ion channels and Ca^{2+} handling proteins increases Ca^{2+} cycling and pacing rate. Similarly, β_2AR also has a functional role in cardiomyocyte contraction[12]. But unlike β_1AR which couples only to G_s, β_2AR also couples to pertussis toxin (PTX)-sensitive G_i proteins[13]. The β_2AR-G_i signaling has negative effects on AC activity, cAMP synthesis, PKA activation, and the inotropic response mediated by G_s.

Importantly, persistent stimulation of β_1AR and β_2AR exhibits distinct outcomes under certain pathological circumstances such as HF. Specifically, persistent stimulation of β_1AR triggers cardiomyocyte apoptosis by a Ca^{2+}/calmodulin-dependent kinase II (CaMKII)-dependent, but PKA independent mechanism[14]. Furthermore, the β_1AR-activated CaMKII signaling, but not the PKA pathway, is involved in catecholamine-induced cardiomyocyte hypertrophy *in vitro*[15] and maladaptive cardiac remodeling *in vivo*[16, 17]. In contrast to the cardiotoxic effects of persistent β_1AR activation, persistent β_2AR stimulation is cardioprotective. The cardioprotective effect of persistent β_2AR signaling is largely mediated by β_2AR-G_i coupling, which activates the $G_{\beta\gamma}$-phosphoinositol 3-kinase (PI3K)-Akt cell survival pathway[18]. Although beneficial in terms of cardiomyocyte viability, the protective effect of β_2AR comes at the cost of compromised contractile support.

Heart failure-associated alterations in βAR signaling

During HF, β_1AR is persistently downregulated at the mRNA and protein levels[19, 20]. Its density on the plasma membrane is reduced by 50%, while that of β_2AR has no such change[21]. The resulting change in the ratio of β_1/β_2AR from an 80:20 distribution in the healthy heart to a ratio of 60:40 in the failing heart may indicate the prominent role of β_2AR signaling in the disease condition. In the failing heart, the selective downregulation of β_1AR is often associated with an upregulation of G_i and an enhanced β_2AR-G_i signaling[22, 23]. Importantly, the β_1AR-mediated contractile response is cross-inhibited by the enhanced β_2AR-G_i signaling in the failing heart. Thus, the enhanced β_2AR-G_i signaling contributes to the dysfunction of both β_1AR- and β_2AR-G_s signaling in the failing heart[24–27].

In addition, the signaling efficiency of β_1AR is also markedly reduced in the failing heart as a result of desensitization[28]. This is attributed, in part, to a significant increase in the expression level of G protein coupled receptor kinase 2 (GRK2)[29], the prototypical member of the GRK family. The process of βAR desensitization involves a series of events, including (a) the translocation of GRK2 to the plasma membrane facilitated by the free $G_{\beta\gamma}$ subunits liberated from the activated heterotrimeric G proteins[30], (b) the phosphorylation of the serine or threonine residues on the C-terminal tail of βARs by GRK2, (c) the recruitment of β-arrestins to the phosphorylated receptor, the physical displacement of $G_{s\alpha}$ from the β-arrestin-associated receptor, and (d) the β-arrestin-dependent internalization of the receptor (endocytosis)[31]. While β_2AR stays at a similar level in the failing heart, its coupling efficiency to G_s is markedly reduced[21]. Desensitization of βARs leads to reduced G_s-mediated responses such as cAMP production and positive inotropic effect. Although receptor downregulation and desensitization are considered to be protective responses against excessive sympathetic stimulation during HF[32, 33], the resultant abnormality in βAR signaling may lead to the activation of signaling pathways that are involved in cardiac remodeling, such as the PI3K cascades[34].

Indeed, in humans or animal models with HF, chronic catecholamine elevation causes marked dysregulation of βARs, resulting in various molecular abnormalities, including the upregulation of GRK2[29, 35] and G_i proteins[22, 23, 36]. Upregulation of both of these proteins have been implicated as causal factors in the development of HF. In particular, GRK2 is the most abundant and best-characterized GRK in the heart[37]. GRK2 expression and activity are markedly elevated and play a central role in the HF-associated defect in βAR signaling[38] and cardiac dysfunction[39]. Myocardial ischemia and hypertension in humans and animal models have also been associated with elevated GRK2 expression and activity[40, 41]. These previous studies have defined GRK2 upregulation as an early common event in cardiac maladaptive remodeling and HF.

Emerging evidence suggests that activation of GRK2 as well as PKA is essentially involved in the activation of the β_2AR-coupled G_i signaling in mammalian cells. First, early work has shown that β_2AR-induced activation of ERK1/2 in HEK293 cells is mediated by a G_i-dependent mechanism, and that phosphorylation of β_2AR by PKA is a prerequisite for the switch of the receptor coupling from G_s to G_i[42]. Second, our recent studies[43] have demonstrated that elevated β_2AR phosphorylation by GRK2 acerbates the G_i signaling, whereas inhibition of GRK2 activity profoundly suppresses the β_2AR-G_i coupling. Since GRK2 upregulation occurs prior to the onset of HF and contributes to the development of HF[44, 45], enhanced GRK2 activation may play an important role in the exacerbated β_2AR-coupled G_i signaling in the failing heart. Indeed, disruption of G_i signaling with PTX or inhibition of GRK2 with a peptide inhibitor, βARK-ct, can restore cardiac contractile response to βAR stimulation in multiple HF models[46–49].

Importantly, cardiac-specific transgenic overexpression of a mutant β_2AR lacking PKA phosphorylation sites (PKA-TG), but not the wild type β_2AR (WT TG) or a mutant β_2AR lacking GRK sites (GRK-TG), led to exaggerated cardiac response to pressure overload, as manifested by markedly exacerbated cardiac maladaptive remodeling and failure, and early mortality[43]. Furthermore, inhibition of G_i signaling with PTX

restores cardiac function in HF associated with increased β_2AR to G_i coupling induced by removing PKA phosphorylation of the receptor and in GRK2 transgenic mice, indicating that enhanced phosphorylation of β_2AR by GRK and resultant increase in G_i-biased β_2AR signaling play an important role in the development of HF[43]. Altogether, our recent studies have demonstrated that enhanced β_2AR phosphorylation by GRK leads the receptor to G_i-biased signaling which, in turn, contributes to the pathogenesis of HF, marking G_i-biased β_2AR signaling as a primary event linking pathological upregulation of GRK to cardiac maladaptive remodeling, failure and cardiodepression. It is also noteworthy that, as is the case in the failing heart, enhanced β_2AR-coupled G_i signaling is responsible for the defects of both β_1AR and β_2AR signaling in the GRK2 transgenic mice[43], and that the previously reported beneficial effects of βARK-ct in improving the function of the failing heart[38, 39, 50-52] is mediated, at least in part, by attenuating GRK-dependent G_i-biased β_2AR signaling.

Carvedilol paradox

In clinical settings, long-term use of β-blockers improves clinical symptom of HF. Treatment with β-blockers improves left ventricular contractile function in the failing heart and reverses cardiac remodeling[8, 9]. In the molecular level, β-blockade may normalize βAR system through the upregulation of β_1AR[53] and the restoration of receptor sensitivity by decreasing the expression of GRK2[50]. However, the effects of different β-blockers are not identical. The use of subtype non-selective β-blockers in early years has caused some major side effects including bronchial and blood vessel constriction[54, 55]. This is largely due to the inhibition of β_2AR in non-cardiac tissues such as the respiratory system and blood vessels. These problems have been partially resolved with the introduction of selective β_1AR antagonists, such as atenolol, metoprolol, bisoprolol and nebivolol. Recent clinical trials have indicated that only 3 out of 16 β-blockers are beneficial in terms of cardiovascular survival[9, 56–58], with carvedilol emerging as the best[59].

Apart from being a non-selective β-blocker, carvedilol also has several properties, such as α_1-adrenergic blockade, anti-oxidant, anti-proliferative, anti-endothelin and anti-arrythmogenic effects[60, 61], which may explain its higher efficacy. Interestingly, carvedilol has been found to be the only one among 16 blockers that activated ERK by a β_2AR-mediated, G protein-independent, and β-arrestin-dependent mechanism[62]. Moreover, among 20 β-blockers tested, only atenolol and carvedilol could induce the β_1AR-mediated transactivation of EGFR and this effect is also β-arrestin-dependent[63]. It has been implicated that this effect may contribute to the special therapeutic effect of carvedilol. In this regard, recent studies have shown that β-arrestin-dependent, G protein-independent activation of EGFR via β_1AR confers cardioprotection in mice chronically stimulated with catecholamine[64]. These data suggest that a ligand can antagonize the G protein-dependent activity of a GPCR and at the same time stimulates signaling pathways in a G protein-independent β-arrestin-dependent fashion[65]. They are also of great relevance to our discussion in the next section about the application of this principle in the development of novel therapeutic agents.

Biased βAR signaling and drug discovery

In the classical paradigm of GPCR signaling, ligand binding leads to conformational change of the receptor from an inactive state R into a single activated state R* that results in the coupling of the receptor to heterotrimeric G proteins. Receptor coupling facilitates the exchange of the bound GDP with GTP in the α subunit of the G protein complex. This triggers dissociation of the complex into G_α and $G_{\beta\gamma}$ subunits. They go on to activate their respective effectors such as AC, phospholipases and ion channels. These receptor mediated reactions often generate signaling molecules called second messengers which activate or inhibit other components of the cellular machinery. Thus, receptor stimulation produces a multitude of cellular responses via the activation of the signal transduction pathways downstream of G proteins. Agonist efficacy, a measure of the ability of an agonist to activate this cascade, quantitatively defines the agonist as partial or full. In this scheme, antagonist is defined as a ligand which binds to the receptor but produces no receptor activation and thus has the ability to block agonist-stimulated G protein activation. This unidirectional understanding of agonist efficacy is contradictory to the aforementioned findings that a ligand for a single GPCR can be an antagonist for the G protein-dependent signals and also an agonist for the β-arrestin-dependent signals[62, 63].

Over the past fifteen years, more and more evidence has accumulated indicating that a ligand for a given GPCR does not simply possess a single defined efficacy. Rather, a ligand possesses multiple efficacies, depending on the downstream signal transduction pathways analyzed. Moreover, GPCR can be differentially activated to target a specific subset of signal transduction pathways by the so-called "biased ligand". In particular, research has revealed that GPCR can be stimulated to produce a β-arrestin-dependent but G protein-independent signal, which differs both spatially and temporally from the β-arrestin-mediated signal stemmed from receptor desensitization[66]. It is believed that the β-arrestin-biased ligand activates the alternative signaling pathway by stabilizing the receptor in a distinct active conformation R*'. Thus, in this new paradigm, GPCR may be stabilized by different ligands in distinct active conformations R^{*1}-R^{*n} each capable of activating a diverse array of signal transduction pathways and responses (Figure 1). This concept, described as functional selectivity, collateral/pluridimensional efficacy, or biased agonism, has major implications for pharmacological therapeutics[65, 67–70].

To add another layer of complexity to this scheme, the signal trafficked by a biased agonist is context-dependent, too. Not only does the selectivity of a ligand towards different signaling pathways change in different cell types, the change in the levels of cytosolic reactants of GPCR also has an impact on the functional selectivity of a ligand. For example, the specific β_2AR antagonist ICI-118551 has been suggested to directly produce a negative inotropic effect by acting as an agonist for the G_i-coupled β_2AR in myocytes from failing human heart[71].

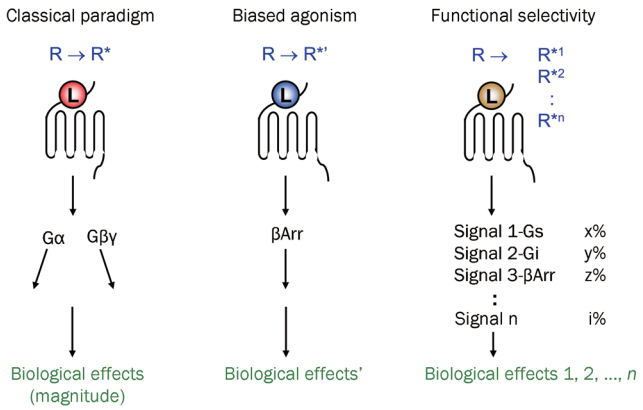

Figure 1. Development of the receptor theory. In the classical paradigm, ligands have linear efficacies, referring to their abilities to stabilize the receptor into a single active state. The emerging concept of biased agonism suggests that a biased ligand may stabilize the receptor into a distinct active state that does not activate G proteins but activates β-arrestins. In the concept of functional selectivity, receptors may exist in multiple active conformations as stabilized by different ligands, and each of these conformations gives rise to different downstream signals and biological effects. βArr, β-arrestin; L, ligand; R, inactive conformation of GPCR; R*, active conformation of GPCR.

This effect is not due to the blocking of the endogenous catecholamines and is also different in principle from an inverse agonistic effect also described for this ligand[72]. It is because this negative inotropic effect of ICI-118551 is PTX-sensitive, is observable at receptor levels with or without overexpression manipulation, and only becomes apparent under the conditions when the levels of G_i are raised.

In a recent study using a cardiomyocyte model[49], we have screened a panel of β_2AR agonists, including zinterol, salbutamol, and procaterol for their receptor-mediated contractility stimulatory activities and the sensitivities of these effects towards PTX. We have found that PTX augmented the contractile responses of most β_2AR agonists but not that of fenoterol. These data indicates that while most β_2AR agonists activate both G_s and G_i, fenoterol selectively activates G_s. This is the first evidence to show that different agonists can activate a receptor to couple to different G-proteins. It was further found that fenoterol fully reversed the diminished β_2AR-mediated inotropic effect in cardiomyocytes isolated from failing spontaneous hypertensive rat hearts even in the absence of PTX. This study is particularly valuable in that fenoterol was identified to be a unique agonist capable of selectively stabilizing the coupled β_2AR-G_s species in conditions that favor β_2AR-G_i coupling. It also reveals the therapeutic potential of fenoterol in the treatment of HF.

The effectiveness of fenoterol in treating HF conditions has been demonstrated in a number of follow-up *in vivo* studies[73–76]. Prolonged use of fenoterol not only improves cardiac function, but also retards cardiac maladaptive remodeling, and that the overall beneficial effects of fenoterol are greater than the salutary effects of β_1AR blockade in a myocardial infarction induced rat model of dilated cardiomyopathy[73]. These studies suggest that selective activation of the β_2-AR-coupled G_s signaling may provide a useful therapeutic target for the treatment of congestive HF. We envision that new G_s-biased β_2AR agonists, such as fenoterol and its derivatives, may be developed into drugs to improve the structure and function of the failing heart.

Fenoterol contains two chiral centers and can exist as four stereoisomers. We have synthesized a cohort of fenoterol derivatives including the *R,R*-, *R,S*-, *S,R*-, and *S,S*-isomers[77, 78]. While the pharmaceutical preparation of fenoterol is a racemic mixture of its *R,R*- and *S,S*-enantiomers, our recent studies have shown that the *R,R*-enantiomer is the only active isomer in receptor binding and cardiomyocyte contraction assays[77, 78]. It has been known for a century that stereoisomers of catecholamines differ in their potency and efficacy. However, the molecular basis for the differences in the efficacies of GPCR ligand stereoisomers has remained poorly defined. We have, therefore, used some of these fenoterol derivatives to examine the hypothesis that the stereochemistry of an agonist determines functional selectivity of a given receptor coupling to different G protein(s) and resultant activation of subset(s) of downstream signaling pathways[79]. We found that while R,R-fenoterol failed to activate G_i signaling, as evidenced by the absence of PTX-sensitivity of its contractile response and its inability to activate G_i-dependent ERK1/2 signaling, S,R-fenoterol exhibited a robust PTX-sensitivity in these responses, suggesting that the S,R-isomer enables β_2AR to activate both G_s and G_i. The same conclusion holds true for some fenoterol derivatives. For instance, S,R-methoxyfenoterol, but not R,R-methoxyfenoterol, activated β_2AR-coupled G_i signaling in cardiomyocytes[79]. Thus, in addition to receptor subtype and phosphorylation status, the different stereoisomers of an agonist selectively activate distinct receptor-G protein interactions and downstream signaling events. This finding is important because it is the first account to show that even the subtle chemical differences within a ligand stereoisomer pair are sufficient to stabilize GPCR conformations with distinct G-protein coupling properties, highlighting how important it is to carefully examine both the "active" and the "inactive" stereoisomer to understand the exact mechanism of action and cellular effects of a GPCR ligand[80].

This finding also has important clinical implications. In particular, it has been shown that long-term (1 year) treatment with racemic fenoterol enhances the beneficial effect of β_1AR blockade with metoprolol in a rat model of dilated cardiomyopathy[75], and the combined (fenoterol+metoprolol) therapy is as good as the clinical combination (metoprolol+ACEI) treatment with respect to mortality, and exceeds the latter with respect to cardiac remodeling and myocardial infarct expansion[76]. It will be interesting to study the effects of different fenoterol derivatives[77, 78, 81] alone or in combination with β_1AR blocker or RAS inhibitor in this model. Continued efforts on this research line may lead to the development of potential novel therapies with greater selectivity, efficacy and fewer side

effects for human congestive HF. Topics related to the translation of this novel treatment regimen have been discussed extensively in another recent review[82], which also contains a pathway map for βAR subtype signaling described in this article.

If suppression of β_2AR-G_i signaling or enhancement of β_2AR-G_s signaling is beneficial in HF, the next question is: what is the difference between β_2AR-G_s signaling and β_1AR-G_s signaling? In a recent elegant study[83], Mangmool and co-authors have elucidated the molecular mechanism of CaMKII activation by β_1AR. They found that stimulation of β_1AR induces the formation of a β-arrestin-CaMKII-Epac1 complex, allowing its recruitment to the plasma membrane, and whereby promotes cAMP-dependent activation of CaMKII. Further studies using chimeric receptors with switched carboxyl-terminal tails of β_1AR or β_2AR suggested that β-arrestin binding to the carboxyl-terminal tail of β_1AR promotes a conformational change within β-arrestin that allows CaMKII and Epac to remain in a stable complex with the receptor. These results demonstrate that only β_1AR but not β_2AR activates CaMKII significantly. As $CaMKII_\delta$ is a common intermediate of diverse death stimuli-induced apoptosis in cardiomyocytes[84], is required for the transition from pressure overload-induced cardiac hypertrophy to HF[85], and promotes life-threatening arrythmias in HF[86], this explains why activation of β_2AR-G_s signaling is usually not accompanied with the adverse effects observed in β_1AR stimulation.

The molecular mechanism of the cardioprotective effect of β_2AR-G_s signaling in HF is unclear. One possibility is the crosstalk of the G_s-AC-cAMP-PKA cascade to the tyrosine kinase receptor-mediated Akt phosphorylation[87–89].

Concluding remark

In summary, recent studies have revealed opposing functional roles of β_1AR and β_2AR in regulating myocyte viability and myocardial remodeling with a cardiac protective effect of β_2AR stimulation and a detrimental effect of β_1AR stimulation. Unlike the sole G_s coupling of β_1AR, β_2AR couples to both G_s and G_i signaling pathways with the G_i coupling negating the G_s-mediated contractile support. In the failing heart, enhanced expression and activity of GRK2 and G_i proteins further promote G_i-biased β_2AR signaling, thus blunting both β_1AR- and β_2AR-mediated cardiac reserve function, resulting in cardiac maladaptive remodeling and failure. These findings defined the β_2AR-G_i signaling as an essential link between pathologic upregulation of GRK and the development of HF. Since GRK2 and resultant G_i-biased β_2AR signaling are pathogenic factors of HF, G_s-biased β_2AR agonists may present an important therapeutic strategy for the treatment of HF caused by various etiologies.

Acknowledgements

This work was supported by the National Basic Research Program of China (2012CB518000) and the National Major Scientific Research Program of China (2012CB910400).

References

1 Rich MW. Epidemiology, pathophysiology, and etiology of congestive heart failure in older adults. J Am Geriatr Soc 1997; 45: 968–74.
2 Lloyd-Jones D, Adams RJ, Brown TM, Carnethon M, Dai S, De Simone G, *et al*. Executive summary: Heart disease and stroke statistics — 2010 update: A report from the American Heart Association. Circulation 2010; 121: 948–54.
3 Levine TB, Francis GS, Goldsmith SR, Simon AB, Cohn JN. Activity of the sympathetic nervous system and renin-angiotensin system assessed by plasma hormone levels and their relation to hemodynamic abnormalities in congestive heart failure. Am J Cardiol 1982; 49: 1659–66.
4 Hasenfuss G, Mulieri LA, Allen PD, Just H, Alpert NR. Influence of isoproterenol and ouabain on excitation-contraction coupling, cross-bridge function, and energetics in failing human myocardium. Circulation 1996; 94: 3155–60.
5 Teerlink JR, Pfeffer JM, Pfeffer MA. Progressive ventricular remodeling in response to diffuse isoproterenol-induced myocardial necrosis in rats. Circ Res 1994; 75: 105–13.
6 Blaufarb IS, Sonnenblick EH. The renin-angiotensin system in left ventricular remodeling. Am J Cardiol 1996; 77: 8C–16C.
7 Overington JP, Al-Lazikani B, Hopkins AL. How many drug targets are there? Nat Rev Drug Disc 2006; 5: 993–6.
8 McMurray JJ, Pfeffer MA. Heart failure. Lancet 2005; 365: 1877–89.
9 Waagstein F, Bristow MR, Swedberg K, Camerini F, Fowler MB, Silver MA, *et al*. Beneficial effects of metoprolol in idiopathic dilated cardiomyopathy. Metoprolol in Dilated Cardiomyopathy (MDC) Trial Study Group. Lancet 1993; 342: 1441–6.
10 Beckwith C, Munger MA. Effect of angiotensin-converting enzyme inhibitors on ventricular remodeling and survival following myocardial infarction. Ann Pharmacother 1993; 27: 755–66.
11 Lee VC, Rhew DC, Dylan M, Badamgarav E, Braunstein GD, Weingarten SR. Meta-analysis: angiotensin-receptor blockers in chronic heart failure and high-risk acute myocardial infarction. Ann Intern Med 2004; 141: 693–704.
12 Xiao RP, Hohl C, Altschuld R, Jones L, Livingston B, Ziman B, *et al*. β_2-adrenergic receptor-stimulated increase in cAMP in rat heart cells is not coupled to changes in Ca^{2+} dynamics, contractility, or phospholamban phosphorylation. J Biol Chem 1994; 269: 19151–6.
13 Xiao RP, Ji X, Lakatta EG. Functional coupling of the β_2-adrenoceptor to a pertussis toxin-sensitive G protein in cardiac myocytes. Mol Pharmacol 1995; 47: 322–9.
14 Zhu WZ, Wang SQ, Chakir K, Yang D, Zhang T, Brown JH, *et al*. Linkage of β_1-adrenergic stimulation to apoptotic heart cell death through protein kinase A-independent activation of Ca^{2+}/calmodulin kinase II. J Clin Invest 2003; 111: 617–25.
15 Sucharov CC, Mariner PD, Nunley KR, Long C, Leinwand, L, Bristow MR. A β_1-adrenergic receptor CaM kinase II-dependent pathway mediates cardiac myocyte fetal gene induction. Am J Physiol Heart Circ Physiol 2006; 291: H1299–308.
16 Bisognano JD, Weinberger HD, Bohlmeyer TJ, Pende A, Raynolds MV, Sastravaha A, *et al*. Myocardial-directed overexpression of the human β_1-adrenergic receptor in transgenic mice. J Mol Cell Cardiol 2000; 32: 817–30.
17 Engelhardt S, Hein L, Wiesmann F, Lohse MJ. Progressive hypertrophy and heart failure in β1-adrenergic receptor transgenic mice. Proc Natl Acad Sci U S A 1999; 96: 7059–64.
18 Zhu WZ, Zheng M, Koch WJ, Lefkowitz RJ, Kobilka BK, Xiao RP. Dual modulation of cell survival and cell death by β_2-adrenergic signaling

in adult mouse cardiac myocytes. Proc Natl Acad Sci U S A 2001; 98: 1607–12.
19 Bristow MR, Ginsburg R, Fowler M, Minobe W, Rassmussen R, Zera P, *et al*. β_1 and β_2-adrenergic-receptor subpopulations in nonfailing and failing human ventricular myocardium: coupling of both receptor subtypes to muscle contraction and selective β_1-receptor down-regulation in heart failure. Circ Res 1986; 59: 297–309.
20 Bristow MR, Minobe WA, Raynolds MV, Port JD, Rasmussen R, Ray PE, *et al*. Reduced β_1 receptor messenger RNA abundance in the failing human heart. J Clin Invest 1993; 92: 2737–45.
21 Bristow MR, Hershberger RE, Port JD, Minobe W, Rasmussen R. β_1- and β_2-adrenergic receptor-mediated adenylate cyclase stimulation in nonfailing and failing human ventricular myocardium. Mol Pharmacol 1989; 35: 295–303.
22 Bohm M, Eschenhagen T, Gierschik P, Larisch K, Lensche H, Mende U, *et al*. Radioimmunochemical quantification of $G_{i\alpha}$ in right and left ventricles from patients with ischaemic and dilated cardiomyopathy and predominant left ventricular failure. J Mol Cell Cardiol 1994; 26: 133–49.
23 Feldman AM, Cates AE, Veazey WB, Hershberger RE, Bristow MR, Baughman KL, *et al*. Increase of the 40 000-mol wt pertussis toxin substrate (G protein) in the failing human heart. J Clin Invest 1988; 82: 189–97.
24 Lokuta AJ, Maertz NA, Meethal SV, Potter KT, Kamp TJ, Valdivia HH, *et al*. Increased nitration of sarcoplasmic reticulum Ca^{2+}-ATPase in human heart failure. Circulation 2005; 111: 988–95.
25 Sato M, Gong H, Terracciano CM, Ranu H, Harding SE. Loss of β-adrenoceptor response in myocytes overexpressing the Na^+/Ca^{2+}-exchanger. J Mol Cell Cardiol 2004; 36: 43–8.
26 Xiao RP, Balke CW. Na^+/Ca^{2+} exchange linking β_2-adrenergic G_i signaling to heart failure: associated defect of adrenergic contractile support. J Mol Cell Cardiol 2004; 36: 7–11.
27 Zhu W, Zeng X, Zheng M, Xiao RP. The enigma of β_2-adrenergic receptor G_i signaling in the heart: the good, the bad, and the ugly. Circ Res 2005; 97: 507–9.
28 Bristow MR, Ginsburg R, Minobe W, Cubicciotti RS, Sageman WS, Lurie K, *et al*. Decreased catecholamine sensitivity and β-adrenergic-receptor density in failing human hearts. N Engl J Med 1982; 307: 205–11.
29 Ungerer M, Bohm M, Elce JS, Erdmann E, Lohse MJ. Altered expression of β-adrenergic receptor kinase and β_1-adrenergic receptors in the failing human heart. Circulation 1993; 87: 454–63.
30 Pitcher JA, Inglese J, Higgins JB, Arriza JL, Casey PJ, Kim C, *et al*. Role of β γ subunits of G proteins in targeting the β-adrenergic receptor kinase to membrane-bound receptors. Science 1992; 257: 1264–7.
31 Lefkowitz RJ. G protein-coupled receptors. III. New roles for receptor kinases and β-arrestins in receptor signaling and desensitization. J Biol Chem 1998; 273: 18677–80.
32 Faulx MD, Ernsberger P, Vatner D, Hoffman RD, Lewis W, Strachan R, *et al*. Strain-dependent β-adrenergic receptor function influences myocardial responses to isoproterenol stimulation in mice. Am J Physiol Heart Circ Physiol 2005; 289: H30–6.
33 Liggett SB, Cresci S, Kelly RJ, Syed FM, Matkovich SJ, Hahn HS, *et al*. A GRK5 polymorphism that inhibits β-adrenergic receptor signaling is protective in heart failure. Nat Med 2008; 14: 510–7.
34 Shioi T, Kang PM, Douglas PS, Hampe J, Yballe CM, Lawitts J, *et al*. The conserved phosphoinositide 3-kinase pathway determines heart size in mice. EMBO J 2000; 19: 2537–48.
35 Ungerer M, Parruti G, Böhm M, Puzicha M, DeBlasi A, Erdmann E, *et al*. Expression of β-arrestins and β-adrenergic receptor kinases in the failing human heart. Circ Res 1994; 74: 206–13.
36 Xiao RP, Avdonin P, Zhou YY, Cheng H, Akhter SA, Eschenhagen T, *et al*. Coupling of β_2-adrenoceptor to G_i proteins and its physiological relevance in murine cardiac myocytes. Circ Res 1999; 84: 43–52.
37 Hata JA, Koch WJ. Phosphorylation of G protein-coupled receptors: GPCR kinases in heart disease. Mol Interv 2003; 3: 264–72.
38 Choi DJ, Koch WJ, Hunter JJ, Rockman HA. Mechanism of β-adrenergic receptor desensitization in cardiac hypertrophy is increased β-adrenergic receptor kinase. J Biol Chem 1997; 272: 17223–9.
39 Perrino C, Naga Prasad SV, Schroder JN, Hata JA, Milano C, Rockman HA. Restoration of β-adrenergic receptor signaling and contractile function in heart failure by disruption of the βARK1/phosphoinositide 3-kinase complex. Circulation 2005; 111: 2579–87.
40 Ungerer M, Kessebohm K, Kronsbein K, Lohse MJ, Richardt G. Activation of β-adrenergic receptor kinase during myocardial ischemia. Circ Res 1996; 79: 455–60.
41 Gros R, Benovic JL, Tan CM, Feldman RD. G-protein-coupled receptor kinase activity is increased in hypertension. J Clin Invest 1997; 99: 2087–93.
42 Daaka Y, Luttrell LM, Lefkowitz RJ. Switching of the coupling of the β_2-adrenergic receptor to different G proteins by protein kinase A. Nature 1997; 390: 88–91.
43 Zhu W, Petrashevskaya N, Ren S, Zhao A, Chakir K, Gao E, *et al*. G_i-biased β_2AR signaling links GRK2 upregulation to heart failure. Circ Res 2011. doi: 10.1161/CIRCRESAHA.111.253260.
44 Rockman HA, Chien KR, Choi DJ, Iaccarino G, Hunter JJ, Ross J Jr, *et al*. Expression of a β-adrenergic receptor kinase 1 inhibitor prevents the development of myocardial failure in gene-targeted mice. Proc Natl Acad Sci U S A 1998; 95: 7000–5.
45 Lymperopoulos A, Rengo G, Gao E, Ebert SN, Dorn GW 2nd, Koch WJ. Reduction of sympathetic activity via adrenal-targeted GRK2 gene deletion attenuates heart failure progression and improves cardiac function after myocardial infarction. J Biol Chem 2010; 285: 16378–86.
46 Chakir K, Daya SK, Aiba T, Tunin RS, Dimaano VL, Abraham TP, *et al*. Mechanisms of enhanced β-adrenergic reserve from cardiac resynchronization therapy. Circulation 2009; 119: 1231–40.
47 Koch WJ, Rockman HA, Samama P, Hamilton RA, Bond RA, Milano CA, *et al*. Cardiac function in mice overexpressing the β-adrenergic receptor kinase or a βARK inhibitor. Science 1995; 268: 1350–3.
48 Tachibana H, Naga Prasad SV, Lefkowitz RJ, Koch WJ, Rockman HA. Level of β-adrenergic receptor kinase 1 inhibition determines degree of cardiac dysfunction after chronic pressure overload-induced heart failure. Circulation 2005; 111: 591–7.
49 Xiao RP, Zhang SJ, Chakir K, Avdonin P, Zhu W, Bond RA, *et al*. Enhanced G_i signaling selectively negates β_2-AR- but not β_1-AR-mediated positive inotropic effect in myocytes from failing rat hearts. Circulation 2003; 108: 1633–9.
50 Iaccarino G, Tomhave ED, Lefkowitz RJ, Koch WJ. Reciprocal *in vivo* regulation of myocardial G protein-coupled receptor kinase expression by β-adrenergic receptor stimulation and blockade. Circulation 1998; 98: 1783–9.
51 White DC, Hata JA, Shah AS, Glower DD, Lefkowitz RJ, Koch WJ. Preservation of myocardial β-adrenergic receptor signaling delays the development of heart failure after myocardial infarction. Proc Natl Acad Sci U S A 2000; 97: 5428–33.
52 Harding VB, Jones LR, Lefkowitz RJ, Koch WJ, Rockman HA. Cardiac βARK1 inhibition prolongs survival and augments β blocker therapy in a mouse model of severe heart failure. Proc Natl Acad Sci U S A 2001; 98: 5809–14.
53 Sigmund M, Jakob H, Becker H, Hanrath P, Schumacher C, Eschenhagen T, *et al*. Effects of metoprolol on myocardial β-adrenoceptors and $G_{i\alpha}$-proteins in patients with congestive heart failure. Eur J Clin

Pharmacol 1996; 51: 127–32.
54 Terpstra GK, Raaijmakers JA, Wassink GA. Propranolol-induced bronchoconstriction: a non-specific side-effect of β-adrenergic blocking therapy. Eur J Pharmacol 1981; 73: 107–8.
55 Eliasson K, Lins LE, Sundqvist K. Vasospastic phenomena in patients treated with β-adrenoceptor blocking agents. Acta Med Scand Suppl 1979; 628: 39–46.
56 CIBIS-II Investigators and Committees. The Cardiac Insufficiency Bisoprolol Study II (CIBIS-II): a randomised trial. Lancet 1999; 353: 9–13.
57 MERIT-HF Study Group. Effect of metoprolol CR/XL in chronic heart failure: Metoprolol CR/XL Randomised Intervention Trial in-Congestive Heart Failure (MERIT-HF). Lancet 1999; 353: 2001–7.
58 Packer M, Coats AJS, Fowler MB, Katus HA, Krum H, Mohacsi P, *et al*. Effect of carvedilol on survival in severe chronic heart failure. N Engl J Med 2001; 344: 1651–8
59 Poole-Wilson PA, Swedberg K, Cleland JG, Di Lenarda A, Hanrath P, Komajda M, *et al*. Comparison of carvedilol and metoprolol on clinical outcomes in patients with chronic heart failure in the Carvedilol Or Metoprolol European Trial (COMET): randomised controlled trial. Lancet 2003; 362: 7–13.
60 Metra M, Cas LD, Di Lenarda A, Poole-Wilson P. β-blockers in heart failure: Are pharmacological differences clinically important? Heart Fail Rev 2005; 9: 123–30.
61 Zhou Q, Xiao J, Jiang D, Wang R, Vembaiyan K, Wang A, *et al*. Carvedilol and its new analogs suppress arrhythmogenic store overload-induced Ca^{2+} release. Nat Med 2011; 17: 1003–9.
62 Wisler JW, DeWire SM, Whalen EJ, Violin JD, Drake MT, Ahn S, *et al*. A unique mechanism of β-blocker action: carvedilol stimulates β-arrestin signaling. Proc Natl Acad Sci U S A 2007; 104: 16657–62.
63 Kim IM, Tilley DG, Chen J, Salazar NC, Whalen EJ, Violin JD, *et al*. β-blockers alprenolol and carvedilol stimulate β-arrestin-mediated EGFR transactivation. Proc Natl Acad Sci U S A 2008; 105: 14555–60.
64 Noma T, Lemaire A, Naga Prasad SV, Barki-Harrington L, Tilley DG, Chen J, *et al*. β-arrestin-mediated β_1-adrenergic receptor transactivation of the EGFR confers cardioprotection. J Clin Invest 2007; 117: 2445–58.
65 Violin JD, Lefkowitz RJ. β-Arrestin-biased ligands at seven-transmembrane receptors. Trends Pharmacol Sci 2007; 28: 416–22.
66 Ahn S, Shenoy SK, Wei H, Lefkowitz RJ. Differential kinetic and spatial patterns of β-arrestin and G protein-mediated ERK activation by the angiotensin II receptor. J Biol Chem 2004; 279: 35518–25.
67 Kenakin T. Principles: Receptor theory in pharmacology. Trends Pharmacol Sci 2004; 25: 186–92.
68 Urban JD, Clarke WP, Zastrow MV, Nichols DE, Kobilka B, Weinstein H, *et al*. Functional selectivity and classical concepts of quantitative pharmacology. Pharmacology 2007; 320: 1–13.
69 Mailman RB. GPCR functional selectivity has therapeutic impact. Trends Pharmacol Sci 2007; 28: 390–6.
70 Kenakin T. Collateral efficacy in drug discovery: taking advantage of the good (allosteric) nature of 7TM receptors. Trends Pharmacol Sci 2007; 28: 407–15.
71 Gong H, Sun H, Koch WJ, Rau T, Eschenhagen T, Ravens U, *et al*. Specific β_2AR blocker ICI 118,551 actively decreases contraction through a G_i-coupled form of the β_2AR in myocytes from failing heart. Circulation 2002; 105: 2497–503.
72 Bond RA, Leff P, Johnson TD, Milano CA, Rockman HA, McMinn TR. Physiological effects of inverse agonists in transgenic mice with myocardial overexpression of the β_2-adrenoceptor. Nature 1995; 374: 272–6.
73 Ahmet I, Krawczyk M, Heller P, Moon C, Lakatta EG, Talan MI. Beneficial effects of chronic pharmacological manipulation of β-adrenoceptor subtype signaling in rodent dilated ischemic cardiomyopathy. Circulation 2004; 110: 1083–90.
74 Ahmet I, Lakatta EG, Talan M. Pharmacological stimulation of β_2-adrenergic receptors (β_2AR) enhances therapeutic effectiveness of β_1AR blockade in rodent dilated ischemic cardiomyopathy. Heart Fail Rev 2005; 10: 289–96.
75 Ahmet I, Krawczyk M, Zhu W, Woo AY, Morrell C, Poosala S, *et al*. Cardioprotective and survival benefits of long-term combined therapy with β_2AR agonist and β_1AR blocker in dilated cardiomyopathy post-myocardial infarction. J Pharmacol Exp Ther 2008; 325: 491–9.
76 Ahmet I, Morrell C, Lakatta EG, Talan MI. Therapeutic efficacy of a combination of a β_1-adrenoreceptor (AR) blocker and β_2-AR agonist in a rat model of postmyocardial infarction dilated heart failure exceeds that of a β_1-AR blocker plus angiotensin-converting enzyme inhibitor. J Pharmacol Exp Ther 2009; 331: 178–85.
77 Beigi F, Bertucci C, Zhu W, Chakir K, Wainer IW, Xiao RP, *et al*. Enantioselective separation and online affinity chromatographic characterization of R,R- and S,S-fenoterol. Chirality 2006; 18: 822–7.
78 Jozwiak K, Khalid C, Tanga MJ, Berzetei-Gurske I, Jimenez L, Kozocas JA, *et al*. Comparative molecular field analysis of the binding of the stereoisomers of fenoterol and fenoterol derivatives to the β_2 adrenergic receptor. J Med Chem 2007; 50: 2903–15.
79 Woo AY, Wang TB, Zeng X, Zhu W, Abernethy DR, Wainer IW, *et al*. Stereochemistry of an agonist determines coupling preference of β_2-adrenoceptor to different G proteins in cardiomyocytes. Mol Pharmacol 2009; 75: 158–65.
80 Seifert R, Dove S. Functional selectivity of GPCR ligand stereoisomers: new pharmacological opportunities. Mol Pharmacol 2009; 75: 13–8.
81 Jozwiak K, Woo AY, Tanga MJ, Toll L, Jimenez L, Kozocas JA, *et al*. Comparative molecular field analysis of fenoterol derivatives: A platform towards highly selective and effective β_2-adrenergic receptor agonists. Bioorg Med Chem 2010; 18: 728–36.
82 Talan MI, Ahmet I, Xiao RP, Lakatta EG. β_2AR in the treatment of congestive heart failure: long path to translation. J Mol Cell Cardiol 2011; 51: 529–33.
83 Mangmool S, Shukla AK, Rockman HA. β-Arrestin-dependent activation of Ca^{2+}/calmodulin kinase II after β_1-adrenergic receptor stimulation. J Cell Biol 2010; 189: 573–87.
84 Zhu W, Woo AY, Yang D, Cheng H, Crow MT, Xiao RP. Activation of $CaMKII_\delta C$ is a common intermediate of diverse death stimuli-induced heart muscle cell apoptosis. J Biol Chem 2007; 282: 10833–9.
85 Ling H, Zhang T, Pereira L, Means CK, Cheng H, Gu Y, *et al*. Requirement for Ca^{2+}/calmodulin-dependent kinase II in the transition from pressure overload-induced cardiac hypertrophy to heart failure in mice. J Clin Invest 2009; 119: 1230–40.
86 Van Oort RJ, McCauley MD, Dixit SS, Pereira L, Yang Y, Respress JL, *et al*. Ryanodine receptor phosphorylation by calcium/calmodulin-dependent protein kinase II promotes life-threatening ventricular arrhythmias in mice with heart failure. Circulation 2010; 122: 2669–79.
87 Chen H, Ma N, Xia J, Liu J, Xu Z. β_2-adrenergic receptor-induced transactivation of EGFR and PDGFR via SRC kinase promotes rat cardiomyocytes survival. Cell Biol Int 2011. doi:10.1042/CBI20110162.
88 Stuenaes JT, Bolling A, Ingvaldsen A, Rommundstad C, Sudar E, Lin FC, *et al*. β2-Adrenoceptor stimulation potentiates insulin-stimulated PKB phosphorylation in rat cardiomyocytes via cAMP and PKA. Br J Pharmacol 2010; 160: 116–29.
89 Morisco C, Condorelli G, Trimarco V, Bellis A, Marrone C, Condorelli G, *et al*. Akt mediates the cross-talk between β-adrenergic and insulin receptors in neonatal cardiomyocytes. Circ Res 2005; 96: 180–8.

Acta Pharmacologica Sinica (2012) 33: 342–350
 1671-4083/12 $32.00
www.nature.com/aps

Review

Role of G protein-coupled receptors in inflammation

Lei SUN[1], Richard D YE[1, 2, *]

[1]School of Pharmacy, Shanghai Jiao Tong University, Shanghai 200240, China; [2]Department of Pharmacology, University of Illinois, Chicago, IL 60612, USA

G protein-coupled receptors (GPCRs) play important roles in inflammation. Inflammatory cells such as polymorphonuclear leukocytes (PMN), monocytes and macrophages express a large number of GPCRs for classic chemoattractants and chemokines. These receptors are critical to the migration of phagocytes and their accumulation at sites of inflammation, where these cells can exacerbate inflammation but also contribute to its resolution. Besides chemoattractant GPCRs, protease activated receptors (PARs) such as PAR1 are involved in the regulation of vascular endothelial permeability. Prostaglandin receptors play different roles in inflammatory cell activation, and can mediate both proinflammatory and anti-inflammatory functions. Many GPCRs present in inflammatory cells also mediate transcription factor activation, resulting in the synthesis and secretion of inflammatory factors and, in some cases, molecules that suppress inflammation. An understanding of the signaling paradigms of GPCRs in inflammatory cells is likely to facilitate translational research and development of improved anti-inflammatory therapies.

Keywords: GPCR; inflammation; leukocytes; chemoattractant; chemokine

Acta Pharmacologica Sinica (2012) 33: 342–350; doi: 10.1038/aps.2011.200; published online 27 Feb 2012

Introduction

Inflammation is characterized by the cardinal signs of rubor (redness), calor (heat), dolor (pain), tumor (swelling) and function laesa (loss of function). These signs reflect tissue response to inflammatory factors that are either external (*eg*, bacterial endotoxin) or host-derived (*eg*, TNFα). GPCRs contribute directly to these clinical manifestations due to their wide presence and diverse functions. Inflammation is shaped not only by leukocytes that accumulate at the site of inflammation, but also by cells in specific tissues and organs such as microglial cells in the brain and synovial fibroblasts in the joints. Endothelial cells in all tissues are actively involved in the process of inflammation and interact closely with leukocytes. GPCRs expressed in these cells play important roles in sensing the presence of chemoattractants, transducing signals that lead to the production of inflammatory cytokines, nociception, and regulation of intracellular and intercellular communications associated with increased blood flow and increased vascular endothelial permeability. Functions mediated by GPCRs can both exacerbate inflammation and promote its resolution.

* To whom correspondence should be addressed.
E-mail yedequan@sjtu.edu.cn
Received 2011-11-16 Accepted 2011-12-19

GPCRs that mediate cell migration and phagocyte activation

It was long observed that phagocytes have the abilities to chase, capture and eventually eliminate invading bacteria. Based on observations made in the last century, it was reported that phagocytes could respond to small molecules derived from invading bacteria and fungi[1]. In addition, these cells also respond to substances produced by the host during the course of sterile inflammation. A number of small molecules was discovered in the 60's and 70's, including activated complement C5a and N-formylated peptides of bacterial origin[2–4]. Evidence that these "classic chemoattractants" act on GPCRs first came from the observation that pertussis toxin (PTX) could alter the binding affinity of chemotactic formyl peptides[5], a characteristic feature of certain GPCR ligands[6]. Working independently, two laboratories reported that PTX could block formyl peptide (*eg*, fMet-Leu-Phe, fMLF)-induced neutrophil functions through ADP-ribosylation of the Gi class of heterotrimeric G proteins[7, 8]. These early studies demonstrate that the chemotactic peptide receptor functionally couples to a heterotrimeric G protein that is a substrate for ADP-ribosylation by PTX. Further characterization of the PTX substrate, also termed "islet-activating protein", found it to be a member of the Gi family of G proteins[9] that is critical to a variety of activities downstream of chemoattractant receptor

signaling. The identity of the receptors for fMLF and C5a was first revealed, among all chemoattractant receptors, through molecular cloning of their cDNAs and analysis of the deduced protein sequence[10, 11]. It was confirmed that these receptors belong to the rhodopsin-like, 7-transmembrane (TM) receptor superfamily[12, 13]. Following these initial cloning efforts, other classic chemoattractant receptors including those for platelet-activating factor (PAF) and leukotriene B4 (LTB4), were subsequently identified as GPCRs[14, 15].

Chemokines (chemotactic cytokines) are small proteins with cysteine residues located at fixed positions. A large number of chemokines have been identified in the mid-80's and early 90's. These chemokines bind to rhodopsin-like GPCRs, although not all of them are signaling receptors[16, 17]. Studies of patients with inflammatory disorders found induced expression of many chemokines, indicating that these small proteins play important roles in the development and progression of inflammatory diseases. Published reports have also shown that genetic deletion of selected chemokine receptors causes reduction in the severity of inflammation in various animal models. For instance, deletion of the CCR2 gene markedly reduced lesion in athrosclerosis-prone ApoE-null mice[18]. Atherosclerosis is an inflammatory disorder and the expression of CCL2, the ligand for CCR2, is upregulated in the atherosclerotic plaque and contributes to local accumulation of monocytes. In addition, CCR2 also contributes to the development of multiple sclerosis, rheumatoid arthritis, scleroderma and ischemia-reperfusion injury. Receptors for the CXCL class of chemokines are found in neutrophils. Among these GPCRs, CXCR1, and CXCR2 are involved in the pathology of myocardial infarction. CXCR1 and CXCR2 interact with CXCL1, CXCL2, and CXCL8, which are present during acute inflammation and acute injury. These chemokines are primarily responsible for the recruitment of neutrophils to the site of inflammation and tissue injury, where these professional phagocytes can affect granule release and reactive oxidant production.

Chemotaxis

All chemoattractant receptors have the ability to mediate cell migration. In inflammatory disorders such as rheumatoid arthritis and atherosclerosis, the presence of leukocytes is crucial to disease progression. FPR1 is also responsible for sensing mitochondrial N-formyl peptides released from damaged cells[19, 20]. Activation of the Gi family of G proteins is critical to chemotaxis, which involves a complex network of intracellular signaling and cytoskeleton reorganization. Phagocytes polarize upon chemoattractant stimulation, forming a leading edge and a trailing edge which is characteristic of a migrating cell. G protein signaling initiates at the leading edge, as evidenced by the production of PIP3 and translocation of proteins with the PIP3-binding PH domain such as Akt and guanine nucleotide exchange factors such as P-Rex1[21] (Figure 1). Cytoskeletal reorganization also requires activation of the small GTPase Rac, whereas RhoA, another small GTPase, is believed to play a role at the trailing edge of a migrating cell[22]. Not all chemotaxis-mediating receptors are 7-TM receptors; other potent chemoattractants such as TGF-β act on other receptors. However, the fact that all chemokines bind to 7-TM receptors illustrates the importance of this class of receptors in cell migration. Until recently, only Gi proteins were implicated in leukocyte chemotaxis. The fact that several chemoattractant receptors could also couple to Gq proteins prompted a study that identified its role in chemotaxis[23]. Using mice lacking Gq proteins, it was observed that chemotaxis of dendritic cells to selected chemokines requires both Gi and Gq proteins. This alternative pathway uses a CD38-dependent mechanism for regulation of chemotaxis. It is presently unclear why in these cells Gq is necessary for chemotaxis whereas in other cells Gi is sufficient, but studies of this sort make it clear that the study of chemotaxis will also expand the understanding of GPCR biology.

Degranulation

A large number of GPCR agonists, including chemotactic peptides, activated complement fragments and histamine, are able to stimulate granule release[24]. In neutrophils, binding of fMLF to the receptor FPR1 or C5a to C5aR, triggers strong degranulation. In fact, exogenous expression of FPR1 or C5aR in a rat basophilic leukemia cell line renders these cells capable of releasing β-hexosaminidase upon stimulation, demonstrates the sufficiency of these receptors to trigger degranulation[25]. Simultaneous activation of several signaling pathways is required for degranulation[26]. As with other secretory cells, fusion of intracellular granules or vesicles in phagocytes requires calcium influx, which is triggered by GPCR signaling (Figure 1). G protein signaling also leads to the activation of several protein kinases, including PKC, cGMP-dependent kinase, and the serine/threonine kinase Akt. Exactly how these kinases promote granule release remains incompletely understood, but it is reported that vesicular fusion-related proteins such as the SNAP proteins are phosphorylated upon cell stimulation and these phosphorylation events precede vesicular fusion[27]. In addition to the protein kinases, small GTPases are activated downstream of GPCRs and are required for fusion of intracellular vesicles.

Superoxide generation

Although the production of reactive oxygen species (ROS) is widespread among different types of cells, phagocytes can produce large amounts of ROS, a requirement for killing phagocytosed bacteria[28]. A number of chemoattractants, including fMLF and C5a, potently stimulate ROS production in neutrophils, although production is extracellular rather than intra-phagosome when induced by these soluble mediators. As a result, these oxygen radicals cause damage to endothelial cells that form the lining of vascular wall. Exposure to even low doses of these chemoattractants also "primes" the phagocytes for more robust oxidant production when stimulated with other inflammatory factors such as LPS[29]. Chemoattractant-induced ROS production requires Gi protein, as it is effectively blocked by PTX treatment. Research con-

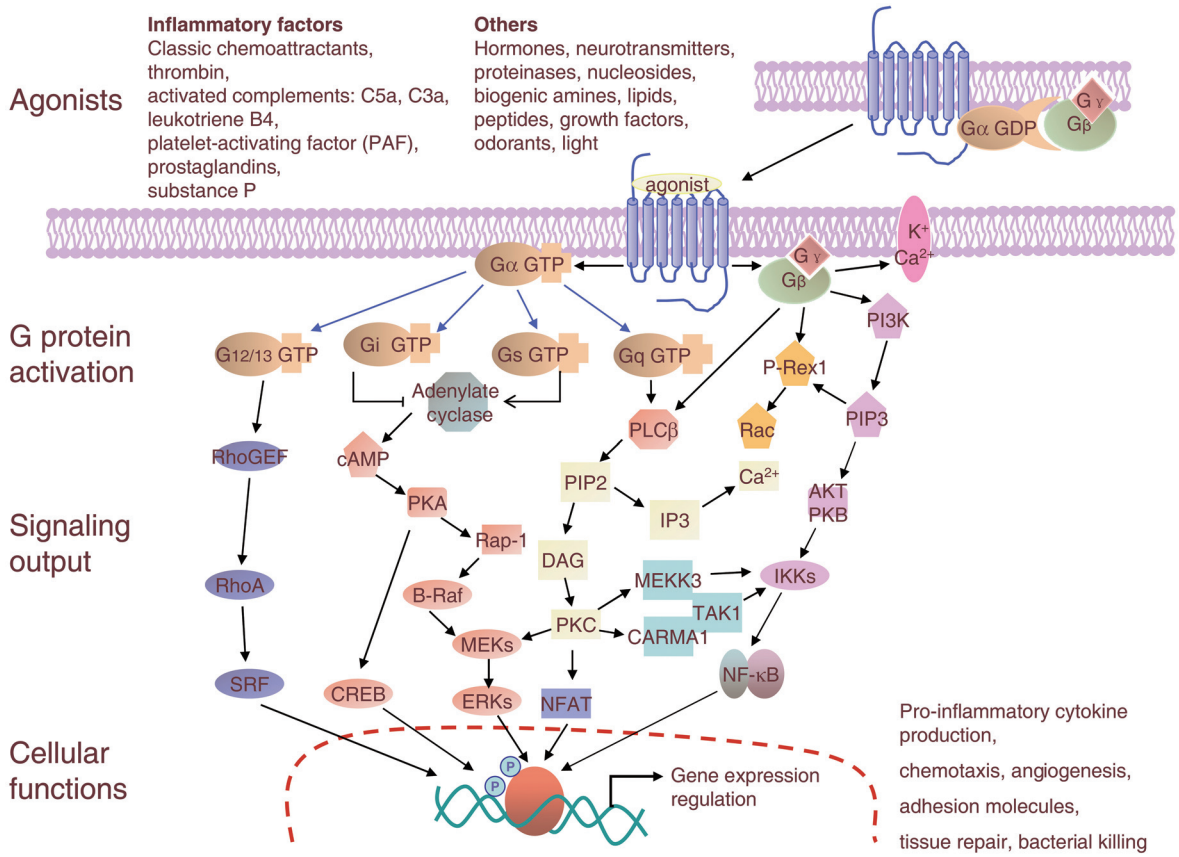

Figure 1. Signaling pathways of GPCRs involved in inflammation. Signaling by GPCRs is initiated by a specific ligand that binds and activates the receptor inducing conformational changes in the receptor. A partial list of the relevant ligands is given in the top panel. All 4 classes of G proteins are involved in the regulation of events that lead to inflammatory cell activation or inactivation. Major effectors, including second messengers and other signaling molecules involved in the regulation of inflammation are shown. These include Ca^{2+}, cAMP, protein kinases, lipid kinases, lipases, phosphoinositides, small GTPases and the relevant guanine nucleotide exchange factors, and transcriptional factors. The final output is manifested as nuclear, cytoplasmic and extracellular activities such as expression of proinflammatory genes, production of oxidants, and generation of tissue damaging and repairing factors.

ducted thus far has found that chemoattractant-induced ROS production shares basic mechanisms with particle-induced ROS production, in that both require membrane translocation of cytosolic components and assembly of a functional NADPH oxidase at membrane. There are, however, major differences in the upstream signaling mechanisms involved. Whereas phagocytosis-induced oxidant production requires primarily tyrosine kinase activation, chemoattractant-induced ROS production relies mostly on the activation of serine/threonine kinases such as Akt and dual-specificity protein kinases such as p38 MAPK. These different signaling pathways then converge at activation of downstream targets such as PKC (Figure 1). Published reports show that upon activation of chemoattractant GPCRs, the released G protein βγ subunits triggers PI3K activation and the production of PIP3[30]. The membrane-bound PIP3 is required for the subsequent activation of Akt and the small GTPase Rac, which is also required for the assembly of a functional NADPH oxidase complex[31, 32]. Thus, chemoattractant-induced ROS production requires simultaneous and sustained activation of multiple signaling pathways, which are also negatively regulated by phosphatases[33]. How chemoattractant GPCRs convert a single binding event to a cascade of signaling events remains incompletely understood. Recent studies have shown that both G protein-dependent and –independent pathways are involved in chemoattractant signaling.

GPCRs and inflammatory pain

Inflammation caused by trauma, infection and other forms of insult to the tissue is often accompanied by the uncomfortable sensation of pain. Inflammatory pain may result from enhanced nociception due to the interaction of inflammatory mediators with neurons and the resulting state of hypersensitivity. Inflammation may also cause damage to neurons and produce neuropathic pain[34]. Being the largest group of sensory receptors, GPCRs play important roles in inflammatory nociception. At the periphery, a number of GPCR agonists produced during inflammation, including bradykinin (BK) and selected prostaglandins (PGs), participate in inflammatory hyperalgesia. BK and kallidin both activate and sensitize

primary afferent neurons. Two classes of BK receptors are present. Experimental data show that B1 BK receptor agonists produce pain only during inflammation, in accordance with the inducible nature of the B1 BK receptor. The B2 BK receptor is constitutively expressed and its blockade reduces inflammatory hyperalgesia in animal models[35].

Prostaglandins (PGs) are lipid-derived autacoids generated through the sequential actions of cyclooxygenase and PG synthase. These metabolites of arachidonic acid include thromboxanes (TXA2), PGD2, PGE2, PGI2, and PGF2a. Collectively, they interact with 9 prostanoid receptors that couple to a variety of G proteins and are responsible for several features of inflammation including pain and edema (Table 1). Nonsteroidal anti-inflammatory drugs (NSAIDs), including acetylsalicylic acid (aspirin) and the more selective COX-2 specific inhibitors, are effective anti-inflammatory and pain-relieving agents primarily because they block the synthesis of PGs[36, 37]. Among the various arachdonic acid metabolites, PGE2 interacts with several GPCRs. The 4 EP receptors are individual gene products but in the case of EP3, there are splice variants as well[38]. The 4 subclasses of EP receptors couple to various G proteins and are responsible for the variety of PGE2 effects. PGE2 is synthesized during the course of inflammation and contributes to tissue edema and hyperalgesia. In the nociceptive primary afferent nerve terminals, PGE2 modulates voltage-gated sodium currents[39], a function mediated through the EP3 receptor[40]. PGE2 is also synthesized in the CNS during peripheral inflammation and contributes to increased pain hypersensitivity[41].

Prostacyclin (PGI), which acts on G protein-coupled IP receptor, is another arachdonic metabolite produced during inflammation that plays a central nociceptive role[42]. Mice lacking the IP receptor display altered pain perception as well as inflammatory responses[43]. Studies have shown that Gs-coupled PG receptors may enhance nociceptor sensitization by reducing the activation threshold for selected sodium channels through a cAMP and PKA-dependent mechanism[44]. GPCRs present in dorsal horn neurons are also involved in transmission of nociception and are responsible for the development of central sensitization. The NK1 receptor for tachykinin is a GPCR that responds to substance P and mediates PKC activation, leading to the phosphorylation and potentiation of N-methyl-*D*-aspartic acid (NMDA) receptors[45]. In addition to the NK1 receptor, the neuromedin U2 receptor (NMU2) plays a central role in nociception. NMU2 knockout mice display reduced sensitivity to pain induced by capsaicin and formalin[46].

Besides functions of GPCRs in inflammatory nociception, there are instances in which GPCRs are antinociceptive. Loperamide, an opioid agonist developed for peripheral use, displays antinociceptive activity in experimental arthritis[47]. Cannabinoids, which are agonists for the CB1 and CB2 receptors, inhibit peripheral sensitization when used topically[48]. Exploration of the roles for GPCRs in inflammatory nociception is bound to provide novel therapeutics for effective control of pain associated with inflammatory diseases.

GPCRs and regulation of vascular endothelial permeability

Edema, an abnormal accumulation of interstitial fluid, often accompanies inflammation. The production of inflammatory factors, many of them GPCR agonists, is largely responsible for increased vascular endothelial permeability, which contributes to edema during inflammation. BK and PAF are well known for their roles in the regulation of vascular wall permeability. It has long been recognized that BK reproduces cardinal signs of inflammation, and the BK effect on vascular permeability is direct rather than dependent on histamine[49]. More recent studies have shown that both the B1 BK receptor and B2 BK receptor are involved in local edema during inflammation, for instance, paw edema and protein extravasation leading to joint swelling[50]. PAF profoundly affects microvascular permeability, allowing extravasation of plasma contents such as albumin[51, 52]. Like BK, PAF acts on endothelial cells directly, increasing gap formation between endothelial cells through the actions of eNOS[53], tyrosine phosphorylation of VE-cadherin[54], and the Rho family small GTPases[55].

Histamine and thrombin are also major regulators of vascular permeability. Histamine is released by basophils and mast cells during the allergic response. It binds to one or more of the four G protein-coupled histamine receptors, stimulating vasodilation and increasing vascular permeability[56]. Histamine also participates in allergic inflammatory diseases such as asthma by inducing chemotaxis and bronchoconstriction[57]. Thrombin is one of the best studied regulators of vascular endothelial permeability[58]. The thrombin receptor was initially identified as a GPCR with a unique mechanism for activation. Upon binding of alpha thrombin, the receptor's N-terminus was cleaved, generating a tethered peptide that becomes an agonist for the receptor[59]. This receptor is the first member of the protease-activated receptor (PAR) subfamily, of which 3 of the 4 PARs bind thrombin (Table 1). Although initially known as a thrombotic agent that catalyzes the conversion of fibrinogen to fibrin, thrombin is also a potent agonist for platelets and its receptors are expressed in human endothelial cells as well as smooth muscle cells (SMC). Its vascular functions include cellular differentiation, migration and proliferation of SMC, angiogenesis and vascular development[60]. PAR1, which is widely studied in this subfamily of GPCRs, couples to multiple G proteins including Gi, Gq, and G12/13. The selectivity for activation of these G proteins depends on the agonists that bind to the receptor[61]. In endothelial cells, thrombin binding to PAR1 leads to activation of p115 RhoGEF, which provides a functional link between G13 and RhoA[62]. Activation of RhoA is responsible for stress fiber formation, and increased calcium flux triggers other signaling pathways which ultimately lead to myosin light chain-dependent contraction of endothelial cells[63]. This process is reversible, and focal adhesion kinase plays a role in the reversal of the increased vascular permeability[64]. Thrombin-induced increase in vascular endothelial permeability contributes to the edema seen in inflammatory disorders such as acute lung injury[65, 66]. Both the receptor and its downstream signaling pathways are targets for therapeutic intervention[67, 68]. In con-

Table 1. A partial list of GPCRs involved in inflammation.

Receptor type		Physiological functions
Chemokine receptors Ref [16, 17]	CC family	Specifically bind and respond to cytokines of CCL chemokine family; responsible for recruiment of T cells, macrophages and eosinophils; involved in atherogenesis and angiogenesis. For instance, CCR2 is highly expressed in monocytes and responsible for their recruitment to atherosclerotic lesions; CCR2 also contributes to development of multiple sclerosis, rheumatoid arthritis, scleroderma and ischemia -reperfusion injury.
	CXC family	Specifically bind and respond to CXCL chemokines; mainly present during acute inflammation and acute injury; responsible for chemoraxis and recruitment of neutrophils and eosinophils; some involvement in neovascularization, hematopoiesis and HIV-1 entry. For instance, CXCR1 and CXCR2 are primary receptors for recruitment of neutrophils to the site of acute inflammation.
	Others	
	CX3CR1	Macrophage recruitment, atherogenesis and HIV-1 coreceptor.
	XCR1	Chemotaxis, recruitment of mononuclear cells to rheumatoid arthritic joint.
Formyl peptide receptors Ref [10, 13]	FPR1 FPR2/ALX FPR3	Detection of bacterial and mitochondrial formyl peptides; binding of other endogenous ligands such as serum amyloid A and annexin A1. Mediates chemotaxis, degranulation and superoxide generation functions in neutrophils; induction of inflammatory cytokine expression. FPR2/ALX is reported to mediate anti-inflammatory functions of lipoxin A4.
Protease-activated receptors Ref [59, 63, 65, 93, 94]	PAR1, PAR2, PAR3, PAR4	PAR1, PAR3 and PAR4 are all considered thrombin receptors, whereas PAR2 is activated by trypsin and other ligands. PARs play roles in hemostasis and thrombosis, platelet signaling, and tissue injury. These receptors are involved in the process of inflammation and tissue repair. For instance, thrombin binding to PAR1 leads to activation of p115 RhoGEF, and RhoA. Activation of RhoA is responsible for stress fiber formation, and increased calcium flux triggers other signaling pathways which ultimately lead to myosin light chain-dependent contraction of endothelial cells. Thrombin-induced increase in vascular endothelial permeability contributes to edema often seen in inflammatory disorders such as acute lung injury.
Lysophos-pholipid receptors Ref [69–71]	S1P1	Binds the lipid signaling molecule sphingosine 1-phosphate (S1P), and highly expressed in endothelial cells. Deficiency of S1P1 leads to embryonic lethality, defective vascular maturation and decrease in Rac-mediated chemotaxis; S1P1 also promotes stabilization of endothelial monolayer barrier function through its downstream signaling that leads to adherens junction assembly in endothelial cells.
Prostaglandin receptors Ref [38–40, 42, 43, 95–98]	DP1, DP2	Inhibits platelet aggregation and histamine release; relaxation of the myometrium and smooth muscle; inhibition of leukotriene B4 and superoxide anion release from human neutrophils; regulation of eosinophil apoptosis; relaxation of pulmonary venous smooth muscle; relaxation of bronchial smooth muscle.
	EP1, EP2, EP3, EP4	PGE2 is synthesized during the course of inflammation and contributes to tissue edema and hyperalgesia. All 4 EPs response to PGE2 for various effects on different tissues, including algesia and regulation of blood pressure, contraction of pulmonary venous smooth muscle, regulation of the peripheral circadian clock, mediation of COX-2-induced cytotoxicity, mediation of acid-induced visceral pain hypersensitivity, inhibition of phagocytosis and apoptotic cell death, promotion of cell growth and follicle growth, neuroprotection, inhibition of TNFα formation. Example: PGE2 binding to EP1 activates Gq pathway, leading to MAP kinase activation and production of pro-inflammatory cytokine such as IL-6 and TNFα. In the nociceptive primary afferent nerve terminals, PGE2 modulates voltage-gated sodium currents, a function mediated through the EP3 receptor that couples to a Gi pathway. Multiple splice variants of EP3 are present.
	FP, IP1, TP	Mediate the responses to PGF2a, PGI2, and thromboxanes, respectively. Example: TP play roles in platelet aggregation, contraction of pulmonary smooth muscle, vasoconstriction, mediation of cellular immune responses and inflammatory tissue injury. Interaction of PGI2 with IP receptor plays a central nociceptive role in inflammation. Mice lacking the IP receptor display altered pain perception as well as inflammatory response.
Bradykinin receptors Ref [35, 99–101]	B1BKR, B2BKR	B2BKR is constantly expressed whereas B1BKR expression is induced by inflammatory factors. Both receptors modulate blood pressure and inflammatory pain. Activation of B1BKR in the kindled rat hippocampus results in increase extracellular glutamate levels. B1 blocking inhibits plasma extravasation in streptozotocin-induced diabetic rats. Modulation of antigen-induced pulmonary inflammation in mice. Blockade of B2BKR prevents tissue swelling and inflammation in animal models.
Tachykinin receptors Ref [45, 102]	NK1	Substance P receptor (SPR) is present in neurons, brainstem, vascular endothelial cells, muscle, and different types of immune cells. SP induces neurogenic inflammation via NK1, not NK2 and NK3, for the transmission of stress signals and pain, the contraction of smooth muscles and inflammation.
Neuromedin U receptors Ref [46, 103]	NMU2	NMU2 binds neuropeptide hormones neuromedin U and neuromedin S. The receptor mediates effects on cardio-vascular, gastrointestinal and CNS functions, and serves as a novel physiological regulator in spinal nociceptive transmission and processing. NMU2-deficient mice display reduced sensitivity to pain induced by capsaicin and formalin.
Cannabinoid receptors Ref [48, 104]	CB1, CB2	Both receptors are activated by endocannabinoids, plant cannabinoids, and synthetic cannabinoids. CB2 is mainly expressed in the immune system and in hematopoietic cells. Its activation causes a reduction in the intracellular levels of cyclic adenosine monophosphate (cAMP) and ultimately suppression of immune function.
Platelet-activating factor receptor Ref [51, 105]	PAFR	Activation of PAFR affects microvascular permeability, allowing extravasation of plasma contents such as albumin and vasodilation during inflammation. PAF directly acts on endothelial cells, increasing gap formation between endothelial cells through the actions of eNOS, tyrosine phosphorylation of VE-cadherin and Rho family small GTPase. PAFR plays roles in cell proliferation, motility and angiogenic response.

trast to thrombin, another GPCR ligand sphingosine 1-phosphate (S1P) promotes stabilization of the endothelial barrier[69]. This effect of S1P is mediated through its receptor S1P1, which promotes adherens junction assembly in endothelial cells, thus fortifying vascular endothelial barrier[70, 71].

GPCRs and regulation of inflammatory gene expression

A large number of GPCRs have been found to participate in transcriptional regulation[72]. G protein signaling leads to activation of transcription factors including CREB, c-Jun, NF-κB, and STAT3, among others (Figure 1). These transcription factors, particularly NF-κB, are closely associated with the expression of genes that encode inflammatory factors. It was first reported that the receptor for PAF could stimulate NF-κB activation through a PTX-insensitive pathway, suggesting that the Gq protein which couples to the PAF receptor is responsible for this function[73]. Subsequent studies identified both PTX-sensitive and PTX-insensitive mechanisms by which GPCRs activate NF-κB[74–78]. The Gi-dependent pathway requires the Gβγ subunits whereas Gq directly activates PLCβ, thus triggering PKC. In addition to PKC, protein kinases that are found to be involved in GPCR activation of NF-κB include the Ser/Thr kinase Akt[77] and tyrosine kinase Pyk2[79]. The β-arrestin pathway was also involved in regulating NF-κB activation. In resting cells, β-arrestins bind to IκBα and protect it from phosphorylation and proteosome degradation[80, 81]. Upon GPCR activation, β-arrestins participate in intracellular signaling leading to activation of multiple pathways that favor NF-κB activation[82–84]. Several intracellular signaling molecules that were initially identified for immune cell functions, including CARMA3 and Bcl10, were found to regulate GPCR signaling leading to NF-κB activation[85, 86]. These latter findings provide evidence for the complexity of signaling pathways downstream of GPCRs.

In addition to agonist-induced, GPCR-mediated NF-κB activation, a number of constitutively activated GPCRs are able to activate NF-κB even in the absence of agonists. Viruses such as KSHV, HHV8, and RCMV encode GPCRs that are constitutivelyactive and, when expressed in mammalian cells, activate NF-κB[87–90]. Like agonist-induced GPCRs, these viral GPCRs couples to more than one G proteins for signaling[88]. Transcriptional activation by these GPCRs is not restricted to NF-κB[87]. These receptors are believed to contribute to their pathological functions including stimulation of angiogenesis in the case of KSHV GPCR, and are potential therapeutic targets[91, 92].

Summary

The diverse actions of inflammatory factors are reflected in the diversity of receptors with which they interact. It is therefore not surprising that inflammatory factors of different nature and composition, including arachidonic acid metabolites, peptides, protein fragments and proteases, are found to partner with the 7-TM GPCRs. The diversity in ligand binding and transmembrane signaling by GPCRs are primarily responsible for the mediation of complex inflammatory (and anti-inflammatory) responses. There is no doubt that GPCRs play important roles in inflammation, as they do in other vital organ functions. A better understanding of these receptors as well as their signaling pathways will help to develop new therapeutic agents with higher specificity than traditional anti-inflammatory agents such as NSAIDs.

Acknowledgements

Due to page limitations, we are unable to cite as many references on GPCRs and inflammation as we wished. We apologize to those whose important work was not mentioned in this article. This work was supported in part by National Basic Research Program of China (973 Program) Grant 2012CB518001 (to Richard D YE).

References

1 Harris H. Role of chemotaxis in inflammation. Physiol Rev 1954; 34: 529–62.
2 Ward PA, Cochrane CG, Muller-eberhard HJ. The role of serum complement in chemotaxis of leukocytes *in vitro*. J Exp Med 1965; 122: 327–46.
3 Ward PA, Lepow IH, Newman LJ. Bacterial factors chemotactic for polymorphonuclear leukocytes. Am J Pathol 1968; 52: 725–36.
4 Schiffmann E, Corcoran BA, Wahl SM. N-formylmethionyl peptides as chemoattractants for leucocytes. Proc Natl Acad Sci U S A 1975; 72: 1059–62.
5 Koo C, Lefkowitz RJ, Snyderman R. Guanine nucleotides modulate the binding affinity of the oligopeptide chemoattractant receptor on human polymorphonuclear leukocytes. J Clin Invest 1983; 72: 748–53.
6 De Lean A, Stadel JM, Lefkowitz RJ. A ternary complex model explains the agonist-specific binding properties of the adenylate cyclase-coupled beta-adrenergic receptor. J Biol Chem 1980; 255: 7108–17.
7 Bokoch GM, Gilman AG. Inhibition of receptor-mediated release of arachidonic acid by pertussis toxin. Cell 1984; 39: 301–8.
8 Lad PM, Olson CV, Smiley PA. Association of the N-formyl-Met-Leu-Phe receptor in human neutrophils with a GTP-binding protein sensitive to pertussis toxin. Proc Natl Acad Sci U S A 1985; 82: 869–73.
9 Simon MI, Strathmann MP, Gautam N. Diversity of G proteins in signal transduction. Science 1991; 252: 802–8.
10 Boulay F, Tardif M, Brouchon L, Vignais P. The human N-formylpeptide receptor: characterization of two cDNA isolates and evidence for a new subfamily of G-protein-coupled receptors. Biochemistry 1990; 29: 11123–33.
11 Gerard NP, Gerard C. The chemotactic receptor for human C5a anaphylatoxin. Nature 1991; 349: 614–7.
12 Gerard C, Gerard NP. C5A anaphylatoxin and its seven transmembrane-segment receptor. Annu Rev Immunol 1994; 12: 775–808.
13 Ye RD, Boulay F, Wang JM, Dahlgren C, Gerard C, Parmentier M, *et al*. International Union of Basic and Clinical Pharmacology. LXXIII. Nomenclature for the formyl peptide receptor (FPR) family. Pharmacol Rev 2009; 61: 119–61.
14 Honda Z, Nakamura M, Miki I, Minami M, Watanabe T, Seyama Y, *et al*. Cloning by functional expression of platelet-activating factor receptor from guinea-pig lung. Nature 1991; 349: 342–6.
15 Yokomizo T, Izumi T, Chang K, Takuwa Y, Shimizu T. A G-protein-

coupled receptor for leukotriene B4 that mediates chemotaxis. Nature 1997; 387: 620–4.
16 Murphy PM, Baggiolini M, Charo IF, Hebert CA, Horuk R, Matsushima K, *et al*. International Union of Pharmacology. XXII. Nomenclature for chemokine receptors. Pharmacol Rev 2000; 52: 145–76.
17 Zlotnik A, Yoshie O. Chemokines: a new classification system and their role in immunity. Immunity 2000; 12: 121–7.
18 Boring L, Gosling J, Cleary M, Charo IF. Decreased lesion formation in CCR2-/- mice reveals a role for chemokines in the initiation of atherosclerosis. Nature 1998; 394: 894–7.
19 Carp H. Mitochondrial N-formylmethionyl proteins as chemoattractants for neutrophils. J Exp Med 1982; 155: 264–75.
20 McDonald B, Pittman K, Menezes GB, Hirota SA, Slaba I, Waterhouse CC, *et al*. Intravascular danger signals guide neutrophils to sites of sterile inflammation. Science 2010; 330: 362–6.
21 Chung CY, Potikyan G, Firtel RA. Control of cell polarity and chemotaxis by Akt/PKB and PI3 kinase through the regulation of PAKa. Mol Cell 2001; 7: 937–47.
22 Xu J, Wang F, Van Keymeulen A, Herzmark P, Straight A, Kelly K, *et al*. Divergent signals and cytoskeletal assemblies regulate self-organizing polarity in neutrophils. Cell 2003; 114: 201–14.
23 Shi G, Partida-Sanchez S, Misra RS, Tighe M, Borchers MT, Lee JJ, *et al*. Identification of an alternative G{alpha}q-dependent chemokine receptor signal transduction pathway in dendritic cells and granulocytes. J Exp Med 2007; 204: 2705–18.
24 Lacy P. Mechanisms of degranulation in neutrophils. Allergy Asthma Clin Immunol 2006; 2: 98–108.
25 Ahamed J, Haribabu B, Ali H. Cutting edge: Differential regulation of chemoattractant receptor-induced degranulation and chemokine production by receptor phosphorylation. J Immunol 2001; 167: 3559–63.
26 Nanamori M, Chen J, Du X, Ye RD. Regulation of leukocyte degranulation by cGMP-dependent protein kinase and phosphoinositide 3-kinase: potential roles in phosphorylation of target membrane SNARE complex proteins in rat mast cells. J Immunol 2007; 178: 416–27.
27 Woska JR Jr, Gillespie ME. SNARE complex-mediated degranulation in mast cells. J Cell Mol Med 2011. doi: 10.1111/j.1582-4934.2011.01443.x.
28 Nauseef WM. Assembly of the phagocyte NADPH oxidase. Histochem Cell Biol 2004; 122: 277–91.
29 Shapira L, Champagne C, Gordon B, Amar S, Van Dyke TE. Lipopolysaccharide priming of superoxide release by human neutrophils: role of membrane CD14 and serum LPS binding protein. Inflammation 1995; 19: 289–95.
30 Li Z, Jiang H, Xie W, Zhang Z, Smrcka AV, Wu D. Roles of PLC-beta2 and -beta3 and PI3Kgamma in chemoattractant-mediated signal transduction. Science 2000; 287: 1046–9.
31 Abo A, Pick E, Hall A, Totty N, Teahan CG, Segal AW. Activation of the NADPH oxidase involves the small GTP-binding protein p21rac1. Nature 1991; 353: 668–70.
32 Knaus UG, Heyworth PG, Evans T, Curnutte JT, Bokoch GM. Regulation of phagocyte oxygen radical production by the GTP-binding protein Rac 2. Science 1991; 254: 1512–5.
33 Qian F, Deng J, Cheng N, Welch EJ, Zhang Y, Malik AB, *et al*. A non-redundant role for MKP5 in limiting ROS production and preventing LPS-induced vascular injury. Embo J 2009; 28: 2896–907.
34 Kidd BL, Urban LA. Mechanisms of inflammatory pain. Br J Anaesth 2001; 87: 3–11.
35 Burgess GM, Perkins MN, Rang HP, Campbell EA, Brown MC, McIntyre P, *et al*. Bradyzide, a potent non-peptide B(2) bradykinin receptor antagonist with long-lasting oral activity in animal models of inflammatory hyperalgesia. Br J Pharmacol 2000; 129: 77–86.
36 Vane JR. Inhibition of prostaglandin synthesis as a mechanism of action for aspirin-like drugs. Nat New Biol 1971; 231: 232–5.
37 Vane JR, Botting RM. Mechanism of action of aspirin-like drugs. Semin Arthritis Rheum 1997; 26: 2–10.
38 Breyer RM, Bagdassarian CK, Myers SA, Breyer MD. Prostanoid receptors: subtypes and signaling. Annu Rev Pharmacol Toxicol 2001; 41: 661–90.
39 Khasar SG, Gold MS, Levine JD. A tetrodotoxin-resistant sodium current mediates inflammatory pain in the rat. Neurosci Lett 1998; 256: 17–20.
40 Minami T, Nakano H, Kobayashi T, Sugimoto Y, Ushikubi F, Ichikawa A, *et al*. Characterization of EP receptor subtypes responsible for prostaglandin E2-induced pain responses by use of EP1 and EP3 receptor knockout mice. Br J Pharmacol 2001; 133: 438–44.
41 Samad TA, Moore KA, Sapirstein A, Billet S, Allchorne A, Poole S, *et al*. Interleukin-1beta-mediated induction of Cox-2 in the CNS contributes to inflammatory pain hypersensitivity. Nature 2001; 410: 471–5.
42 Doi Y, Minami T, Nishizawa M, Mabuchi T, Mori H, Ito S. Central nociceptive role of prostacyclin (IP) receptor induced by peripheral inflammation. Neuroreport 2002; 13: 93–6.
43 Murata T, Ushikubi F, Matsuoka T, Hirata M, Yamasaki A, Sugimoto Y, *et al*. Altered pain perception and inflammatory response in mice lacking prostacyclin receptor. Nature 1997; 388: 678–82.
44 England S, Bevan S, Docherty RJ. PGE2 modulates the tetrodotoxin-resistant sodium current in neonatal rat dorsal root ganglion neurones via the cyclic AMP-protein kinase A cascade. J Physiol 1996; 495: 429–40.
45 Thompson SW, Dray A, Urban L. Injury-induced plasticity of spinal reflex activity: NK1 neurokinin receptor activation and enhanced A- and C-fiber mediated responses in the rat spinal cord *in vitro*. J Neurosci 1994; 14: 3672–87.
46 Zeng H, Gragerov A, Hohmann JG, Pavlova MN, Schimpf BA, Xu H, *et al*. Neuromedin U receptor 2-deficient mice display differential responses in sensory perception, stress, and feeding. Mol Cell Biol 2006; 26: 9352–63.
47 DeHaven-Hudkins DL, Burgos LC, Cassel JA, Daubert JD, DeHaven RN, Mansson E, *et al*. Loperamide (ADL 2-1294), an opioid antihyperalgesic agent with peripheral selectivity. J Pharmacol Exp Ther 1999; 289: 494–502.
48 Piomelli D, Giuffrida A, Calignano A, Rodriguez de Fonseca F. The endocannabinoid system as a target for therapeutic drugs. Trends Pharmacol Sci 2000; 21: 218–24.
49 Gaponiuk P, Oivin VI. Direct effect of bradykinin on vascular permeability. Biull Eksp Biol Med 1971; 71: 23–5.
50 Bhoola K, Ramsaroop R, Plendl J, Cassim B, Dlamini Z, Naicker S. Kallikrein and kinin receptor expression in inflammation and cancer. Biol Chem 2001; 382: 77–89.
51 Handley DA, Arbeeny CM, Lee ML, Van Valen RG, Saunders RN. Effect of platelet activating factor on endothelial permeability to plasma macromolecules. Immunopharmacology 1984; 8: 137–42.
52 Burhop KE, Garcia JG, Selig WM, Lo SK, van der Zee H, Kaplan JE, *et al*. Platelet-activating factor increases lung vascular permeability to protein. J Appl Physiol 1986; 61: 2210–7.
53 Hatakeyama T, Pappas PJ, Hobson RW 2nd, Boric MP, Sessa WC, Duran WN. Endothelial nitric oxide synthase regulates microvascular hyperpermeability *in vivo*. J Physiol 2006; 574: 275–81.
54 Hudry-Clergeon H, Stengel D, Ninio E, Vilgrain I. Platelet-activating factor increases VE-cadherin tyrosine phosphorylation in mouse

endothelial cells and its association with the PtdIns3'-kinase. FASEB J 2005; 19: 512–20.
55 Knezevic II, Predescu SA, Neamu RF, Gorovoy MS, Knezevic NM, Easington C, *et al*. Tiam1 and Rac1 are required for platelet-activating factor-induced endothelial junctional disassembly and increase in vascular permeability. J Biol Chem 2009; 284: 5381–94.
56 Bakker RA, Timmerman H, Leurs R. Histamine receptors: specific ligands, receptor biochemistry, and signal transduction. Clin Allergy Immunol 2002; 17: 27–64.
57 Hamid Q, Tulic M. Immunobiology of asthma. Annu Rev Physiol 2009; 71: 489–507.
58 Mehta D, Malik AB. Signaling mechanisms regulating endothelial permeability. Physiol Rev 2006; 86: 279–367.
59 Vu TK, Hung DT, Wheaton VI, Coughlin SR. Molecular cloning of a functional thrombin receptor reveals a novel proteolytic mechanism of receptor activation. Cell 1991; 64: 1057–68.
60 Patterson C, Stouffer GA, Madamanchi N, Runge MS. New tricks for old dogs: nonthrombotic effects of thrombin in vessel wall biology. Circ Res 2001; 88: 987–97.
61 McLaughlin JN, Shen L, Holinstat M, Brooks JD, Dibenedetto E, Hamm HE. Functional selectivity of G protein signaling by agonist peptides and thrombin for the protease-activated receptor-1. J Biol Chem 2005; 280: 25048–59
62 Kozasa T, Jiang X, Hart MJ, Sternweis PM, Singer WD, Gilman AG, *et al*. p115 RhoGEF, a GTPase activating protein for Galpha12 and Galpha13. Science 1998; 280: 2109–11.
63 Tiruppathi C, Minshall RD, Paria BC, Vogel SM, Malik AB. Role of Ca^{2+} signaling in the regulation of endothelial permeability. Vascul Pharmacol 2002; 39: 173–85.
64 Holinstat M, Knezevic N, Broman M, Samarel AM, Malik AB, Mehta D. Suppression of RhoA activity by focal adhesion kinase-induced activation of p190RhoGAP: role in regulation of endothelial permeability. J Biol Chem 2006; 281: 2296–305.
65 Garcia JG, Siflinger-Birnboim A, Bizios R, Del Vecchio PJ, Fenton JW 2nd, Malik AB. Thrombin-induced increase in albumin permeability across the endothelium. J Cell Physiol 1986; 128: 96–104.
66 Lum H, Aschner JL, Phillips PG, Fletcher PW, Malik AB. Time course of thrombin-induced increase in endothelial permeability: relationship to $[Ca^{2+}]_i$ and inositol polyphosphates. Am J Physiol 1992; 263: L219–25.
67 Kaneider NC, Leger AJ, Agarwal A, Nguyen N, Perides G, Derian C, *et al*. 'Role reversal' for the receptor PAR1 in sepsis-induced vascular damage. Nat Immunol 2007; 8: 1303–12.
68 Cirino G, Severino B. Thrombin receptors and their antagonists: an update on the patent literature. Expert Opin Ther Pat 2010; 20: 875–84.
69 English D, Kovala AT, Welch Z, Harvey KA, Siddiqui RA, Brindley DN, *et al*. Induction of endothelial cell chemotaxis by sphingosine 1-phosphate and stabilization of endothelial monolayer barrier function by lysophosphatidic acid, potential mediators of hemato-poietic angiogenesis. J Hematother Stem Cell Res 1999; 8: 627–34.
70 McVerry BJ, Peng X, Hassoun PM, Sammani S, Simon BA, Garcia JG. Sphingosine 1-phosphate reduces vascular leak in murine and canine models of acute lung injury. Am J Respir Crit Care Med 2004; 170: 987–93.
71 Mehta D, Konstantoulaki M, Ahmmed GU, Malik AB. Sphingosine 1-phosphate-induced mobilization of intracellular Ca^{2+} mediates rac activation and adherens junction assembly in endothelial cells. J Biol Chem 2005; 280: 17320–8.
72 Ho MK, Su Y, Yeung WW, Wong YH. Regulation of transcription factors by heterotrimeric G proteins. Curr Mol Pharmacol 2009; 2: 19–31.
73 Kravchenko VV, Pan Z, Han J, Herbert JM, Ulevitch RJ, Ye RD. Platelet-activating factor induces NF-kappa B activation through a G protein-coupled pathway. J Biol Chem 1995; 270: 14928–34.
74 Cowen DS, Molinoff PB, Manning DR. 5-hydroxytryptamine1A receptor-mediated increases in receptor expression and activation of nuclear factor-kappaB in transfected Chinese hamster ovary cells. Mol Pharmacol 1997; 52: 221–6.
75 Hsu MH, Wang M, Browning DD, Mukaida N, Ye RD. NF-kappaB activation is required for C5a-induced interleukin-8 gene expression in mononuclear cells. Blood 1999; 93: 3241–9.
76 Shahrestanifar M, Fan X, Manning DR. Lysophosphatidic acid activates NF-kappaB in fibroblasts. A requirement for multiple inputs. J Biol Chem 1999; 274: 3828–33.
77 Xie P, Browning DD, Hay N, Mackman N, Ye RD. Activation of NF-kappa B by bradykinin through a Galpha(q)- and Gbeta gamma-dependent pathway that involves phosphoinositide 3-kinase and Akt. J Biol Chem 2000; 275: 24907–14.
78 Yang M, Sang H, Rahman A, Wu D, Malik AB, Ye RD. G alpha 16 couples chemoattractant receptors to NF-kappa B activation. J Immunol 2001; 166: 6885–92.
79 Shi CS, Kehrl JH. PYK2 links G(q)alpha and G(13)alpha signaling to NF-kappa B activation. J Biol Chem 2001; 276: 31845–50.
80 Gao H, Sun Y, Wu Y, Luan B, Wang Y, Qu B, *et al*. Identification of beta-arrestin2 as a G protein-coupled receptor-stimulated regulator of NF-kappaB pathways. Mol Cell 2004; 14: 303–17.
81 Witherow DS, Garrison TR, Miller WE, Lefkowitz RJ. beta-Arrestin inhibits NF-kappaB activity by means of its interaction with the NF-kappaB inhibitor IkappaBalpha. Proc Natl Acad Sci U S A 2004; 101: 8603–7.
82 Yang M, Zhang H, Voyno-Yasenetskaya T, Ye RD. Requirement of Gbetagamma and c-Src in D2 dopamine receptor-mediated nuclear factor-kappaB activation. Mol Pharmacol 2003; 64: 447–55.
83 Sun J, Lin X. Beta-arrestin 2 is required for lysophosphatidic acid-induced NF-kappaB activation. Proc Natl Acad Sci U S A 2008; 105: 17085–90.
84 Yang M, He RL, Benovic JL, Ye RD. beta-Arrestin1 interacts with the G-protein subunits beta1gamma2 and promotes beta1gamma2-dependent Akt signalling for NF-kappaB activation. Biochem J 2009; 417: 287–96.
85 Grabiner BC, Blonska M, Lin PC, You Y, Wang D, Sun J, *et al*. CARMA3 deficiency abrogates G protein-coupled receptor-induced NF-{kappa} B activation. Genes Dev 2007; 21: 984–96.
86 Wang D, You Y, Lin PC, Xue L, Morris SW, Zeng H, *et al*. Bcl10 plays a critical role in NF-kappaB activation induced by G protein-coupled receptors. Proc Natl Acad Sci U S A 2007; 104: 145–50.
87 Schwarz M, Murphy PM. Kaposi's sarcoma-associated herpesvirus G protein-coupled receptor constitutively activates NF-kappa B and induces proinflammatory cytokine and chemokine production via a C-terminal signaling determinant. J Immunol 2001; 167: 505–13.
88 Shepard LW, Yang M, Xie P, Browning DD, Voyno-Yasenetskaya T, Kozasa T, *et al*. Constitutive activation of NF-kappa B and secretion of interleukin-8 induced by the G protein-coupled receptor of Kaposi's sarcoma-associated herpesvirus involve G alpha(13) and RhoA. J Biol Chem 2001; 276: 45979–87.
89 Couty JP, Geras-Raaka E, Weksler BB, Gershengorn MC. Kaposi's sarcoma-associated herpesvirus G protein-coupled receptor signals through multiple pathways in endothelial cells. J Biol Chem 2001; 276: 33805–11.
90 Gruijthuijsen YK, Casarosa P, Kaptein SJ, Broers JL, Leurs R, Bruggeman CA, *et al*. The rat cytomegalovirus R33-encoded G

protein-coupled receptor signals in a constitutive fashion. J Virol 2002; 76: 1328–38.
91 Cannon M. The KSHV and other human herpesviral G protein-coupled receptors. Curr Top Microbiol Immunol 2007; 312: 137–56.
92 Vischer HF, Hulshof JW, de Esch IJ, Smit MJ, Leurs R. Virus-encoded G-protein-coupled receptors: constitutively active (dys)regulators of cell function and their potential as drug target. Ernst Schering Found Symp Proc 2006; 2: 187–209.
93 Kahn ML, Zheng YW, Huang W, Bigornia V, Zeng D, Moff S, *et al*. A dual thrombin receptor system for platelet activation. Nature 1998; 394: 690–4.
94 Cunningham MA, Rondeau E, Chen X, Coughlin SR, Holdsworth SR, Tipping PG. Protease-activated receptor 1 mediates thrombin-dependent, cell-mediated renal inflammation in crescentic glomerulonephritis. J Exp Med 2000; 191: 455–62.
95 Hata AN, Breyer RM. Pharmacology and signaling of prostaglandin receptors: multiple roles in inflammation and immune modulation. Pharmacol Ther 2004; 103: 147–66.
96 Boie Y, Rushmore TH, Darmon-Goodwin A, Grygorczyk R, Slipetz DM, Metters KM, *et al*. Cloning and expression of a cDNA for the human prostanoid IP receptor. J Biol Chem 1994; 269: 12173–8.
97 Boie Y, Sawyer N, Slipetz DM, Metters KM, Abramovitz M. Molecular cloning and characterization of the human prostanoid DP receptor. J Biol Chem 1995; 270: 18910–6.
98 Matsuoka T, Hirata M, Tanaka H, Takahashi Y, Murata T, Kabashima K, *et al*. Prostaglandin D2 as a mediator of allergic asthma. Science 2000; 287: 2013–7.
99 Leeb-Lundberg LM, Marceau F, Muller-Esterl W, Pettibone DJ, Zuraw BL. International Union of Pharmacology. XLV. Classification of the kinin receptor family: from molecular mechanisms to pathophysiological consequences. Pharmacol Rev 2005; 57: 27–77.
100 Kuduk SD, Bock MG. Bradykinin B1 receptor antagonists as novel analgesics: a retrospective of selected medicinal chemistry developments. Curr Top Med Chem 2008; 8: 1420–30.
101 Duchene J, Ahluwalia A. The kinin B(1) receptor and inflammation: new therapeutic target for cardiovascular disease. Curr Opin Pharmacol 2009; 9: 125–31.
102 Duffy RA. Potential therapeutic targets for neurokinin-1 receptor antagonists. Expert Opin Emerg Drugs 2004; 9: 9–21.
103 Torres R, Croll SD, Vercollone J, Reinhardt J, Griffiths J, Zabski S, *et al*. Mice genetically deficient in neuromedin U receptor 2, but not neuromedin U receptor 1, have impaired nociceptive responses. Pain 2007; 130: 267–78.
104 Kaminski NE. Immune regulation by cannabinoid compounds through the inhibition of the cyclic AMP signaling cascade and altered gene expression. Biochem Pharmacol 1996; 52: 1133–40.
105 Yost CC, Weyrich AS, Zimmerman GA. The platelet activating factor (PAF) signaling cascade in systemic inflammatory responses. Biochimie 2010; 92: 692–7.

Acta Pharmacologica Sinica (2012) 33: 351–362
 1671-4083/12 $32.00
www.nature.com/aps

Review

GPCRs and cancer

Rosamaria LAPPANO, Marcello MAGGIOLINI*

Department of Pharmaco-Biology, University of Calabria, Rende (CS), Italy

G-protein-coupled receptors (GPCRs), which represent the largest gene family in the human genome, play a crucial role in multiple physiological functions as well as in tumor growth and metastasis. For instance, various molecules like hormones, lipids, peptides and neurotransmitters exert their biological effects by binding to these seven-transmembrane receptors coupled to heterotrimeric G-proteins, which are highly specialized transducers able to modulate diverse signaling pathways. Furthermore, numerous responses mediated by GPCRs are not dependent on a single biochemical route, but result from the integration of an intricate network of transduction cascades involved in many physiological activities and tumor development. This review highlights the emerging information on the various responses mediated by a selected choice of GPCRs and the molecular mechanisms by which these receptors exert a primary action in cancer progression. These findings provide a broad overview on the biological activity elicited by GPCRs in tumor cells and contribute to the identification of novel pharmacological approaches for cancer patients.

Keywords: cancer; G-protein-coupled receptors; heterotrimeric G-proteins; hormones; lipids; peptides; signal transduction

Acta Pharmacologica Sinica (2012) 33: 351–362; doi: 10.1038/aps.2011.183; published online 23 Jan 2012

Introduction

The seven-transmembrane G protein-coupled receptors (GPCRs), which belong to the largest superfamily of signal transduction proteins, regulate multiple biological functions coupling to a heterotrimeric G-protein associated with the inner surface of the plasma membrane[1]. The heterotrimer that is composed of the Gα, Gβ, and Gγ subunits, binds to the guanine nucleotide GDP in its basal state. Upon activation by ligand binding, GDP is released and replaced by GTP, which leads to subunit dissociation into a βγ dimer and the GTP-bound α monomer[2] (Figure 1). On the basis of the sequence identity, the Gα subunit has been classified into four families: $G\alpha_s$, $G\alpha_i$, $G\alpha_q$, and $G\alpha_{12}$. Each Gα family can relay the GPCR signal stimulating different downstream effectors[2]. Some GPCRs, such as the lysophosphatidic acid (LPA) receptors, can couple to more than one G protein triggering consequently diverse signaling cascades, whereas other GPCRs like sphingosine-1-phosphate (S1P) receptor 1 (S1P1) couple exclusively to one G protein[3, 4].

An increasing number of studies links aberrant GPCR expression and activation to numerous types of human malignancies[5, 6] (Figure 1). For instance, several GPCRs are overexpressed in different tumors[6] and GPCR variants can lead to increased cancer risk. In this regard, it should be mentioned that in genetic association studies melanocortin-1 receptor (MC1R) polymorphisms were associated with an enhanced threat of skin cancer[7]. In addition, an aberrant activation of GPCRs by high levels of ligands like LPA, S1P and chemokines was involved in cell transformation, proliferation, angiogenesis, metastasis and drug resistance[6]. Conversely, some members of GPCRs, such as the orexin receptor OX1R, were shown to mediate a pro-apoptotic action in various cancer cells[8].

Cross-talk among different receptors including GPCRs triggers relevant biological functions in normal and neoplastic cells[9]. In this context, it has been reported that many GPCRs activate numerous signaling pathways interacting with other plasma membrane receptors[9] (Figure 1). For example, the cross-talk between acetylcholine muscarinic receptors (mAChRs) and epidermal growth factor (EGFR) as well as platelet-derived growth factor (PDGFR) receptors leads to the activation of mitogenic pathways which mediate cell proliferation, differentiation and survival[10]. In addition, several GPCR ligands like bradikinin (BK), LPA, Gastrin-releasing peptide (GrP) and bombesin (BN) transactivate EGFR, then inducing stimulatory effects in different types of tumors[6].

Currently, many agents targeting GPCRs, such as gonadotropin-releasing factor and somatostatin receptors, are used for cancer treatment on the basis of valuable experimental data and clinical benefits[11, 12]. Moreover, various inhibitors of GPCRs are currently under evaluation in clinical trials as anticancer agents (http://www.clinicaltrials.gov/). This

* To whom correspondence should be addressed.
E-mail marcellomaggiolini@yahoo.it
Received 2011-10-13 Accepted 2011-12-01

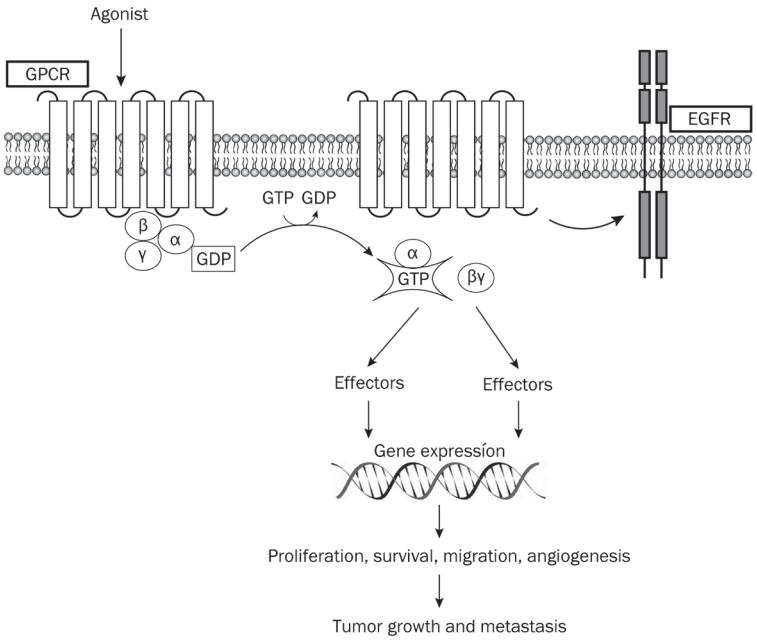

Figure 1. Agonist binding to GPCRs promotes the dissociation of GDP bound to the Gα subunit and its replacement with GTP leading to the activation of the heterotrimeric G proteins and the subunit dissociation into a βγ dimer and the GTP-bound α monomer. Both subunits activate multiple downstream effectors which induce gene transcription and relevant biological responses. A cross-talk between several GPCRs and other membrane receptors as Epidermal Growth Factor Receptor (EGFR) contributes to the growth stimulation and invasion of cancer cells.

review recapitulates our current understanding regarding the mechanisms through which various GPCRs may contribute to tumor progression. On these bases, GPCRs may be considered as promising targets in novel pharmacological approaches for cancer patients.

GPCRs activated by bio-active lipids

GPCRs activated by the bio-active lipids LPA and S1P have been implicated in aberrant signaling in a wide range of tumors. LPA1, LPA2 and LPA3 represent the most widely expressed and well-characterized receptors for LPA and its analogues[3]. Upon binding to these receptors, LPA triggers a variety of signaling pathways engaging the heterotrimeric G proteins and their downstream effectors[3]. As a consequence, the transcriptional activation of multiple cancer-associated genes leads to cell survival and proliferation, migration, chemotaxis, vascular remodeling and angiogenesis[13]. Aberrant expressions and mutations of LPA receptors have been found in several types of tumors, suggesting their involvement in the growth advantage of cancer cells[3, 14, 15]. For instance, LPA1 was inversely correlated in breast cancer tissues with the Nm23 metastases regulator[16] and contributed to bone metastasis in breast cancer xenografts[17]. Furthermore, LPA induced migration in breast cancer cells by activating LPA1, which promoted the phosphorylation of nonmuscle myosin II (NM II) light chain through the activation of ROCK and RhoA activity[18]. In addition, the expression of LPA1, LPA2, and LPA3 in mammary epithelium of transgenic mice induced a high frequency of late-onset, estrogen receptor (ER)-positive, invasive and metastatic mammary cancer[19]. LPA stimulated also tumorigenesis and metastasis in ovarian malignancy[20]. For instance, LPA exerted a growth factor-similar action and prevented apoptosis in ovarian cancer cells through redox-dependent activation of ERK, Akt and NF-κB-dependent signaling[21]. Recently, the LPA/LPA1-induced Rac activation as well as the integrity of SOS1/EPS8/ABI1 tri-complex were required for ovarian cancer metastasis[22]. Closely resembling the LPA-effects in human ovarian cancer cells, LPA induced metastasis of epithelial ovarian cancer in immuno-competent mice[23]. As other GPCR ligands, LPA promoted stimulatory effects in different types of tumors by transactivating EGFR and triggering a functional cross-talk between its cognate receptors and EGFR-mediated signaling[6]. In this regard, it should be mentioned that EGFR activity was required for the activation of Gi-dependent cellular responses induced by LPA in ovarian cancer cells[24]. Moreover, a cross-talk between LPA receptors and EGFR occurred in ovarian cancer cells as demonstrated by the increase of LPA production following ligand-dependent EGFR transactivation[25]. In addition to breast and ovarian malignancies, LPA was involved in other types of tumors. In a murine xenograft model of lung adenocarcinoma, mesenchymal stem cells were recently shown to stimulate angiogenesis through a LPA1-dependent mechanism[26]. Likewise, an engineered three-dimensional tumor xenograft model of non-small cell lung cancer (NSCLC) in nude mice regressed and lost vascularity in response to BrP-LPA, which acts as a LPA receptor antagonist and autotaxin inhibitor[27].

The bio-active lipid S1P has been involved in various aspects of tumor development, including cell proliferation, motility and invasiveness, apoptosis, differentiation, angiogenesis and inflammation[28]. However, S1P can mediate both proliferative[29] and antiproliferative[30] effects in neoplastic cells. These opposite responses to S1P were attributed to the different activities exerted by its five receptors, which are coupled to distinct members of the G protein family and display a specific tissue expression pattern[28]. In particular, S1P1 mediated pro-migratory effects[31], whereas S1P2 inhibited cell migration[32]. An increased S1P1 expression, which was recently induced by

the activator of transcription-3 (STAT3), up-regulated IL-6 and accelerated tumor growth and metastasis[33]. In glioblastoma and in Wilms tumor cells S1P-dependent S1P1 signaling induced cell migration and invasion[34, 35], whereas in glioblastoma and melanoma cells S1P-dependent S1P2 pathway negatively directed migration and invasion[32, 36]. Paralleling the aforementioned observations, S1P1 and S1P2 exerted opposite effects on tumor angiogenesis. For instance, S1P1 stimulated angiogenesis[37] and accordingly the administration of monoclonal anti-S1P antibody prevented tumor growth by inhibiting angiogenesis and motility, survival and proliferation[38]. In addition, S1P1 was shown to be up-regulated in vessels at sites of tumor implantation, whereas S1P1 silencing resulted in the inhibition of tumor growth[39]. In contrast to the Gi-dependent S1P1 stimulation of tumor angiogenesis, S1P2 mediated inhibitory effects on tumor angiogenesis through G12/Rho signaling[40]. Together, these data suggest that the different action elicited by S1P1 and S1P2 may serve for novel pharmacological strategies based on therapeutics able to inhibit S1P1 and to activate S1P2 simultaneously.

GPCRs activated by peptides

The endothelin receptors (ET_AR and ET_BR) have been broadly involved in the regulation of mitogenesis, cell survival, angiogenesis, lymphangiogenesis, invasion and metastatic dissemination as well as epithelial-to-mesenchymal transition (EMT) in diverse types of malignancies[41]. Accordingly, high plasma endothelin-1 (ET-1) levels correlated with the tumor stage in cancer patients, suggesting that ET-1 can also serve as a prognostic marker[41, 42]. Emerging data demonstrate that interfering with the ET receptors-dependent pathways may provide a significant chance for the development of novel anticancer strategies, in particular using ET_AR antagonists in combination with EGFR inhibitors as well as cytotoxic drugs[43]. Nevertheless, antagonists of ET receptors, like atrasentan and zibotentan (ZD4054), used alone have also gained considerable interest in human clinical trials on the basis of their potential anticancer activity[43]. For instance, the ET_AR blockade with the specific ET_AR antagonist zibotentan restored drug sensitivity to cytotoxic-induced apoptosis and inhibited ovarian cancer cell invasion[44].

The four receptors for the Gastrin-releasing peptide (GrP) were shown to be able to transactivate EGFR in lung, head and neck squamous tumor cells[45, 46]. In addition, ligand-stimulation of GrP receptors contributed to the growth of several malignancies through the activation of diverse phospholipases and protein kinases[47]. As GrP receptors were found overexpressed in a wide variety of tumors, their inhibition has been suggested as a promising objective in some malignancies[47]. Hence, the use of antagonists of GrP receptors represents a potential approach to inhibit the GrP-dependent effects on tumor growth. In this regard, it was demonstrated that the anti-tumor activity of GrP antagonists involves different mechanisms as the reduction of EGFR and Her2 levels, the alteration of MAPK, PKC, pAkt, and COX-2 signaling, the attenuation of c-fos and c-jun expression, the modulation of wild-type and mutated forms of p53 along with an alteration of Bcl-2/BAX ratio, the inhibition of vascular endothelial growth factor (VEGF)[47]. Radiolabeled GrP analogues represent another chance in targeting GrP receptors, thus they are currently considered promising radiopharmaceuticals for detection and treatment of different types of tumors[48, 49].

Protease-activated receptors (PARs) are a unique class of GPCRs that are activated by proteolytic cleavage of their extracellular domains[50]. PAR-1 exerted a functional role in the growth, migration and metastasis in various tumors[51-53]. For instance, its proteolytic activation by thrombin caused persistent activation of EGFR/ERK signaling, promoting thereafter breast carcinoma cell invasion[54]. Moreover, PAR-1 negatively regulated the expression of the Maspin tumor-suppressor gene contributing to the metastatic phenotype of melanoma[55]. It has been recently reported that metalloprotease-1 (MMP1) may function as a protease agonist of PAR-1 which then stimulates migration, invasion and angiogenesis in breast and ovarian malignancies[56, 57].

Activation of the canonical Wnt pathway occurs through the seven-transmembrane Frizzled (Fzd) family receptors and the co-receptors lipoprotein receptor-related protein (LRP) in order to initiate the β-catenin signaling cascade[58]. The activated β-catenin translocates from the cytoplasm to the nucleus inducing the transcription of Wnt-responsive genes[58]. Numerous studies have shown that the dysregulation of the canonical Wnt pathway may lead to cancer development and progression[58]. In this regard, mutations of β-catenin, axin and other components of the Wnt pathway[59] as well as the activation of tissue-specific Wnt target genes[60, 61] were found in a variety of human tumors. In addition, the non-canonical Wnt pathways that act independently of β-catenin promote the invasiveness and progression of tumors[62]. Several Fzd receptors are highly expressed in a variety of malignancies and involved in cancer cell growth, survival and invasion through both canonical and non-canonical Wnt pathways[6]. For instance, the pharmacological inhibition of Fzd7, which is frequently overexpressed in hepatocellular carcinoma (HCC), displayed anti-tumor properties by involving β-catenin and PKCδ signals[63]. Fzd7 was also crucial through the canonical Wnt pathway for cell proliferation and invasiveness in triple negative breast cancer cells as well as for tumor formation in xenograft models[64]. Moreover, the increased expression of Fzd4 through the up-regulation of β-catenin dependent Wnt signaling promoted in invasive glioma cells the acquisition of glioma stem cell-like properties and resistance to apoptosis[65]. Next, a cross-talk between Wnt pathways and EGFR signaling occurred in multiple stages of cancer development[59].

The Hedgehog (Hh) signaling, which plays a key role in embryonic development, has been involved in the development of multiple malignancies[66]. Hh ligands are secreted from different tissues at various stages of development and generate intracellular signaling by binding to and inactivating the Hh receptor Patched-1 (Ptch1), which relieves its catalytic inhibition of the GPCR-like signal transducer Smoothened (Smo). The activation of Smo triggers downstream events

that culminate in the stimulation of the glioma-associated oncogene homologue (GLI) transcription factors, the up-regulation of target genes like cyclins, Bcl-2 and SNAIL and the production of VEGF and angiopoietins[66]. Consequently, Hh signaling contributes to cancer cell proliferation and survival, angiogenesis and metastasis[66]. In addition, mutations in components of the Hh pathway, such as Smo and Ptch1, lead to a constitutively activated Hh signaling in the absence of ligands in diverse cancer types, including basal cell carcinoma, medulloblastoma and non-small cell lung carcinoma[66–68]. The overexpression of Hh ligands have been also identified in several tumors as a stimulating factor acting in an autocrine manner to induce cell proliferation and survival[69]. Likewise, Hh ligands produced by stromal cells can promote tumor growth and survival in a paracrine manner[69]. Conversely, tumor cells can produce Hh ligands which activate transduction pathways in stromal cells[69]. Several small molecule antagonists for Smo have been developed with a promising preclinical efficacy in multiple tumors. For instance, the Smo inhibitor CUR61414 inhibited in mice skin the Hh signaling, blocked the induction of hair follicle anagen and shrank in basal cell carcinomas (BCCs), although in a phase I clinical study it did not show any activity in human superficial or nodular BCCs[70]. Several other Smo antagonists, such as IPI-926, BMS-833923 and GDC-0449, are currently under evaluation in clinical trials as anticancer agents (http://www.clinicaltrials.gov/). In particular, GDC-0449 produced promising antitumor responses in a phase I study in patients with advanced BCCs as well as in a 26-year-old man with metastatic medulloblastoma which was unmanageable by conventional therapies[71]. However, the response of this patient to GDC-0449 treatment was only transient due to a mutation of Smo[71]. Recently, a number of Hh pathway antagonists targeting Smo mutants[72] as well as inhibitors able to block both wild-type and Smo mutants have been identified[73]. In addition to Smo antagonists, other inhibitors were used to block Hh signaling like the small molecule inhibitor of GLI1 and GLI2 transcription factors, GANT61, which induced colon carcinoma cell death in a higher extent respect to the conventional Smo inhibitor cyclopamin[74]. The treatment with GANT61 reduced also the expression of the target gene Patched and decreased the viability of chronic lymphocytic leukemia cells[75]. Recently, the systemic antifungal itraconazole which failed to bind to Smo at the same binding site of cyclopamine, showed a potent antagonism for the Hh signaling pathway associated with anti-tumor activity in a mouse medulloblastoma allograft model[76].

GPCRs activated by chemokines

Besides their functions in the immune system as mediators of leukocyte migration, chemokines and the cognate receptors play a critical role in tumor initiation and progression, including angiogenesis, attraction of leukocytes and induction of cell migration and homing in metastatic sites[77]. The first described angiogenic chemokine, CXCL8/IL-8, which binds to CXCR1 and CXCR2[78], is secreted by a variety of normal and tumor cells exposed to pro-inflammatory cytokines like IL-1 and TNF-α[79]. CXCR2 was associated to multiple signaling pathways involved in tumorigenesis, angiogenesis, proliferation and metastasis in several malignancies, including melanoma[80], lung[81], pancreatic[79, 82], gastric[83], and ovarian[57] tumors. For instance, the overexpression of CXCR2 induced an aggressive phenotype of melanoma cells consisting with an enhanced proliferation, migration and tumor growth in mice[84].

The homeostatic chemokine stromal cell-derived factor-1, CXCL12/SDF-1, which regulates cardiac and neuronal development, stem cell motility and neovascularization, was also involved in diverse tumorigenic processes[77]. The CXCL12/SDF-1 interaction with the widely expressed tumor cell surface receptor CXCR4 initiates divergent signaling pathways which can result in a variety of responses like chemotaxis, cell survival, proliferation and metastasis[80]. CXCR4 is capable of orchestrating a complex signaling network, including the up-regulation of E-cadherin and c-myc as well as the modulation of molecules facilitating mammary epithelia cell transformation[85]. Enhanced CXCR4 signaling was also involved in the resistance to endocrine therapy in breast cancer[86] and in the drug resistance of colon[87] and pancreatic cancer cells[88]. Of note, CXCR4 expression and phosphorylation has been considered a negative prognostic marker in various types of cancer including acute myelogenous leukemia and B-acute lymphoblastic leukemia, breast and colon carcinomas, as it correlated with worse prognosis and decreased survival of patients[86, 89–92]. Increased levels of VEGF, the activation of nuclear factor kappa B (NF-κB) and some oncoproteins up-regulate CXCR4 expression, in particular during cancer progression[93, 94] and under hypoxic conditions[95]. CXCR4/SDF-1 contributes to tumor progression also through the activation of tumor-associated integrin and the production of matrix metalloproteases[93], as observed in human basal carcinoma cells[96] and oral squamous cell carcinomas[97]. Recently, CXCR7/RDC1 has been identified as a novel receptor for CXCL12/SDF-1 and CXCL11[98], although its coupling to G-proteins remains controversial. CXCR7 is expressed in diverse cell types including malignant cells[98] as well as in tumor-associated blood vessels[99]. CXCR7-dependent signals promote the growth of breast and lung tumors, enhance lung metastasis and tumor aggressiveness in prostate cancer[99, 100]. Antagonists of CXCR7 prevented tumor growth in animal models, hence validating this receptor as a potential target for the development of novel anti-cancer therapeutics[98].

GPCRs activated by hormones

Numerous hormone-activated GPCRs are overexpressed in hormone-dependent and independent tumors and trigger multiple transduction pathways, which mediate relevant biological effects in diverse cancer cells. For instance, angiotensin II (Ang-II) and bradykinin (BK) receptors are overexpressed in prostate cancer[101, 102] and mediate cell growth through $G\alpha_q$ and/or $G\alpha_{13}$ which activate RhoA-dependent signaling[103]. In this regard, it was shown that Rho is involved in the androgen-like activity of androgen receptor (AR) antagonists[104] and

able to sensitize AR to low androgens levels[105]. On the basis of these studies, it can be assumed that GPCRs may contribute to androgen-dependent and independent growth of prostate cancer[103]. Recently, Ang-II exhibited *in vitro* and *in vivo* the potential to enhance the expression of AR in prostate cancer cells through angiotensin II type-1 receptor (AT1R)[106]. In addition, Ang-II and BK receptors have been implicated in the development, growth, angiogenesis and metastasis in a wide number of tumors[101, 102, 107–111]. For instance, Ang-II and BK stimulated DNA synthesis in pancreatic cancer cells[112]. In the context of this malignancy, a cross-talk between insulin/insulin like growth factor-I (IGF-1) receptors and Ang-II and BK-activated GPCRs has been reported[111-114]. In particular, insulin induced the potentiation of Ang-II and BK-dependent signaling through the PI3K/Akt/mTOR transduction pathway[113]. Metformin, which is one of the most used drug in the treatment of type 2 diabetes, disrupted in pancreatic cancer cells the cross-talk between insulin receptor and GPCR signaling through the activation AMP kinase, which negatively regulated mTOR function[113]. Further supporting these observations, metformin prevented the growth of pancreatic cancer cells in xenograft models[114, 115]. Cumulatively, these findings suggest that the cross-talk between insulin/IGF-1 receptors and GPCR-activated signaling can be considered as a mechanism involved in the development of certain tumors and a promising target for novel anti-cancer strategies.

As it concerns the renin-angiotensin system, an abundant generation of Ang-II stimulated by the angiotensin-converting enzyme (ACE) and the up-regulation of AT1R have been demonstrated in various tumors[110, 116]. In this respect, ACE inhibitors and angiotensin II receptor blockers (ARBs) have recently acquired an increasing interest as chemopreventive agents[110, 117, 118]. Of note, ARBs have been associated with reduced cancer occurrence in patients with essential hypertension and a longer exposure to ARBs has been related with major benefits in cancer patients[119]. Nevertheless, ARBs did not show the ability to reduce considerably cancer development in a meta-analysis of randomized controlled trials[120].

Among the GPCR family members, the gonadotropin-releasing hormone (GnRH) receptor is a well established target in the clinical practice of cancer treatment[121]. Several antagonist analogues of GnRH have been clinically tested and numerous orally active antagonists are under development[121]. The GnRH receptor is one of the smallest GPCRs as it lacks the characteristic intracellular carboxyl-terminal domain with a very short extracellular amino-terminus. GnRH receptors are expressed not only in the pituitary and in normal peripheral tissues[122], but also in various tumor cells like melanoma, prostate and endometrial carcinomas, leiomyomas, leiomyosarcomas, breast cancer, choriocarcinoma, epithelial and stromal tumors of the ovary[122, 123]. The activation of the peripheral GnRH receptor, which is coupled to the Gi protein in uterine leiomyosarcoma, ovarian and endometrial carcinomas, decreased intracellular cAMP levels leading to a down-regulation of gene transcription and antiproliferative effects in tumor cells[122]. Indeed, the repressive action of GnRH-I receptor on cell proliferation has been demonstrated in hormone-related tumors like prostate, breast, ovary and endometrium cancer[124]. GnRH and the cognate receptors were also involved in the stimulation of motility and invasion in ovarian cancer cells[125, 126], however several studies suggested a protective role elicited by GnRH analogues against gonadal damage during chemotherapy in diverse types of tumors[122]. On the basis of these findings, GnRH analogues are used in many endocrine-dependent malignancies such as breast, endometrial, epithelial and stromal ovarian cancer. The antitumor activity of GnRH analogues was presumed to result from desensitization and/or decrease of GnRH receptors in the pituitary, with the consequent decline in gonadotropin secretion and gonadal hormone production. Nevertheless, GnRH analogues were shown to suppress directly the growth of endometrial, ovarian, breast and prostate tumors and uterine leiomyoma[122, 127, 128]. Likewise, the growth of prostate cancer cells *in vitro* and in tumor xenografts was inhibited by activating the GnRH receptor or by GnRH receptor blockade[129]. In line with these observations, phase III trial data have demonstrated that GnRH agonists are effective and well tolerated in the treatment of hormone-sensitive prostate cancer[130]. Recently, the possibility of using GnRH analogues to carry cytotoxic agents directly to cancer cells expressing GnRH receptors has been evaluated[131]. For instance, AN-152 conjugate which is made from doxorubicin being linked to [*D*-Lys6]GnRH agonist, reduced the proliferation of breast, ovarian and endometrial cancer cells *in vitro* and in xenografted nude mice[132, 133].

Estrogens influence many physiological processes, but are also implicated in the development or progression of various types of cancer[134]. The multiple biological actions elicited by these hormones have traditionally been attributed to the classical nuclear estrogen receptor (ER)α and ERβ, which act as ligand-activated transcription factors[134]. Surprisingly, a member of the GPCR family, GPR30/GPER, was recently shown to mediate the multifaceted actions of estrogens in different tissues including cancer cells[135]. Importantly, GPER overexpression was associated with lower survival rates in endometrial and ovarian cancer patients and with an elevated risk of developing metastases in patients with breast cancer[136-138]. GPER by transactivating EGFR triggers numerous transduction pathways including the intracellular cAMP, calcium mobilization, MAPK, PI3-K and phospholipase C activation in a variety of cell types[139]. Moreover, it has been shown that the activation of the $G\alpha_s$ protein by GPER is responsible for the estrogen, phyto- and xenoestrogens stimulation of adenylate cyclase and the ensuing increase in cAMP in breast cancer cells[140, 141]. The signaling events upon GPER activation by both estrogens and notably ER antagonists can lead to gene transcription as well as to the growth and migration in diverse hormone-sensitive tumors like breast, endometrial and ovarian cancer[142–149]. Notably, GPER was also involved in the stimulatory effects elicited by estrogens and ER antagonists in cancer-associated fibroblasts[147, 150].

GPCRs activated by neurotransmitters

Emerging findings support the hypothesis that the development, progression and responsiveness to treatments in most tumors is strongly influenced by an imbalance in stimulatory and inhibitory neurotransmission[151]. The neurotransmitters adrenaline and noradrenaline act as powerful regulators of numerous cellular and tissue functions and can promote tumor growth and metastases through the β-adrenergic receptors (β-AR), which are Gs-protein coupled receptors[152–154]. For instance, noradrenaline stimulates tumor progression in diverse types of malignancies activating β-AR which in turn induces the production of VEGF, interleukin-6 (IL-6) and matrix metalloproteinases[153, 155].

As for β-adrenergic compounds[156], the action of muscarinic acetylcholine receptors (mAchRs) on the proliferation of cancer cells is still questioned[157]. In fact, these receptors interact with distinct G protein subunits triggering various cellular functions through specific downstream effectors. As it concerns M2 and M4 receptors, they interact with Gi proteins inhibiting adenylyl cyclase-dependent signaling. On the contrary, M1, M3 and M5 receptors coupled with Gq proteins activate phospholipase C, PKC and induce an increase of intracellular calcium[153]. These mAchR subtypes can protect cells from the apoptosis subsequent to DNA damage, oxidative stress and mitochondrial dysfunction[158]. Although muscarinic receptor expression was identified in cells derived from brain, breast, colon, lung, ovary, pancreas, prostate, skin, stomach and uterus malignancies[157], only for some of these receptors a functional role has been demonstrated. In ovarian cancer the expression of muscarinic receptors was associated with reduced survival[159], while in leukemia cells their activation resulted in increased intracellular calcium and up-regulation of the oncogene c-fos[160]. Activation of M3 receptor by cholinergic agonists stimulated proliferation of primary astrocytoma cells in a ERK and NF-κB dependent manner[157]. In breast cancer cells, M1 and M2 receptors were involved in angiogenesis and cell proliferation, whereas M3 receptor was associated only with cell growth[161]. Agonist binding to M3 receptor resulted in the activation of EGFR/MAPK transduction pathway, which then stimulated the proliferation in colon cancer cells[162].

Somatostatin receptors (SSTRs), particularly SSTR subtype 2, were found highly expressed in many neoplastic cells and in tumoral blood vessels[163]. SST analogues decreased tumor cell growth and angiogenesis as well as stimulated apoptosis in cancer cells[164]. These findings contributed to develop various cytotoxic SST conjugates that displayed relevant anti-tumor abilities targeting selectively SSTR2-specific sites[165].

β-arrestins: novel transducers of GPCR signals

The sensitivity of GPCRs is regulated by G protein-coupled receptor kinases (GRKs) and β-arrestins families, that are known to exert a central role in GPCR endocytosis, intracellular trafficking, desensitization and resensitization[166, 167]. As it concerns β-arrestins, they can also function as molecular mediators of G protein-independent signaling by activating a variety of transduction proteins like Src family kinases and components of the MAPK cascades[166, 168, 169]. On the basis of these findings, β-arrestins were included among the signaling factors mediating the action of diverse GPCRs in cancer[170]. For instance, β-arrestin/Ral signaling was involved in the migration and invasion of breast cancer cells induced by LPA[170]. In addition, prostaglandin E2 induced the association of prostaglandin E receptor 4 with β-arrestin 1 and c-Src, that formed a signaling complex able to induce the migration and metastasis of colorectal carcinoma cells[171]. In accordance with these data, β-arrestin 1 interacting with Src and ET_AR triggered EGFR transactivation and β-catenin phosphorylation, which stimulated invasion and metastasis in ovarian cancer cells[172]. Moreover, β-arrestin 1 forming a trimeric complex with ET_AR and axin contributed to the inactivation of glycogen synthase kinase (GSK)-3 and stabilization of β-catenin[172]. Collectively, these results indicate that β-arrestins exert an important role in GPCR-mediated signaling as well as a pivotal role in cancer invasion and metastasis. Novel pharmacological approaches targeting the β-arrestins pathway would provide further therapeutical opportunities in diverse types of tumors.

Orphan GPCRs and cancer

Relevant efforts were recently made in the deorphanization of the over 130 GPCRs for which ligands have not yet been identified. Some of these GPCRs have been linked to cancer development and progression on the basis of their overexpression and/or up-regulation by diverse factors[173–175]. For instance, an elevated expression of the orphan G-protein-coupled receptor GPR49 was involved in the formation and proliferation of basal cell carcinoma[176], while GPR18 was found associated with melanoma metastases[177]. In lung, cervix, skin, urinary bladder, testis, head and neck squamous cell carcinomas were detected high levels of GPR87[178, 179] for which UDP-glucose, cysteinyl-leukotrienes and LPA exhibited binding properties[180]. In breast and colon cancer cells, DNA damage has been recently found to regulate GPR87 expression in a p53-dependent manner[173]. Taken together, these results suggest that GPR87 may elicit survival and anti-apoptotic actions, while its overexpression plays a pivotal role in the development and progression of diverse types of tumors. On the contrary, GPR56 inhibited prostate cancer progression and suppressed tumor growth and metastasis in melanoma xenografs[181]. Moreover, GPR56 inhibited VEGF production from melanoma cells and prevented melanoma angiogenesis and growth[182]. Accordingly, the expression of GPR56 has been found inversely correlated with melanoma malignancies, suggesting its potential role in cancer development and metastasis[175, 182].

Targeting deorphanized GPCRs also in combination with well-known anti-cancer agents would be expected to increase the effectiveness of the current therapeutical approaches. In this regard, extensive studies are required to completely decipher the biology of these receptors in order to provide the basis for the design and use of new drugs in different types of human tumors.

Concluding remarks

Despite GPCRs form the largest superfamily of cell surface receptors involved in signal transmission, in clinical practice only few anticancer compounds are currently used in order to interfere with GPCR-mediated signaling. Although the role played by GPCRs and their ligands in tumor pathophysiology is intricate, an increasing body of evidence has recently emerged linking indubitably these molecules to the development and progression of cancer. Consequently, GPCRs and their downstream-activated effectors represent a rich source of potential drug targets for innovative strategies in tumor prevention and treatment. Next, the identification of the transduction network maps connecting several GPCR-dependent signals with other transduction pathways will facilitate further investigations regarding the biological potential of these receptors, opening in the mean time a new valuable scenario for the discovery of novel anti-cancer therapeutics. Finally, the ongoing efforts to fully characterize the numerous orphan GPCRs will certainly lead in the near future to the identification of new targets toward innovative pharmacological strategies in cancer patients.

Acknowledgements

This work was supported by Associazione Italiana per la Ricerca sul Cancro (AIRC, project No 8925/2009 and project Calabria 2011) (http://www.airc.it/), Fondazione Cassa di Risparmio di Calabria e Lucania, Ministero dell'Istruzione, dell'Università e della Ricerca (MIUR) (project PRIN 2008PK2WCW/2008) (http://www.istruzione.it/).

References

1 Pierce KL, Premont RT, Lefkowitz RJ. Seven-transmembrane receptors. Nat Rev Mol Cell Biol 2002; 3: 639–50.
2 Neves SR, Ram PT, Iyengar R. G protein pathways. Science 2002; 296: 1636–9.
3 Noguchi K, Herr D, Mutoh T, Chun J. Lysophosphatidic acid (LPA) and its receptors. Curr Opin Pharmacol 2009; 9: 15–23.
4 Sanchez T, Hla T. Structural and functional characteristics of S1P receptors. J Cell Biochem 2004; 92: 913.
5 Dorsam RT, Gutkind JS. G-protein-coupled receptors and cancer. Nature Rev Cancer 2007; 7: 79–94.
6 Lappano R, Maggiolini M. G protein-coupled receptors: novel targets for drug discovery in cancer. Nat Rev Drug Discov 2011; 10: 47–60.
7 Demenais F, Mohamdi H, Chaudru V, Goldstein AM, Newton Bishop JA, Bishop DT, *et al.* Association of MC1R variants and host phenotypes with melanoma risk in CDKN2A mutation carriers: a GenoMEL study. J Natl Cancer Inst 2010; 102: 1568–83.
8 Voisin T, El Firar A, Fasseu M, Rouyer-Fessard C, Descatoire V, Walker F, *et al*. Aberrant expression of OX1 receptors for orexins in colon cancers and liver metastases: an openable gate to apoptosis. Cancer Res 2011; 71: 3341–51.
9 Almendro V, García-Recio S, Gascón P. Tyrosine kinase receptor transactivation associated to G protein-coupled receptors. Curr Drug Targets 2010; 11: 1169–80.
10 Luttrell LM. Location, location, location: activation and targeting of MAP kinases by G protein-coupled receptors. J Mol Endocrinol 2003; 30: 117–26.
11 Gnant M, Mlineritsch B, Schippinger W, Luschin-Ebengreuth G, Pöstlberger S, Menzel C, *et al*. Endocrine therapy plus zoledronic acid in premenopausal breast cancer. N Engl J Med 2009; 360: 679–91.
12 Hejna M, Schmidinger M, Raderer M. The clinical role of somatostatin analogues as antineoplastic agents: much ado about nothing? Ann Oncol 2002; 13: 653–68.
13 Mills GB, Moolenaar WH. The emerging role of lysophosphatidic acid in cancer. Nat Rev Cancer 2003; 3: 582–91.
14 Fujita T, Miyamoto S, Onoyama I, Sonoda K, Mekada E, Nakano H. Expression of lysophosphatidic acid receptors and vascular endothelial growth factor mediating lysophosphatidic acid in the development of human ovarian cancer. Cancer Lett 2003; 192: 161–9.
15 Shida D, Watanabe T, Aoki J, Hama K, Kitayama J, Sonoda H. Aberrant expression of lysophosphatidic acid (LPA) receptors in human colorectal cancer. Lab Investigation 2004; 84: 1352–62.
16 Horak CE, Mendoza A, Vega-Valle E, Albaugh M, Graff-Cherry C, McDermott WG, *et al*. Nm23-H1 suppresses metastasis by inhibiting expression of the lysophosphatidic acid receptor EDG2. Cancer Res 2007; 67: 11751–9.
17 Boucharaba A, Serre CM, Guglielmi J, Bordet JC, Clezardin P, Peyruchaud O. The type 1 lysophosphatidic acid receptor is a target for therapy in bone metastases. Proc Natl Acad Sci U S A 2006; 103: 9643–8.
18 Kim JH, Adelstein RS. LPA(1)-induced migration requires nonmuscle myosin II light chain phosphorylation in breast cancer cells. J Cell Physiol 2011; 226: 2881–93.
19 Liu S, Umezu-Goto M, Murph M, Lu Y, Liu W, Zhang F, *et al*. Expression of autotaxin and lysophosphatidic acid receptors increases mammary tumorigenesis, invasion, and metastases. Cancer Cell 2009; 15: 539–50.
20 Bian D, Su S, Mahanivong C, Cheng RK, Han Q, Pan ZK, *et al*. Lysophosphatidic acid stimulates ovarian cancer cell migration via a Ras-MEK kinase 1 pathway. Cancer Res 2004; 64: 4209–17.
21 Saunders JA, Rogers LC, Klomsiri C, Poole LB, Daniel LW. Reactive oxygen species mediate lysophosphatidic acid induced signaling in ovarian cancer cells. Free Radic Biol Med 2010; 49: 2058–67.
22 Chen H, Wu X, Pan ZK, Huang S. Integrity of SOS1/EPS8/ABI1 tricomplex determines ovarian cancer metastasis. Cancer Res 2010; 70: 9979–90.
23 Li H, Wang D, Zhang H, Kirmani K, Zhao Z, Steinmetz R, *et al*. Lysophosphatidic acid stimulates cell migration, invasion, and colony formation as well as tumorigenesis/metastasis of mouse ovarian cancer in immunocompetent mice. Mol Cancer Ther 2009; 8: 1692–701.
24 Oyesanya RA, Greenbaum S, Dang D, Lee Z, Mukherjee A, Wu J, *et al*. Differential requirement of the epidermal growth factor receptor for G protein-mediated activation of transcription factors by lysophosphatidic acid. Mol Cancer 2010; 9: 8.
25 Snider AJ, Zhang Z, Xie Y, Meier KE. Epidermal growth factor increases lysophosphatidic acid production in human ovarian cancer cells: roles for phospholipase D_2 and receptor transactivation. Am J Physiol Cell Physiol 2010; 298: C163–70.
26 Jeon ES, Lee IH, Heo SC, Shin SH, Choi YJ, Park JH, *et al*. Mesenchymal stem cells stimulate angiogenesis in a murine xenograft model of A549 human adenocarcinoma through an LPA1 receptor-dependent mechanism. Biochim Biophys Acta 2010; 1801: 1205–13.
27 Xu X, Prestwich GD. Inhibition of tumor growth and angiogenesis by a lysophosphatidic acid antagonist in an engineered three-dimensional lung cancer xenograft model. Cancer 2010; 116: 1739–50.

28 Pyne NJ, Pyne S. Sphingosine 1-phosphate and cancer. Nat Rev Cancer 2010; 10: 489–503.
29 Goetzl EJ, Dolezalova H, Kong Y, Zeng L. Dual mechanisms for lysophospholipid induction of proliferation of human breast carcinoma cells. Cancer Res 1999; 59: 4732–7.
30 Yamashita H, Kitayama J, Shida D, Yamaguchi H, Mori K, Osada M, *et al*. Sphingosine 1-phosphate receptor expression profile in human gastric cancer cells: differential regulation on the migration and proliferation. J Surg Res 2006; 130: 80–7.
31 Bergelin N, Löf C, Balthasar S, Kalhori V, Törnquist K. S1P1 and VEGFR-2 form a signaling complex with extracellularly regulated kinase 1/2 and protein kinase C-alpha regulating ML-1 thyroid carcinoma cell migration. Endocrinology 2010; 151: 2994–3005.
32 Lepley D, Paik JH, Hla T, Ferrer F. The G protein-coupled receptor S1P2 regulates Rho/Rho kinase pathway to inhibit tumor cell migration. Cancer Res 2005; 65: 3788–95.
33 Lee H, Deng J, Kujawski M, Yang C, Liu Y, Herrmann A, *et al*. STAT3-induced S1PR1 expression is crucial for persistent STAT3 activation in tumors. Nat Med 2010; 16: 1421–8.
34 Li MH, Sanchez T, Yamase H, Hla T, Oo ML, Pappalardo A, *et al*. S1P/S1P1 signaling stimulates cell migration and invasion in Wilms tumor. Cancer Lett 2009; 276: 171–9.
35 Young N, Pearl DK, Van Brocklyn JR. Sphingosine-1-phosphate regulates glioblastoma cell invasiveness through the urokinase plasminogen activator system and CCN1/Cyr61. Mol Cancer Res 2009; 7: 23–32.
36 Arikawa K, Takuwa N, Yamaguchi H, Sugimoto N, Kitayama J, Nagawa H, *et al*. Ligand-dependent inhibition of B16 melanoma cell migration and invasion via endogenous S1P2 G protein-coupled receptor. Requirement of inhibition of cellular RAC activity. J Biol Chem 2003; 278: 32841–51.
37 Takuwa Y, Du W, Qi X, Okamoto Y, Takuwa N, Yoshioka K. Roles of sphingosine-1-phosphate signaling in angiogenesis. World J Biol Chem 2010; 1: 298–306.
38 Visentin B, Vekich JA, Sibbald BJ, Cavalli AL, Moreno KM, Matteo RG, *et al*. Validation of an anti-sphingosine-1-phosphate antibody as a potential therapeutic in reducing growth, invasion, and angiogenesis in multiple tumor lineages. Cancer Cell 2006; 9: 225–38.
39 Chae SS, Paik JH, Furneaux H, Hla T. Requirement for sphingosine 1-phosphate receptor-1 in tumor angiogenesis demonstrated by *in vivo* RNA interference. J Clin Invest 2004; 114: 1082–9.
40 Du W, Takuwa N, Yoshioka K, Okamoto Y, Gonda K, Sugihara K, *et al*. S1P(2), the G protein-coupled receptor for sphingosine-1-phosphate, negatively regulates tumor angiogenesis and tumor growth *in vivo* in mice. Cancer Res 2010; 70: 772–81.
41 Bagnato A, Rosanò L. The endothelin axis in cancer. Int J Biochem Cell Biol 2008; 40: 1443–51.
42 Arun C, London NJ, Hemingway DM. Prognostic significance of elevated endothelin-1 levels in patients with colorectal cancer. Int J Biol Markers 2004; 19: 32–7.
43 Bagnato A, Loizidou M, Pflug BR, Curwen J, Growcott J. Role of the endothelin axis and its antagonists in the treatment of cancer. Br J Pharmacol 2011; 163: 220–33.
44 Rosanò L, Cianfrocca R, Spinella F, Di Castro V, Nicotra MR, Lucidi A, *et al*. Acquisition of chemoresistance and EMT phenotype is linked with activation of the endothelin A receptor pathway in ovarian carcinoma cells. Clin Cancer Res 2011; 17: 2350–60.
45 Thomas SM, Grandis JR, Wentzel AL, Gooding WE, Lui VW, Siegfried JM. Gastrin-releasing peptide receptor mediates activation of the epidermal growth factor receptor in lung cancer cells. Neoplasia 2005; 7: 426–31.
46 Lui VW, Thomas SM, Zhang Q, Wentzel AL, Siegfried JM, Li JY, *et al*. Mitogenic effects of gastrin-releasing peptide in head and neck squamous cancer cells are mediated by activation of the epidermal growth factor receptor. Oncogene 2003; 22: 6183–93.
47 Hohla F, Schally AV. Targeting gastrin releasing peptide receptors: New options for the therapy and diagnosis of cancer. Cell Cycle 2010; 9: 1738–41.
48 Mu L, Honer M, Becaud J, Martic M, Schubiger PA, Ametamey SM, *et al*. *In vitro* and *in vivo* characterization of novel ^{18}F-labeled bombesin analogues for targeting GRPR-positive tumors. Bioconjug Chem 2010; 21: 1864–71.
49 Honer M, Mu L, Stellfeld T, Graham K, Martic M, Fischer CR, *et al*. ^{18}F-labeled bombesin analog for specific and effective targeting of prostate tumors expressing gastrin-releasing peptide receptors. J Nucl Med 2011; 52: 270–8.
50 Coughlin SR. Thrombin signalling and protease-activated receptors. Nature 2000; 407: 258–64.
51 Yang E, Boire A, Agarwal A, Nguyen N, O'Callaghan K, Tu P, *et al*. Blockade of PAR1 signaling with cell-penetrating pepducins inhibits Akt survival pathways in breast cancer cells and suppresses tumor survival and metastasis. Cancer Res 2009; 69: 6223–31.
52 Wysoczynski M, Liu R, Kucia M, Drukala J, Ratajczak MZ. Thrombin regulates the metastatic potential of human rhabdomyosarcoma cells: distinct role of PAR1 and PAR3 signaling. Mol Cancer Res 2010; 8: 677–90.
53 García-López MT, Gutiérrez-Rodríguez M, Herranz R. Thrombin-activated receptors: promising targets for cancer therapy? Curr Med Chem 2010; 17: 109–28.
54 Arora P, Cuevas BD, Russo A, Johnson GL, Trejo J. Persistent transactivation of EGFR and ErbB2/HER2 by protease-activated receptor-1 promotes breast carcinoma cell invasion. Oncogene 2008; 27: 4434–45.
55 Villares GJ, Zigler M, Dobroff AS, Wang H, Song R, Melnikova VO, *et al*. Protease activated receptor-1 inhibits the Maspin tumor-suppressor gene to determine the melanoma metastatic phenotype. Proc Natl Acad Sci U S A 2011; 108: 626–31.
56 Boire A, Covic L, Agarwal A, Jacques S, Sherifi S, Kuliopulos A. PAR1 is a matrix metalloprotease-1 receptor that promotes invasion and tumorigenesis of breast cancer cells. Cell 2005; 120: 303–13.
57 Agarwal A, Tressel SL, Kaimal R, Balla M, Lam FH, Covic L, *et al*. Identification of a metalloprotease-chemokine signaling system in the ovarian cancer microenvironment: implications for antiangiogenic therapy. Cancer Res 2010; 70: 5880–90.
58 Clevers H. Wnt/beta-catenin signaling in development and disease. Cell 2006; 127: 469–80.
59 Hu T, Li C. Convergence between Wnt-β-catenin and EGFR signaling in cancer. Mol Cancer 2010; 9: 236.
60 Jones KA, Kemp CR. Wnt-induced proteolytic targeting. Genes Dev 2008; 22: 3077–81.
61 Ojalvo LS, Whittaker CA, Condeelis JS, Pollard JW. Gene expression analysis of macrophages that facilitate tumor invasion supports a role for Wnt-signaling in mediating their activity in primary mammary tumors. J Immunol 2010; 184: 702–12.
62 Lai SL, Chien AJ, Moon RT. Wnt/Fz signaling and the cytoskeleton: potential roles in tumorigenesis. Cell Res 2009; 19: 532–45.
63 Nambotin SB, Lefrancois L, Sainsily X, Berthillon P, Kim M, Wands JR, *et al*. Pharmacological inhibition of Frizzled-7 displays anti-tumor properties in hepatocellular carcinoma. J Hepatol 2011; 54: 288–99.
64 Yang L, Wu X, Wang Y, Zhang K, Wu J, Yuan YC, *et al*. FZD7 has a critical role in cell proliferation in triple negative breast cancer.

Oncogene 2011; 30: 4437–46.
65 Jin X, Jeon HY, Joo KM, Kim JK, Jin J, Kim SH, *et al*. Frizzled 4 regulates stemness and invasiveness of migrating glioma cells established by serial intracranial transplantation. Cancer Res 2011; 71: 3066–75.
66 Scales SJ, de Sauvage FJ. Mechanisms of Hedgehog pathway activation in cancer and implications for therapy. Trends Pharmacol Sci 2009; 30: 303–12.
67 Teglund S, Toftgard R. Hedgehog beyond medulloblastoma and basal cell carcinoma. Biochim Biophys Acta 2010; 1805: 181–208.
68 Singh S, Wang Z, Liang Fei D, Black KE, Goetz JA, Tokhunts R, *et al*. Hedgehog-producing cancer cells respond to and require autocrine Hedgehog activity. Cancer Res 2011; 71: 4454–63.
69 Merchant AA, Matsui W. Targeting Hedgehog–a cancer stem cell pathway. Clin Cancer Res 2010; 16: 3130–40.
70 Tang T, Tang JY, Li D, Reich M, Callahan CA, Fu L, *et al*. Targeting superficial or nodular Basal cell carcinoma with topically formulated small molecule inhibitor of smoothened. Clin Cancer Res 2011; 17: 3378–87.
71 Metcalfe C, de Sauvage FJ. Hedgehog fights back: mechanisms of acquired resistance against Smoothened antagonists. Cancer Res 2011; 71: 5057–61.
72 Dijkgraaf GJ, Alicke B, Weinmann L, Januario T, West K, Modrusan Z, *et al*. Small molecule inhibition of GDC-0449 refractory smoothened mutants and downstream mechanisms of drug resistance. Cancer Res 2011; 71: 435–44.
73 Tao H, Jin Q, Koo DI, Liao X, Englund NP, Wang Y, *et al*. Small molecule antagonists in distinct binding modes inhibit drug-resistant mutant of smoothened. Chem Biol 2011; 18: 432–7.
74 Mazumdar T, DeVecchio J, Shi T, Jones J, Agyeman A, Houghton JA. Hedgehog signaling drives cellular survival in human colon carcinoma cells. Cancer Res 2011; 71: 1092–102.
75 Desch P, Asslaber D, Kern D, Schnidar H, Mangelberger D, Alinger B, *et al*. Inhibition of GLI, but not Smoothened, induces apoptosis in chronic lymphocytic leukemia cells. Oncogene 2010; 29: 4885–95.
76 Kim J, Tang JY, Gong R, Kim J, Lee JJ, Clemons KV, *et al*. Itraconazole, a commonly used antifungal that inhibits Hedgehog pathway activity and cancer growth. Cancer Cell 2010; 17: 388–99.
77 Vandercappellen J, Van Damme J, Struyf S. The role of CXC chemokines and their receptors in cancer. Cancer Lett 2008; 267: 226–44.
78 Thelen M. Dancing to the tune of chemokines. Nat Immunol 2001; 2: 129–34.
79 Kamohara H, Takahashi M, Ishiko T, Ogawa M, Baba H. Induction of interleukin-8 (CXCL-8) by tumor necrosis factor-alpha and leukemia inhibitory factor in pancreatic carcinoma cells: Impact of CXCL-8 as an autocrine growth factor. Int J Oncol 2007; 31: 627–32.
80 Balkwill F. Cancer and the chemokine network. Nat Rev Cancer 2004; 4: 540–50.
81 Yanagawa J, Walser TC, Zhu LX, Hong L, Fishbein MC, Mah V, *et al*. Snail promotes CXCR2 ligand-dependent tumor progression in non-small cell lung carcinoma. Clin Cancer Res 2009; 15: 6820–9.
82 Matsuo Y, Raimondo M, Woodward TA, Wallace MB, Gill KR, Tong Z, *et al*. CXC-chemokine/CXCR2 biological axis promotes angiogenesis *in vitro* and *in vivo* in pancreatic cancer. Int J Cancer 2009; 125: 1027–37.
83 Xu J, Zhang C, He Y, Wu H, Wang Z, Song W, *et al*. Lymphatic endothelial cell-secreted CXCL1 stimulates lymphangiogenesis and metastasis of gastric cancer. Int J Cancer 2011. doi: 10.1002/ijc.26035.
84 Singh S, Nannuru KC, Sadanandam A, Varney ML, Singh RK. CXCR1 and CXCR2 enhances human melanoma tumourigenesis, growth and invasion. Br J Cancer 2009; 100: 1638–46.
85 Su H, Sobrino Najul EJ, Toth TA, Ng CM, Lelievre SA, Fred M, *et al*. Chemokine receptor CXCR4-mediated transformation of mammary epithelial cells by enhancing multiple RTKs expression and deregulation of the p53/MDM2 axis. Cancer Lett 2011; 307: 132–40.
86 Rhodes LV, Short SP, Neel NF, Salvo VA, Zhu Y, Elliott S, *et al*. Cytokine receptor CXCR4 mediates estrogen-independent tumorigenesis, metastasis, and resistance to endocrine therapy in human breast cancer. Cancer Res 2011; 71: 603–13.
87 Dessein AF, Stechly L, Jonckheere N, Dumont P, Monté D, Leteurtre E, *et al*. Autocrine induction of invasive and metastatic phenotypes by the MIF-CXCR4 axis in drug-resistant human colon cancer cells. Cancer Res 2010; 70: 4644–54.
88 Singh S, Srivastava SK, Bhardwaj A, Owen LB, Singh AP. CXCL12-CXCR4 signalling axis confers gemcitabine resistance to pancreatic cancer cells: a novel target for therapy. Br J Cancer 2010; 103: 1671–9.
89 Li YM, Pan Y, Wei Y, Cheng X, Zhou BP, Tan M, *et al*. CXCR4 is a prognostic marker in acute myelogenous leukemia. Cancer Cell 2004; 6: 459–69.
90 Kim J, Takeuchi H, Lam ST, Turner RR, Wang HJ, Kuo C, *et al*. Chemokine receptor CXCR4 expression in colorectal cancer patients increases the risk for recurrence and for poor survival. J Clin Oncol 2005; 23: 2744–53.
91 Konoplev S, Jorgensen JL, Thomas DA, Lin E, Burger J, Kantarjian HM, *et al*. Phosphorylated CXCR4 is associated with poor survival in adults with B-acute lymphoblastic leukemia. Cancer 2011; 117: 4689–95.
92 Rombouts EJ, Pavic B, Lowenberg B, Ploemacher RE. Relation between CXCR-4 expression, Flt3 mutations, and unfavorable prognosis of adult acute myeloid leukemia. Blood 2004; 104: 550–7.
93 Furusato B, Mohamed A, Uhlén M, Rhim JS. CXCR4 and cancer. Pathol Int 2010; 60: 497–505.
94 Miyanishi N, Suzuki Y, Simizu S, Kuwabara Y, Banno K, Umezawa K. Involvement of autocrine CXCL12/CXCR4 system in the regulation of ovarian carcinoma cell invasion. Biochem Biophys Res Commun 2010; 403: 154–9.
95 Schutyser E, Su Y, Yu Y, Gouwy M, Zaja-Milatovic S, Van Damme J, *et al*. Hypoxia enhances CXCR4 expression in human microvascular endothelial cells and human melanoma cells. Eur Cytokine Netw 2007; 18: 59–70.
96 Chu CY, Cha ST, Chang CC, Hsiao CH, Tan CT, Lu YC, *et al*. Involvement of matrix metalloproteinase-13 in stromal-cell-derived factor 1 alphadirected invasion of human basal cell carcinoma cells. Oncogene 2007; 26: 2491–501.
97 Yu T, Wu Y, Helman JI, Wen Y, Wang C, Li L. CXCR4 promotes oral squamous cell carcinoma migration and invasion through inducing expression of MMP-9 and MMP-13 via the ERK signaling pathway. Mol Cancer Res 2011; 9: 161–72.
98 Burns JM, Summers BC, Wang Y, Melikian A, Berahovich R, Miao Z, *et al*. A novel chemokine receptor for SDF-1 and I-TAC involved in cell survival, cell adhesion, and tumor development. J Exp Med 2006; 203: 2201–13.
99 Miao Z, Luker KE, Summers BC, Berahovich R, Bhojani MS, Rehemtulla A, *et al*. CXCR7 (RDC1) promotes breast and lung tumor growth *in vivo* and is expressed on tumor-associated vasculature. Proc Natl Acad Sci U S A 2007; 104: 15735–40.
100 Wang J, Shiozawa Y, Wang J, Wang Y, Jung Y, Pienta KJ, *et al*. The role of CXCR7/RDC1 as a chemokine receptor for CXCL12/SDF-1 in

prostate cancer. J Biol Chem 2008; 283: 4283–94.
101 Uemura H, Hoshino K, Kubota Y. Engagement of renin-angiotensin system in prostate cancer. Curr Cancer Drug Targets 2011; 11: 442–50.
102 Taub JS, Guo R, Leeb-Lundberg LM, Madden JF, Daaka Y. Bradykinin receptor subtype 1 expression and function in prostate cancer. Cancer Res 2003; 63: 2037–41.
103 Daaka Y. G proteins in cancer: the prostate cancer paradigm. Sci STKE 2004; 2004: re2.
104 Metzger E, Müller JM, Ferrari S, Buettner R, Schüle R. A novel inducible transactivation domain in the androgen receptor: implications for PRK in prostate cancer. EMBO J 2003; 22: 270–80.
105 Müller JM, Isele U, Metzger E, Rempel A, Moser M, Pscherer A, *et al*. FHL2, a novel tissue-specific coactivator of the androgen receptor. EMBO J 2000; 19: 359–69.
106 Hoshino K, Ishiguro H, Teranishi JI, Yoshida SI, Umemura S, Kubota Y, *et al*. Regulation of androgen receptor expression through angiotensin II type 1 receptor in prostate cancer cells. Prostate 2011; 71: 964–75.
107 Deshayes F, Nahmias C. Angiotensin receptors: a new role in cancer? Trends Endocrinol Metab 2005; 16: 293–9.
108 Lau ST, Leung PS. Role of the RAS in pancreatic cancer. Curr Cancer Drug Targets 2011; 11: 412–20.
109 Ino K, Shibata K, Yamamoto E, Kajiyama H, Nawa A, Mabuchi Y, *et al*. Role of the renin-angiotensin system in gynecologic cancers. Curr Cancer Drug Targets 2011; 11: 405–11.
110 Molina L, Matus CE, Astroza A, Pavicic F, Tapia E, Toledo C, *et al*. Stimulation of the bradykinin B(1) receptor induces the proliferation of estrogen-sensitive breast cancer cells and activates the ERK1/2 signaling pathway. Breast Cancer Res Treat 2009; 118: 499–510.
111 Lu DY, Leung YM, Huang SM, Wong KL. Bradykinin-induced cell migration and COX-2 production mediated by the bradykinin B1 receptor in glioma cells. J Cell Biochem 2010; 110: 141–50.
112 Guha S, Lunn JA, Santiskulvong C, Rozengurt E. Neurotensin stimulates protein kinase C-dependent mitogenic signaling in human pancreatic carcinoma cell line PANC-1. Cancer Res 2003; 63: 2379–87.
113 Kisfalvi K, Rey O, Young SH, Sinnett-Smith J, Rozengurt E. Insulin potentiates Ca^{2+} signaling and phosphatidylinositol 4,5-bisphosphate hydrolysis induced by Gq protein-coupled receptor agonists through an mTOR-dependent pathway. Endocrinology 2007; 148: 3246–57.
114 Rozengurt E, Sinnett-Smith J, Kisfalvi K. Crosstalk between insulin/insulin-like growth factor-1 receptors and G protein-coupled receptor signaling systems: a novel target for the antidiabetic drug metformin in pancreatic cancer. Clin Cancer Res 2010; 16: 2505–11.
115 Kisfalvi K, Eibl G, Sinnett-Smith J, Rozengurt E. Metformin disrupts crosstalk between G protein-coupled receptor and insulin receptor signaling systems and inhibits pancreatic cancer growth. Cancer Res 2009; 69: 6539–45.
116 Dolley-Hitze T, Jouan F, Martin B, Mottier S, Edeline J, Moranne O, *et al*. Angiotensin-2 receptors (AT1-R and AT2-R), new prognostic factors for renal clear-cell carcinoma? Br J Cancer 2010; 103: 1698–705.
117 Arrieta O, Guevara P, Escobar E, Garcìa-Navarrete R, Pineda B, Sotelo J. Blockage of angiotensin II type I receptor decreases the synthesis of growth factors and induces apoptosis in C6 cultured cells and C6 rat glioma. Br J Cancer 2005; 92: 1247–52.
118 Kosugi M, Miyajima A, Kikuchi E, Horiguchi Y, Murai M. Angiotensin II type 1 receptor antagonist candesartan as an angiogenic inhibitor in a xenograft model of bladder cancer. Clin Cancer Res 2006; 12: 2888–93.
119 Huang CC, Chan WL, Chen YC, Chen TJ, Lin SJ, Chen JW, *et al*. Angiotensin II receptor blockers and risk of cancer in patients with systemic hypertension. Am J Cardiol 2011; 107: 1028–33.
120 Sipahi I, Debanne SM, Rowland DY, Simon DI, Fang JC. Angiotensin-receptor blockade and risk of cancer: meta-analysis of randomised controlled trials. Lancet Oncol 2010; 11: 627–36.
121 Pommerville PJ, de Boer JG. GnRH antagonists in the treatment of advanced prostate cancer. Can J Urol 2010; 17: 5063–70.
122 Yu B, Ruman J, Christman G. The role of peripheral gonadotropin-releasing hormone receptors in female reproduction. Fertil Steril 2011; 95: 465–73.
123 Halmos G, Arencibia JM, Schally AV, Davis R, Bostwick DG. High incidence of receptors for luteinizing hormone-releasing hormone (LHRH) and LHRH receptor gene expression in human prostate cancers. J Urol 2001; 163: 623–9.
124 Gründker C, Günthert AR, Westphalen S, Emons G. Biology of the gonadotropin-releasing hormone system in gynecological cancers. Eur J Endocrinol 2002; 146: 1–14.
125 Cheung LW, Mak AS, Cheung AN, Ngan HY, Leung PC, Wong AS. P-cadherin cooperates with insulin-like growth factor-1 receptor to promote metastatic signaling of gonadotropin-releasing hormone in ovarian cancer via p120 catenin. Oncogene 2011; 30: 2964–74.
126 Ling Poon S, Lau MT, Hammond GL, Leung PC. Gonadotropin-releasing hormone-II increases membrane type I metalloproteinase production via beta-catenin signaling in ovarian cancer cells. Endocrinology 2011; 152: 764–72.
127 Schubert A, Hawighorst T, Emons G, Gründker C. Agonists and antagonists of GnRH-I and -II reduce metastasis formation by triple-negative human breast cancer cells *in vivo*. Breast Cancer Res Treat 2011; 130: 783–90
128 Kraus S, Levy G, Hanoch T, Naor Z, Seger R. Gonadotropin releasing hormone induces apoptosis of prostate cancer cells: Role of c-Jun NH_2-terminal kinase, protein kinase B, and extracellular signal-regulated kinase pathways. Cancer Res 2004; 64: 5736–44.
129 Kim DK, Yang JS, Maiti K, Hwang JI, Kim K, Seen D, *et al*. A gonadotropin releasing hormone-II antagonist induces autophagy of prostate cancer cells. Cancer Res 2009; 69: 923–31.
130 Van Poppel H. Evaluation of degarelix in the management of prostate cancer. Cancer Manag Res 2010; 2: 39–52.
131 Schally AV, Varga JL. Antagonists of growth hormone-releasing hormone in oncology. Comb Chem High Throughput Screen 2006; 9: 163–70.
132 Szepeshazi K, Schally AV, Nagy A. Effective treatment of advanced estrogen-independent MXT mouse mammary cancers with targeted cytotoxic LH-RH analogs. Breast Cancer Res Treat 1999; 56: 267–76.
133 Grundker C, Volker P, Griesinger F, Ramaswamy A, Nagy A, Schally AV, *et al*. Antitumor effects of the cytotoxic luteinizing hormone-releasing hormone analog AN-152 on human endometrial and ovarian cancers xenografted into nude mice. Am J Obstet Gynecol 2002; 187: 528–37.
134 Chen GG, Zeng Q, Tse GM. Estrogen and its receptors in cancer. Med Res Rev 2008; 28: 954–74.
135 Maggiolini M, Picard D. The unfolding stories of GPR30, a new membrane bound estrogen receptor. J Endocrinol 2010; 204: 105–14.
136 Smith HO, Leslie KK, Singh M, Qualls CR, Revankar CM, Joste NE, *et al*. GPR30: a novel indicator of poor survival for endometrial carcinoma. Am J Obstet Gynecol 2007; 196: 386.e1–9.
137 Smith HO, Arias-Pulido H, Kuo DY, Howard T, Qualls CR, Lee SJ, *et al*. GPR30 predicts poor survival for ovarian cancer. Gynecol Oncol 2009; 114: 465–71.

138 Filardo EJ, Graeber CT, Quinn JA, Resnick MB, Giri D, DeLellis RA, *et al*. Distribution of GPR30, a seven membrane-spanning estrogen receptor, in primary breast cancer and its association with clinicopathologic determinants of tumor progression. Clin Cancer Res 2006; 12: 6359–66.
139 Prossnitz ER, Maggiolini M. Mechanisms of estrogen signaling and gene expression via GPR30. Mol Cell Endocrinol 2009; 308: 32–8.
140 Thomas P, Pang Y, Filardo EJ, Dong J. Identity of an estrogen membrane receptor coupled to a G protein in human breast cancer cells. Endocrinology 2005; 146: 624–32.
141 Thomas P, Dong J. Binding and activation of the seven-transmembrane estrogen receptor GPR30 by environmental estrogens: a potential novel mechanism of endocrine disruption. J Steroid Biochem Mol Biol 2006; 102: 175–9.
142 Maggiolini M, Vivacqua A, Fasanella G, Recchia AG, Sisci D, Pezzi V, *et al*. The G protein coupled receptor GPR30 mediates c-fos up-regulation by 17β-estradiol and phytoestrogens in breast cancer cells. J Biol Chem 2004; 279: 27008–16.
143 Vivacqua A, Bonofiglio D, Recchia AG, Musti AM, Picard D, Andò S, *et al*. The G protein-coupled receptor GPR30 mediates the proliferative effects induced by 17β-estradiol and hydroxytamoxifen in endometrial cancer cells. Mol Endocrinol 2006; 20: 631–46.
144 Albanito L, Madeo A, Lappano R, Vivacqua A, Rago V, Carpino A, *et al*. G protein-coupled receptor 30 (GPR30) mediates gene expression changes and growth response to 17beta-estradiol and selective GPR30 ligand G-1 in ovarian cancer cells. Cancer Res 2007; 67: 1859–66.
145 Albanito L, Lappano R, Madeo A, Chimento A, Prossnitz ER, Cappello AR, *et al*. G-protein-coupled receptor 30 and estrogen receptor-alpha are involved in the proliferative effects induced by atrazine in ovarian cancer cells. Environ Health Perspect 2008; 116: 1648–55.
146 Albanito L, Sisci D, Aquila S, Brunelli E, Vivacqua A, Madeo A, *et al*. Epidermal growth factor induces G protein-coupled receptor 30 expression in estrogen receptor-negative breast cancer cells. Endocrinology 2008; 149: 3799–808.
147 Pandey DP, Lappano R, Albanito L, Madeo A, Maggiolini M, Picard D. Estrogenic GPR30 signalling induces proliferation and migration of breast cancer cells through CTGF. EMBO J 2009; 28: 523–32.
148 Vivacqua A, Lappano R, De Marco P, Sisci D, Aquila S, De Amicis F, *et al*. G protein-coupled receptor 30 expression is upregulated by EGF and TGFalpha in estrogen receptor alpha-positive cancer cells. Mol Endocrinol 2009; 11: 1815–26.
149 Lappano R, Rosano C, De Marco P, De Francesco EM, Pezzi V, Maggiolini M. Estriol acts as a GPR30 antagonist in estrogen receptor-negative breast cancer cells. Mol Cell Endocrinol 2010; 320: 162–70.
150 Madeo A, Maggiolini M. Nuclear alternate estrogen receptor GPR30 mediates 17beta-estradiol-induced gene expression and migration in breast cancer-associated fibroblasts. Cancer Res 2010; 70: 6036–46.
151 Schuller HM. Neurotransmission and cancer: implications for prevention and therapy. Anticancer Drugs 2008; 19: 655–71.
152 Thaker PH, Han LY, Kamat AA, Arevalo JM, Takahashi R, Lu C, *et al*. Chronic stress promotes tumor growth and angiogenesis in a mouse model of ovarian carcinoma. Nat Med 2006; 12: 939–44.
153 Yang EV, Kim SJ, Donovan EL, Chen M, Gross AC, Webster Marketon JI, *et al*. Norepinephrine upregulates VEGF, IL-8, and IL-6 expression in human melanoma tumor cell lines: implications for stress-related enhancement of tumor progression. Brain Behav Immun 2009; 23: 267–75.
154 Sloan EK, Priceman SJ, Cox BF, Yu S, Pimentel MA, Tangkanangnukul V, *et al*. The sympathetic nervous system induces a metastatic switch in primary breast cancer. Cancer Res 2010, 70: 7042–52.
155 Lutgendorf SK, Cole S, Costanzo E, Bradley S, Coffin J, Jabbari S, *et al*. Stress-related mediators stimulate vascular endothelial growth factor secretion by two ovarian cancer cell lines. Clin Cancer Res 2003; 9: 4514–21.
156 Lüthy IA, Bruzzone A, Piñero CP, Castillo LF, Chiesa IJ, Vázquez SM, *et al*. Adrenoceptors: non conventional target for breast cancer? Curr Med Chem 2009; 16: 1850–62.
157 Shah N, Khurana S, Cheng K, Raufman JP. Muscarinic receptors and ligands in cancer. Am J Physiol Cell Physiol 2009; 296: C221–32.
158 De Sarno P, Shestopal SA, King TD, Zmijewska A, Song L, Jope RS. Muscarinic receptor activation protects cells from apoptotic effects of DNA damage, oxidative stress, and mitochondrial inhibition. J Biol Chem 2003; 278: 11086–93.
159 Oppitz M, Mobus V, Brock S, Drews U. Muscarinic receptors in cell lines from ovarian carcinoma: negative correlation with survival of patients. Gynecol Oncol 2002; 85: 159–64.
160 Kawashima K, Fujii T. Extraneuronal cholinergic system in lymphocytes. Pharmacol Ther 2000; 86: 29–48.
161 Español AJ, de la Torre E, Fiszman GL, Sales ME. Role of non-neuronal cholinergic system in breast cancer progression. Life Sci 2007; 80: 2281–5.
162 Cheng K, Zimniak P, Raufman JP. Transactivation of the epidermal growth factor receptor mediates cholinergic agonist-induced proliferation of H508 human colon cancer cells. Cancer Res 2003; 63: 6744–50.
163 Reubi JC, Waser B, Schaer JC, Laissue JA. Somatostatin receptor sst1-sst5 expression in normal and neoplastic human tissues using receptor autoradiography with subtype-selective ligands. Eur J Nucl Med 2001; 28: 836–46.
164 Dizeyi N, Konrad L, Bjartell A, Wu H, Gadaleanu V, Hansson J, *et al*. Localization and mRNA expression of somatostatin receptor subtypes in human prostatic tissue and prostate cancer cell lines. Urol Oncol 2002; 7: 91–8.
165 Sun LC, Coy DH. Somatostatin receptor-targeted anti-cancer therapy. Curr Drug Deliv 2011; 8: 2–10.
166 Luttrell LM, Lefkowitz RJ. The role of beta-arrestins in the termination and transduction of G-protein-coupled receptor signals. J Cell Sci 2002; 115: 455–65.
167 Ribas C, Penela P, Murga C, Salcedo A, García-Hoz C, Jurado-Pueyo M, *et al*. The G protein-coupled receptor kinase (GRK) interactome: role of GRKs in GPCR regulation and signaling. Biochim Biophys Acta 2007; 1768: 913–22.
168 Lefkowitz RJ, Shenoy SK. Transduction of receptor signals by beta-arrestins. Science 2005; 308: 512–7.
169 Rakesh K, Yoo B, Kim IM, Salazar N, Kim KS, Rockman HA. beta-Arrestin-biased agonism of the angiotensin receptor induced by mechanical stress. Sci Signal 2010; 3: ra46.
170 Li TT, Alemayehu M, Aziziyeh AI, Pape C, Pampillo M, Postovit LM, *et al*. Beta-arrestin/Ral signaling regulates lysophosphatidic acid-mediated migration and invasion of human breast tumor cells. Mol Cancer Res 2009; 7: 1064–77.
171 Buchanan FG, Gorden DL, Matta P, Shi Q, Matrisian LM, DuBois RN. Role of beta-arrestin 1 in the metastatic progression of colorectal cancer. Proc Natl Acad Sci U S A 2006; 103: 1492–7.
172 Rosanò L, Cianfrocca R, Masi S, Spinella F, Di Castro V, Biroccio A, *et al*. Beta-arrestin links endothelin A receptor to beta-catenin signaling to induce ovarian cancer cell invasion and metastasis. Proc Natl Acad Sci U S A 2009; 106: 2806–11.
173 Zhang Y, Qian Y, Lu W, Chen X. The G protein-coupled receptor 87 is

necessary for p53-dependent cell survival in response to genotoxic stress. Cancer Res 2009; 69: 6049–56.

174 Zhang Y, Scoumanne A, Chen X. G protein-coupled receptor 87: a promising opportunity for cancer drug discovery. Mol Cell Pharmacol 2010; 2: 111–6.

175 Jin Z, Luo R, Piao X. GPR56 and its related diseases. Prog Mol Biol Transl Sci 2009; 89: 1–13.

176 Tanese K, Fukuma M, Yamada T, Mori T, Yoshikawa T, Watanabe W, *et al*. G-protein-coupled receptor GPR49 is up-regulated in basal cell carcinoma and promotes cell proliferation and tumor formation. Am J Pathol 2008; 173: 835–43.

177 Qin Y, Verdegaal EM, Siderius M, Bebelman JP, Smit MJ, Leurs R, *et al*. Quantitative expression profiling of G-protein-coupled receptors (GPCRs) in metastatic melanoma: the constitutively active orphan GPCR GPR18 as novel drug target. Pigment Cell Melanoma Res 2011; 24: 207–18.

178 Gugger M, White R, Song S, Waser B, Cescato R, Rivière P, *et al*. GPR87 is an overexpressed G-protein coupled receptor in squamous cell carcinoma of the lung. Dis Markers 2008; 24: 41–50.

179 Glatt S, Halbauer D, Heindl S, Wernitznig A, Kozina D, Su KC, *et al*. hGPR87 contributes to viability of human tumor cells. Int J Cancer 2008; 122: 2008–16.

180 Tabata K, Baba K, Shiraishi A, Ito M, Fujita N. The orphan GPCR GPR87 was deorphanized and shown to be a lysophosphatidic acid receptor. Biochem Biophys Res Commun 2007; 363: 861–6.

181 Xu L, Begum S, Barry M, Crowley D, Yang L, Bronson RT, *et al*. GPR56 plays varying roles in endogenous cancer progression. Clin Exp Metastasis 2010; 27: 241–9.

182 Yang L, Chen G, Mohanty S, Scott G, Fazal F, Rahman A, *et al*. GPR56 Regulates VEGF production and angiogenesis during melanoma progression. Cancer Res 2011; 71: 5558–68.

Acta Pharmacologica Sinica (2012) 33: 363–371
 1671-4083/12 $32.00
www.nature.com/aps

Review

Orphan G protein-coupled receptors (GPCRs): biological functions and potential drug targets

Xiao-long TANG[1], Ying WANG[2], Da-li LI[1], Jian LUO[1, *], Ming-yao LIU[1, 2, *]

[1]*Shanghai Key Laboratory of Regulatory Biology, Institute of Biomedical Sciences and School of Life Sciences, East China Normal University, Shanghai 200241, China;* [2]*Alkek Institute of Biosciences and Technology, Texas A&M University Health Science Center, Houston, Texas 77030, USA*

The superfamily of G protein-coupled receptors (GPCRs) includes at least 800 seven-transmembrane receptors that participate in diverse physiological and pathological functions. GPCRs are the most successful targets of modern medicine, and approximately 36% of marketed pharmaceuticals target human GPCRs. However, the endogenous ligands of more than 140 GPCRs remain unidentified, leaving the natural functions of those GPCRs in doubt. These are the so-called orphan GPCRs, a great source of drug targets. This review focuses on the signaling transduction pathways of the *Adhesion* GPCR family, the LGR subfamily, and the PSGR subfamily, and their potential functions in immunology, development, and cancers. In this review, we present the current approaches and difficulties of orphan GPCR deorphanization and characterization.

Keywords: G protein-coupled receptors; orphan GPCR; deorphanization; *Adhesion* GPCR family; LGR subfamily; PSGR; Gpr48/Lgr4

Acta Pharmacologica Sinica (2012) 33: 363–371; doi: 10.1038/aps.2011.210; published online 27 Feb 2012

Introduction

GPCRs represent the largest superfamily and most diverse group of mammalian transmembrane proteins. The main characteristic feature of these proteins is that they share a common seven-transmembrane (7TM) configuration. GPCRs have attracted a great deal of interest owing to their numerous physiological and pathological roles in transducing extracellular signals into intracellular effector pathways through the activation of heterotrimeric G protein by binding to a broad range of ligands, including proteins[1], peptides[2], organic compounds[3, 4], and eicosanoids[5]. This makes GPCRs and their signal transduction pathways important specific targets for a variety of physiological functions and therapeutic approaches, ranging from the control of blood pressure, allergic response, kidney function, hormonal disorders, and neurological diseases to the progression of cancer[6]. Owing to the features of GPCR structure and function, approximately 36% of currently marketed drugs target human GPCRs[7]. GPCRs have huge potential in biomedical research and drug development.

Human GPCRs can be divided into five main families on the basis of phylogenetic criteria, *Glutamate*, *Rhodopsin*, *Adhesion*, *Frizzled/Taste2*, and *Secretin*[8]. Among the five GPCRs families, *Rhodopsin* is the most studied. It comprises the largest group of GPCRs. Notably, in recent years, the leucine-rich repeat-containing G-protein coupled receptor (LGR) subfamily, part of *Rhodopsin*, have displayed enormously important physiological functions in knockout mice studies especially LGR4 and LGR5. Olfactory receptors are also members of *Rhodopsin* family of GPCRs and are mainly expressed in sensory neurons of olfactory system. These form a multigene family. The PSGR subfamily belongs to the olfactory receptor group. The family has restricted expression in human prostate tissues and is upregulated in prostate cancer. The second largest GPCR family, with 33 members, is the *Adhesion* family. This family is very special because of its members' secondary structures, with distinctive long N-termini containing adhesion domains[8]. Limited studies have shown that *Adhesion* GPCRs are involved in the signaling of cell adhesion, motility, embryonic development, and the immune system. There are still GPCRs for which the natural ligands remain to be identified. These are called orphan GPCRs.

LGRs and PSGR belong to *Rhodopsin* subfamily and they represent as classical GPCRs in structure and signal transduction. On the other hand, *Adhesion* GPCRs are novel, and their structures and signal transduction are distinct to the classical GPCRs. In this review, we focused our discussion on LGR subfamily, PSGR subfamily, and *Adhesion* GPCRs family. We

* To whom correspondence should be addressed.
E-mail jluo@bio.ecnu.edu.cn (Jian LUO);
mliu@ibt.tamhsc.edu (Ming-yao LIU)
Received 2011-12-12 Accepted 2011-12-28

also discussed current screening systems for the deorphanization and characterization of the orphan GPCRs.

Orphan GPCRs

The first GPCR to be identified was rhodopsin in 1878. It was later proven that rhodopsin consists of the GPCR protein opsin and a reversibly covalently bound cofactor, retinal[9, 10]. After completion of the human genome sequence in 2004[11, 12], the number of human GPCRs increased to about 800 based on the screening approaches, such as low-stringency hybridization[13], PCR-derived methods[14], and bioinformatic analyses[15]. Besides the olfactory receptor family, more than 140 GPCRs have not yet been linked to endogenous ligands. These are the so-called orphan GPCRs (Figure 1)[16].

Biological functions of the LGR subfamily

LGRs 4–8 are members of the rhodopsin GPCR family, which can be divided into two groups, LGRs 4, 5, and 6 and LGRs 7 and 8 in terms of their natural ligand. R-spondins have recently been identified as the ligands for LGRs 4, 5, and 6[17]. LGRs 7 and 8 are relaxin family peptide (RXFP) receptors[18]. According to sequence similarity, LGRs 4, 5, and 6 are closely related to each other, showing almost 50% identities. The three orphan receptors have a substantially large N-terminal extracellular domain (ECD) composed of 17 leucine rich repeats (LRR) (Figure 2)[19]. Lgr4, also known as Gpr48, has been reported to have many physiological functions by the generation of knockout mice. The loss of Lgr4 results in developmental defects in many areas, including intrauterine growth retardation associated with embryonic and perinatal lethality[20], abnormal renal development[21], defective postnatal development of the male reproductive tract[22], ocular anterior segment dysgenesis[23], bone formation and remodeling dysfunction[6], impaired hair placode formation[24], and defective development of the gall bladder and cystic ducts[25]. Lgr5 has been proven to be a marker of gastrointestinal tract and hair follicle stem cells[26, 27]. Knockout of Lgr5 in mice leads to total neonatal lethality accompanied with ankyloglossia and gastrointestinal distension[28]. Lgr6 also has been shown to be a stem cell marker in hair follicles, and Lgr6-positive stem cells have been found to produce all cell lineages of the skin[29]. LGR4 and LGR5 are also highly expressed in several types of cancers. LGR5 is up-regulated in human colon and ovarian tumors and promotes cell proliferation and tumor formation in basal cell carcinoma[30, 31]. Overexpression of LGR4 enhances cervical and colon cancer cell invasiveness and metastasis[32]. However, despite their critical function in development and cancer, LGR4 and LGR5 will still be considered orphan receptors until R-spondins reported to function as their natural ligands can be proven to regulate Wnt/β-catenin signaling pathway. Some observations of Lgr4 and Lgr5 knockout mice have been strongly relevant to Wnt/β-catenin signaling[33, 34]. This suggests that LGR4 and LGR5 could be involved in the Wnt pathway. One author stated that

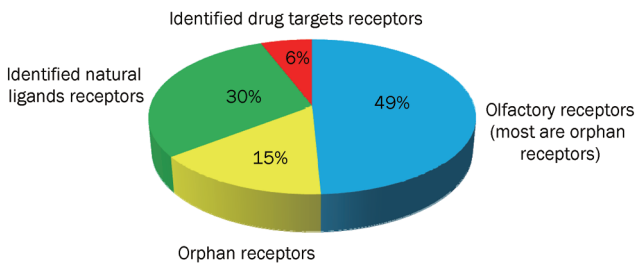

Figure 1. Percentage of the orphan GPCRs in GPCR superfamily. GPCRs constitute a large transmembrane family of more than 800 members. Among them, 6% are utilized as drug target in clinical applications, and 30% are natural ligand receptors. However, 49% are olfactory receptors (most of them are orphan GPCRs), and 15% are orphan GPCRs. (Data were summarized from a review paper[122])

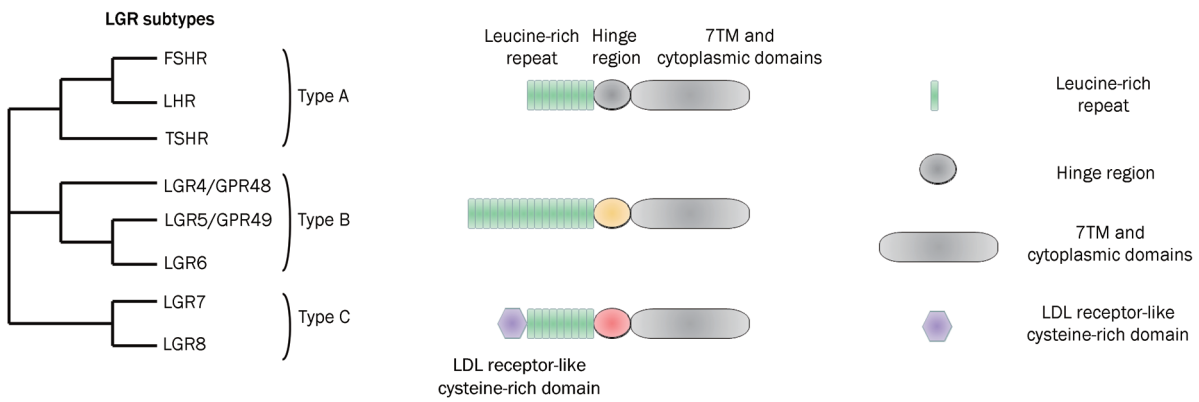

Figure 2. LGR subfamily GPCRs. The Type A LGRs includes the follicle-stimulating hormone receptor (FSHR), the luteinizing hormone receptor (LHR) and the thyroid-stimulating hormone receptor (TSHR). The Type B LGR comprises three members, Gpr48/LGR4, LGR5, and LGR6 which remain orphan GPCRs at the present time. By contrast, Type C LGRs have only two members, LGR7 and LGR8 which have been demonstrated to be the relaxin family receptors. Type A contains 9 LRRs in the ectodomain, whereas Type B contains 17 LRRs. By contrast, Type C has an N-terminal LDL receptor-like cysteine-rich domain not found in other LGRs. 7TM, seven-transmembrane; LDL, low-density lipoprotein; LRR, leucine-rich repeat; LGR, leucine-rich repeat-containing G-protein-coupled receptor; FSHR, follicle-stimulating hormone receptor; LHR, luteinizing hormone receptor; TSHR, thyroid-stimulating hormone receptor.

R-spondins-Lgr4 induced the signal transduction pathway in a manner independent of G proteins[17]. However, two independent groups have reported that Lgr4/Gpr48 is associated with the Gαs-cAMP pathway by generating constitutively active forms of Lgr4/Gpr48[23, 35]. Therefore, the existence of endogenous ligands for the activation of classical G-protein coupled signaling pathways for Lgr4/Gpr48 is still a question. LGR7 and LGR8 share 54% identity. Besides 10 LRRs motif, LGR7 and LGR8 also have an LDL class A (LDLa) motif in the N-terminal, which is an important domain for signal transduction (Figure 2). Traditionally, relaxin/LGR7 has been thought to be a hormone receptor for pregnancy and parturition[18]. Recently, it has been reported that relaxin/LGR7 also has significant function in non-reproductive organs, such as the heart, and even plays a role in cancer growth and metastasis[36]. Insulin-like peptide 3 (INSL3), which is a ligand of LGR8, is highly expressed in the Leydig cells of the testis and knocking out Insl3 in mice generates a cryptorchid phenotype. However, reports have been conflicting with respect to LGR8 mutations related to human cryptorchidism[18]. The role of INSL3 in human adult male is still not clear.

PSGRs subfamily in prostate cancer

Mammalian olfactory receptors, which are the members of the Rhodopsin family of GPCRs and mainly expressed in sensory neurons of the olfactory epithelium in the nose, are used to sense the chemical environment[37]. Recently, some olfactory receptors have also been found in other organs. For example, MOR23 is expressed both in the olfactory epithelium and in sperm and functions as a chemosensing receptor during sperm-egg communication, thereby modulating fertilization in the reproductive system[38]. The new olfactory receptor family members PSGR1 and PSGR2 have been found to have restricted expression in human prostate tissues, as shown by Northern blot and real-time PCR analysis of over 20 different human tissue types[39–41]. PSGR subfamily expression increases significantly in the epithelial cells of prostate intraepithelial neoplasia (PIN) patients and in prostate cancer patients relative to non-cancerous controls and benign prostatic hyperplasia tissues, suggesting that the PSGR subfamily may play an important role in early prostate cancer development[42]. The PSGR subfamily has been proven to be strongly associated with the clinical parameters (clinical stages, Gleason scores, recurrence status, and metastasis) and its members could serve as biomarkers for prostate cancer[42, 43]. PSGR subfamily transcripts even can be used as diagnostic markers in urine[44]. It has also been reported that PSGR expression detection together with the well-known prostate cancer marker prostate-specific antigen (PSA), prostate cancer gene 3 (PCA3), and α-methylacyl-CoA racemase (AMACR) can increases diagnostic specificity in the detection of prostate cancer[43–45]. Recently, Neuhaus EM *et al* reported that through intracellular Ca^{2+} flux using a bank of steroid hormones and through odorant-related compound screening, certain steroids and β-ionone have been proven to be active ligands for PSGR[46]. PSGR-induced Ca^{2+} signaling was found to require the involvement of endogenous Ca^{2+}-selective transient receptor potential vanilloid type 6 (TRPV6) channels[47]. Incubation of prostate cancer cells with β-ionone inhibits cell proliferation[46]. This suggests that PSGR signaling is also involved in prostate cancer cell progression.

Adhesion GPCR family

GPCRs in the *Adhesion* family have a relative long N-terminal domain, which contains many so-called adhesion domains (Figure 3). These adhesion domains only existed in some adhesion molecules, such as integrins, cadherins, and selectins; and the domains are thought to have adhesive properties. Another striking characteristic of all the *Adhesion* GPCRs is that there is a GPS (GPCR proteolytic site) domain linking the 7TM region to the extracellular domain, which acts as an autocatalytic site[48, 49]. As a novel GPCRs family, most of the members are orphan and only a few of them have been identified as having natural ligands and functions.

Adhesion GPCRs in immunology

Immune response is coordinated by an assortment of membrane receptors, including TLRs, integrins, lectins, the Ig superfamily, selectins, and GPCRs, which are found on leukocytes[10, 50, 51]. The first *Adhesion* GPCR to be discovered, epidermal growth factor-like module containing mucin-like receptor protein 1 (EMR1, F4/80 receptor), which is an epidermal growth factor (EGF)-seven transmembrane (7M) receptor, have a predominantly leukocyte-restricted expression pattern[52]. Though the expression of Emr1 is restricted, the function of this receptor remained unknown until the generation of Emr1 knock-out mice. The mouse model indicates that Emr1 is critical to the induction of $CD8^+$ regulatory T-cells in peripheral tolerance[53]. Besides EMR1, the EGF-TM7 subfamily includes EMR2, EMR3, EMR4, and CD97, all of which belong to the *Adhesion* GPCR family. Unlike the highly specific expression of EMR1, the other EGF-TM7 receptors are expressed largely in myeloid cells (monocytes, macrophages, neutrophils, and dendritic cells) and in some lymphoid cells (T and B cells)[54]. Chondroitin sulfate has recently been identified as the ligand for EMR2 and CD97, which mediate cell attachment[55]. CD97, the leukocyte activation antigen, also has been shown to bind to the complement regulatory protein DAF/CD55 (decay accelerating factor) and the longest splice variant of CD97 has the highest capacity to bind to CD55-expressing cells. Although CD97 and EMR2 differ by only 3 amino acids (in the EGF domain), the activity of EMR2 binding to CD55 is significantly weaker[56, 57]. The precise function of the CD97-CD55 interaction is still not fully understood. Using knock-out mice and x-ray crystallography, Abbott RJ *et al* demonstrated that T cells and complement regulatory activities of CD55 occur on opposite faces of the molecule, suggesting that the CD97-CD55 complex might simultaneously regulate both the innate and adaptive immune responses[58, 59]. EMR3 has been reported as a marker for mature granulocytes, and it can interact with the ligand that expresses at the surface of monocyte-derived macrophages and activated human neutrophils[60, 61]. EMR4 has been reported to interact with a cell surface protein as a ligand

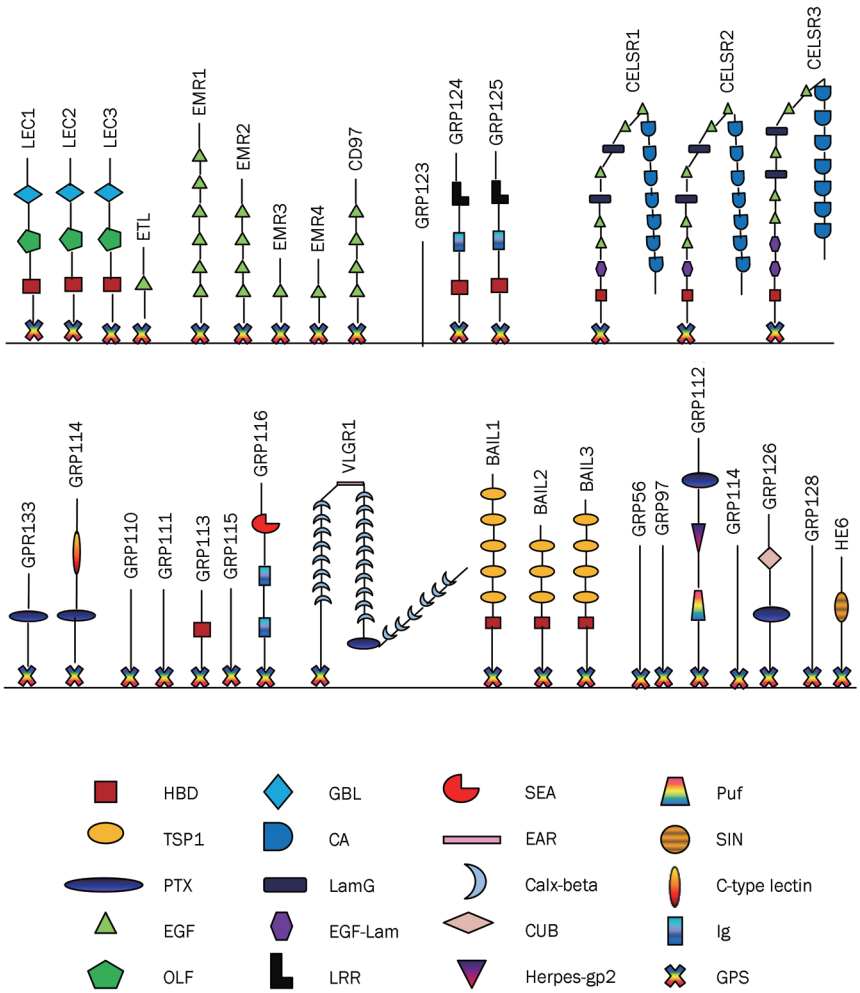

Figure 3. Schematic diagram of the extracellular N-terminal domain within the *Adhesion* GPCRs. The extracellular N-terminal domains of 33 *Adhesion* GPCRs was predicted by the RPS-BLAST against the conserved domain database (CCD). CA, cadherin domain; calx-beta, domain found in Na^+–Ca^{2+} exchangers; CUB, resembles the structure of immunoglobins; EAR, epilepsy-associated repeat; EGF-Lam, laminin EGF-like domain; EGF, epidermal growth factor domain; HBD, hormone-binding domain; herpes-gp2, resembles the equine herpes virus glycoprotein gp2 structure; GBL, galactose-binding lectin domain; Ig, immunoglobulin domain; OLF, olfactomedin domain; LamG, laminin G domain; LRR, leucine-rich repeat domain; PTX, pentraxin domain; Puf, displays structural similarity to RNA-binding protein from the Puf family; SEA, domain found in sea-urchin sperm protein; SIN, resembles the primary structure of the SIN component of the histone deacetylase complex; TSP1, thrombospondin domain. C-type lectin, similar to the C-type lectin or carbohydrate-recognition domain; GPS, GPCR proteolytic site domain.

on A20 B-lymphoma cells[62].

Adhesion GPCRs in development

The most extensively studied *Adhesion* GPCRs in embryonic development are the so-called 7TM-cadherin subfamily (*Celsr/Flamingo/Starry night*). All the members of this subfamily posses extracellular domains containing nine atypical cadherin repeats which have linked the combination of EGF-like and laminin G-like domains[63]. The 7TM-cadherins are an evolutionarily conserved gene subfamily with homologues discovered from ascidians to mammals[63]. In mammals, the subfamily comprises 3 genes, *Celsr1*, *Celsr2*, and *Celsr3*. There are 4 genes (*fmila*, *fmilb*, *fmi2*, and *fmi3*) in zebrafish and only one homologue, called *flamingo* and *starry night*, in *Drosophila*. *Drosophila* studies provide us with a distinct function view of Flamingo/Starry night as a core planar polarity protein[64]. Its functions include regulating dendrite extension from sensory neurons[65, 66], modulating target selection by photoreceptor axons[67], accelerating axon advance from sensory and motor neurons[68], and limiting ectopic neuromuscular junction formation and maintenance of motor axon terminals[69]. Gene knockout and knockdown of 7TM-cadherins has also confirmed this observation in vertebrates. 7TM-cadherins regulate morphogenetic movements, neural tube closure, orientation of sensory hair cells in inner ear, and hair follicle patterning[63, 70–73]. Recently, *Adhesion* GPCRs Gpr124 and Gpr126, which are not 7TM-cadherins, have been shown to regulate the development of different tissues in mice. Gpr124 affects CNS-specific angiogenesis and Gpr126 affects Schwann cells to initiate myelination[74–77]. This suggests that more members of this family may be involved in development and that this may be due to the adhesive or other properties of N-terminal domains.

Adhesion GPCRs in cancers

Because cell adhesion molecules have a vital role in cancer progression, it is reasonable to speculate that *Adhesion* GPCRs also play important functions in cancer progression and metastasis. Leukocyte *Adhesion* GPCR EMR2 has been proven to be overexpressed in human breast cancer and is associated with patient survival[78]. CD97 is involved in tumor-environment interactions and mediates tumor invasion[79]. It has been reported that the 7TM-cadherin receptors may also be involved in human cancers, such as gastric cancer, lung cancer, and melanoma[80]. Interestingly, unlike other *Adhesion* GPCRs, GPR56 has been shown to suppress some cancer cell

growth and metastasis through interacting with tissue transglutaminase (TG2)[81, 82].

Signal transduction mediated by *Adhesion* GPCRs

Most *Adhesion* GPCRs are orphan receptors, which is the main reason whether or not *Adhesion* GPCRs are involved in G protein signaling. In addition, the complicated structure of *Adhesion* GPCRs, comprising both largely ECD and 7TM domains, make it possible for *Adhesion* GPCRs to go through the signaling pathway in a G-protein-independent manner[83]. For example, Gpr124 regulates angiogenic sprouting into neural tissues through TGF-beta pathway in mouse[76]. BAI1 can function as an engulfment receptor in response to "eat me" signal phosphatidylserine, which leads to BAI1 directly bind and activate the ELMO/DOCK180/RAC module[84]. It has been reported that GPR124 and GPR125 can interact with several viral oncoproteins by its cytoplasmic PDZ domain. And the rat Ig-Hepta (GPR116) has been shown to form a homodimer that is linked by disulphide bonds. Moreover, this receptor undergoes two proteolytic cleavages, and cleaved product in the SEA domain might act as a ligand to bind to GPR116[85–87]. Therefore, these 7TM receptors may mediate G-protein independent signaling pathway in cellular functions.

Though some *Adhesion* GPCRs go through G-protein-independent pathways, others have been proven to go through the classic G-protein-dependent pathway. Lectomedin receptor-1 was co-purified with the $G_{\alpha o}$[88]. Also, GPR56 has been shown to form a complex with $G_{q/11}$ and $G_{12/13}$ in the neural progenitor cells[89, 90]. Gpr126 modulates Schwann cells, initiating myelination by classic cAMP pathway[74]. Latrophilin, which is activated by the ligand LTX, can transduce the intercellular Ca^{2+} signal pathway. These observations indicate that this family can transmit signals through both classical G-protein-dependent and G-protein-independent mechanisms.

Deorphanization strategy

GPCRs are the most prominent family of pharmacological targets in biomedicine[91]. The deorphanization of orphan GPCRs is one of the most important missions in orphan GPCR research. Deorphanization is the process of identifying ligands that are highly selective for orphan GPCRs. In general, the standard assays are radio-ligand binding, calcium flux, GTPγ binding, and modulation of cAMP levels[92–98].

With the development of molecular technology, several lines of approaches have been used for deorphanization. The first, according to the sequence and function similarity, ligands of the identified receptors are used to examine GPCRs with identical sequences or domains. This sequence similarity strategy resulted in the identification of the ligands of Edg3 and Edg5, whose sequences are similar to that of the S1P receptors, with >50% amino acid identity[99–101]. The function similarity strategy lead to the identification of the ligands of Lgr5 homologues, R-spondins, which stimulate the growth of intestinal stem cells[17]. However, this approach must be carefully evaluated because its predictions are not always accurate. For example, alkyl imidazole functions as dual histamine H3/H4 receptor ligands, while histamine H3/H4 receptors share very little sequence identity[102, 103]. Although the EGF domain of CD97 and EMR2 share 97% identity, only CD97 shows high affinity with CD55 but not with EMR2. The second strategy used to identify natural ligands works by determining the expression profile relationship between receptor and the putative ligand. This technique led to the identification of the receptors of RDC7 and RDC8 as adenosine A_1 and A_{2A} receptors, all of which are highly transcribed in the brain cortex, thyroid follicular cells, and testis[104, 105]. The third technique is used to identify GPCRs that have specific expression profiles and distinct cytoplasm signal pathways. This method uses extracts of tissues that contain potential ligands to screen by the GPCRs mediated signaling assays. Some hormone proteins, such as nociptin, orexins, apelin, prolactin, and ghrelin, were successfully identified using this strategy[106–109]. The fourth strategy has been used successfully to deorphanize *Adhesion* GPCRs. It involves engineering recombinant soluble extracellular regions of *Adhesion* GPCRs with an Fc-fragment in N-terminal and biotinylation signal at the C-terminal. This acts as probe to screen the extracellular matrix components. This led to the identification of certain ligands for myeloid cell *Adhesion* GPCR[51, 110]. In recent years, the so-called reverse pharmacology strategy has also been used to identify the ligands of orphan GPCRs[98]. This is carried out by expressing these orphan GPCRs in eukaryotic cells by DNA transfection and then coupling them to ligands to examine the binding affinity of the cells and ligands[111, 112]. With this approach, many peptide hormones, including ghrelin, which stimulates hunger; kisspeptin and metastin, which are involved in puberty development and cancer metastasis; orexin and hypocretin, which mediate food intake and induce wakefulness and energy expenditure, have been discovered within the last decade[113]. However, the successful application of reverse pharmacology method depends on three major elements: sufficient orphan receptor expression, high-quality ligands and robust screening assays to detect receptor activation[114, 115]. Fortunately, with development of membrane protein expression and purification techniques, neuropeptides and synthetic ligands have been applied to large-scale screening[116]. Of the three elements outlined above, choosing an appropriate detection assay is the most problematic.

The rate of GPCR deorphanization decreased drastically at the turn of the century, suggesting some gap the processes exit. Herein, we discuss several factors that may account for the problem. The greatest challenge in deorphanization of the receptors is the limited knowledge about them, especially with respect to their physiological functions and their roles as transmitters of signal pathways. Thus, experimental design is rendered difficult by the lack of signal transduction assays and positive controls[113]. Second, the majority of approaches to deorphanization rely on monitoring changes at the second messenger level, which is regulated by G proteins. However, GPCRs can transduce signal pathways diversely, sometimes even beyond G proteins. In this case, identifying the relevant

signaling pathway is key point to deorphanization. For example, some orphan GPCRs require accessory proteins for their activity. This working model has been shown in calcitonin GPCRs, which require RAMPs (receptor activity-modifying proteins) for their activation. To identify the ligand of this kind of GPCR, new screening assays for specific accessory proteins must be set up[117, 118]. Third, there is a possibility that some transmitters are only expressed at a particular time during the life span or at certain specific conditions[9]. Although it is risky and challenging, it is necessary to find more effective transmitters for deorphanization and put them to use. Lastly, some orphan GPCRs can form heterodimers with other GPCRs and function in a ligand-independent manner, and there is no outcome for the identification of the ligands of this kind of orphan GPCRs. For example, GABABR1 and GABABR2 form well-known heterodimer receptors and GABABR1 is involved in ligand-binding, whereas GABABR2 only acts as the signaling unit. GABABR2 is an orphan receptor in the heterodimer complex without any known ligand[119-121].

Perspectives in the research of orphan GPCRs

In recent years, the numbers of new orphan GPCRs have increased and several members have been relatively well characterized. However, the progress of orphan GPCR function research has been hampered by the lack of identified ligands and by the unique structures of the GPCR themselves. Further investigation of their signaling pathways is valuable to understand the physiological and pathological roles of these new orphan GPCRs. The development of orphan GPCR knockout mice has also been shown to be a successful method for the characterization of their physiological and pathological functions. The knockout approach for orphan GPCRs are essential for our understanding of these receptor functions and their potential pathways. Functional and specific antibodies can serve probes not only for the ligands, but also for developing therapies for tumors and genetic disorders in which orphan GPCRs are involved. Although progress is very difficult, searching for the ligands of orphan GPCRs and identifying their physiological functions will continue. With recent discoveries of more and more orphan GPCR signaling pathways, understanding of their particular physiological functions and deorphanization for therapeutic purposes should accelerate in the coming years.

Acknowledgements

This work is partially supported by grants from National Basic Research Program of China (2012CB910400), National Natural Science Foundation of China (30800653, 30930055, and 81071437), the Science and Technology Commission of Shanghai Municipality (11DZ2260300), and by grants from NIH (5R01CA134731) and DOD (W81XWH-10-10147).

References

1 Parmentier M, Libert F, Maenhaut C, Lefort A, Gerard C, Perret J, *et al*. Molecular cloning of the thyrotropin receptor. Science 1989; 246: 1620–2.

2 Masu Y, Nakayama K, Tamaki H, Harada Y, Kuno M, Nakanishi S. cDNA cloning of bovine substance-K receptor through oocyte expression system. Nature 1987; 329: 836–8.

3 Dixon RA, Kobilka BK, Strader DJ, Benovic JL, Dohlman HG, Frielle T, *et al*. Cloning of the gene and cDNA for mammalian beta-adrenergic receptor and homology with rhodopsin. Nature 1986; 321: 75–9.

4 Kobilka BK, MacGregor C, Daniel K, Kobilka TS, Caron MG, Lefkowitz RJ. Functional activity and regulation of human beta 2-adrenergic receptors expressed in *Xenopus* oocytes. J Biol Chem 1987; 262: 15796–802.

5 Felder CC, Briley EM, Axelrod J, Simpson JT, Mackie K, Devane WA. Anandamide, an endogenous cannabimimetic eicosanoid, binds to the cloned human cannabinoid receptor and stimulates receptor-mediated signal transduction. Proc Natl Acad Sci U S A 1993; 90: 7656–60.

6 Luo J, Zhou W, Zhou X, Li D, Weng J, Yi Z, *et al*. Regulation of bone formation and remodeling by G-protein-coupled receptor 48. Development 2009; 136: 2747–56.

7 Rask-Andersen M, Almen MS, Schioth HB. Trends in the exploitation of novel drug targets. Nat Rev Drug Discov 2011; 10: 579–90.

8 Fredriksson R, Lagerstrom MC, Lundin LG, Schioth HB. The G-protein-coupled receptors in the human genome form five main families. Phylogenetic analysis, paralogon groups, and fingerprints. Mol Pharmacol 2003; 63: 1256–72.

9 Chung S, Funakoshi T, Civelli O. Orphan GPCR research. Br J Pharmacol 2008; 153: S339–46.

10 Oh DY, Kim K, Kwon HB, Seong JY. Cellular and molecular biology of orphan G protein-coupled receptors. Int Rev Cytol 2006; 252: 163–218.

11 Lander ES, Linton LM, Birren B, Nusbaum C, Zody MC, Baldwin J, *et al*. Initial sequencing and analysis of the human genome. Nature 2001; 409: 860–921.

12 Venter JC, Adams MD, Myers EW, Li PW, Mural RJ, Sutton GG, *et al*. The sequence of the human genome. Science 2001; 291: 1304–51.

13 Bunzow JR, Van Tol HH, Grandy DK, Albert P, Salon J, Christie M, *et al*. Cloning and expression of a rat D_2 dopamine receptor cDNA. Nature 1988; 336: 783–7.

14 Libert F, Parmentier M, Lefort A, Dinsart C, Van Sande J, Maenhaut C, *et al*. Selective amplification and cloning of four new members of the G protein-coupled receptor family. Science 1989; 244: 569–72.

15 Vassilatis DK, Hohmann JG, Zeng H, Li F, Ranchalis JE, Mortrud MT, *et al*. The G protein-coupled receptor repertoires of human and mouse. Proc Natl Acad Sci U S A 2003; 100: 4903–8.

16 Levoye A, Dam J, Ayoub MA, Guillaume JL, Jockers R. Do orphan G-protein-coupled receptors have ligand-independent functions? New insights from receptor heterodimers. EMBO Rep 2006; 7: 1094–8.

17 Carmon KS, Gong X, Lin Q, Thomas A, Liu Q. R-spondins function as ligands of the orphan receptors LGR4 and LGR5 to regulate Wnt/beta-catenin signaling. Proc Natl Acad Sci U S A 2011; 108: 11452–7.

18 Kong RC, Shilling PJ, Lobb DK, Gooley PR, Bathgate RA. Membrane receptors: structure and function of the relaxin family peptide receptors. Mol Cell Endocrinol 2010; 320: 1–15.

19 Hsu SY, Kudo M, Chen T, Nakabayashi K, Bhalla A, van der Spek PJ, *et al*. The three subfamilies of leucine-rich repeat-containing G protein-coupled receptors (LGR): identification of LGR6 and LGR7 and the signaling mechanism for LGR7. Mol Endocrinol 2000; 14: 1257–71.

20 Mazerbourg S, Bouley DM, Sudo S, Klein CA, Zhang JV, Kawamura K, *et al*. Leucine-rich repeat-containing, G protein-coupled receptor 4 null mice exhibit intrauterine growth retardation associated with

embryonic and perinatal lethality. Mol Endocrinol 2004; 18: 2241–54.
21 Kato S, Matsubara M, Matsuo T, Mohri Y, Kazama I, Hatano R, *et al*. Leucine-rich repeat-containing G protein-coupled receptor-4 (LGR4, Gpr48) is essential for renal development in mice. Nephron Exp Nephrol 2006; 104: e63–75.
22 Mendive F, Laurent P, Van Schoore G, Skarnes W, Pochet R, Vassart G. Defective postnatal development of the male reproductive tract in LGR4 knockout mice. Dev Biol 2006; 290: 421–34.
23 Weng J, Luo J, Cheng X, Jin C, Zhou X, Qu J, *et al*. Deletion of G protein-coupled receptor 48 leads to ocular anterior segment dysgenesis (ASD) through down-regulation of Pitx2. Proc Natl Acad Sci U S A 2008; 105: 6081–6.
24 Mohri Y, Kato S, Umezawa A, Okuyama R, Nishimori K. Impaired hair placode formation with reduced expression of hair follicle-related genes in mice lacking Lgr4. Dev Dyn 2008; 237: 2235–42.
25 Yamashita R, Takegawa Y, Sakumoto M, Nakahara M, Kawazu H, Hoshii T, *et al*. Defective development of the gall bladder and cystic duct in Lgr4-hypomorphic mice. Dev Dyn 2009; 238: 993–1000.
26 Barker N, van Es JH, Kuipers J, Kujala P, van den Born M, Cozijnsen M, *et al*. Identification of stem cells in small intestine and colon by marker gene Lgr5. Nature 2007; 449: 1003–7.
27 Jaks V, Barker N, Kasper M, van Es JH, Snippert HJ, Clevers H, *et al*. Lgr5 marks cycling, yet long-lived, hair follicle stem cells. Nat Genet 2008; 40: 1291–9.
28 Morita H, Mazerbourg S, Bouley DM, Luo CW, Kawamura K, Kuwabara Y, *et al*. Neonatal lethality of LGR5 null mice is associated with ankyloglossia and gastrointestinal distension. Mol Cell Biol 2004; 24: 9736–43.
29 Snippert HJ, Haegebarth A, Kasper M, Jaks V, van Es JH, Barker N, *et al*. Lgr6 marks stem cells in the hair follicle that generate all cell lineages of the skin. Science 2010; 327: 1385–9.
30 McClanahan T, Koseoglu S, Smith K, Grein J, Gustafson E, Black S, *et al*. Identification of overexpression of orphan G protein-coupled receptor GPR49 in human colon and ovarian primary tumors. Cancer Biol Ther 2006; 5: 419–26.
31 Tanese K, Fukuma M, Yamada T, Mori T, Yoshikawa T, Watanabe W, *et al*. G-protein-coupled receptor GPR49 is up-regulated in basal cell carcinoma and promotes cell proliferation and tumor formation. Am J Pathol 2008; 173: 835–43.
32 Gao Y, Kitagawa K, Hiramatsu Y, Kikuchi H, Isobe T, Shimada M, *et al*. Up-regulation of GPR48 induced by down-regulation of p27Kip1 enhances carcinoma cell invasiveness and metastasis. Cancer Res 2006; 66: 11623–31.
33 Ootani A, Li X, Sangiorgi E, Ho QT, Ueno H, Toda S, *et al*. Sustained *in vitro* intestinal epithelial culture within a Wnt-dependent stem cell niche. Nat Med 2009; 15: 701–6.
34 Sato T, van Es JH, Snippert HJ, Stange DE, Vries RG, van den Born M, *et al*. Paneth cells constitute the niche for Lgr5 stem cells in intestinal crypts. Nature 2011; 469: 415–8.
35 Gao Y, Kitagawa K, Shimada M, Uchida C, Hattori T, Oda T, *et al*. Generation of a constitutively active mutant of human GPR48/LGR4, a G-protein-coupled receptor. Hokkaido Igaku Zasshi 2006; 81: 101–5, 7, 9.
36 Feng S, Agoulnik IU, Truong A, Li Z, Creighton CJ, Kaftanovskaya EM, *et al*. Suppression of relaxin receptor RXFP1 decreases prostate cancer growth and metastasis. Endocr Relat Cancer 2010; 17: 1021–33.
37 Spehr M, Munger SD. Olfactory receptors: G protein-coupled receptors and beyond. J Neurochem 2009; 109: 1570–83.
38 Fukuda N, Yomogida K, Okabe M, Touhara K. Functional characterization of a mouse testicular olfactory receptor and its role in chemosensing and in regulation of sperm motility. J Cell Sci 2004; 117: 5835–45.
39 Xu LL, Stackhouse BG, Florence K, Zhang W, Shanmugam N, Sesterhenn IA, *et al*. PSGR, a novel prostate-specific gene with homology to a G protein-coupled receptor, is overexpressed in prostate cancer. Cancer Res 2000; 60: 6568–72.
40 Weng J, Wang J, Hu X, Wang F, Ittmann M, Liu M. PSGR2, a novel G-protein coupled receptor, is overexpressed in human prostate cancer. Int J Cancer 2006; 118: 1471–80.
41 Xia C, Ma W, Wang F, Hua S, Liu M. Identification of a prostate-specific G-protein coupled receptor in prostate cancer. Oncogene 2001; 20: 5903–7.
42 Weng J, Wang J, Cai Y, Stafford LJ, Mitchell D, Ittmann M, *et al*. Increased expression of prostate-specific G-protein-coupled receptor in human prostate intraepithelial neoplasia and prostate cancers. Int J Cancer 2005; 113: 811–8.
43 Wang J, Weng J, Cai Y, Penland R, Liu M, Ittmann M. The prostate-specific G-protein coupled receptors PSGR and PSGR2 are prostate cancer biomarkers that are complementary to alpha-methylacyl-CoA racemase. Prostate 2006; 66: 847–57.
44 Rigau M, Morote J, Mir MC, Ballesteros C, Ortega I, Sanchez A, *et al*. PSGR and PCA3 as biomarkers for the detection of prostate cancer in urine. Prostate 2010; 70: 1760–7.
45 Rigau M, Ortega I, Mir MC, Ballesteros C, Garcia M, Llaurado M, *et al*. A three-gene panel on urine increases PSA specificity in the detection of prostate cancer. Prostate 2011; 71: 1736-45.
46 Neuhaus EM, Zhang W, Gelis L, Deng Y, Noldus J, Hatt H. Activation of an olfactory receptor inhibits proliferation of prostate cancer cells. J Biol Chem 2009; 284: 16218–25.
47 Spehr J, Gelis L, Osterloh M, Oberland S, Hatt H, Spehr M, *et al*. G protein-coupled receptor signaling via Src kinase induces endogenous human transient receptor potential vanilloid type 6 (TRPV6) channel activation. J Biol Chem 2011; 286: 13184–92.
48 Krasnoperov VG, Bittner MA, Beavis R, Kuang Y, Salnikow KV, Chepurny OG, *et al*. alpha-Latrotoxin stimulates exocytosis by the interaction with a neuronal G-protein-coupled receptor. Neuron 1997; 18: 925–37.
49 Baud V, Chissoe SL, Viegas-Pequignot E, Diriong S, N'Guyen VC, Roe BA, *et al*. EMR1, an unusual member in the family of hormone receptors with seven transmembrane segments. Genomics 1995; 26: 334–44.
50 Taylor PR, Martinez-Pomares L, Stacey M, Lin HH, Brown GD, Gordon S. Macrophage receptors and immune recognition. Annu Rev Immunol 2005; 23: 901–44.
51 Yona S, Lin HH, Stacey M. Immunity and adhesion-GPCRs. Adv Exp Med Biol 2010; 706: 121–7.
52 Austyn JM, Gordon S. F4/80, a monoclonal antibody directed specifically against the mouse macrophage. Eur J Immunol 1981; 11: 805–15.
53 Lin HH, Faunce DE, Stacey M, Terajewicz A, Nakamura T, Zhang-Hoover J, *et al*. The macrophage F4/80 receptor is required for the induction of antigen-specific efferent regulatory T cells in peripheral tolerance. J Exp Med 2005; 201: 1615–25.
54 Kwakkenbos MJ, Pouwels W, Matmati M, Stacey M, Lin HH, Gordon S, *et al*. Expression of the largest CD97 and EMR2 isoforms on leukocytes facilitates a specific interaction with chondroitin sulfate on B cells. J Leukoc Biol 2005; 77: 112–9.
55 Stacey M, Chang GW, Davies JQ, Kwakkenbos MJ, Sanderson RD, Hamann J, *et al*. The epidermal growth factor-like domains of the human EMR2 receptor mediate cell attachment through chondroitin

sulfate glycosaminoglycans. Blood 2003; 102: 2916–24.
56 Hamann J, Vogel B, van Schijndel GM, van Lier RA. The seven-span transmembrane receptor CD97 has a cellular ligand (CD55, DAF). J Exp Med 1996; 184: 1185–9.
57 Hamann J, Stortelers C, Kiss-Toth E, Vogel B, Eichler W, van Lier RA. Characterization of the CD55 (DAF)-binding site on the seven-span transmembrane receptor CD97. Eur J Immunol 1998; 28: 1701–7.
58 Abbott RJ, Spendlove I, Roversi P, Fitzgibbon H, Knott V, Teriete P, *et al*. Structural and functional characterization of a novel T cell receptor co-regulatory protein complex, CD97–CD55. J Biol Chem 2007; 282: 22023–32.
59 Capasso M, Durrant LG, Stacey M, Gordon S, Ramage J, Spendlove I. Costimulation via CD55 on human CD4+ T cells mediated by CD97. J Immunol 2006; 177: 1070–7.
60 Matmati M, Pouwels W, van Bruggen R, Jansen M, Hoek RM, Verhoeven AJ, *et al*. The human EGF-TM7 receptor EMR3 is a marker for mature granulocytes. J Leukoc Biol 2007; 81: 440–8.
61 Stacey M, Lin HH, Hilyard KL, Gordon S, McKnight AJ. Human epidermal growth factor (EGF) module-containing mucin-like hormone receptor 3 is a new member of the EGF-TM7 family that recognizes a ligand on human macrophages and activated neutrophils. J Biol Chem 2001; 276: 18863–70.
62 Stacey M, Chang GW, Sanos SL, Chittenden LR, Stubbs L, Gordon S, *et al*. EMR4, a novel epidermal growth factor (EGF)-TM7 molecule up-regulated in activated mouse macrophages, binds to a putative cellular ligand on B lymphoma cell line A20. J Biol Chem 2002; 277: 29283–93.
63 Formstone CJ. 7TM-Cadherins: developmental roles and future challenges. Adv Exp Med Biol 2010; 706: 14–36.
64 Lawrence PA, Casal J, Struhl G. Cell interactions and planar polarity in the abdominal epidermis of *Drosophila*. Development 2004; 131: 4651–64.
65 Grueber WB, Jan LY, Jan YN. Tiling of the Drosophila epidermis by multidendritic sensory neurons. Development 2002; 129: 2867–78.
66 Sweeney NT, Li W, Gao FB. Genetic manipulation of single neurons *in vivo* reveals specific roles of flamingo in neuronal morphogenesis. Dev Biol 2002; 247: 76–88.
67 Chen PL, Clandinin TR. The cadherin Flamingo mediates level-dependent interactions that guide photoreceptor target choice in *Drosophila*. Neuron 2008; 58: 26–33.
68 Steinel MC, Whitington PM. The atypical cadherin Flamingo is required for sensory axon advance beyond intermediate target cells. Dev Biol 2009; 327: 447–57.
69 Bao H, Berlanga ML, Xue M, Hapip SM, Daniels RW, Mendenhall JM, *et al*. The atypical cadherin flamingo regulates synaptogenesis and helps prevent axonal and synaptic degeneration in *Drosophila*. Mol Cell Neurosci 2007; 34: 662–78.
70 Curtin JA, Quint E, Tsipouri V, Arkell RM, Cattanach B, Copp AJ, *et al*. Mutation of Celsr1 disrupts planar polarity of inner ear hair cells and causes severe neural tube defects in the mouse. Curr Biol 2003; 13: 1129–33.
71 Carreira-Barbosa F, Kajita M, Morel V, Wada H, Okamoto H, Martinez Arias A, *et al*. Flamingo regulates epiboly and convergence/extension movements through cell cohesive and signalling functions during zebrafish gastrulation. Development 2009; 136: 383–92.
72 Ciruna B, Jenny A, Lee D, Mlodzik M, Schier AF. Planar cell polarity signalling couples cell division and morphogenesis during neurulation. Nature 2006; 439: 220–4.
73 Ravni A, Qu Y, Goffinet AM, Tissir F. Planar cell polarity cadherin Celsr1 regulates skin hair patterning in the mouse. J Invest Dermatol 2009; 129: 2507–9.
74 Monk KR, Naylor SG, Glenn TD, Mercurio S, Perlin JR, Dominguez C, *et al*. A G protein-coupled receptor is essential for Schwann cells to initiate myelination. Science 2009; 325: 1402–5.
75 Kuhnert F, Mancuso MR, Shamloo A, Wang HT, Choksi V, Florek M, *et al*. Essential regulation of CNS angiogenesis by the orphan G protein-coupled receptor GPR124. Science 2010; 330: 985–9.
76 Anderson KD, Pan L, Yang XM, Hughes VC, Walls JR, Dominguez MG, *et al*. Angiogenic sprouting into neural tissue requires Gpr124, an orphan G protein-coupled receptor. Proc Natl Acad Sci U S A 2011; 108: 2807–12.
77 Monk KR, Oshima K, Jors S, Heller S, Talbot WS. Gpr126 is essential for peripheral nerve development and myelination in mammals. Development 2011; 138: 2673–80.
78 Davies JQ, Lin HH, Stacey M, Yona S, Chang GW, Gordon S, *et al*. Leukocyte adhesion-GPCR EMR2 is aberrantly expressed in human breast carcinomas and is associated with patient survival. Oncol Rep 2011; 25: 619–27.
79 Galle J, Sittig D, Hanisch I, Wobus M, Wandel E, Loeffler M, *et al*. Individual cell-based models of tumor-environment interactions: Multiple effects of CD97 on tumor invasion. Am J Pathol 2006; 169: 1802–11.
80 Katoh M. WNT/PCP signaling pathway and human cancer (review). Oncol Rep 2005; 14: 1583–8.
81 Xu L, Begum S, Hearn JD, Hynes RO. GPR56, an atypical G protein-coupled receptor, binds tissue transglutaminase, TG2, and inhibits melanoma tumor growth and metastasis. Proc Natl Acad Sci U S A 2006; 103: 9023–8.
82 Xu L, Begum S, Barry M, Crowley D, Yang L, Bronson RT, *et al*. GPR56 plays varying roles in endogenous cancer progression. Clin Exp Metastasis 2010; 27: 241–9.
83 Mizuno N, Itoh H. Signal transduction mediated through adhesion-GPCRs. Adv Exp Med Biol 2010; 706: 157–66.
84 Park D, Tosello-Trampont AC, Elliott MR, Lu M, Haney LB, Ma Z, *et al*. BAI1 is an engulfment receptor for apoptotic cells upstream of the ELMO/Dock180/Rac module. Nature 2007; 450: 430–4.
85 Abe J, Fukuzawa T, Hirose S. Cleavage of Ig-Hepta at a "SEA" module and at a conserved G protein-coupled receptor proteolytic site. J Biol Chem 2002; 277: 23391–8.
86 Abe J, Suzuki H, Notoya M, Yamamoto T, Hirose S. Ig-hepta, a novel member of the G protein-coupled hepta-helical receptor (GPCR) family that has immunoglobulin-like repeats in a long N-terminal extracellular domain and defines a new subfamily of GPCRs. J Biol Chem 1999; 274: 19957–64.
87 Fukuzawa T, Hirose S. Multiple processing of Ig-Hepta/GPR116, a G protein-coupled receptor with immunoglobulin (Ig)-like repeats, and generation of EGF2-like fragment. J Biochem 2006; 140: 445–52.
88 Lelianova VG, Davletov BA, Sterling A, Rahman MA, Grishin EV, Totty NF, *et al*. Alpha-latrotoxin receptor, latrophilin, is a novel member of the secretin family of G protein-coupled receptors. J Biol Chem 1997; 272: 21504–8.
89 Little KD, Hemler ME, Stipp CS. Dynamic regulation of a GPCR-tetraspanin-G protein complex on intact cells: central role of CD81 in facilitating GPR56-Galpha q/11 association. Mol Biol Cell 2004; 15: 2375–87.
90 Iguchi T, Sakata K, Yoshizaki K, Tago K, Mizuno N, Itoh H. Orphan G protein-coupled receptor GPR56 regulates neural progenitor cell migration via a G alpha 12/13 and Rho pathway. J Biol Chem 2008; 283: 14469–78.
91 Lappano R, Maggiolini M. G protein-coupled receptors: novel targets for drug discovery in cancer. Nat Rev Drug Discov 2011; 10: 47–60.
92 Crouch MF, Osmond RI. New strategies in drug discovery for GPCRs:

high throughput detection of cellular ERK phosphorylation. Comb Chem High Throughput Screen 2008; 11: 344–56.
93 Bikkavilli RK, Tsang SY, Tang WM, Sun JX, Ngai SM, Lee SS, *et al*. Identification and characterization of surrogate peptide ligand for orphan G protein-coupled receptor mas using phage-displayed peptide library. Biochem Pharmacol 2006; 71: 319–37.
94 Overton HA, Babbs AJ, Doel SM, Fyfe MC, Gardner LS, Griffin G, *et al*. Deorphanization of a G protein-coupled receptor for oleoylethanolamide and its use in the discovery of small-molecule hypophagic agents. Cell Metab 2006; 3: 167–75.
95 Pausch MH. G-protein-coupled receptors in Saccharomyces cerevisiae: high-throughput screening assays for drug discovery. Trends Biotechnol 1997; 15: 487–94.
96 Bates B, Zhang L, Nawoschik S, Kodangattil S, Tseng E, Kopsco D, *et al*. Characterization of Gpr101 expression and G-protein coupling selectivity. Brain Res 2006; 1087: 1–14.
97 Suga H, Haga T. Ligand screening system using fusion proteins of G protein-coupled receptors with G protein alpha subunits. Neurochem Int 2007; 51: 140–64.
98 Howard AD, McAllister G, Feighner SD, Liu Q, Nargund RP, Van der Ploeg LH, *et al*. Orphan G-protein-coupled receptors and natural ligand discovery. Trends Pharmacol Sci 2001; 22: 132–40.
99 Okamoto H, Takuwa N, Yatomi Y, Gonda K, Shigematsu H, Takuwa Y. EDG3 is a functional receptor specific for sphingosine 1-phosphate and sphingosylphosphorylcholine with signaling characteristics distinct from EDG1 and AGR16. Biochem Biophys Res Commun 1999; 260: 203–8.
100 An S, Zheng Y, Bleu T. Sphingosine 1-phosphate-induced cell proliferation, survival, and related signaling events mediated by G protein-coupled receptors Edg3 and Edg5. J Biol Chem 2000; 275: 288–96.
101 Pyne S, Pyne NJ. Sphingosine 1-phosphate signalling in mammalian cells. Biochem J 2000; 349: 385–402.
102 Lovenberg TW, Roland BL, Wilson SJ, Jiang X, Pyati J, Huvar A, *et al*. Cloning and functional expression of the human histamine H3 receptor. Mol Pharmacol 1999; 55: 1101–7.
103 Oda T, Morikawa N, Saito Y, Masuho Y, Matsumoto S. Molecular cloning and characterization of a novel type of histamine receptor preferentially expressed in leukocytes. J Biol Chem 2000; 275: 36781–6.
104 Maenhaut C, Van Sande J, Libert F, Abramowicz M, Parmentier M, Vanderhaegen JJ, *et al*. RDC8 codes for an adenosine A2 receptor with physiological constitutive activity. Biochem Biophys Res Commun 1990; 173: 1169–78.
105 Libert F, Schiffmann SN, Lefort A, Parmentier M, Gerard C, Dumont JE, *et al*. The orphan receptor cDNA RDC7 encodes an A1 adenosine receptor. EMBO J 1991; 10: 1677–82.
106 de Lecea L, Kilduff TS, Peyron C, Gao X, Foye PE, Danielson PE, *et al*. The hypocretins: hypothalamus-specific peptides with neuroexcitatory activity. Proc Natl Acad Sci U S A 1998; 95: 322–7.
107 Hinuma S, Habata Y, Fujii R, Kawamata Y, Hosoya M, Fukusumi S, *et al*. A prolactin-releasing peptide in the brain. Nature 1998; 393: 272–6.
108 Sakurai T, Amemiya A, Ishii M, Matsuzaki I, Chemelli RM, Tanaka H, *et al*. Orexins and orexin receptors: a family of hypothalamic neuropeptides and G protein-coupled receptors that regulate feeding behavior. Cell 1998; 92: 573–85.
109 Tatemoto K, Hosoya M, Habata Y, Fujii R, Kakegawa T, Zou MX, *et al*. Isolation and characterization of a novel endogenous peptide ligand for the human APJ receptor. Biochem Biophys Res Commun 1998; 251: 471–6.
110 Lin HH, Chang GW, Huang YS, Hsiao CC, Stacey M, Gordon S. Multivalent protein probes for the identification and characterization of cognate cellular ligands for myeloid cell surface receptors. Methods Mol Biol 2009; 531: 89–101.
111 Libert F, Vassart G, Parmentier M. Current developments in G-protein-coupled receptors. Curr Opin Cell Biol 1991; 3: 218–23.
112 Mills A, Duggan MJ. Orphan seven transmembrane domain receptors: reversing pharmacology. Trends Biotechnol 1994; 12: 47–9.
113 Ozawa A, Lindberg I, Roth B, Kroeze WK. Deorphanization of novel peptides and their receptors. AAPS J 2010; 12: 378–84.
114 Marchese A, George SR, Kolakowski LF Jr, Lynch KR, O'Dowd BF. Novel GPCRs and their endogenous ligands: expanding the boundaries of physiology and pharmacology. Trends Pharmacol Sci 1999; 20: 370–5.
115 Lerner MR. Tools for investigating functional interactions between ligands and G-protein-coupled receptors. Trends Neurosci 1994; 17: 142–6.
116 Wise A, Jupe SC, Rees S. The identification of ligands at orphan G-protein coupled receptors. Annu Rev Pharmacol Toxicol 2004; 44: 43–66.
117 McLatchie LM, Fraser NJ, Main MJ, Wise A, Brown J, Thompson N, *et al*. RAMPs regulate the transport and ligand specificity of the calcitonin-receptor-like receptor. Nature 1998; 393: 333–9.
118 Hay DL, Poyner DR, Sexton PM. GPCR modulation by RAMPs. Pharmacol Ther 2006; 109: 173–97.
119 Galvez T, Duthey B, Kniazeff J, Blahos J, Rovelli G, Bettler B, *et al*. Allosteric interactions between GB1 and GB2 subunits are required for optimal $GABA_B$ receptor function. EMBO J 2001; 20: 2152–9.
120 Jones KA, Borowsky B, Tamm JA, Craig DA, Durkin MM, Dai M, *et al*. $GABA_B$ receptors function as a heteromeric assembly of the subunits $GABA_BR1$ and $GABA_BR2$. Nature 1998; 396: 674–9.
121 Robbins MJ, Calver AR, Filippov AK, Hirst WD, Russell RB, Wood MD, *et al*. $GABA_{B2}$ is essential for g-protein coupling of the $GABA_B$ receptor heterodimer. J Neurosci 2001; 21: 8043–52.
122 Lagerstrom MC, Schioth HB. Structural diversity of G protein-coupled receptors and significance for drug discovery. Nat Rev Drug Discov 2008; 7: 339–57.

Acta Pharmacologica Sinica (2012) 33: 372–384
 1671-4083/12
www.nature.com/aps

Open
Review

Tools for GPCR drug discovery

Ru ZHANG[1], Xin XIE[1, 2, *]

[1]*Shanghai Key Laboratory of Signaling and Disease Research, Laboratory of Receptor-based Bio-medicine, School of Life Sciences and Technology, Tongji University, Shanghai 200092, China;* [2]*State Key Laboratory of Drug Research, the National Center for Drug Screening, Shanghai Institute of Materia Medica, Chinese Academy of Sciences, Shanghai 201203, China*

G-protein-coupled receptors (GPCRs) mediate many important physiological functions and are considered as one of the most successful therapeutic targets for a broad spectrum of diseases. The design and implementation of high-throughput GPCR assays that allow the cost-effective screening of large compound libraries to identify novel drug candidates are critical in early drug discovery. Early functional GPCR assays depend primarily on the measurement of G-protein-mediated 2nd messenger generation. Taking advantage of the continuously deepening understanding of GPCR signal transduction, many G-protein-independent pathways are utilized to detect the activity of GPCRs, and may provide additional information on functional selectivity of candidate compounds. With the combination of automated imaging systems and label-free detection systems, such assays are now suitable for high-throughput screening (HTS). In this review, we summarize the most widely used GPCR assays and recent advances in HTS technologies for GPCR drug discovery.

Keywords: G-protein-coupled receptors (GPCRs); high-throughput screening; high-content screening; functional assay; G-protein-dependent assay; G-protein-independent assay; label-free assay; functional selectivity

Acta Pharmacologica Sinica (2012) 33: 372–384; doi: 10.1038/aps.2011.173; published online 23 Jan 2012

Introduction

G-protein-coupled receptors (GPCRs), also known as 7 transmembrane receptors, are the largest family of cell surface receptors and account for approximately 4% of the protein-coding human genome[1]. They are activated by a wide variety of stimulants, including light, odorant molecules, peptide and non-peptide neurotransmitters, hormones, growth factors and lipids, and control a wide variety of physiological processes including sensory transduction, cell–cell communication, neuronal transmission, and hormonal signaling.

After agonist binding, activated receptors catalyze the exchange of guanidine diphosphate (GDP) for guanidine triphosphate (GTP) on the α-subunit of heterotrimeric G proteins (composed of α-, β-, and γ-subunits), which in turn engages conformational changes that lead to the dissociation of Gα from the dimeric Gβγ subunits[2]. GPCRs coupled to $G\alpha_s$ and $G\alpha_{i/o}$ proteins activate or inhibit, respectively, adenylate cyclase, the enzyme responsible for converting adenosine triphosphate (ATP) to 3′,5′-cyclic adenosine monophosphate (cAMP). cAMP serves as a second messenger that activates protein kinase A (PKA) and other downstream effectors (previously reviewed[3]). GPCRs coupled to $G\alpha_{q/o}$ alternatively activate phospholipase Cβ (PLCβ), which catalyzes the formation of diacylglycerol (DAG) and inositol-1,4,5-trisphosphate (IP_3). IP_3 then binds and opens the endoplasmic IP3-gated calcium channel, causing the release of calcium into the cytoplasm. GPCRs coupling to $G\alpha_{12/13}$ further activate the guanine nucleotide exchange factor RhoGEF, which in turn activates the small G protein RhoA.

In the presence of continuous agonist stimulation, GPCRs are phosphorylated by specific GPCR kinases (GRKs), and the recruitment of β-arrestins to the phosphorylated GPCRs eventually terminates G protein signaling and leads to a coordinated process of receptor desensitization, inactivation and internalization[3]. The β-arrestins also facilitate the formation of multi-molecular complexes and provide a means for G protein-independent signaling of GPCRs, including those involving mitogen-activated protein (MAP) kinases, receptor and non-receptor tyrosine kinases, phosphatidylinositol 3-kinases (PI3K) and others[4].

Given their importance in health and disease, together with their potential for therapeutic intervention via using small molecules as regulators, GPCRs represent the largest family of druggable targets. These receptors are the target of >50% of the current therapeutic agents on the market, including more than a quarter of the 100 top-selling drugs, with profits in the range of several billion US dollars each year[5]. Therefore, GPCR assay development and GPCR ligand screening remain

* To whom correspondence should be addressed.
E-mail xxie@mail.shcnc.ac.cn
Received 2011-09-30 Accepted 2011-11-15

the major focus of drug discovery research worldwide. Historically, radioligand binding assays with receptor-containing membranes were used to identify compounds that target GPCRs. However, binding affinity data do not tell us whether the compound is an agonist or an antagonist, or more importantly, the overall potency of a compound under physiological conditions. Efforts have been made in the past few decades to develop signaling-dependent cell-based functional assays to provide more accurate and comprehensive data of the compounds targeting GPCRs.

An ideal assay for GPCR ligand screening should be simple, nonradioactive, robust, homogenous, and easily adapted to a microtiter plate format (96-, 384-, or 1536-well) for robotic automation. Since GPCR signaling consists of a series of spatial and temporal events, another important consideration is whether to measure a proximal or distal signaling step after GPCR stimulation. Measurement of events proximal to receptor activation will reduce the incidence of false positives[6]; however, moving down the signal transduction cascade will enhance the signal-to-noise ratio due to signal amplification. Many GPCRs also activate multiple signaling pathways. Biased signaling, a phenomenon in which certain agonists display better efficacies in activating one pathway over others, is another critical issue to consider in functional screen development[4, 7]. If a functional assay capturing only one signaling pathway is selected for screening compound libraries, potentially valuable compounds could be missed if the compound does display biased activity. Therefore, multiplexing of signaling pathways or assays representing an overall cellular response may be used to resolve such problems. In this review, we summarize the most widely used GPCR assays and recent advances in high-throughput screening (HTS) technology for GPCR drug discovery (Table 1).

Receptor binding assay

Receptor binding assay can be used to characterize in great detail the interaction between receptor and its ligands, such as the intrinsic affinity of ligands to the receptor, association/dissociation rates, and the density of receptor in tissues or cells[8]. Receptor binding assay is a cell-free method theoretically suitable for any GPCR screening without involving downstream signaling from the receptor. This type of assay can also obtain agonists and antagonists in one experiment, but without distinguishing whether the candidate compound is an agonist, antagonist, or inverse agonist. However, the availability of labeled ligands greatly limits the application of this assay. It is practically useless for GPCR deorphanization.

The first radioligand binding assay was performed in 1970 by Lefkowitz *et al* using a radiolabeled hormone to determine the binding affinity for its receptor[9]. Since then, ^{3}H- or ^{125}I-labeled ligands have been widely used to characterize the affinity of a compound for a target GPCR, while nonlabeled compounds can be characterized by their ability to displace the binding of a radiolabeled molecule to the target (orthosteric agonists/antagonists) or to modulate the affinity of a radiolabeled molecule for the target (some allosteric modulators)[10]. The traditional radioligand binding assays require washing and filtration steps, which can only be scaled down to a 96-well format.

A homogenous scintillation proximity assay (SPA), which can be easily scaled down and automated for HTS applications, was developed more recently (reviewed in[11]). In SPA, only the radiolabeled molecules binding to the GPCR immobilized on the surface of SPA beads can activate the scintillation beads, which produce photons detectable with a scintillation counter. SPA thus allows binding reactions to be tested without washing or filtration steps. Although radioligand binding gives a clear, unmistakable signal, radioligands are relatively expensive, problematic to dispose of, and some isotopes have inconveniently short half-lives. These drawbacks have led to the creation of highly sensitive nonradioactive alternatives.

Many new binding assays are based on time-resolved fluorescence resonance energy transfer (TR-FRET) technology, such as DELFIA™ TRF from PerkinElmer, the LanthaScreen™ system from Invitrogen, and the Tag-lite™ system from Cisbio. Tag-lite™ is a newly developed homogeneous time-resolved fluorescence (HTRF) technology[12] for assaying GPCR ligand binding in HTS format. A suicide enzyme (either SNAP- or CLIP-tag) is fused to the N-terminus of a GPCR without affecting its binding and activity, and a non-permeant substrate labeled with terbium cryptate fluorophore (Lumi4-Tb) is used to specifically and covalently label the receptors expressed on the cell surface. The ligands are labeled with red or green acceptors. The long fluorescence lifetime of the terbium cryptate allows a time-resolved measurement of FRET emission when all natural fluorescence disappears. The assay is carried out in a "mix and measure" format, which can be used not only for ligand binding studies but also for receptor activity analysis and GPCR dimerization assessment (as discussed below). The availability of Tagged-GPCR expressing cell lines and the fluorophore-labeled ligands are some of the limitations in this approach.

G-protein dependent functional assays

Ligand-binding assays are useful to identify new compounds that target GPCRs. Further analysis of the biological responses after compound binding will help complete the whole picture concerning the overall characteristics of the compound. Upon ligand binding, GPCRs change their conformation and activate coupled G proteins, which subsequently promote second messenger production via downstream effectors. The corresponding assays measuring either G protein activation or G protein-mediated events, including second messenger generation and reporter activation, are therefore defined as G-protein-dependent functional assays (Figure 1).

GTPγS binding assay

GTPγS binding assays directly measure the guanine nucleotide exchange of G proteins, an early event after GPCR activation, which is not subjected to amplification or regulation by other cellular processes[6]. Typically, the accumulation of non-hydrolysable GTP analog, such as [^{35}S]-GTPγS, on the plasma

Table 1. Summary of GPCR screening technologies.

Assay classification	Commonly used assays	Commercial HTS Technology (Company)	Pros	Cons	Suitable GPCRs
Receptor binding assay	Radioligand binding assay	• Filtration assay (PerkinElmer) • SPA (GE Healthcare or PerkinElmer)	High-throughput; less interference; obtain agonist and antagonist in one assay	Availability of radioligand; generation of radioactive waste; need secondary functional assay	any GPCR
	Other tagged-ligand binding	• DELFIA™ TRF (PerkinElmer); • LanthaScreen™ system (Invitrogen); • Tag-lite™ system (Cisbio)	Non-radioactive; high-throughput; obtain agonist and antagonist in one assay	Availability of tagged-ligand; need secondary functional assay	any GPCR
G-protein dependent assays	GTPγS binding	• Filtration assay (PerkinElmer) • SPA (GE Healthcare or PerkinElmer) • DELFIA™ GTP Binding Assay (PerkinElmer)	Functional cell-free assay; discrimination between full or partial agonists, neutral antagonists, inverse agonists, allosteric regulators	Relatively low signal to background window	$G\alpha_{i/o}$
	CRE/MRE reporter assay		Homogenous assay; high-throughput; large signal to background window	Need to know the coupling mechanism, not good for orphan GPCR	any GPCR
	cAMP assay	• SPA cAMP assay (GE Healthcare or PerkinElmer) • HitHunter™ (DiscoveRx); • AlphaScreen™ (PerkinElmer); • Fluorescence polarization-based cAMP kits (PerkinElmer, Molecular Devices and GE Healthcare); • HTRF™-based cAMP (Cisbio); • cAMP Glosensor™ (Promega)	High-throughput; very sensitive	Need to know the coupling mechanism, not good for orphan GPCR	$G\alpha_s$, $G\alpha_{i/o}$
	Ca^{2+}	• Fluo-3 or Fluo-4 (Invitrogen) and FLIPR™ automated real-time fluorescence plate readers (Molecular Device)	High-throughput; functional assay for live cells; obtain agonist, antagonist and allosteric modulator in one assay	Fluorescent interference from compounds; not good for inverse agonist and slow binding agonist	$G\alpha_q$ (with $G\alpha_{15/16}$, could be universal)
	$IP_{1/3}$	• SPA IP_3 assay (PerkinElmer) • AlphaScreen™ (PerkinElmer); • HitHunter™ Fluorescence Polarization (DiscoveRx); • HTRF IP-One™ (Cisbio)	High-throughput; functional assay for live cells; good for slow binding ligands	Limited industrial validation	$G\alpha_q$ (with $G\alpha_{15/16}$, could be universal)
G-protein independent assays	Receptor trafficking	• Cellomics ArrayScan™ (Thermo Scientificf); • INCell™ Analyzer 3000 (GE Healthcare); • Opera™ (Evotec Technologies); • Acumen™ Explorer (TTP Lab Tech)	Image based, high-content; functional assay for live cells; generic method for all GPCRs	Image based, relatively low throughput	any GPCR
	β-Arrestin recruitment assay	• Transfluor™(Molecular Device); • BRET/FRET • Tango™ (Invitrogen); • PathHunter™ (DiscoveRx);	High-throughput; image or non-image based; functional assay for live cells; useful in biased signal detection; generic method for all GPCRs	Affinity for β-arrestin binding varies amone GPCRs; less sensitive; need further pathway analysis	any GPCR
	Label-free assay	• BIND™ RWG biosensors (SRU Biosystems) • Epic™ RWG biosensors systems (Corning Inc); • ECIS™ (Applied Biophysics); • xCELLigence™ System (Roche and ACEA Biosciences) • CellKey™ (MDS)	Label-free functional assay in native live cells; summation of all cellular events	Possibly higher false positive and false negative rates; need special instrument and costly microplate; need further pathway analysis	any GPCR
Receptor dimerization assay		• BRET/FRET; • PathHunter™ (DiscoveRx); • Tag-lite™ (Cisbio)	GPCR heterodimers are considered new pharmacological targets	Very artificial system, can not assess GPCR dimerization in native state	any GPCR

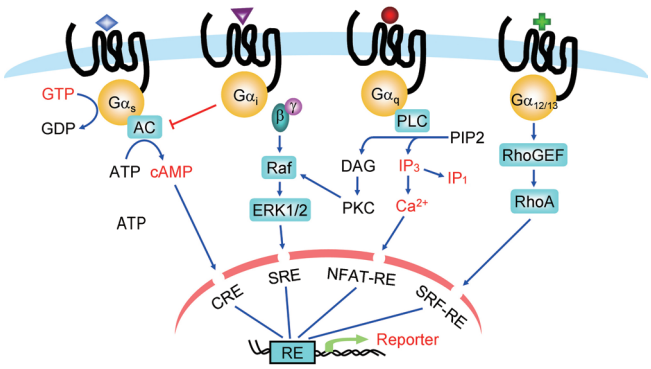

Figure 1. Receptor binding and G-protein-dependent assays. Schematic representation of receptor binding and major pathways activated by different G proteins. Red indicates the detection points of commonly used HTS assays: GTPγS binding, cAMP detection, IP_3/IP_1 detection, Ca^{2+} flux and reporter expression.

membrane prepared from cells expressing GPCRs of interest is measured after agonist stimulation. Unlike receptor binding assays, the GTPγS binding assay allows discrimination between full or partial agonists, neutral antagonists, inverse agonists, and allosteric regulators[13]. In reality, this assay is experimentally more feasible for receptors coupled to $G\alpha_{i/o}$, which is the most abundant G protein in many cells and has a faster GDP-GTP exchange rate than other G proteins[6]. Nevertheless, [^{35}S]-GTPγS binding assays can also be used with GPCRs that couple to the $G\alpha_s$ and $G\alpha_q$ families of G proteins, especially in artificial expression systems, or using receptor-Gα chimeras, or by immunoprecipitation of [^{35}S]-GTPγS-labeled Gα (reviewed in[13]). A problem with this assay is that it requires a filtration step through glass fiber to separate free and bound [^{35}S]-GTPγS, which limits assay throughput. With the development of SPA technology, the filtration step can be omitted and GTPγS binding assays can be adopted for high-throughput screening[14, 15].

With the increased desire to move assays to a non-radioactive format, a GTP binding assay based on time-resolved fluorescence (TRF) technology utilizing a non-radioactive, non-hydrolysable, europium-labeled GTP analog, GTP-Eu, has been developed for GPCR screening (DELFIA™ GTP binding assay from PerkinElmer)[16]. However, this assay still requires filtration and washing steps. The DELFIA™ GTP binding assay has been validated on several GPCRs, including α2-adrenergic[17], neuropeptide FF2 receptor[18], dopamine D3 receptor[19] and muscarinic receptors[20], and the results are comparable with those obtained using traditional [^{35}S]-GTPγS binding assays[21].

cAMP assay

Assays measuring cellular levels of cAMP are dependent on the activity of adenylyl cyclase, which is regulated by GPCRs coupled to $G\alpha_s$ or $G\alpha_{i/o}$ protein. $G\alpha_s$ positively stimulates the activity of adenylate cyclase, resulting in increased cellular cAMP. In contrast, activation of $G\alpha_i$ leads to a negative regulation of adenylate cyclase and a decrease in cAMP levels. Screening $G\alpha_s$-coupled receptors is generally straightforward, whereas screening $G\alpha_{i/o}$-coupled receptors, especially for $G\alpha_{i/o}$-coupled receptor antagonists, could be extremely difficult to achieve with high precision using cAMP detection methods. This difficulty arises because of the requirement to pre-stimulate adenylate cyclase with forskolin, which should be titrated during assay optimization, to inhibit the response with agonist and then measure reversal of the agonist effect with antagonists. In addition, to counteract the natural degradation of cAMP to AMP by phosphodiesterase (PDE) enzymes, an inhibitor of PDE (*eg*, IBMX) might be required in the system during assay optimization. cAMP levels are typically measured using a competition assay in which cellular cAMP competes with an introduced, labeled form of cAMP for binding to an anti-cAMP antibody.

Radiometric assays, such as the SPA cAMP assay from GE Healthcare and the FlashPlate™ cAMP assay from PerkinElmer using ^{125}I-labeled cAMP, are widely used. More recently, these assays have been replaced with fluorescence- or luminescence-based homogenous assays to avoid the use of radioactivity. There are several newer radio-free approaches for cAMP detection. One such assay is based on Enzyme Fragment Complementation (HitHunter™) and was introduced by DiscoveRx (http://www.discoverx.com). Cellular cAMP competes with cAMP labeled with a small peptide fragment of β-galactosidase for binding to an anti-cAMP antibody. The resulting free labeled-cAMP complements with the enzyme fragment, producing active β-galactosidase, which is detected with fluorescent or luminescent substrates[22, 23]. AlphaScreen™ from PerkinElmer is a sensitive bead-based proximity chemiluminescent assay. Cellular cAMP competes with a biotinylated cAMP probe recognized by a streptavidin donor and anti-cAMP antibody-conjugated acceptor beads. Release of the biotinylated cAMP from the antibody results in the dissociation of the streptavidin donor from its acceptor, which can be measured as a decrease in the chemiluminescent signal (http://www.perkinelmer.com). In addition, fluorescence polarization (FP)-based cAMP kits are available from PerkinElmer, Molecular Devices and GE Healthcare. When exposed to polarized light, the emission from an antibody-bound fluorescent-labeled cAMP is also polarized due to restricted molecular rotation. When the labeled cAMP is replaced on the antibody by cellular cAMP, the emission becomes more depolarized because it can rotate freely in solution. With the availability of red-shifted fluorophores, the signal-to-noise ratios have been greatly improved[24]. Furthermore, HTRF-based cAMP detection is available from Cisbio. With this method, novel donor (cAMP antibody labeled with europium cryptate) and acceptor (cAMP labeled with a modified allophycocyanin dye) pairs are designed to increase the stability of the signal and make this assay highly sensitive and reproducible for cAMP measurement[12]. Finally, the cAMP Glosensor™ assay is a luciferase biosensor-based assay from Promega[25]. Upon cAMP binding, the conformational change in the biosensor leads to the activation of luciferase and increased light output.

This type of assay can be used to measure GPCR function in a non-lytic live-cell format, enabling facile kinetic measurements of cAMP accumulation or turnover in living cells. The assay also offers a broad dynamic range, showing up to 500-fold changes in light output. Extreme sensitivity allows the detection of $G\alpha_i$-coupled receptor activation or inverse agonist activity in the absence of artificial stimulation by compounds such as forskolin (http://www.promega.com/glosensor). A direct comparison of AlphaScreen™, HTRF, HitHunter™, and FP cAMP assays suggests that there are advantages and disadvantages in each method[26]. The AlphaScreen™ and HTRF assays are recommended for cells expressing low levels of GPCRs because of their higher sensitivities.

IP_3/IP_1 and Ca^{2+} assays

Stimulation of $G\alpha_q$ or $G\alpha_i$ coupled-GPCRs activates phospholipase C (PLC), which hydrolyzes phosphatidylinositol bisphosphate (PIP_2) to form two second messengers, inositol 1,4,5-triphosphate (IP_3) and DAG. While DAG activates protein kinase C (PKC), IP_3 activates the IP_3 receptor on the endoplasmic reticulum (ER) resulting in an efflux of Ca^{2+} from the ER to the cytoplasm and an elevation of intracellular Ca^{2+}. IP_3 is very rapidly hydrolyzed to IP_2, then to IP_1 and finally to inositol by a series of enzymatic reactions[27]. The radioactive IP_3 assay measures ^{3}H-inositol incorporation and is a traditional assay for the assessment of PLC activity, but it is not suitable for the screening of large compound collections because it requires a cell wash step and generates radioactive waste. An SPA platform has been developed to achieve higher throughput and homogenous assays in measuring IP accumulation.

There are a few non-radiometric technologies used for the measurement of IP_3, including AlphaScreen™ (PerkinElmer) and HitHunter™ Fluorescence Polarization (DiscoveRx) assay. Recently, a homogeneous, non-radioactive TRF assay for measuring IP accumulation, IP-One HTRF™, was released by Cisbio (http://www.htrf.com). The basis for the assay is a reduction in energy transfer between acceptor IP_1 and a europium-conjugated IP_1 antibody as cellular IP_1 accumulates and replaces the acceptor IP_1 in binding the IP_1 antibody. Compared to earlier kits using IP_3-binding proteins to specifically measure IP_3, the IP-One assay takes advantage of the fact that LiCl inhibits the degradation of IP_1, the final step in the inositol phosphate cascade, allowing it to accumulate in the cell and to be measured as a substitute for IP_3. This assay also does not require a kinetic readout. Data reported by Cisbio show that the assay can be used with endogenously or heterologously expressed GPCRs in either adherent or suspension cells to quantitate the activity of agonists, antagonists, and inverse agonists. Additionally, the efficacy data from the IP-One assay correlate well with those from calcium assays and traditional IP_3 assays (http://www.htrf.com). This assay can be adopted for ultra high-throughput screening in the 1536-well plate format and has been tested with cell lines expressing M_1 acetylcholine, FFAR1, vasopressin V1b, and neuropeptide S receptors[28].

As previously mentioned, intracellular Ca^{2+} is another second messenger for GPCR signaling. GPCRs that naturally couple to $G\alpha_q$ produce a ligand-dependent increase in intracellular Ca^{2+}. However, $G\alpha_{i/o}$, $G\alpha_s$, or $G\alpha_{12}$-coupled GPCRs can also be "switched" to induce an increase in intracellular Ca^{2+} either by the expression of a chimeric G-protein ($G\alpha_{qi5}$ or $G\alpha_{qo5}$) or a promiscuous G-protein ($G\alpha_{16}$ or $G\alpha_{15}$) (reviewed in[29]). The Ca^{2+} assay is very popular in GPCR screening owing to the availability of cell-permeable Ca^{2+}-sensitive fluorescent dyes (such as Fluo-3 and Fluo-4) and automated real-time fluorescence plate readers, such as FLIPR™ from Molecular Device. Molecular Device also offers fluorescent dye kits, which contain proprietary quenching molecules that allow cellular loading of dye without the need of subsequent cell washing to remove excess dye[30]. The integrated pipetting capabilities of the FLIPR™ allow ultra high-throughput screening in 384- or 1536-well format with the ability to detect agonists, antagonists, and allosteric modulators all in one assay. The use of fluorescent dyes can also be replaced by the use of Ca^{2+}-sensitive biosensors. Recombinant expression of the jellyfish photoprotein aequorin, which provides an intense luminescent signal in response to elevated intracellular Ca^{2+} in the presence of a coelenterazine derivative, has also been developed for functional screens of GPCRs[31]. With the overexpression of promiscuous G-proteins, the Ca^{2+} assay does not require the prior knowledge of G protein coupling conditions and signaling pathways of the receptor, so it is widely used to de-orphan GPCRs[32, 33].

Although Ca^{2+} assays are robust and easily amenable to HTS, there are some important shortcomings. They cannot be used to screen for inverse agonists because increases in basal Ca^{2+} are not observed in cells expressing constitutively active $G\alpha_q$-coupled receptors. In addition, calcium flux occurs rapidly and transiently and is not suitable to detect slow binding agonists. In such conditions, an IP_1 accumulation assay will be more useful. Furthermore, false positive signals obtained from fluorescent and nuisance compounds are a problem, and the sensitivity is often insufficient to allow the use of primary cells.

Reporter assay

GPCR activation is well known to alter gene transcription via responsive elements for second messengers including the cAMP response element (CRE), the nuclear factor of activated T-cells response element (NFAT-RE), the serum response element (SRE) and the serum response factor response element (SRF-RE, a mutant form of SRE), all of which are located within the gene promoter regions (reviewed in[34]). Therefore, cell-based reporter assays provide another popular and cost-effective HTS platform for GPCR screening. Reporter gene constructs usually contain second messenger responsive elements upstream of a minimal promoter, which in turn regulate the expression of a selected reporter protein. Commonly used reporters are enzyme proteins with activities linked to a variety of colorimetric, fluorescent or luminescent readouts, such as luciferase, alkaline phosphatase, β-galactosidase,

β-lactamase and a variety of fluorescent proteins. Among them, luciferase is the reporter of choice, especially in high-throughput screening due to its sensitivity, broad dynamic range, lack of endogenous activity and low interference coming from the compounds[35].

The advantages of reporter gene assays include the wide linearity and sensitivity of the technique and a large signal-to-background ratio, making them suitable for the detection of weak GPCR agonists or allosteric modulators. Reporter gene assays are also easy to set up and can be scaled down to extremely low assay volumes in 1536- or 3456-well formats. Despite these advantages, some concerns have been raised, such as the requirement for long incubation periods, difficulty in antagonist detection due to reporter accumulation and the higher potential for false positives because the signal event is distal from receptor activation. Concerns about the long incubation time and accumulation of reporter have been addressed through the use of destabilized reporters (available from Promega). The higher false positive rate due to the distal signaling event could be partially resolved with by the co-expression of a constitutively expressed internal control[35], so compounds nonspecifically affecting gene transcription could be ruled out. Chen *et al* demonstrated that by combining pathway-specific reporter assays, all four major G protein subfamilies and downstream pathways could be studied in one luciferase reporter assay format. This combination could help establish receptor-G protein profiles for specific receptors and aid drug screening for pathway-specific GPCR modulators[34].

Generic G-protein independent functional assays

Receptor internalization assay

The concept of the GPCR internalization assay is based on the common phenomenon of GPCR desensitization, which has been demonstrated for numerous GPCRs (reviewed in[36]). In the desensitization process, GRKs phosphorylate agonist-activated GPCRs on specific serine and threonine residues, and cytosolic β-arrestins are recruited to the cell membrane by GRK-phosphorylated GPCRs. β-Arrestins uncouple GPCRs from their cognate G proteins and target the receptors to clathrin-coated pits for endocytosis. With the development of image-based, high-content screening (HCS) systems, the internalization of GPCRs is now a quantifiable process.

To date, most high-throughput, cell-based screens have been whole-well cell assays that quantify one molecular event or provide a single readout of a complex biological process (*eg*, measurement of intracellular Ca^{2+} concentration for $G\alpha_q$-coupled GPCR activation) — they have been one-dimensional. HCS is a relatively new technology, introduced approximately 10 years ago, that combines high-resolution fluorescence microscopy with automated image analysis (reviewed in[37]). This technology offers multi-dimensional or multi-parametric readouts by monitoring various biomolecules labeled with different fluorophores. The multi-parametric data generated by HCS can also provide temporal and spatial information for biomolecules, thus enabling a more sophisticated understanding of responses in the cell after stimulation. There are a few HCS systems currently available; some are based on automated epi-fluorescent microscopes, such as the Cellomics ArrayScan™ Series from Thermo Scientific (http://www.thermo.com.cn/HCS), while others are equipped with confocal optics, such as the INCell™ Analyzer 3000 from GE Healthcare and Opera™ from Evotec Technologies. More recently, the development of a laser-scanning fluorescence microplate cytometer, for example, the Acumen™ Explorer from TTP Lab Tech, offers even higher throughput in these multiplexing assays.

In contrast to the aforementioned Ca^{2+}, cAMP and reporter assays, the internalization assay is independent of the associated G protein subclass or individual GPCR intracellular signaling pathway. Thus, there is no need to have prior knowledge of the signaling pathways of a GPCR before using this assay. The internalization assay is particularly useful for de-orphaning GPCRs, while the imaging-based GPCR internalization assays also offer the general advantage of the HCS format.

There are several ways to monitor the internalization process of GPCRs. For GPCRs with known ligands, fluorophore-labeled specific ligands can be used to detect the internalization of the receptors. Fluorescent ligands have been used since the mid-1970s. When coupled to the growing exploitation of imaging-based HCS analysis, it is clear that fluorescent molecules offer a safer, more powerful and more versatile alternative to traditional radioligand binding assays[38]. Another way to visualize the internalization of a GPCR is to co-internalize a specific antibody, directed either against an extracellular domain of the receptor or against an N-terminal epitope tag[39]. The primary antibody is co-internalized with the receptor upon agonist stimulation and then detected with a fluorophore-labeled secondary antibody. Considering the cost of antibodies and the tedious procedure of immunofluorescent staining, this method is commonly used for GPCR signaling studies but not large-scale drug screening. GPCRs tagged with fluorescent proteins (GFP or RFP) are the most common setup for HCS of receptor internalization (Figure 2) and are widely used for receptor deorphanization. When internalized, these tagged-GPCRs form grain-like objects within the cells. The Spot detector bio-application in the ArrayScan™ system or the granularity analysis module of the INCell™ Analyzer can identify, analyze and quantify these grain-like structures[40, 41]. With the EGFP-tagged GPR120 internalization assay, Hirasawa and colleagues de-orphaned this receptor and found that unsaturated long-chain free fatty acids activate GPR120 and promote GLP-1 secretion[42].

β-arrestin recruitment assay

β-arrestins are cytosolic proteins that bind to ligand-activated GPCRs, uncouple the receptors from G proteins and target the receptors to clathrin-coated endocytic vesicles. β-arrestin recruitment is a ubiquitous mechanism of negative regulation of GPCR signaling that has been demonstrated for almost all GPCRs[43]. More recently, β-arrestins have themselves been shown to act as signaling scaffolds for numerous pathways,

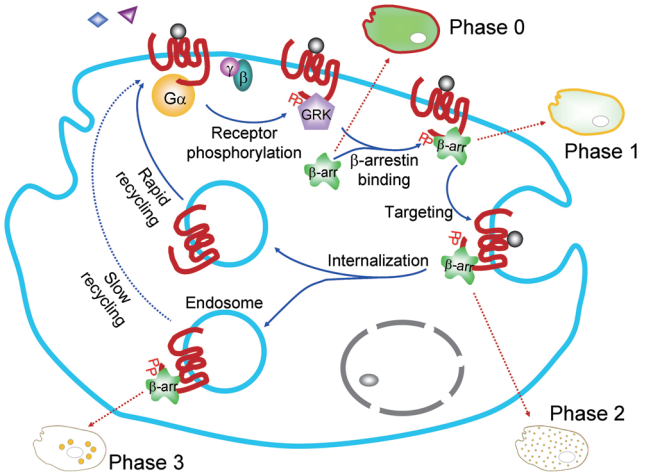

Figure 2. Transfluor™ and receptor internalization assays. Schematic representation of Transfluor™ β-arrestin recruitment assay multiplexed with a receptor internalization assay. The receptor is tagged at the C-terminus with RFP, and β-arrestin is tagged with GFP. In the resting state, the receptor is located on the cell membrane and β-arrestin is localized in the cytoplasm (Phase 0). A few seconds to several minutes after stimulation, the receptor is phosphorylated by GRK and β-arrestin is recruited to the cell membrane (Phase 1). β-arrestin binding leads to the internalization of the receptor-β-arrestin complex, initially forming internalization pits (Phase 2). For fast-recycling GPCRs, the receptor dissociates with β-arrestin and returns to the plasma membrane. For slow-recycling GPCRs, the receptor-β-arrestin complex traffics towards the endosome and forms large vesicles (Phase 3).

such as c-Src, ERK 1/2, and Akt, in a G protein-independent manner[4]. G protein and β-arrestin pathways were found to be distinct and could be pharmacologically modulated independently with "biased ligands"[44]. Therefore, β-arrestin-based assays are more interesting, potentially providing new insights into the functional selectivity (biased agonism) of GPCR signaling. These insights may help eliminate undesirable side effects by activating certain pathways but not others. Therefore, β-arrestin recruitment assays provide novel, universal, and G-protein independent ways for GPCR screening and drug discovery. Such assays are particularly useful for the screening of $G\alpha_i$-coupled GPCRs, which traditionally suffer from a small assay window in second messenger detection systems, and orphan GPCRs.

The first commercialized β-arrestin recruitment assay, Transfluor™, was originally licensed by Norak Biosciences in 1999 from Duke University Medical Center and is now available from Molecular Devices. The Transfluor™ assay is performed using GFP-tagged β-arrestin. The redistribution of diffuse β-arrestin-GFP from the cytoplasm to agonist-occupied receptor-containing pits or vesicles can be monitored quantitatively with a high content imaging system, such as the INCell™ Analyzer, ArrayScan™, Acumen™ or ImageXpress™ [45–47]. Taking advantage of these HCS instruments, the Transfluor™ assay provides robust high-throughput screening for compounds targeting GPCRs[48, 49]. The benefits of this assay include the following: (1) no fluorescent dyes or secondary substrates are required; (2) the cell imaging assay allows parallel detection of putative compound liabilities, such as cytotoxicity; (3) visualization of β-arrestin localization (to the membrane or to the vesicles) and (4) multiplexing with the receptor internalization assay (Figure 2) and providing additional information regarding drug effect with respect to ligand-induced trafficking. Like any other imaging-based assays, to obtain high quality images for further software analysis, the cell type used should be grown in a monolayer, have good adherence properties and have a large cytoplasm-to-nucleus ratio. Before conducting a HTS screening for orphan GPCRs, a ligand independent translocation assay (LITe™), which utilizes a constitutively active GRK2 to phosphorylate the receptor and initiate GPCR-β-arrestin interaction, is required to verify that the receptor can indeed recruit β-arrestin-GFP after stimulation[50].

Alternatively, several non-imaging-based β-arrestin recruitment assays, such as Bioluminescence Resonance Energy Transfer (BRET), PathHunter™ technology (DiscoveRx) and the Tango™ assay (Invitrogen), are available. The BRET assay was one of the earliest approaches utilized for assessing GPCR-β-arrestin interactions and can be scaled for HTS[51, 52]. The receptor of interest is tagged at the C-terminus with a fluorescent protein tag (such as eGFP2, GFP10 or YFP) and the β-arrestin is tagged with a *Renilla* luciferase (RLuc) or vise versa. Upon β-arrestin recruitment, the two tags come into close proximity and the light emitted from the RLuc reaction excites the GFP, which then emits a detectable signal at a higher wavelength (Figure 3A). BRET is calculated as the ratio of the two emissions (GFP/RLuc). It was reported that increased BRET sensitivity can be achieved by using RLuc8/YPet and RLuc8/RGFP as donor/acceptor couples[53].

Invitrogen's Tango™ GPCR Assay System is a platform based on a protease-activated reporter gene (Figure 3B). β-arrestin is fused to a TEV protease, while GPCR is extended at its C-terminus with a protease cleavage site followed by the transcription factor Gal-VP16[54]. Upon GPCR activation, protease-tagged arrestin is recruited to the receptor and the Gal-VP16 that is fused to the receptor is cleaved and enters the nucleus to regulate the transcription of a β-lactamase reporter gene. The β-lactamase catalyzes the cleavage of a modified substrate tagged with two fluorophores, and the change in FRET signal between these two fluorophores can be monitored. Tango™ GPCR assays have been validated for a diverse array of GPCRs, including receptors related to each of the major G protein pathways and activated by a variety of ligand types[55, 56].

The PathHunter™ assay developed by DiscoveRx utilizes enzyme fragment complementation of β-galactosidase and subsequent enzymatic activity to measure receptor−β-arrestin interactions (Figure 3C). In this assay, β-arrestin is fused to an N-terminal deletion mutant of β-galactosidase that is catalytically inactive, and GPCR is tagged at the C-terminus with a small (4 kDa) fragment derived from the deleted N-terminal sequence of β-galactosidase (ProLink™). Upon GPCR-β-arrestin interaction, the two parts of β-galactosidase

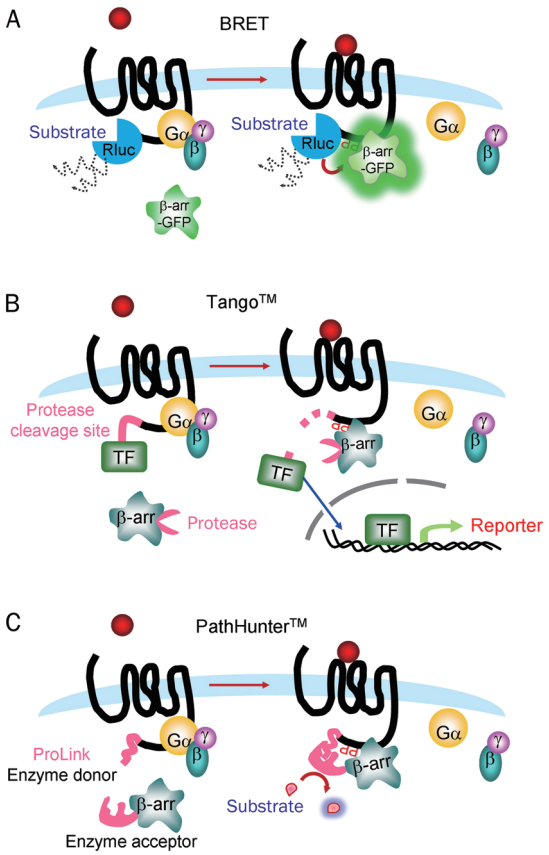

Figure 3. Non-imaging-based β-arrestin recruitment assays. (A) BRET assay. The GPCR is tagged with a RLuc, and β-arrestin is tagged with GFP, or vice versa. Upon β-arrestin recruitment, the two tags come into close proximity and the light emitted from the RLuc reaction excites the GFP, which then emits a detectable signal at a higher wavelength. (B) Tango™ assay. β-arrestin is fused to a protease, while GPCR is extended at its C-terminus with a protease cleavage site followed by a transcription factor (TF). Upon β-arrestin recruitment, the TF fused to the receptor is cleaved and enters the nucleus to regulate the transcription of a reporter gene. (C) PathHunter™ assay. β-arrestin is fused to a deletion mutant of β-galactosidase that is catalytically inactive, and GPCR is tagged with a small fragment derived from the deleted sequence of the enzyme (ProLink™). Upon GPCR-β-arrestin interaction, the two parts of β-galactosidase are brought into close proximity, which results in cleavage of the substrate and generation of a chemiluminescent signal.

are brought into proximity, which results in the activation of the enzyme, cleavage of the substrate and generation of a chemiluminescent signal. Similar to Tango™ GPCR assays, PathHunter™ has also been validated for a diverse array of GPCRs and is widely accepted in industrial and academic drug-screening laboratories[57, 58]. Both assays also have commercially available, assay-ready cell lines for a large number of GPCRs. There are several advantages in the PathHunter™ assay, including a homogeneous assay with enzyme-amplified robust signal. The chemiluminescent signal is also low in background and resistant to interference from fluorescent compounds. One disadvantage of this platform is that the time window for measurement is limited, so the assay only captures a snapshot of β-arrestin-receptor binding during the period of substrate incubation. However, this limitation can also be viewed as an advantage when using instruments capable of real-time detection to study the kinetics of GPCR-β-arrestin interaction.

Label-free whole cell assays

Label-free technologies, which emerged within the past few years, have the potential to substantially change some aspects of whole-cell assays, including GPCR screening (reviewed in[59]). Many assays widely employed for GPCR ligand discovery tend to provide reductionist views of cell signaling. These assays are extremely robust and have been successfully implemented for measuring one particular functional activity of GPCRs, but often fail to account for the summation of events associated with the activation of one or more receptors. The emergence of label-free technologies presents a different strategy in measuring signal transduction, with integrated or cumulative responses rather than the resolution of individual events. Label-free, whole cell assays generally employ a biosensor that converts the summation of ligand-induced changes in living cells to optical, electrical, calorimetric, acoustic, magnetic or other quantifiable signals. They can detect changes in cellular features including adhesion, proliferation, migration, and cell death.

Most of the label-free instruments available for GPCR screening use either an optical or electrical biosensor to detect cellular changes after stimulation. The optical biosensors are also called resonant waveguide grating (RWG) biosensors, which utilize grating structures embedded in the bottom of microtiter plates (Figure 4B). When illuminated with broadband or monochromatic light, these grating surfaces reflect a narrow band of light that is characteristic of the refractive index near the grating surface. These instruments can detect

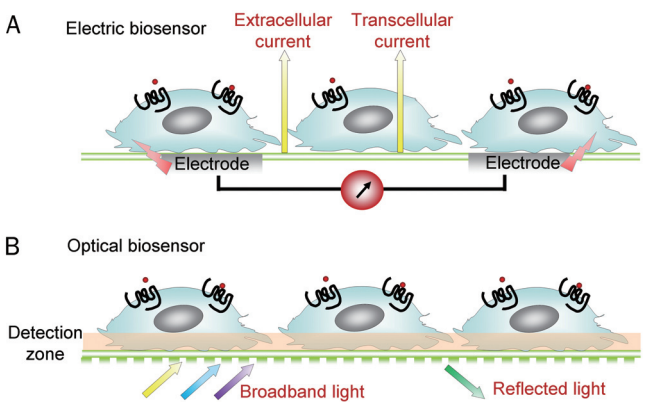

Figure 4. Principles of the biosensors for label-free, whole-cell detection. (A) Schematic representation of an electrical biosensor. Cells are cultured on the surface of arrayed gold microelectrodes. A low AC voltage at variable frequencies is applied to the cell layer and both the extracellular current and transcellular current are measured. (B) Schematic representation of an optical biosensor. Cells are cultured on the surface of the biosensor with an embedded grating structure. Only the mass redistribution within the bottom portion of cells is directly measured.

either angle- or wavelength-shift[60]. The refractive index is influenced by the physical properties of the cell layer in contact with the grating surface. When a GPCR is activated and subsequent signal transduction changes the biomolecular concentration within an approximately 200 nm range of the contact surface, the disturbance in local refractive index can be detected as a shift in resonant angle or wavelength. The current optical-based instruments include BIND™ (SRU Biosystems) and Epic™ (Corning Inc) systems. Although initially designed for *in vitro* molecular binding assays, both systems were successful in studying cell morphological changes and GPCR signaling[61, 62].

Electrical biosensors, also known as impedance-based biosensors, mainly consist of a substrate, an electrode and a cell layer in close contact with the electrode (Figure 4A). Giaever and Keese of GE first reported the use of impedance to measure cellular processes[63]. In their early studies, fibroblasts cultured on thin-film gold electrodes were found to impede the flow of a very weak alternating current. The impedance change could be monitored in real-time, and the fluctuation of impedance was dependent on ATP concentration and actin polymerization, and was thus linked to cellular motion[64]. Since then, electrical-based detections have been applied to study a wide variety of cellular events, including cell adhesion and spreading[65], cell morphological changes[66], and cell death[67]. It is now generally accepted that the impedance value is the sum of cellular events, including the relative density of cells over the electrode surface and the relative adherence of these cells.

Applied Biophysics launched ECIS™, the first commercially available instrument for electrical-based whole cell detection with high-throughput capability (up to 96-well detection), in 1995. The more recently available (2008) xCELLigence™ System from Roche Applied Science and ACEA Biosciences is also built to fit into cell culture incubators and to measure long-term cellular responses that occur over hours to days. Both systems have been used to detect GPCR activity for hours[68, 69]. A more high-throughput system, CellKey™, was developed by MDS Analytical Technologies, which is designed to detect acute cellular responses in 96- and 384-well formats.

Based on both the CellKey™ and Epic™ systems, scientists observed distinct response profiles depending on the G-protein pathway activated[62, 70, 71]. Several studies compared the Epic™ system and traditional Ca^{2+} or cAMP assays using CHO cells expressing the muscarinic M2, M3 or dopamine D3 receptors. Most of the results from the Epic™ were consistent with data from cAMP or Ca^{2+} readouts with few exceptions, and the Epic™ was found to detect weak activity that was not observed with the label-based assays[72, 73]. Many studies with GPCR ligand sets also demonstrated similar rank-order potency values between CellKey™ impedance and traditional Ca^{2+} or cAMP assays[74–76].

The sensitivity, precision and high-throughput of some label-free instruments warrant their use in HTS, although the cost of consumables might limit broader application. These systems have also been used for ligand selectivity studies[76–78], endogenous receptor profiling in cell lines commonly used in drug discovery[62, 74, 77], systemic cell biology studies of GPCR signaling[77, 79], and many other aspects of GPCR research. Like any other functional assay, label-free, whole cell assays are also prone to false positives. Another unique problem associated with label-free systems is the possibility that signaling through multiple pathways with opposing effects may cause a lack of overall response, resulting in a false negative outcome[70]. In combination with traditional assays, biosensor-based label-free methods have a promising future and should further strengthen the role of GPCRs in drug discovery and development.

Receptor dimerization assay

Many, but perhaps not all[80], GPCRs interact with each other at the plasma membrane to form dimers, oligomers or even higher-order complexes. The dimerization of GPCRs can be observed early after biosynthesis and profoundly impacts receptor pharmacology and signaling (reviewed in[81]). For class C GPCRs, heterodimerization is obligatory for receptor function. Many class A GPCRs, however, can function as homodimers when individually expressed in cells, and heterodimerization between class A GPCRs may lead to distinct and unique signaling properties even when stimulated with the same ligand, a phenomenon termed "heteromer-directed signaling specificity." Such phenomena are believed to be involved in the physiological roles of GPCRs and in disease-specific dysregulation of a receptor effect[82, 83]. Therefore, compounds that specifically target GPCR heterodimers or affect receptor dimerization may have the potential to achieve specific therapeutic effects[84]. As a result, there is considerable interest in designing assays to assess the effect of compounds on GPCR dimerization. Various technologies have been established to monitor receptor dimerization, including resonance energy transfer approaches (FRET or BRET) and the recently developed PathHunter™ GPCR dimerization system (DiscoveRx) and Tag-lite™ GPCR dimer assay (Cisbio).

In commonly used FRET or BRET-based approaches, donor and acceptor molecules are genetically fused to the C-terminus of GPCRs, which are overexpressed in the cells (Figure 5A). Resonance energy transfer occurs when donor and acceptor molecules are brought into close proximity as a consequence of GPCR dimerization (reviewed in[85, 86]). However, one limitation of such traditional FRET and BRET assays is that in the overexpression system, resonance energy transfer can also occur within the intracellular compartments such that it is difficult to demonstrate a specific signal resulting only from a direct interaction of proteins at the cell surface. In addition, low signal-to-noise ratio resulting from the intrinsic fluorescence background of a cell and the overlap between the emission spectra of FRET donors and acceptors is another limitation of the commonly used resonance energy transfer techniques.

The GPCR dimerization assay with Tag-lite™ is a method combining TR-FRET with SNAP-tag™ technology (Cisbio), enabling quantitative analysis of protein-protein interactions

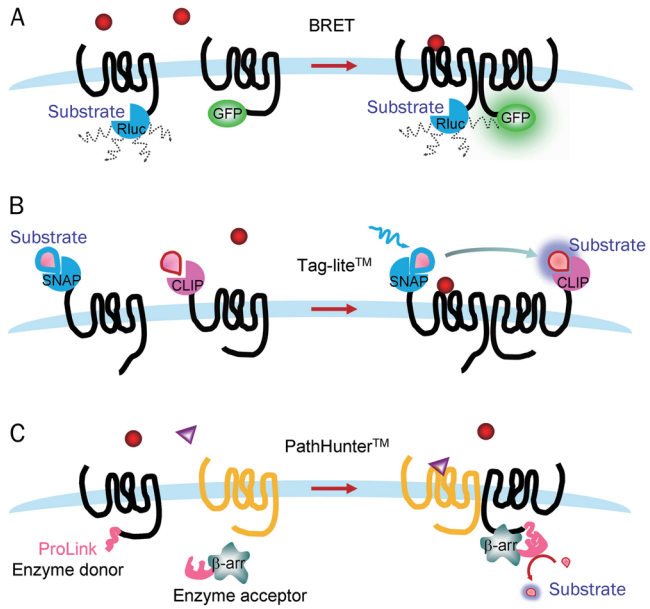

Figure 5. Receptor dimerization assays. (A) BRET dimerization assay. GPCRs are tagged with a RLuc donor and a GFP acceptor. Upon receptor dimerization, the two tags come into close proximity and energy transfer occurs. (B) Tag-lite™ dimerization assay. GPCRs are tagged with either a SNAP- or CLIP-tag at the N-terminus, which can be subsequently labeled with their corresponding cell-impermeable substrates carrying appropriate TR-FRET-compatible fluorophores. (C) PathHunter™ heterodimerization assay. β-arrestin is fused to the larger portion of a β-galactosidase enzyme acceptor, and the ProLink™ tag is attached to one of the GPCR targets. A second untagged GPCR can be introduced into the cells, and the transactivation effects of the untagged GPCR on the ProLink™-tagged GPCR can be measured by the recruitment of β-arrestin to the tagged-GPCR using PathHunter detection reagents.

at the surface of living cells in a 96- or 384-well format. In this assay, GPCRs are tagged with either a SNAP- or CLIP-tag at the N-terminus, which can be subsequently labeled with their corresponding cell-impermeable substrates carrying appropriate TR-FRET-compatible fluorophores, typically using terbium cryptate as a donor and a green or red fluorescent molecule as an acceptor (Figure 5B). Several possible dimer combinations exist in this assay: 1/4 of the dimers contain both receptors labeled with the donor, 1/4 of the dimers contain both receptors labeled with the acceptors, and 1/2 of the dimers contain one receptor labeled with the donor and one receptor labeled with the acceptor. Only the last fraction will emit the FRET signal[87]. This assay was validated with well-known GPCR dimers and the oligomeric assembly of both class A and class C GPCRs was confirmed[88].

The PathHunter™ GPCR dimerization system from DiscoveRx is another platform for GPCR heterodimerization analysis. Cell lines utilized in the previously described PathHunter™ β-arrestin recruitment assay can be used as the starting material. In these cell lines, β-arrestin is fused to the larger portion of the β-galactosidase enzyme acceptor, and the smaller 42-amino acid ProLink™ tag is attached to one of the GPCR targets. A second untagged GPCR can be introduced into the cells and the transactivation effects of the untagged GPCR on the ProLink™-tagged GPCR can be measured by the recruitment of β-arrestin to the tagged-GPCR using PathHunter detection reagents (Figure 5C). The transactivation strength can be estimated as a ratio between the cellular response to the agonist of the untagged GPCR and the response to the agonist of Prolink™-GPCR. The assay can be used to investigate the interaction between GPCR pairs, as well as screen for compounds that modulate GPCP activity through enhancing or disrupting GPCR heterodimerization in a 384-well format (http://www.discoverx.com/documents/DRx_poster_Heterodimer_DOT09_REV1.pdf).

In silico drug discovery

GPCR drug discovery usually relies on HTS for hit identification. However, with the development and maturation of computational methods for drug discovery, HTS may be complemented by *in silico* screening. This combination of approaches will reduce both time and cost through reducing the number of compounds to be experimentally tested and increase the probability of identifying novel lead compounds. Both ligand-based and structure-based methods for *in silico* screening have been successfully applied to GPCR drug discovery.

Structure-based screening requires reliable 3D structures for the target protein, which poses a challenge for GPCRs because of the heterogeneity of this receptor family and the lack of crystallographic data. Until 2008, the only available GPCR structure was that of bovine rhodopsin[89]. In the last few years, a number of different technological developments[90] have resulted in the structures of several new GPCRs, including β2 adrenergic receptor[91], A2a adenosine receptor[92], CXCR4 chemokine receptor[93], dopamine D3 receptor[94] and histamine H1 receptor[95]. Additionally, the first structure of a signal transduction complex (β2 adrenergic receptor and $G\alpha_s$) has also been reported[96]. Nevertheless, the relatively limited 3D information for GPCRs is an obstacle for structure-based drug discovery. In the absence of crystal structures, both homology modeling and *ab initio* techniques have been applied to model the 3D structures of GPCRs and used for *in silico* screening (reviewed in[97, 98]).

When a crystal structure of the targeted protein is not available and reliable modeling is not feasible, a problem common to many GPCRs, ligand-based drug discovery methods remain the major computational approach for the analysis of the growing data sets for GPCR ligands. Ligand-based screening is highly efficient and can be productive with sufficient information on known ligands. Incorporating ligand information with homology modeling has also been applied with good results (reviewed in[97, 99, 100]).

Conclusion

Choosing the right primary HTS assay for GPCRs, one of the most important protein families for therapeutic targeting, is critical in early drug discovery. With the availability of all the aforementioned assays, a few important things must also be

considered. First, the choice of cell line for GPCR expression might affect assay development because such cell line might lack correct post-translational modification and dimerization of GPCRs, and the expression of important signaling molecules. Second, the level of GPCR expression also needs to be carefully monitored because significant overexpression might lead to ligand-independent signaling and shifts in G protein coupling. Third, the functional selectivity (biased signaling) of ligands might complicate the screening process. Assays based on one signaling pathway might miss potentially valuable compounds acting on other pathways. Therefore, multiplexing of assays or a summed readout should always be considered. With the advancement of high-content imaging and label-free, whole cell technologies, new GPCR functional assays might provide more comprehensive and physiologically relevant information on lead compounds and might improve the success rate in drug discovery.

Acknowledgements

The authors thank Chang-sheng DU for discussion and critical reading of this manuscript. This work was supported by grants from the Ministry of Science and Technology of China (2009ZX09302-001 and 2008DFB30150), the National Natural Science Foundation of China (31071227 and 90713047), and the Shanghai Commission of Science and Technology (09DZ2260100).

Refferences

1 Fredriksson R, Lagerstrom MC, Lundin LG, Schioth HB. The G-protein-coupled receptors in the human genome form five main families. Phylogenetic analysis, paralogon groups, and fingerprints. Mol Pharmacol 2003; 63: 1256–72.
2 Bourne HR, Sanders DA, McCormick F. The GTPase superfamily: conserved structure and molecular mechanism. Nature 1991; 349: 117–27.
3 Pierce KL, Premont RT, Lefkowitz RJ. Seven-transmembrane receptors. Nat Rev Mol Cell Biol 2002; 3: 639–50.
4 Lefkowitz RJ, Shenoy SK. Transduction of receptor signals by beta-arrestins. Science 2005; 308: 512–7.
5 Klabunde T, Hessler G. Drug design strategies for targeting G-protein-coupled receptors. Chembiochem 2002; 3: 928–44.
6 Milligan G. Principles: extending the utility of [^{35}S]GTP gamma S binding assays. Trends Pharmacol Sci 2003; 24: 87–90.
7 Kenakin T. Efficacy at G-protein-coupled receptors. Nat Rev Drug Discov 2002; 1: 103–10.
8 Bylund DB, Toews ML. Radioligand binding methods: practical guide and tips. Am J Physiol 1993; 265: L421–9.
9 Lefkowitz RJ, Roth J, Pastan I. Radioreceptor assay of adrenocorticotropic hormone: new approach to assay of polypeptide hormones in plasma. Science 1970; 170: 633–5.
10 Trankle C, Weyand O, Schroter A, Mohr K. Using a radioalloster to test predictions of the cooperativity model for gallamine binding to the allosteric site of muscarinic acetylcholine M(2) receptors. Mol Pharmacol 1999; 56: 962–5.
11 Glickman JF, Schmid A, Ferrand S. Scintillation proximity assays in high-throughput screening. Assay Drug Dev Technol 2008; 6: 433–55.
12 Degorce F, Card A, Soh S, Trinquet E, Knapik GP, Xie B. HTRF: A technology tailored for drug discovery — a review of theoretical aspects and recent applications. Curr Chem Genomics 2009; 3: 22–32.
13 Harrison C, Traynor JR. The [^{35}S]GTPgammaS binding assay: approaches and applications in pharmacology. Life Sci 2003; 74: 489–508.
14 Ferrer M, Kolodin GD, Zuck P, Peltier R, Berry K, Mandala SM, *et al*. A fully automated [^{35}S]GTPgammaS scintillation proximity assay for the high-throughput screening of Gi-linked G protein-coupled receptors. Assay Drug Dev Technol 2003; 1: 261–73.
15 Johnson EN, Shi X, Cassaday J, Ferrer M, Strulovici B, Kunapuli P. A 1536-well [^{35}S]GTPgammaS scintillation proximity binding assay for ultra-high-throughput screening of an orphan galphai-coupled GPCR. Assay Drug Dev Technol 2008; 6: 327–37.
16 Labrecque J, Wong RS, Fricker SP. A time-resolved fluorescent lanthanide (Eu)-GTP binding assay for chemokine receptors as targets in drug discovery. Methods Mol Biol 2009; 552: 153–69.
17 Frang H, Mukkala VM, Syysto R, Ollikka P, Hurskainen P, Scheinin M, *et al*. Nonradioactive GTP binding assay to monitor activation of g protein-coupled receptors. Assay Drug Dev Technol 2003; 1: 275–80.
18 Engstrom M, Narvanen A, Savola JM, Wurster S. Assessing activation of the human neuropeptide FF2 receptor with a non-radioactive GTP binding assay. Peptides 2004; 25: 2099–104.
19 Leopoldo M, Lacivita E, Colabufo NA, Contino M, Berardi F, Perrone R. First structure-activity relationship study on dopamine D3 receptor agents with N-[4-(4-arylpiperazin-1-yl)butyl]arylcarboxamide structure. J Med Chem 2005; 48: 7919–22.
20 Zhang HY, Watson ML, Gallagher M, Nicolle MM. Muscarinic receptor-mediated GTP-Eu binding in the hippocampus and prefrontal cortex is correlated with spatial memory impairment in aged rats. Neurobiol Aging 2007; 28: 619–26.
21 Koval A, Kopein D, Purvanov V, Katanaev VL. Europium-labeled GTP as a general nonradioactive substitute for [^{35}S]GTPgammaS in high-throughput G protein studies. Anal Biochem 2010; 397: 202–7.
22 Eglen RM, Singh R. Beta galactosidase enzyme fragment complementation as a novel technology for high throughput screening. Comb Chem High Throughput Screen 2003; 6: 381–7.
23 Weber M, Ferrer M, Zheng W, Inglese J, Strulovici B, Kunapuli P. A 1536-well cAMP assay for Gs- and Gi-coupled receptors using enzyme fragmentation complementation. Assay Drug Dev Technol 2004; 2: 39–49.
24 Williams C. cAMP detection methods in HTS: selecting the best from the rest. Nat Rev Drug Discov 2004; 3: 125–35.
25 Wigdal SS, Anderson JL, Vidugiris GJ, Shultz J, Wood KV, Fan F. A novel bioluminescent protease assay using engineered firefly luciferase. Curr Chem Genomics 2008; 2: 16–28.
26 Gabriel D, Vernier M, Pfeifer MJ, Dasen B, Tenaillon L, Bouhelal R. High throughput screening technologies for direct cyclic AMP measurement. Assay Drug Dev Technol 2003; 1: 291–303.
27 Berridge MJ. Inositol trisphosphate and calcium signalling. Nature 1993; 361: 315–25.
28 Liu K, Titus S, Southall N, Zhu P, Inglese J, Austin CP, *et al*. Comparison on functional assays for Gq-coupled GPCRs by measuring inositol monophospate-1 and intracellular calcium in 1536-well plate format. Curr Chem Genomics 2008; 1: 70–8.
29 Emkey R, Rankl NB. Screening G protein-coupled receptors: measurement of intracellular calcium using the fluorometric imaging plate reader. Methods Mol Biol 2009; 565: 145–58.
30 Zhang Y, Kowal D, Kramer A, Dunlop J. Evaluation of FLIPR calcium 3 assay kit — a new no-wash fluorescence calcium indicator reagent. J

Biomol Screen 2003; 8: 571–7.
31 Eglen RM, Reisine T. Photoproteins: important new tools in drug discovery. Assay Drug Dev Technol 2008; 6: 659–71.
32 Robas NM, Fidock MD. Identification of orphan G protein-coupled receptor ligands using FLIPR assays. Methods Mol Biol 2005; 306: 17–26.
33 Hansen KB, Brauner-Osborne H. FLIPR assays of intracellular calcium in GPCR drug discovery. Methods Mol Biol 2009; 552: 269–78.
34 Cheng Z, Garvin D, Paguio A, Stecha P, Wood K, Fan F. Luciferase reporter assay system for deciphering GPCR pathways. Curr Chem Genomics 2010; 4: 84–91.
35 Fan F, Wood KV. Bioluminescent assays for high-throughput screening. Assay Drug Dev Technol 2007; 5: 127–36.
36 Salahpour A, Barak LS. Visualizing receptor endocytosis and trafficking. Methods Mol Biol 2011; 756: 311–23.
37 Zanella F, Lorens JB, Link W. High content screening: seeing is believing. Trends Biotechnol 2010; 28: 237–45.
38 Middleton RJ, Kellam B. Fluorophore-tagged GPCR ligands. Curr Opin Chem Biol 2005; 9: 517–25.
39 Hislop JN, von Zastrow M. Analysis of GPCR localization and trafficking. Methods Mol Biol 2011; 746: 425–40.
40 Taylor HD, Haskins JR, Giuliano KA. High content screening: A powerful approach to systems cell biology and drug discovery totowa. New Jersery Humana Press Inc; 2007.
41 Haasen D, Schnapp A, Valler MJ, Heilker R. G protein-coupled receptor internalization assays in the high-content screening format. Methods Enzymol 2006; 414: 121–39.
42 Hirasawa A, Tsumaya K, Awaji T, Katsuma S, Adachi T, Yamada M, *et al*. Free fatty acids regulate gut incretin glucagon-like peptide-1 secretion through GPR120. Nat Med 2005; 11: 90–4.
43 Luttrell LM, Lefkowitz RJ. The role of beta-arrestins in the termination and transduction of G-protein-coupled receptor signals. J Cell Sci 2002; 115: 455–65.
44 Violin JD, Lefkowitz RJ. Beta-arrestin-biased ligands at seven-transmembrane receptors. Trends Pharmacol Sci 2007; 28: 416–22.
45 Bowen WP, Wylie PG. Application of laser-scanning fluorescence microplate cytometry in high content screening. Assay Drug Dev Technol 2006; 4: 209–21.
46 Eggeling C, Brand L, Ullmann D, Jager S. Highly sensitive fluorescence detection technology currently available for HTS. Drug Discov Today 2003; 8: 632–41.
47 Haasen D, Wolff M, Valler MJ, Heilker R. Comparison of G-protein coupled receptor desensitization-related beta-arrestin redistribution using confocal and non-confocal imaging. Comb Chem High Throughput Screen 2006; 9: 37–47.
48 Oakley RH, Hudson CC, Cruickshank RD, Meyers DM, Payne RE Jr, Rhem SM, *et al*. The cellular distribution of fluorescently labeled arrestins provides a robust, sensitive, and universal assay for screening G protein-coupled receptors. Assay Drug Dev Technol 2002; 1: 21–30.
49 Garippa RJ, Hoffman AF, Gradl G, Kirsch A. High-throughput confocal microscopy for beta-arrestin-green fluorescent protein translocation G protein-coupled receptor assays using the Evotec Opera. Methods Enzymol 2006; 414: 99–120.
50 Oakley RH, Hudson CC, Sjaastad MD, Loomis CR. The ligand-independent translocation assay: an enabling technology for screening orphan G protein-coupled receptors by arrestin recruitment. Methods Enzymol 2006; 414: 50–63.
51 Bertrand L, Parent S, Caron M, Legault M, Joly E, Angers S, *et al*. The BRET2/arrestin assay in stable recombinant cells: a platform to screen for compounds that interact with G protein-coupled receptors (GPCRS). J Recept Signal Transduct Res 2002; 22: 533–41.
52 Hamdan FF, Audet M, Garneau P, Pelletier J, Bouvier M. High-throughput screening of G protein-coupled receptor antagonists using a bioluminescence resonance energy transfer 1-based beta-arrestin2 recruitment assay. J Biomol Screen 2005; 10: 463–75.
53 Kamal M, Marquez M, Vauthier V, Leloire A, Froguel P, Jockers R, *et al*. Improved donor/acceptor BRET couples for monitoring beta-arrestin recruitment to G protein-coupled receptors. Biotechnol J 2009; 4: 1337–44.
54 Barnea G, Strapps W, Herrada G, Berman Y, Ong J, Kloss B, *et al*. The genetic design of signaling cascades to record receptor activation. Proc Natl Acad Sci U S A 2008; 105: 64–9.
55 Doucette C, Vedvik K, Koepnick E, Bergsma A, Thomson B, Turek-Etienne TC. Kappa opioid receptor screen with the Tango beta-arrestin recruitment technology and characterization of hits with second-messenger assays. J Biomol Screen 2009; 14: 381–94.
56 Hanson BJ, Wetter J, Bercher MR, Kopp L, Fuerstenau-Sharp M, Vedvik KL, *et al*. A homogeneous fluorescent live-cell assay for measuring 7-transmembrane receptor activity and agonist functional selectivity through beta-arrestin recruitment. J Biomol Screen 2009; 14: 798–810.
57 Yin H, Chu A, Li W, Wang B, Shelton F, Otero F, *et al*. Lipid G protein-coupled receptor ligand identification using beta-arrestin PathHunter assay. J Biol Chem 2009; 284: 12328–38.
58 Zhao X, Jones A, Olson KR, Peng K, Wehrman T, Park A, *et a*l. A homogeneous enzyme fragment complementation-based beta-arrestin translocation assay for high-throughput screening of G-protein-coupled receptors. J Biomol Screen 2008; 13: 737–47.
59 Scott CW, Peters MF. Label-free whole-cell assays: expanding the scope of GPCR screening. Drug Discov Today 2010; 15: 704–16.
60 Fang Y. Label-free cell-based assays with optical biosensors in drug discovery. Assay Drug Dev Technol 2006; 4: 583–95.
61 Fang Y, Ferrie AM, Li G. Probing cytoskeleton modulation by optical biosensors. FEBS Lett 2005; 579: 4175–80.
62 Fang Y, Li G, Ferrie AM. Non-invasive optical biosensor for assaying endogenous G protein-coupled receptors in adherent cells. J Pharmacol Toxicol Methods 2007; 55: 314–22.
63 Giaever I, Keese CR. Monitoring fibroblast behavior in tissue culture with an applied electric field. Proc Natl Acad Sci U S A 1984; 81: 3761–4.
64 Giaever I, Keese CR. Micromotion of mammalian cells measured electrically. Proc Natl Acad Sci U S A 1991; 88: 7896–900.
65 Tiruppathi C, Malik AB, Del Vecchio PJ, Keese CR, Giaever I. Electrical method for detection of endothelial cell shape change in real time: assessment of endothelial barrier function. Proc Natl Acad Sci U S A 1992; 89: 7919–23.
66 Giaever I, Keese CR. A morphological biosensor for mammalian cells. Nature 1993; 366: 591–2.
67 Zhu J, Wang X, Xu X, Abassi YA. Dynamic and label-free monitoring of natural killer cell cytotoxic activity using electronic cell sensor arrays. J Immunol Methods 2006; 309: 25–33.
68 Yu N, Atienza JM, Bernard J, Blanc S, Zhu J, Wang X, *et al*. Real-time monitoring of morphological changes in living cells by electronic cell sensor arrays: an approach to study G protein-coupled receptors. Anal Chem 2006; 78: 35–43.
69 McLaughlin JN, Shen L, Holinstat M, Brooks JD, Dibenedetto E, Hamm HE. Functional selectivity of G protein signaling by agonist peptides and thrombin for the protease-activated receptor-1. J Biol Chem 2005; 280: 25048–59.
70 Peters MF, Vaillancourt F, Heroux M, Valiquette M, Scott CW. Comparing label-free biosensors for pharmacological screening with cell-

based functional assays. Assay Drug Dev Technol 2010; 8: 219–27.
71 Leung G, Tang HR, McGuinness R, Verdonk E, Michelotti JM, Liu VF. Cellular dielectric spectroscopy: A label-free technology for drug discovery. J Lab Autom 2005; 10: 258–69.
72 Dodgson K, Gedge L, Murray DC, Coldwell M. A 100K well screen for a muscarinic receptor using the Epic label-free system — a reflection on the benefits of the label-free approach to screening seven-transmembrane receptors. J Recept Signal Transduct Res 2009; 29: 163–72.
73 Tran E, Ye F. Duplexed label-free G protein-coupled receptor assays for high-throughput screening. J Biomol Screen 2008; 13: 975–85.
74 Ciambrone GJ, Liu VF, Lin DC, McGuinness RP, Leung GK, Pitchford S. Cellular dielectric spectroscopy: a powerful new approach to label-free cellular analysis. J Biomol Screen 2004; 9: 467–80.
75 Peters MF, Knappenberger KS, Wilkins D, Sygowski LA, Lazor LA, Liu J, *et al*. Evaluation of cellular dielectric spectroscopy, a whole-cell, label-free technology for drug discovery on Gi-coupled GPCRs. J Biomol Screen 2007; 12: 312–9.
76 McGuinness RP, Proctor JM, Gallant DL, van Staden CJ, Ly JT, Tang FL, *et al*. Enhanced selectivity screening of GPCR ligands using a label-free cell based assay technology. Comb Chem High Throughput Screen 2009; 12: 812–23.
77 Verdonk E, Johnson K, McGuinness R, Leung G, Chen YW, Tang HR, *et al*. Cellular dielectric spectroscopy: a label-free comprehensive platform for functional evaluation of endogenous receptors. Assay Drug Dev Technol 2006; 4: 609–19.
78 Lee PH, Gao A, van Staden C, Ly J, Salon J, Xu A, *et al*. Evaluation of dynamic mass redistribution technology for pharmacological studies of recombinant and endogenously expressed g protein-coupled receptors. Assay Drug Dev Technol 2008; 6: 83–94.
79 Fang Y, Li GG, Peng J. Optical biosensor provides insights for bradykinin B(2) receptor signaling in A431 cells. FEBS Lett 2005; 579: 6365–74.
80 Meyer BH, Segura JM, Martinez KL, Hovius R, George N, Johnsson K, *et al*. FRET imaging reveals that functional neurokinin-1 receptors are monomeric and reside in membrane microdomains of live cells. Proc Natl Acad Sci U S A 2006; 103: 2138–43.
81 Rozenfeld R, Devi LA. Exploring a role for heteromerization in GPCR signalling specificity. Biochem J 2011; 433: 11–8.
82 Rozenfeld R, Gupta A, Gagnidze K, Lim MP, Gomes I, Lee-Ramos D, *et al*. AT1R-CBR heteromerization reveals a new mechanism for the pathogenic properties of angiotensin II. EMBO J 2011; 30: 2350–63.
83 Gassmann M, Shaban H, Vigot R, Sansig G, Haller C, Barbieri S, *et al*. Redistribution of GABAB(1) protein and atypical GABAB responses in GABAB(2)-deficient mice. J Neurosci 2004; 24: 6086–97.
84 Rozenfeld R, Devi LA. Receptor heteromerization and drug discovery. Trends Pharmacol Sci 2010; 31: 124–30.
85 Achour L, Kamal M, Jockers R, Marullo S. Using quantitative BRET to assess G protein-coupled receptor homo- and heterodimerization. Methods Mol Biol 2011; 756: 183–200.
86 Cottet M, Albizu L, Comps-Agrar L, Trinquet E, Pin JP, Mouillac B, *et al*. Time resolved FRET strategy with fluorescent ligands to analyze receptor interactions in native tissues: application to GPCR oligomerization. Methods Mol Biol 2011; 746: 373–87.
87 Comps-Agrar L, Maurel D, Rondard P, Pin JP, Trinquet E, Prezeau L. Cell-surface protein-protein interaction analysis with time-resolved FRET and snap-tag technologies: application to G protein-coupled receptor oligomerization. Methods Mol Biol 2011; 756: 201–14.
88 Maurel D, Comps-Agrar L, Brock C, Rives ML, Bourrier E, Ayoub MA, *et al*. Cell-surface protein-protein interaction analysis with time-resolved FRET and snap-tag technologies: application to GPCR oligomerization. Nat Methods 2008; 5: 561–7.
89 Palczewski K, Kumasaka T, Hori T, Behnke CA, Motoshima H, Fox BA, *et al*. Crystal structure of rhodopsin: A G protein-coupled receptor. Science 2000; 289: 739–45.
90 Hanson MA, Stevens RC. Discovery of new GPCR biology: one receptor structure at a time. Structure 2009; 17: 8–14.
91 Rasmussen SG, Choi HJ, Rosenbaum DM, Kobilka TS, Thian FS, Edwards PC, *et al*. Crystal structure of the human beta2 adrenergic G-protein-coupled receptor. Nature 2007; 450: 383–7.
92 Jaakola VP, Griffith MT, Hanson MA, Cherezov V, Chien EY, Lane JR, *et al*. The 2.6 angstrom crystal structure of a human A2A adenosine receptor bound to an antagonist. Science 2008; 322: 1211–7.
93 Wu B, Chien EY, Mol CD, Fenalti G, Liu W, Katritch V, *et al*. Structures of the CXCR4 chemokine GPCR with small-molecule and cyclic peptide antagonists. Science 2010; 330: 1066–71.
94 Chien EY, Liu W, Zhao Q, Katritch V, Han GW, Hanson MA, *et al*. Structure of the human dopamine D3 receptor in complex with a D2/D3 selective antagonist. Science 2010; 330: 1091–5.
95 Shimamura T, Shiroishi M, Weyand S, Tsujimoto H, Winter G, Katritch V, *et al*. Structure of the human histamine H1 receptor complex with doxepin. Nature 2011; 475: 65–70.
96 Rasmussen SG, Devree BT, Zou Y, Kruse AC, Chung KY, Kobilka TS, *et al*. Crystal structure of the beta(2) adrenergic receptor-Gs protein complex. Nature 2011; 477: 549–55.
97 Sela I, Golan G, Strajbl M, Rivenzon-Segal D, Bar-Haim S, Bloch I, *et al*. G protein coupled receptors — *in silico* drug discovery and design. Curr Top Med Chem 2010; 10: 638–56.
98 Senderowitz H, Marantz Y. G Protein-Coupled Receptors: target-based *in silico* screening. Curr Pharm Des 2009; 15: 4049–68.
99 Gruber CW, Muttenthaler M, Freissmuth M. Ligand-based peptide design and combinatorial peptide libraries to target G protein-coupled receptors. Curr Pharm Des 2010; 16: 3071–88.
100 Tropsha A, Wang SX. QSAR modeling of GPCR ligands: methodologies and examples of applications. Ernst Schering Found Symp Proc 2006; (2): 49–73.

Acta Pharmacologica Sinica (2012) 33: 385–392

www.nature.com/aps

Original Article

Rapamycin prevents the mutant huntingtin-suppressed GLT-1 expression in cultured astrocytes

Lei-lei CHEN[1], Jun-chao WU[1], Lin-hui WANG[1], Jin WANG[1], Zheng-hong QIN[1], Marian DIFIGLIA[2], Fang LIN[1, *]

[1]*Laboratory of Aging and Nervous Diseases and Department of Pharmacology, Soochow University School of Pharmaceutical Science, Suzhou 215123, China;* [2]*Laboratory of Cellular Neurobiology, Massachusetts General Hospital and Harvard Medical School, Charlestown, MA 02129, USA*

Aim: To investigate the effects of rapamycin on glutamate uptake in cultured rat astrocytes expressing N-terminal 552 residues of mutant huntingtin (Htt-552).

Methods: Primary astrocyte cultures were prepared from the cortex of postnatal rat pups. An astrocytes model of Huntington's disease was established using the astrocytes infected with adenovirus carrying coden gene of N-terminal 552 residues of Huntingtin. The protein levels of glutamate transporters GLT-1 and GLAST, the autophagic marker microtubule-associated protein 1A/1B-light chain 3 (LC3) and the autophagy substrate p62 in the astrocytes were examined using Western blotting. The mRNA expression levels of GLT-1 and GLAST in the astrocytes were determined using Real-time PCR. [^{3}H]glutamate uptake by the astrocytes was measured with liquid scintillation counting.

Results: The expression of mutant Htt-552 in the astrocytes significantly decreased both the mRNA and protein levels of GLT-1 but not those of GLAST. Furthermore, Htt-552 significantly reduced [^{3}H]glutamate uptake by the astrocytes. Treatment with the autophagy inhibitor 3-MA (10 mmol/L) significantly increased the accumulation of mutant Htt-552, and reduced the expression of GLT-1 and [^{3}H]glutamate uptake in the astrocytes. Treatment with the autophagy stimulator rapamycin (0.2 mg/mL) significantly reduced the accumulation of mutant Htt-552, and reversed the changes in GLT-1 expression and [^{3}H]glutamate uptake in the astrocytes.

Conclusion: Rapamcin, an autophagy stimulator, can prevent the suppression of GLT-1 expression and glutamate uptake by mutant Htt-552 in cultured astrocytes.

Keywords: Huntington's disease; huntingtin-552; GLT-1; glutamate uptake; autophagy; rapamycin; 3-MA

Acta Pharmacologica Sinica (2012) 33: 385–392; doi: 10.1038/aps.2011.162; published online 23 Jan 2012

Introduction

Huntington's disease (HD) is a neurological disorder that is caused by an expansion of a polyglutamine tract in the protein huntingtin (Htt). Although mutant huntingtin is widely expressed in neuronal and non-neuronal cells, it preferentially accumulates in striatal neurons and causes neurodegeneration in the brain[1]. This phenomenon has led to extensive studies of mutant huntingtin on neurons. Later studies have found that in a neuron-glia co-culture system, wild-type glial cells protect neurons against neurotoxicity caused by mutant Htt, whereas glial cells expressing mutant Htt increased neuronal vulnerability[2]. These studies indicate that cell-cell interactions between neurons and glial cells play an important role in HD pathology[3, 4]. In addition, mutant Htt expressed in glial cells could exacerbate neurological symptoms in HD transgenic mice, so the role of glial cells in HD neuropathology should not be neglected[5].

Recently, some studies have proven that the selective degeneration of striatal neurons is relevant to dysfunctional glial protective mechanisms in HD pathology[2, 6]. On the membranes of astrocytes, which are the major subtype of glial cells, there are two types of glutamate transporters (GLT-1 and GLAST) that do most of the work in clearing extracellular excitatory neurotransmitters[7, 8]. It has been shown that small fragments of N-terminal mutant Htt (such as N-208, N-171), which were reported to be more pathogenic than full-length mutant Htt, caused decreased expression of GLT-1[2, 5]. However, these fragments had been cut occasionally and might not exist in physiological and pathological conditions, so they could not simulate the condition of HD patients completely. In this study, a termination codon was inserted into Htt at the N-terminal 552 amino acid of caspase2/3 and generated a truncated Htt fragment 1-552 aa (Htt-552). Mutant Htt-552 had been found in the brains of HD patients, which allows us

* To whom correspondence should be addressed.
E-mail bluestonelin@hotmail.com
Received 2011-07-04 Accepted 2011-11-03

to achieve a similar pathological condition of HD. Moreover, we intended to find out if mutant Htt-552 expressed in cultured astrocytes had the same effects as N-208 and N-171.

It was reported that the decreased glutamate uptake in astrocytes was mainly caused by the decreased expression of GLT-1, which has a gene promoter that carries multiple Sp1 binding sites[9]. The transcription of GLT-1 was Sp1-dependent, and it had been reported that mutant Htt bound more Sp1 and reduced Sp1-mediated GLT-1 expression in astrocytes. This could lead to defective glial glutamate uptake and increased neuronal excitotoxicity[10]. Therefore, we want to know if the expression of GLT-1 would return to a normal level after mutant Htt had been cleared.

Autophagy is a major degradation pathway for misfolded proteins, especially for long-lived proteins. It was reported that enhancing autophagy with rapamycin treatment increased mutant huntingtin clearance and decreased the levels of soluble proteins and aggregates in HD cell models[11]. In contrast, inhibition of autophagy during autophagosome formation by 3-MA decreased mutant huntingtin clearance and increased the levels of soluble and aggregated mutant huntingtin[12]. In our previous studies, we also found that activated autophagy could clear mutant Htt effectively[13]. Therefore, in this study, we used rapamycin, an autophagy activator, to enhance autophagy in astrocytes and to investigate if the expression of GLT-1 could be returned to its initial level.

Materials and methods

Reagents

Huntingtin antibody (1:2000, Cat.MAB2166, Chemicon, Billerica, MA, USA); β-actin antibody (1:5000, Cat.A5441, Sigma, St Louis, MO, USA); LC3 antibody (1:1000, Cat.Ab62721, Abcam, University of Cambridge, UK); p62 antibody (1:2000, Cat.PW9860, Enzo Life Science, Lausen, CH, USA); GFAP (1:2000, Cat.c9205, Sigma, St Louis, MO, USA); DAPI (1:10000, Cat. D9564, Sigma, St Louis, MO, USA); GLT-1 (1:3000, Cat. ab58571, Abcam, University of Cambridge, UK); GLAST (1:5000, Cat.ab416, Abcam, University of Cambridge, UK); Cy3-conjugated anti-mouse IgG and HRP-conjugated anti-mouse IgG (1:5000, Cat 715-165-150 and Cat 715-035-1500, Jackson ImmunoResearch, West Grove, PA, USA); rapamycin (Cat. R0395, Sigma, St Louis, MO, USA); 3-MA (3-methyladenine, Cat. M9281, Sigma, St Louis, MO, USA); DHK (dihydrokainate, Cat.D1064, Sigma, St Louis, MO, USA); and [^{3}H]glutamate (Cat.NET1082250UC, Perkin Elmer, Waltham, MA, USA) were used in this study.

Primary astrocyte culture

Primary astrocyte cultures were prepared from the cortex of 1- to 2-day-old postnatal SD rat pups as described in a previous study[14]. The ethical committee of Soochow University approved this study. Microglial cells were dissociated from the culture by shaking cultured glial cells. An immunoassay with antibodies against GFAP was used to identify the purity of the astrocytes.

Western blot analysis

Astrocytes were harvested 24 h, 48 h, or 72 h after infection. The boiled samples (each containing 10–20 μg of protein) were subjected to SDS-PAGE on a 10% acrylamide gel and transferred to nitrocellulose membranes (Bio-Rad, Hercules, CA, USA). The membranes were blocked for 1 h in TBST containing 5% non-fat milk. The membranes were then incubated with mouse anti-Htt monoclonal antibody 2166 (1:2000, Chemicon) at 4 °C overnight, incubated with horseradish peroxidase-conjugated donkey anti-mouse IgG secondary antibody (Sigma) at a dilution of 1:5000 for 2 h and finally visualized with an enhanced chemiluminescence (ECL) kit (Shanghai Sangon Biological Engineering Technology, Shanghai, China) according to the manufacturer's protocol.

Real-time PCR

The real-time PCR experiments were performed according to the protocol of the Real-time PCR kit (Cat.DRR041A, TAKARA). The primers were as follows: GAPDH: forward primer: 5′-gacaactttggcatcgtgga-3′, reverse primer: 5′-atgcaggatgatgttctgg-3′; GLAST: forward primer: 5′-gcctttgtgctactcaccgtca-3′, reverse primer: 5′-ctgcagcatccgcatcaga-3′; GLT-1: forward primer: 5′-gcaggtggaagtgcgcatgcac-3′, reverse primer: 5′-cacatactgctcccaggatgaca-3′.

Glutamate uptake assay

After being infected with Ad-Htt-552-18Q, Ad-Htt-552-100Q, or Ad-null, the astrocytes were washed with normal saline. Half of the cells were pre-incubated with 1 mmol/L dihydrokainate (DHK; Sigma Aldrich) for 1 h at 37 °C, and the other half were pre-incubated without DHK treatment. After pre-incubation, [^{3}H]glutamate at a concentration of 25 nmol/L was added into the solution and incubated for 15 min. The incubation was terminated by rapidly removing the solution, and the astrocytes were washed with 4 mL of ice-cold normal saline three times. The astrocytes were lysed in 0.3% NaOH with sonication, and the radioactivity was determined by using a liquid scintillation counter (Perkin Elmer, Waltham, MA, USA). The protein concentration was measured to normalize the scintillation counting results. The astrocytes pre-incubated with 10 mmol/L of unlabeled glutamate served as a control to obtain a background value. The difference between the DHK-treated and non-treated samples was obtained and reflected GLT-1–specific glutamate uptake (nmol·mg protein^{-1}·15 min^{-1}).

Statistical analysis

Statistical significance was assessed by using one-way ANOVA with the Newman-Keuls multiple comparison test. Calculations were performed using Sigma Plot 4.11 and Prism (version 4) software. Statistical significance was considered when $P<0.05$.

Results

Expression of Htt-552 in cultured primary astrocytes

The purity of astrocytes reached approximately 98% and met

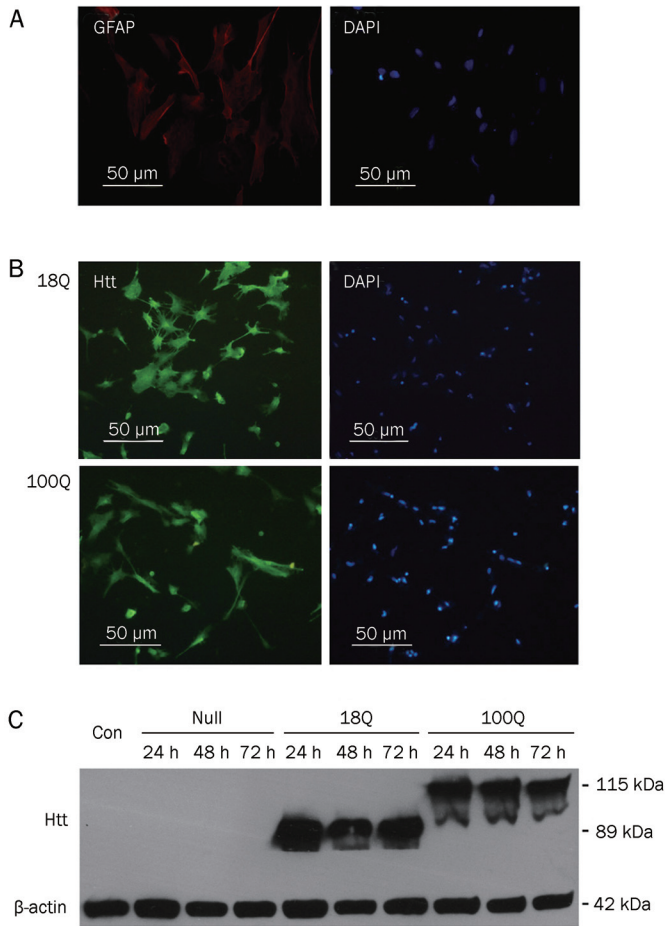

Figure 1. Expression of Htt-552 in cultured astrocytes. (A) Astrocytes were collected from 1- to 2-day-old postnatal rats and purified to the third generation. GFAP is a marker of astrocytes. DAPI stains cell nuclei. Immunofluorescence labeling showed more than 98% of the GFAP-positive (red) astrocytes. (B) Immunofluorescent images of cultured glial cells that were infected with Ad-Htt-552-18Q (wild type Htt) or Ad-Htt-552-100Q (mutant Htt) for 24 h show that the ratio of Htt-positive cells to DAPI-positive cells is almost 80%. (C) Western blotting analysis of Htt-552 in cultured astrocytes 24, 48, and 72 h after infection, showing persistent expression of wild type Htt and mutant Htt.

our study's needs (Figure 1A). The astrocytes were harvested after being infected with Ad-Htt-552-18Q or Ad-Htt-552-100Q for 24 h, 48 h, or 72 h. Then immunohistochemistry staining and Western blot analysis were performed to identify the expression of wild-type Htt (Htt-552-18Q) and mutant Htt (Htt-552-100Q) in the astrocytes. The proper ratio of infection is very important to this study. We found that the adenoviral tier, which resulted in 80% of the cultured astrocytes expressing mutant Htt, was thought to be ideal (Figure 1B). Western blot analysis showed that persistent stable expression of Htt in the astrocytes lasted for at least 72 h after infection (Figure 1C).

Decreased expression of GLT-1 and glutamate uptake in astrocytes

Western blot analysis revealed decreased expression of GLT-1 in astrocytes expressing mutant Htt (Ad-Htt-552-100Q), and the decreased expression of GLT-1 appeared to correlate with the time-dependent expression of mutant Htt in astrocytes (Figure 2A). However, the level of expression of GLAST appeared to be variable in astrocytes but not significantly decreased (Figure 2C). Real-time PCR confirmed that GLT-1 transcripts were significantly reduced in astrocytes expressing mutant Htt for 48 or 72 h (Figure 2B), while GLAST transcripts showed no significant changes (Figure 2D). There was no obvious effect on either GLT-1 mRNA or GLT-1 proteins by wild-type Htt expression (Ad-Htt-552-18Q).

An interesting question is whether fewer glutamate transporters could alter glutamate uptake in astrocytes. We decided to infect astrocytes with Ad-null, Ad-Htt-552-18Q or Ad-Htt-100Q for 72 h and then measure their uptake of [^{3}H]glutamate as described in the methods section. The result showed significantly decreased glutamate uptake in astrocytes expressing mutant Htt, which was closely correlated with altered expression of GLT-1 (Figure 2E). It was reported that DHK could specifically inhibit the activity of GLT-1 in astrocytes[15]. After infecting the astrocytes with Ad-null, Ad-Htt-552-18Q or Ad-Htt-552-100Q for 72 h, we pre-incubated the astrocytes with 1 mmol/L DHK for 1 h at 37 °C, and the control was pre-incubated without DHK treatment. The difference between the astrocytes that received the DHK treatment and those that did not received the DHK treatment revealed the specific contribution of GLT-1 to transporting [^{3}H]glutamate. Consistent with the decreased expression of GLT-1, GLT-1-specific glutamate uptake was more significantly decreased in astrocytes expressing mutant Htt, demonstrating a close association between GLT-1 expression and glutamate uptake in astrocytes.

Enhancing Htt clearance by activation of autophagy

After transfection of cells with Ad-Htt-552-18Q or Ad-Htt-552-100Q for 48 h, the cells were treated with rapamycin (0.2 μg/mL), an activator of autophagy, or 3-MA (10 mmol/L), an inhibitor of autophagy. The astrocytes were then harvested for Western blot analysis 24 h later. The microtubule-associated protein 1A/1B-light chain 3 (LC3) is thought to be an autophagic marker[16]. An increased ratio of LC3II to LC3I was observed when the astrocytes were treated with rapamycin. On the contrary, when infected astrocytes were treated with 3-MA, the expression of LC3II did not seem to change significantly. But compared with the control, the expression of LC3I increased, so the rate of LC3II/LC3I decreased. These results suggested that autophagy was activated by rapamycin and inhibited by 3-MA (Figure 3A). p62/SQSTM1 is an ubiquitin- and LC3-binding protein that could be degraded by autophagy and is thought to be a substrate of autophagy[17]. We found that the amount of p62 was decreased when cells were treated with rapamycin (100Q-rap *vs* 100Q) (Figure 3B), while the amount of p62 was increased when cells were treated with 3-MA (100Q-3-MA *vs* 100Q) (Figure 3C). These results confirmed that autophagy was enhanced by rapamycin and inhibited by 3-MA.

Furthermore, we detected the protein levels of Htt. Western

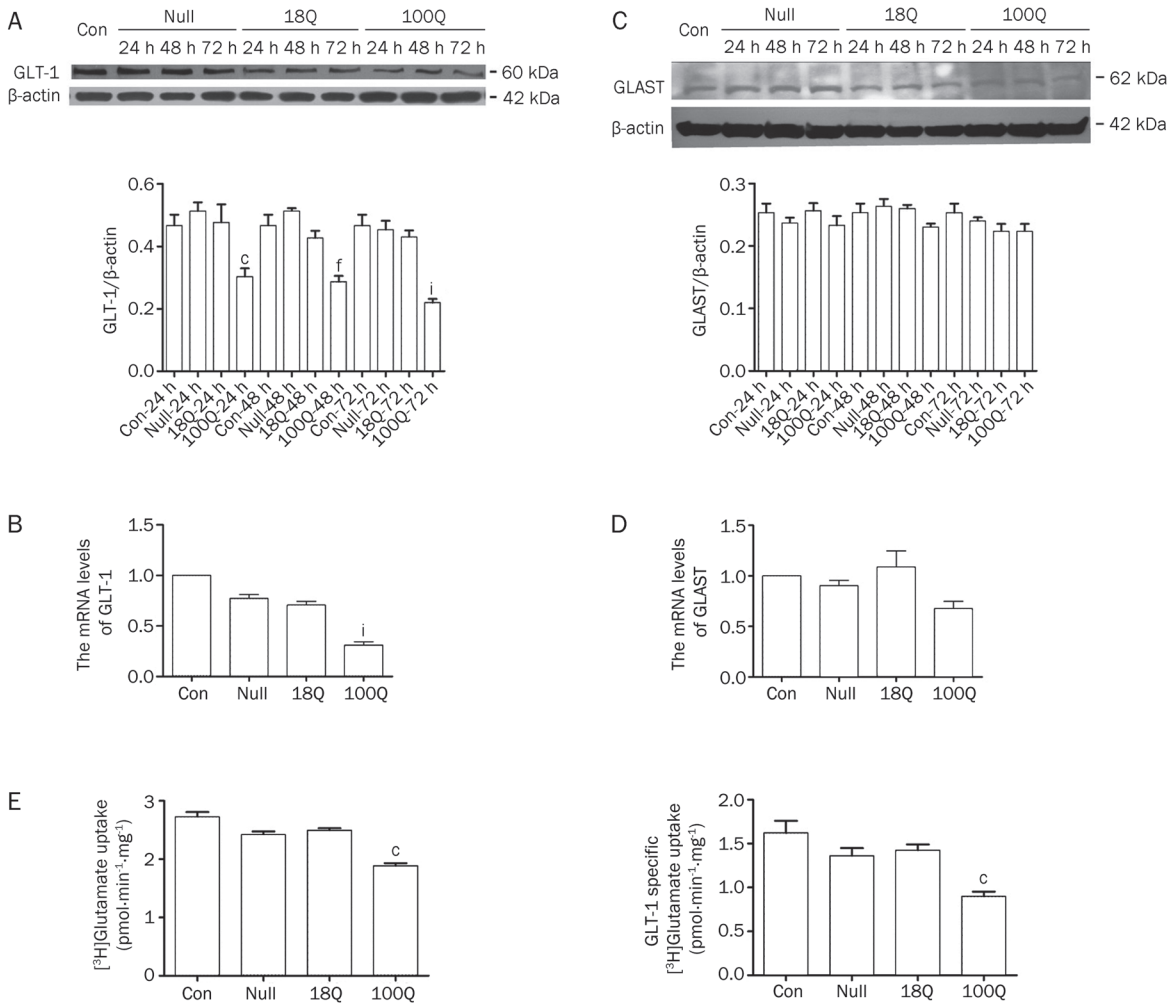

Figure 2. Decreased expression of GLT-1 and glutamate uptake in astrocytes. Cultured astrocytes were harvested after expression of Htt-552 for 24, 48, or 72 h. The results are shown as means±SD (n=3). (A) Western blotting analysis was performed, showing decreased expression of GLT-1 in astrocytes expressing mutant Htt. ^{c}P<0.01, 100Q-24 h *vs* (con-24 h, null-24 h, 18Q-24 h); ^{f}P<0.01, 100Q-48 h *vs* (con-48 h, null-48 h, 18Q-48 h); ^{i}P<0.01, 100Q-72 h *vs* (con-72 h, null-72 h, 18Q-72 h). (B) The total RNA in astrocytes was extracted after expression of Htt-552 for 72 h. Real-time PCR showed decreased GLT-1 transcription in astrocytes expressing mutant Htt for 72 h (^{i}P<0.01 compared with con, null and 18Q). (C) Western blotting analysis showed no significant difference in the expression of GLAST in astrocytes after expression of mutant and wild-type Htt-552. (D) The total RNA in astrocytes was extracted after expression of Htt-552 for 72 h. Real-time PCR showed no significant difference in GLAST mRNA levels in astrocytes. (E) Decreased glutamate uptake by astrocytes expressing mutant Htt. GLT-1-specific glutamate uptake was significantly decreased in astrocytes expressing mutant Htt (^{c}P<0.01, 100Q *vs* cont, null, 18Q), as well as the total uptake level (^{c}P<0.01, 100Q vs cont, null, 18Q). After expression of Htt-552 for 72 h, the astrocytes were pre-incubated with 1 mmol/L DHK (specific inhibitor of GLT-1) for 1 h at 37 ºC , and GLT-1-specific glutamate uptake was determined (one-way ANOVA with Newman-Keuls multiple comparison test).

blot analysis showed a significant reduction of mutant Htt when autophagy was stimulated (100Q-rap *vs* 100Q) (Figure 3B), and a significant accumulation of mutant Htt was observed when autophagy was inhibited (100Q-3-MA *vs* 100Q) (Figure 3C).

Recovery of GLT-1 expression and function by rapamycin

It has been reported that the decreased expression of GLT-1 had been mainly caused by mutant Htt. As the mutant Htt is cleared by enhanced autophagy, could the expression of GLT-1 be resumed? In this study, we detected the expression of GLT-1 and glutamate uptake by astrocytes after treatment with rapamycin. Western blot analysis showed a recovery of GLT-1 levels in astrocytes when autophagy was activated by rapamycin (Figure 4A). With the treatment of 3-MA, which could inhibit the activity of autophagy, the decrease in expression of GLT-1 appeared to be exacerbated (Figure 4B). At the same time, uptake of [^{3}H]glutamate by astrocytes infected with Htt-552 in the presence of rapamycin or 3-MA was determined. The result showed a recovery of glutamate uptake by astrocytes after treatment with rapamycin. In contrast, treatment with 3-MA slightly accelerated the decline of [^{3}H]glutamate uptake in astrocytes expressing mutant Htt-552, but the effect was not as significant (Figure 4C).

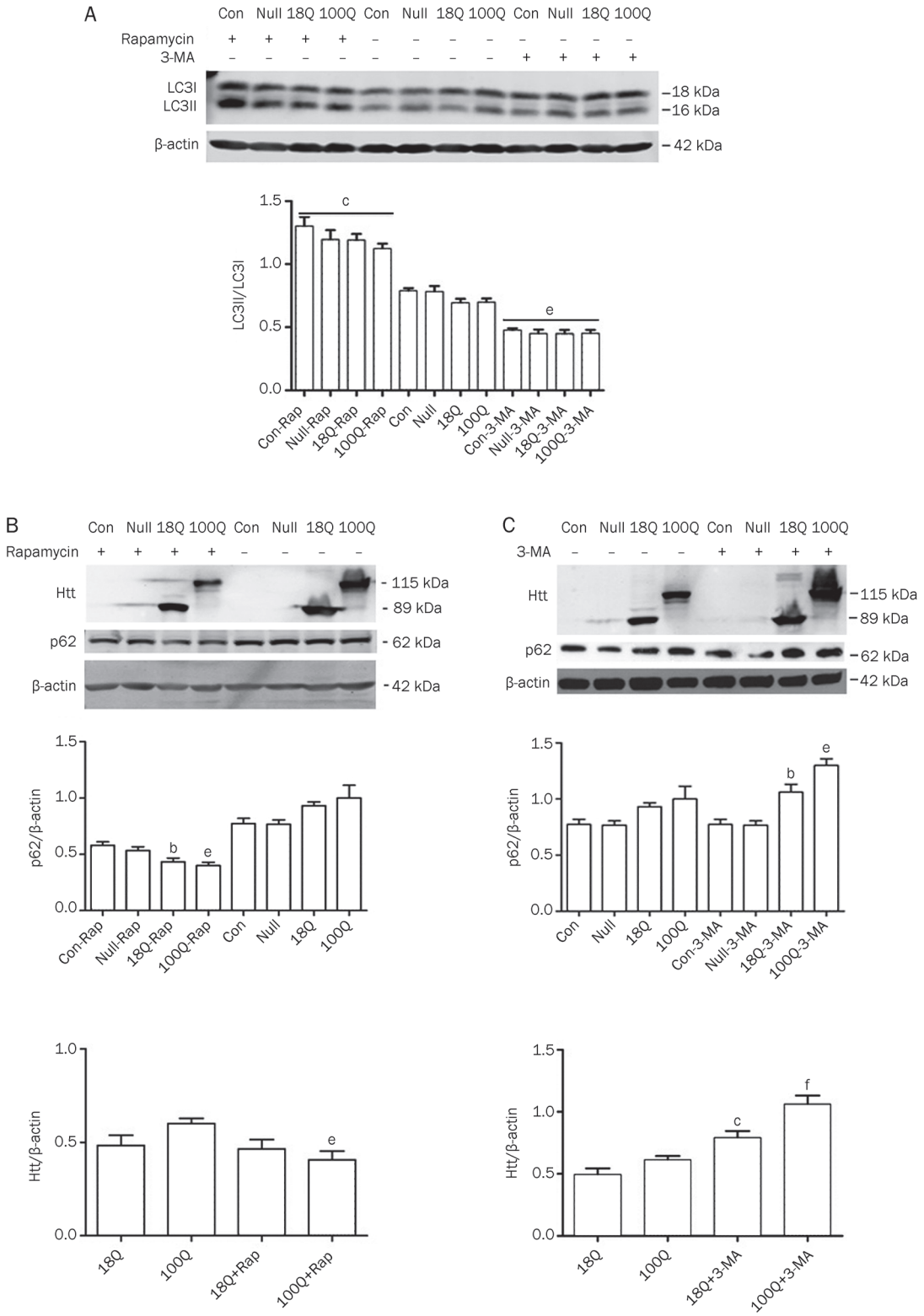

Figure 3. Mutant Htt-552 was reduced by enhanced autophagy. (A) Astrocytes were harvested after being infected for 72 h and treated with rapamycin (0.2 μg/mL) or 3-MA (10 mmol/L) for the last 24 h. Western blotting results showed increased LC3II/LC3I with treatment of rapamycin and decreased LC3II/LC3I with the treatment of 3-MA (^{c}P<0.01, rapamycin treatment *vs* control; ^{e}P<0.05, 3-MA treatment *vs* control). (B) Western blotting results showed p62 expression level were decreased (^{b}P<0.05, 18Q-Rap *vs* 18Q, ^{e}P<0.05, 100Q-Rap *vs* 100Q) and the level of mutant Htt decreased with rapamycin treatment (^{e}P<0.05, 100Q-Rap *vs* 100Q). (C) Western blotting results showed P62 expression level were increased (^{b}P<0.05, 18Q-3-MA *vs* 18Q; ^{e}P<0.05, 100Q-3-MA *vs* 100Q) and the level of Htt increased (^{c}P<0.01, 18Q-3-MA *vs* 18Q; ^{f}P<0.001, 100Q-3-MA *vs* 100Q) with 3-MA treatment.

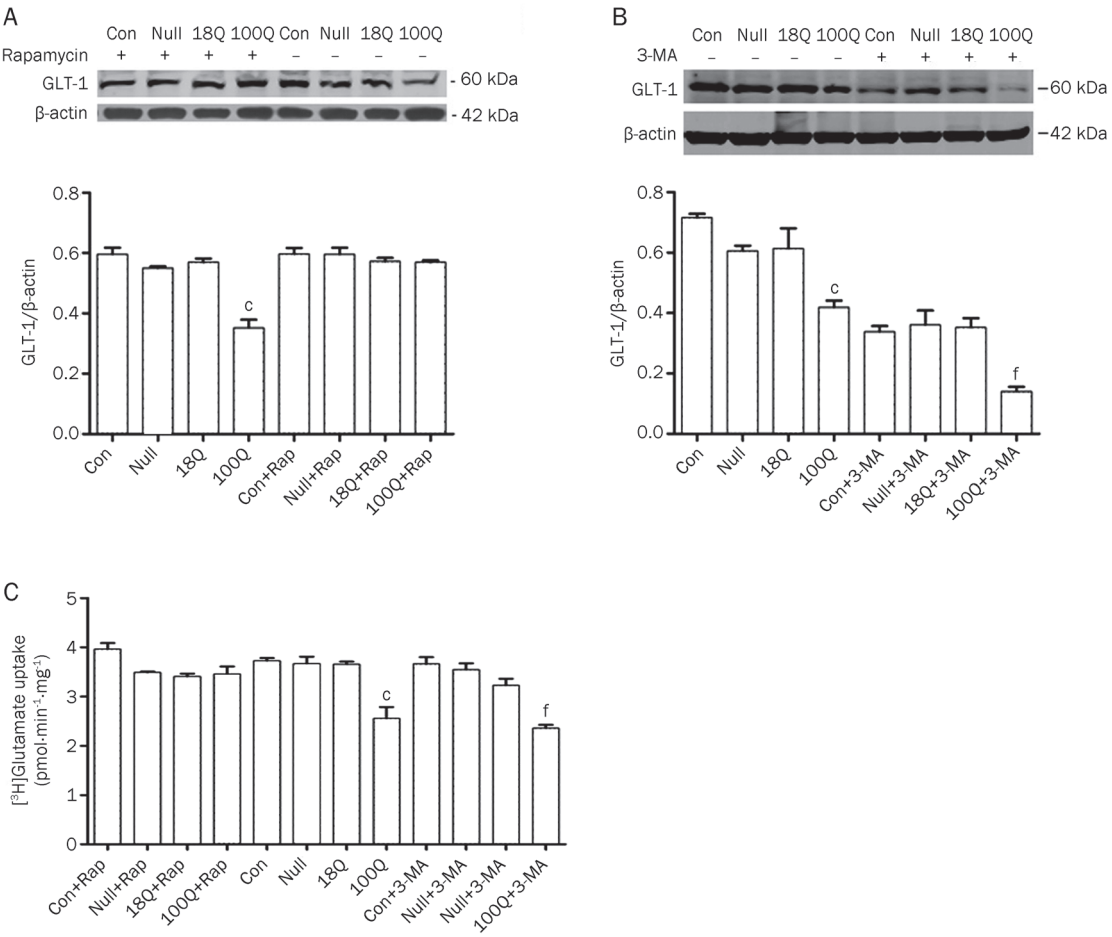

Figure 4. Recovered expression of GLT-1 and glutamate uptake by autophagy stimulator. The densities of respective protein bands in each group were analyzed with Sigma Scan Pro 5, and β-actin was used as a reference. All the results are shown as mean±SD (n=3). (A) Astrocytes were harvested after being infected for 72 h and treated with rapamycin (0.2 μg/mL) during the last 24 h. (A) Western blotting showing recovery of GLT-1 expression with stimulation of autophagy (^{c}P<0.01, 100Q-Rap *vs* 100Q). (B) Astrocytes were harvested after being infected for 72 h and treated with 3-MA during the last 24 h. Western blotting analysis showed decreased expression of GLT-1 with 3-MA treatment . ^{f}P<0.01, 100Q-3-MA *vs* (con-3-MA, null-3-MA, 18Q-3-MA); ^{c}P<0.01, 100Q *vs* (con, null, 18Q). (C) Glutamate uptake was recovered by astrocytes expressing mutant Htt after treatment with rapamycin but not with 3-MA. Astrocytes were harvested after expression of Htt-552 for 72 h and treated with rapamycin (0.2 μg/mL) or 3-MA (10 mmol/L) for the last 24 h, followed with incubation with [^{3}H]glutamate for 15 min as described in the methods section. ^{f}P<0.01, 100Q-3-MA *vs* (con-3-MA, null-3-MA, 18Q-3-MA); ^{c}P<0.01, 100Q *vs* (con, null, 18Q).

Discussion

In HD, mutant Htt is expressed in various types of cells, including neurons and non-neuronal cells, but it preferentially aggregates in striatal neurons and causes dysfunction in striatal neurons. There are two possible explanations for this phenomenon. First, compared with glial cells, lower and impaired neuronal ubiquitin-proteasome system activity, which plays a critical role in clearing misfolded proteins[18], may account for the preferential accumulation of misfolded Htt in neurons as well as their selective vulnerability[19–21]. Second, the expression of mutant huntingtin in glial cells, which could clear excess excitatory neurotransmitters from extracellular space, contributed to neuronal excitotoxicity[2, 5, 22, 23].

In this paper, we intended to find out the effect of Htt-552, the fragment of Htt that exists in physiological and pathological conditions, on glutamate uptake in astrocytes. GLT-1 and GLAST, two important types of glutamate transporters that are primarily expressed in astrocytes, were thought to be the predominant glutamate transporters and did the most work to clear extracellular excitatory glutamate[8]. Previous studies showed that mutant Htt expressed in astrocytes caused decreased GLT-1 both in HD mouse brains and in cultured glial cells, but there was no report about mutant Htt-552, which existed in the brains of HD patients. Consistent with prior research, we have provided direct evidence that mutant Htt-552 in glial cells reduced the expression of GLT-1 but not of GLAST and decreased glutamate uptake in astrocytes, which was mainly caused by decreased expression of GLT-1. Because there are Sp1-binding sites in the promoter of GLT-1 and the transcription of GLT-1 is Sp1-dependent[24, 25], previous reports of mutant Htt binding more Sp1 and reducing Sp1-mediated GLT-1 expression in astrocytes may explain this

phenomenon[10].

Autophagy is thought to be involved in neurodegenerative diseases[26], such as HD[27–29], Parkinson's disease[30–33], and Alzheimer's disease[34–36]. It is a major degradation pathway for long-lived misfolded proteins, such as mutant Htt in HD. In this study, we used rapamycin, an enhancer of autophagy, to activate autophagy. Although autophagy could be slightly activated by mutant Htt, which might be the normal stress reaction of astrocytes, the effect of rapamycin would be more powerful. The present study showed that the expression and the glutamate uptake function of GLT-1 could be resumed after reducing mutant Htt-552 levels by stimulating autophagy. On the basis of our results, we postulated that a reduction in mutant Htt levels would increase the availability of Sp1 to the GLT-1 promoter and increase GLT-1 transcription back to initial levels. The dysfunction of the glutamate transporter GLT-1 caused by mutant Htt can be returned to normal after clearing mutant Htt. Our results give futher evidence for enhancing clearance of mutant Htt by autophagy may protect neurons survival by lower excitotoxicity in Huntington's disease[37].

Acknowledgements

We thank Prof Hai-yan LIU at Soochow University for providing help in the measurement of [^{3}H]-glutamate. This work is supported by grants from the National Natural Science Foundation of China (No 30600197).

Author contribution

Dr Fang LIN designed the research; Lei-lei CHEN, Jun-chao WU, and Lin-hui WANG performed the research; Dr Zheng-Hong QIN, Dr Marian DIFIGILA, and Dr Jin WANG revised the paper.

References

1 Li H, Li S, Johnston H, Shelbourne P, Li X. Amino-terminal fragments of mutant huntingtin show selective accumulation in striatal neurons and synaptic toxicity, Nat Genet 2000; 25: 385–9.
2 Shin JY, Fang ZH, Yu ZX, Wang CE, Li SH, Li XJ. Expression of mutant huntingtin in glial cells contributes to neuronal excitotoxicity. J Cell Biol 2005; 171: 1001–12.
3 Gu X, Li C, Wei W, Lo V, Gong S, Li S, *et al*. Pathological cell-cell interactions elicited by a neuropathogenic form of mutant Huntingtin contribute to cortical pathogenesis in HD mice. Neuron 2005; 46: 433–44.
4 Gu X, Andre V, Cepeda C, Li S, Li X, Levine M, *et al*. Pathological cell-cell interactions are necessary for striatal pathogenesis in a conditional mouse model of Huntington's disease. Mol Neurodegener 2007; 2: 8.
5 Bradford J, Shin JY, Roberts M, Wang CE, Sheng G, Li S, *et al*. Mutant huntingtin in glial cells exacerbates neurological symptoms of Huntington disease mice. J Biol Chem 2010; 285: 10653–61.
6 Maragakis NJ, eeRothstein JD. Glutamate transporters in neurologic disease. Arch Neurol 2001; 58 : 365–70.
7 Faideau M, Kim J, Cormier K, Gilmore R, Welch M, Auregan G, *et al*. *In vivo* expression of polyglutamine-expanded huntingtin by mouse striatal astrocytes impairs glutamate transport: a correlation with Huntington's disease subjects. Hum Mol Genet 2010; 19: 3053–7.
8 Rothstein JD, Dykes-Hoberg M, Pardo CA, Bristol LA, Jin L, Kuncl RW, *et al*. Knockout of glutamate transporters reveals a major role for astroglial transport in excitotoxicity and clearance of glutamate. Neuron 1996; 16: 675–86.
9 Su ZZ, Leszczyniecka M, Kang D, Sarkar D, Chao W, Volsky DJ, *et al*. Insights into glutamate transport regulation in human astrocytes: Cloning of the promoter for excitatory amino acid transporter 2 (EAAT2). Proc Natl Acad Sci U S A 2003; 100: 1955–60.
10 Bradford J, Shin JY, Roberts M, Wang CE, Li XJ, Li S. Expression of mutant huntingtin in mouse brain astrocytes causes age-dependent neurological symptoms. Proc Natl Acad Sci U S A 2009; 106:22480–5.
11 Berger Z, RavikumarB, Menzies FM, Oroz LG, Underwood BR, Pangalos MN, *et al*. Rapamycin alleviates toxicity of different aggregate-prone proteins. Hum Mol Genet 2006; 15: 433–42.
12 Ravikumar B, Rubinsztein DC. Aggregate-prone proteins with polyglutamine and polyalanine expansions are degraded by autophagy. Hum Mol Genet 2002; 11: 1107–17.
13 Qin ZH, Qin YM, Kegel KB, Kazantsev A, Apostol BL, Thompson LM, *et al*. Autophagy regulates the processing of amino terminal huntingtin fragments. Hum Mol Genet 2003; 12: 3231–44.
14 Wang LH, Lin F, Wu JC, Qin ZH. High efficiency adenovirus-mediated expression of truncated N-terminal huntingtin fragment (htt552) in primary rat astrocytes. Acta Biochim Biophys Sin 2009; 41: 325–34.
15 Kawahara K, Hosoya R, Sato H, Tanaka M, Nakajima T, Iwabuchi S. Selective blockade of astrocytic glutamate transporter GLT-1 with dihydrokainate prevents neuronal death during ouabain treatment of astrocyte/neuron cocultures. Glia 2002; 40: 337–49.
16 Tanida I, UenoT, Kominami E. LC3 and Autophagy. Methods Mol Biol 2008; 445: 77–88.
17 Pankiv S, Clausen TH, Lamark T, Brech A, Bruun JA, Outzen H, *et al*. p62/SQSTM1 binds directly to Atg8/LC3 to facilitate degradation of ubiquitinated protein aggregates by autophagy. J Biol Chem 2007; 282: 24131–45.
18 Li H, Li XJ, Li S. Clearance of mutant huntingtin. Autophagy 2010; 6: 663–4.
19 Tydlacka S, Wang CE, Wang X, Li S, Li XJ. Differential activities of the ubiquitin-proteasome system in neurons versus glia may account for the preferential accumulation of misfolded proteins in neurons. J Neurosci 2008; 28: 13285–95.
20 Wang J, Wang CE, Orr A, Tydlacka S, Li S, Li XJ. Impaired ubiquitin-proteasome system activity in the synapses of Huntington's disease mice. J Cell Biol 2008; 180: 1177–89.
21 Bennett EJ, Shaler TA, Woodman B, Ryu KY, Zaitseva TS, Becker CH, *et al*. Global changes to the ubiquitin system in Huntington's disease. Nature 2007; 448: 704–8.
22 Brusilow WSA. Is Huntington's a glutamine storage disease? Neuroscientist 2006; 12: 300–4.
23 McBride JL, Ramaswamy S, Gasmi M, Bartus RT, Herzog CD, Brandon EP, *et al*. Viral delivery of glial cell line-derived neurotrophic factor improves behavior and protects striatal neurons in a mouse model of Huntington's disease. Proc Natl Acad Sci U S A 2006; 103: 9345–50.
24 Dunah AW, Jeong H, Griffin A, Kim YM, Standaert DG, Hersch SM, *et al*. Sp1 and TAFII130 transcriptional activity disrupted in early Huntington's disease. Science 2002; 296: 2238–43.
25 Li S, Cheng AL, Zhou H, Lam S, Rao M, Li H, *et al*. Interaction of Huntington disease protein with transcriptional activator Sp1. Mol Cell Biol 2002; 22: 1277–87.
26 Hara T, Nakamura K, Matsui M, Yamamoto A, Nakahara Y, Suzuki-Migishima R, *et al*. Suppression of basal autophagy in neural cells causes neurodegenerative disease in mice. Nature 2006; 441:

885–9.
27 Sarkar S, Rubinsztein DC. Huntington's disease: degradation of mutant huntingtin by autophagy. FEBS J 2008; 275: 4263–70.
28 Heng MY, Detloff PJ, Paulson HL, Albin RL. Early alterations of autophagy in Huntington disease-like mice. Autophagy 2010; 6: 1206–8.
29 Bauer PO, Nukina N. Enhanced degradation of mutant huntingtin by rho kinase inhibition is mediated through activation of proteasome and macroautophagy. Autophagy 2009; 5: 747–8.
30 Pan T, Rawal P, Wu Y, Xie W, Jankovic J, Le W. Rapamycin protects against rotenone-induced apoptosis through autophagy induction. Neuroscience 2009; 164: 541–51.
31 Dadakhujaev S, Noh HS, Jung EJ, Cha JY, Baek SM, Ha JH, *et al*. Autophagy protects the rotenone-induced cell death in alpha-synuclein overexpressing SH-SY5Y cells. Neurosci Lett 2009; 472: 47–52.
32 Winslow AR, Chen CW, Corrochano S, Acevedo-Arozena A, Gordon DE, Peden AA, *et al*. Rubinsztein DC, α-Synuclein impairs macroautophagy: implications for Parkinson's disease. J Cell Biol 2010; 190: 1023–37.
33 Webb JL, Ravikumar B, Atkins J, Skepper JN, Rubinsztein DC. Alpha–synuclein is degraded by both autophagy and the proteasome. J Biol Chem 2003; 278: 25009–13.
34 Yang DS, Lee JH, Nixon RA. Monitoring autophagy in Alzheimer's disease and related neurodegenerative diseases. Methods Enzymol 2009; 453: 111–44.
35 Boland B, Kumar A, Lee S, Platt FM, Wegiel J, Yu WH, *et al*. Autophagy induction and autophagosome clearance in neurons: relationship to autophagic pathology in Alzheimer's disease. J Neurosci 2008; 28: 6926–37.
36 Nixon RA, Yang DS. Autophagy failure in Alzheimer's disease-locating the primary defect. Neurobiol Dis 2011; 43: 38–45.
37 Ravikumar B, Vacher C, Berger Z, Davies JE, Luo S, Oroz LG, *et al*. Inhibition of mTOR induces autophagy and reduces toxicity of polyglutamine expansions in fly and mouse models of Huntington disease. Nat Genet 2004; 36: 585–95.

Acta Pharmacologica Sinica (2012) 33: 393–400
 1671-4083/12 $32.00
www.nature.com/aps

Original Article

High-sodium intake aggravates myocardial injuries induced by aldosterone via oxidative stress in Sprague-Dawley rats

Jing-yi LI[1, $], Shao-ling ZHANG[1], Meng REN[1], Yan-ling WEN[2], Li YAN[1], Hua CHENG[1, *]

[1]Department of Endocrinology, The Second Affiliated Hospital, Sun Yat-sen University, Guangzhou 510120, China; [2]Department of Ultrasound, The Second Affiliated Hospital, Sun Yat-sen University, Guangzhou 510120, China

Aim: To evaluate the effects of aldosterone with or without high sodium intake on blood pressure, myocardial structure and left ventricular function in rats, and to investigate the mechanisms underlying the effects.
Methods: Eight-week-old male Sprague-Dawley rats were randomly divided into 3 groups: (1) control (CON) group fed a normal sodium diet, (2) aldosterone (ALD) group receiving aldosterone infusion and a normal sodium diet, and (3) high sodium plus aldosterone (HS-ALD) group receiving 1% NaCl diet in conjunction with aldosterone infusion. Aldosterone was administered through continuously subcutaneous infusion with osmotic minipump at the rate of 0.75 μg/h for 8 weeks. The myocardium structure was observed using transthoracic echocardiography and transmission electron microscopy. The collagen deposition in left ventricle was evaluated with Masson's trichrome staining. The expression of IL-18, p22phox, and p47phox proteins was examined using Western blot analysis.
Results: The systolic blood pressure in the ALD and HS-ALD groups was significantly higher than that in the CON group after 2-week treatment. But the blood pressure showed no significant difference between the HS-ALD and ALD groups. The left ventricular hypertrophy, myocardial collagen deposition and oxidative stress were predominantly found in the HS-ALD and ALD group. Furthermore, the breakdown of myocardial structure and oxidative stress were more apparent in the HS-ALD group as compared with those in the ALD group.
Conclusion: Long-term infusion of aldosterone results in hypertension and profibrotic cardiovascular responses in rats fed a normal sodium diet, which were mediated by oxidative stress. High-sodium intake could aggravate myocardial injuries induced by aldosterone.

Keywords: sodium intake; aldosterone; blood pressure; myocardial injury; left ventricular hypertrophy; oxidative stress

Acta Pharmacologica Sinica (2012) 33: 393–400; doi: 10.1038/aps.2011.179; published online 23 Jan 2012

Introduction

A series of recent studies have revealed that patients with primary aldosteronism have higher incidence of cardiovascular complications compared with demographically and hemodynamically similar essential hypertension patients[1]. Furthermore, two clinical trials, the randomized aldactone evaluation study (RALES)[2] and the eplerenone post-acute myocardial infarction heart failure efficacy and survival study (EPHESUS)[3], have shown that mineralocorticoid receptor (MR) antagonists reduce mortality in patients with heart failure.

Experimental studies have shown that the combined administration of aldosterone and high sodium in uninephrectomized rats induces cardiovascular injuries[4, 5]. However, it has remained unclear whether the cardiac injury was due to the direct action of aldosterone, the sodium loading or uninephrectomy. The contribution of dietary sodium intake is illustrated by the finding that the nitric oxide synthase inhibitor N^{ω}-nitro-*L*-arginine methyl ester (*L*-NAME)/angiotensin II treated animals fed a low-salt diet do not develop vascular damage, even though plasma aldosterone levels were 10-fold higher than those of animals on a high-salt diet, suggesting that blood levels of aldosterone alone are insufficient to cause vascular injury on a low-salt diet[6]. In modern society, humans could easily increase sodium intake via food diversity[7]. Little information is available concerning the effect of excess aldosterone on cardiac injury of rats on a normal sodium diet. To clarify these issues, we performed experiments to evaluate the effects of chronic subcutaneous aldosterone infusion with or without the addition of 1% sodium chloride on blood pressure, myo-

[$] At present in the Department of Endocrinology, The first Affiliated Hospital, Tsinghua University, Beijing 100016, China
* To whom correspondence should be addressed.
E-mail hcheng4374@21cn.com
Received 2011-08-22 Accepted 2011-11-24

cardial structure and left ventricular (LV) function in normotensive Sprague-Dawley (SD) rats.

Materials and methods

Animals model

This study was approved by the Ethics Committee of Sun Yat-sen University (Guangzhou, China). All procedures were performed in accordance with "Institutional Guidelines for Animal Research of Sun Yat-sen University" and "Guide for the Care and Use of Laboratory Animals of National Institutes of Health". Eight week-old male SD rats with an initial body weight of 260–280 g were purchased (Laboratory Animal Center of Sun Yat-sen University, Guangzhou, China) and used in this study. The rats were randomly divided into three groups (n=8 in each group) and assigned to one of the following protocols for 8 weeks: vehicle (CON group), excess aldosterone and a normal sodium diet (ALD group), or 1% (*w/v*) NaCl in conjunction with excess aldosterone (HS-ALD group). All of the rats were anesthetized, and implanted subcutaneously with an osmotic minipump (Alzet model 2004, DURECT Corp, Cupertino, CA, USA). The CON group received a continuously subcutaneous infusion of 5% (*v/v*) ethanol (vehicle, Sigma-Aldrich, St Louis, MO, USA). The ALD group and the HS-ALD group received continuously subcutaneous infusion of aldosterone (0.75 μg/h, Sigma-Aldrich, St Louis, MO, USA) dissolved in 5% ethanol. The mini-osmotic pumps were replaced every 4 weeks under anesthesia. In addition to standard rat chow [Na, 0.3% (*w/v*)], all of the animals had free access to tap water (the CON group and the ALD group) or 1% NaCl solution (the HS-ALD group). The animals were maintained in an environment with a constant temperature and 12 h light-dark cycles. Systolic blood pressure (SBP) was measured in conscious rats by the tail-cuff method (BP-98A; Softron Co, Tokyo, Japan) before treatment and at 1-week interval thereafter.

Echocardiographic assessment

Transthoracic echocardiographic studies were performed at week 8 using an echocardiographic system equipped with 13-MHz echocardiographic probe (Technos MPX, Biosound Esaote, Indianapolis, IN, USA). A single investigator unaware of the make-up of the experimental groups performed the task. The rats were anesthetized, and were held in the dorsal decubitus. M-mode tracings were recorded through the LV anterior and posterior walls (AW and PW, respectively) at the papillary muscle level to measure the AW thickness at end diastole, PW thickness at end diastole, LV end-diastolic dimension (LVEDD), fractional shortening (FS), and LV ejection fraction (EF). Pulse-wave Doppler spectra of mitral inflow were recorded from the apical 4-chamber view, with the sample volume placed near the tips of the mitral leaflets and adjusted to the position at which the velocity was maximal and the flow pattern laminar. Mitral inflow measurements of early and late filling velocities (E_{max} and A_{max}, respectively) were obtained. The ratio of E_{max} to A_{max} (E/A) was also recorded.

Tissue and blood collection and analysis

The rats were transferred to metabolic cages prior to the completion of the experiment. Body weight, food intake and urine volume of 24 h were recorded. The sodium and potassium in the urine and plasma were measured. The rats were then sacrificed at week 8. Blood samples from puncturing heart were collected into heparin tubes for the measurement of plasma sodium and potassium, into EDTA tubes for the measurement of plasma renin activity (PRA, RIA kit, DiaSorin, Saluggia, Italy) and into xeransis tubes for the measurement of serum aldosterone (RIA kit, Diagnostic System Laboratories, Webster, TX, USA) and 8-isoprostane (ELISA kit, Assay Designs 900-010, Assay Designs Inc, Ann Arbor, MI, USA). The hearts were divided into right ventricle (RV) and LV plus septum. Hearts was rapidly excised and weighed. The LV mass index (LVMI) was determined as the ratio of the LV mass to the body weight. Part of the left ventricle was fixed in glutaraldehyde and freshly prepared 4% (*w/v*) paraformaldehyde in phosphate buffer solution for morphometric studies. The remaining left ventricle was frozen in liquid nitrogen for later protein extraction.

Transmission electron microscopy examination for myocardial ultrastructure

Heart tissue was thinly sliced and placed in primary electron microscopy fixative. After secondary fixation, the specimens were placed on a rocker overnight, embedded, and polymerized at 60 °C for 24 h. The 85-nm thin sections were stained with 5% uranyl acetate and Sato's Triple lead stain, and then viewed by a transmission electron microscopy (TEM) (CM10, Philips, Amsterdam, Holland).

Masson's trichrome-stained method for interstitial and perivascular collagen

The middle of the LV was excised, fixed in 4% (*w/v*) paraformaldehyde, and embedded in paraffin. Sections, 5 μm thickness, were made and stained with Masson's trichrome-stained method. Collagen fibers were shown in blue, and muscles were shown in red. Ten fields in each LV section were recorded randomly by photograhy (T-B2.5XA, Nikon, Tokyo, Japan). The collagen volume fraction (CVF) was determined by measuring the area of stained blue tissue within a given field. The area stained blue was calculated as a percentage of the total area within a field. CVF examination excluded scars, artifacts, perivascular collagen areas and incomplete tissue. For each LV section, five cut cross-sectional intramyocardial coronary arteries were examined individually. The area of collagen immediately surrounding the blood vessels was calculated, and the perivascular collagen was determined as the ratio of the area of collagen surrounding the vessel wall to the total area of the vessel (perivascular collagen area/vessel luminal area, PVCA/VA). It was determined by quantitative morphometry with Image-pro plus 5.0 (Media Cybernetics, Bethesda, MD, USA). The operator was blinded to the experimental group during the analysis.

Immunohistochemical staining for ED1 expression

To evaluate the focal inflammatory infiltration of the LV myocardium, we evaluated changes in inflammatory markers. At sites of injury, infiltrating monocytes differentiate into macrophages and express ED-1. Therefore, an ED-1 monoclonal antibody (Millipore Biotechnology, Billerica, MA, working dilution 1:50) was used to identify the macrophages. For immunohistochemical staining, sections were labeled with primary antibody of mouse monoclonal antibody against ED1 after antigen retrieval. The binding of the primary antibodies was revealed by horseradish peroxidase-conjugated secondary antibodies (DAKO, Carpinteria, CA, USA) and detected with diaminobenzidine staining (DAKO, Carpinteria, CA, USA). Positive staining appeared as brown. Controls for immunospecificity were included in all experiments, and the primary antibody was replaced by phosphate buffered saline.

Western blot analysis for IL-18, p22phox, and p47phox protein expression

NADPH oxidase is a critical source of ROS production within the vascular wall and heart[8]. p22phox and p47phox subunits seem to be key molecules of NADPH oxidase[9]. In addition, IL-18 is a pleiotropic cytokine and several lines of evidence support a causal role for it in the pathogenesis of cardiovascular disease. Therefore, to demonstrate the relationship among IL-18, oxidative stress and aldosterone treatment, we analyzed the expression of IL-18, p22phox, and p47phox subunits in the LV. About 100 mg LV was homogenized in 50 mmol/l Tris buffer (pH 7.4), 150 mol/L NaCl, 1% (*v/v*) Triton X-100, 1% sodium(*w/v*) deoxycholate, 0.1% (*w/v*) SDS and some inhibitors with a homogenizer on the ice and then centrifuged at 12000 r/min for 15 min at 4°C. The resulting supernatants were collected and either frozen at -80 °C or used immediately. Protein concentrations were determined using the BCA method. Equal amounts of protein (20 μg per sample) were analyzed by 12% sodium dodecylsulfate-polyacrylamide gel electrophoresis (SDS-PAGE) and electrotransferred onto polyvinylidene difluoride (PVDF) membranes for 1 h at 200 mA (Bio-Rad, Hercules, CA). The membranes were blocked in 5% nonfat milk (Santa Cruz Biotechnology, Santa Cruz, CA) for 2 h at room temperature and then incubated in primary antibody against IL-18 (R&D Systems, Minneapolis, MN, working dilution 2 μg/mL) p22phox (Santa Cruz Biotechnology, Santa Cruz, CA, working dilution 1:500) or p47phox (Millipore Biotechnology, Billerica, MA, working dilution 1:1000) overnight at 4 °C. The binding of the primary antibodies was revealed by horseradish peroxidase-conjugated secondary antibodies (Santa Cruz Biotechnology, Santa Cruz, CA). The proteins of the membranes were detected using an enhanced chemiluminescence immunoblotting detection system (Thermo Fisher Scientific, Rockford, IL). The results were quantified by densitometric analysis using Image-Quant software. Values were corrected by the absorbance of the internal control (GAPDH).

Statistical analysis

Data were expressed as mean±standard deviation. Statistical analysis was performed with software (SPSS version 13.0; SPSS, Chicago, IL) between two groups using two-tailed Student's *t*-test for unpaired values, and $P<0.05$ was considered statistically significant.

Results

Physiological characteristics and time-course of SBP in SD rats

The body weight and food intake did not differ between the CON, ALD, and HS-ALD groups. The serum aldosterone level was higher and the PRA was lower in the ALD group compared with those in the CON group (aldosterone level 1664.9±389.9 *vs* 623.1±80.1 pg/mL, $P<0.01$; PRA 4.17±0.25 *vs* 7.22±0.07 ng·mL^{-1}·h^{-1}, $P<0.01$). Urine output and urinary potassium excretion were increased, plasma sodium concentrations were higher and the plasma potassium levels were lower in the ALD group compared with those in the CON group. Serum aldosterone levels were not significantly different between the HS-ALD group and the ALD group. However, the HS-ALD group exhibited a lower PRA(1.04±0.89 ng·mL^{-1}·h^{-1} in the HS-ALD group *vs* 4.17±0.25 ng·mL^{-1}·h^{-1} in the ALD group, $P<0.01$), greater urine output, increased urinary sodium and potassium excretion, and a lower plasma potassium level ($P<0.05$) (Table 1).

The time-course of SBP in the rats of the three groups was shown in Figure 1. At the first week of treatment, aldosterone infusion had not significantly increased the animals' blood pressure. However, following 2-week aldosterone treatment alone, the SBP of the ALD group was slightly but significantly higher than that of the CON group (140±5 *vs* 125±4 mmHg, $P<0.01$). Following 8-week aldosterone treatment, the SBP of the ALD group was moderately and significantly higher than that of the CON group (162±4 *vs* 127±3 mmHg, $P<0.01$). The SBP was not significantly different between the ALD group and the HS-ALD group.

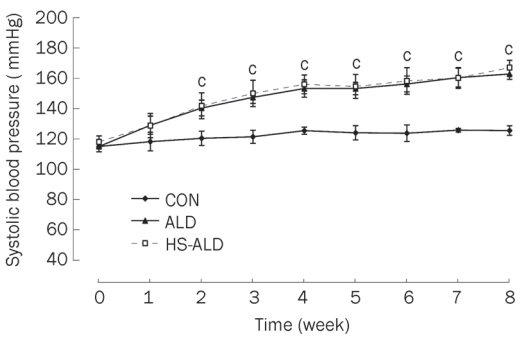

Figure 1. Systolic blood pressure of control rats (CON), aldosterone alone-infused rats (ALD) and 1% sodium chloride intake in conjunction with excess aldosterone (HS-ALD) at 0, 1, 2, 3, 4, 5, 6, 7, and 8 weeks. Mean±SD. $n=8$. $^cP<0.01$ *vs* CON.

LV weight, echocardiographic analysis and ultrastructure

Cardiac structure and function were examined to determine the effects of aldosterone infusion with or without the addition

Table 1. Physiologic and morphologic characteristics in Sprague-Dawley rats. Mean±SD. *n*=8. [b]*P*<0.05, [c]*P*<0.01 *vs* CON; [e]*P*<0.05, [f]*P*<0.01 *vs* ALD.

	CON	ALD	HS-ALD
Body weight (g)	438.7±14.7	429.2±28.7	416.7±24.6
Food intake (g/100 g BW)	5.85±0.81	5.67±0.34	5.89±0.84
Urinary volume (mL/100 g BW)	2.8±0.8	5.6±1.4[c]	12.3±1.5[f]
Urinary sodium (mmol/24 h)	1.06±0.42	1.39±0.41	6.80±1.15[f]
Urinary potassium (mmol/24 h)	1.48±0.37	2.24±0.46[b]	2.98±0.58[e]
Plasma sodium (mmol/L)	141.5±2.4	148.7±1.1[b]	149.5±0.8
Plasma potassium (mmol/L)	4.3±0.2	3.1±0.3[b]	2.5±0.1[e]
Serum aldosterone (pg/mL)	623.1±80.1	1664.9±389.9[c]	1474.3±452.4
PRA (ng·mL^{-1}·h^{-1})	7.22±0.07	4.17±0.25[c]	1.04±0.89[f]
LVMI (mg/g)	2.06±0.10	2.36±0.17[b]	2.67±0.24[e]

CON, control rats; ALD, aldosterone-infused rats; HS-ALD, 1% NaCl in conjunction with aldosterone in rats. BW, body weight; PRA, plasma renin activity; LVMI, left ventricular mass index.

of 1% sodium chloride on the heart. Cardiac hypertrophy, as suggested by LVMI, was observed. LVMI was significantly higher in the ALD group compared with that in the CON group (2.36±0.17 *vs* 2.06±0.10, *P*<0.05). The LVMI was also significantly higher in the HS-ALD group compared with that in the ALD group (2.67±0.24 *vs* 2.36±0.17, *P*<0.05) (Table 1).

As shown by echocardiographic analysis in Figure 2A, the thickness of both the LVAW and the LVPW (2.30±0.19 mm and 2.32±0.21 mm, respectively) in the ALD group was significantly greater after 8 weeks compared with that in the CON group (1.90±0.25 mm and 1.99±0.16 mm, respectively; *P*<0.05). The E/A was significantly lower in the ALD group compared with that in the CON group (0.94±0.19 *vs* 1.74±0.18, *P*<0.05). Furthermore, the LVAW and LVPW thickness were significantly greater in the HS-ALD group (2.58±0.17 mm and 2.53±0.20 mm, respectively) compared with that in the ALD group (*P*<0.05). Other echocardiographic parameters, including HR (441±34, 435±36, and 428±36 bpm in the CON, ALD,and HS-ALD groups, respectively; *P*>0.05), LVEDD (5.52±0.69, 6.10±0.76, and 5.71±1.11 mm in the CON, ALD,

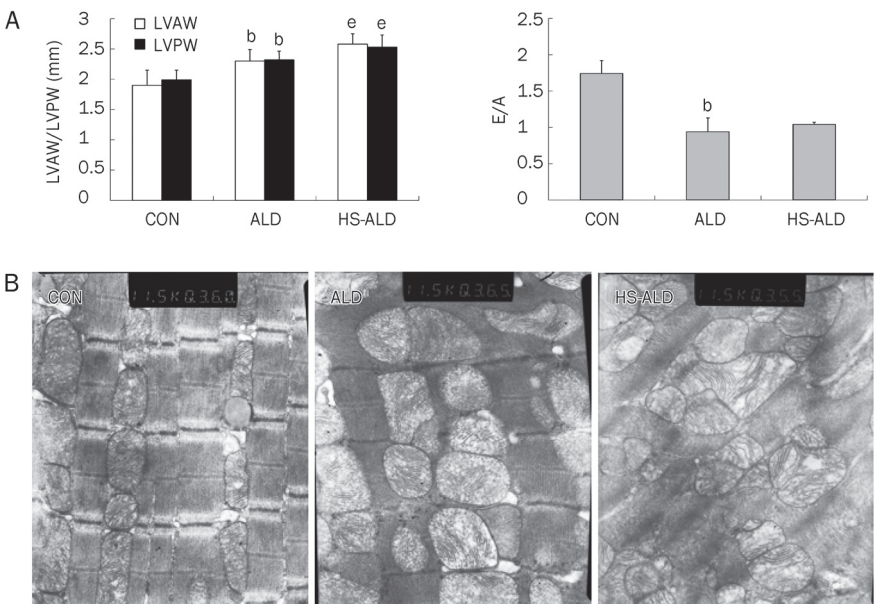

Figure 2. Aldosterone infusion with or without additional 1% sodium chloride intake induce left ventricular (LV) hypertrophy by echocardiographic analysis and ultrastructural remodeling visible by TEM in rats. (A) aldosterone infusion with or without additional 1% sodium chloride intake induce LV hypertrophy and diastolic dysfunction. LVAW, LV anterior wall thickness at end diastole; LVPW, LV posterior wall thickness at end diastole; E/A, the ratio of mitral inflow measurements of early to late filling velocities; CON, control rats; ALD, excess aldosterone alone-infused rats; HS-ALD, 1% NaCl in conjunction with aldosterone in rats. Mean±SD. *n*=8. [b]*P*<0.05 *vs* CON; [e]*P*<0.05 *vs* ALD. (B) Representative image from CON demonstrating a line of sarcolemmal mitochondria just beneath the sarcomeres (the distance between two Z lines) of the myocardium. Representative remodeled mitochondria in ALD rats. This image represents marked increase of swollen and denatured mitochondria. The myocardial ultrastructure was disappeared in some spaces and mitochondria of myocardium were dissolved in HS-ALD group. Original magnifications: ×10 000.

and HS-ALD groups, respectively; $P>0.05$), FS (45.4±3.9, 54.1%±5.2%, and 45.8%±3.4% in the CON, ALD, and HS-ALD groups, respectively; $P>0.05$), and EF (81.8%±3.6%, 87.9%±6.1%, and 82.3%±3.2% in the CON, ALD, and HS-ALD groups, respectively; $P>0.05$) were not significantly changed by aldosterone infusion with or without the addition of 1% sodium chloride.

To further evaluate the changes in cardiac morphology, the cardiac ultrastructure was observed using TEM. TEM images of the rat heart following aldosterone infusion with or without the addition of 1% sodium chloride revealed striking changes in the mitochondria and myofilaments. The myofilaments were sparser, and there was a marked increase in swollen and denatured mitochondria in the ALD group. Moreover, the myocardial ultrastructure was not visible in some spaces and mitochondria were seriously damaged in the HS-ALD group (Figure 2B).

LV collagen deposition

Cardiac fibrosis in rats following aldosterone infusion with or without the addition of 1% sodium chloride was shown in Figure 3. The CVF and PVCA/VA were higher in the ALD group (3.61%±0.63% and 0.57±0.062, respectively) than those in the CON group (1.44%±0.41% and 0.28±0.01, respectively; $P<0.01$). CVF was 4.55%±0.52% and PVCA/VA was 0.71±0.04 in the HS-ALD group. The CVF was not significantly different between the ALD group and the HS-ALD group. However, PVCA/VA was higher in the HS-ALD group compared with that in the ALD group ($P<0.01$). We found that aldosterone infusion alone induced a significant increase in cardiac fibrosis, in terms of collagen deposition, in the myocardial interstitium (Figure 3A and 3C) and the perivascular space of the intramyocardial coronary arteries (Figure 3B and 3D). Furthermore, high sodium in conjunction with aldosterone induced more obvious myocardial fibrosis, especially in the perivascular space of the intramyocardial coronary arteries (Figure 3).

LV inflammatory infiltration and oxidative stress

As shown in Figure 4A, LV inflammatory infiltration was not detected in the CON group. Focal inflammatory infiltration in LV characterized by ED-1-positive cells (macrophages) was observed in the ALD group. More obvious inflammatory infiltration was detected in the HS-ALD group.

The expression of NADPH oxidase was determined by Western blot detection of the subunits p22phox and p47phox. In addition, we analyzed the expression of the IL-18 protein in three groups. Our results showed that the expressions of

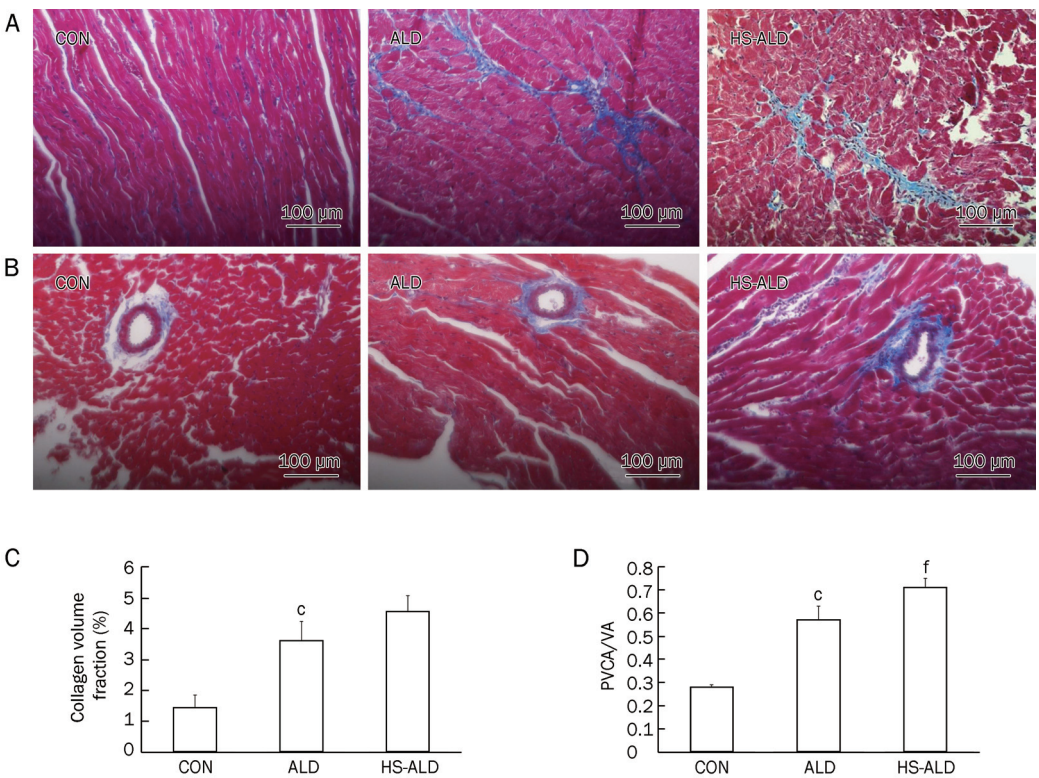

Figure 3. Effects of aldosterone infusion with or without additional 1% sodium chloride intake on cardiac fibrosis. Representative photomicrographs show collagen changes in midmyocardium (A, C) and perivascular space of intramyocardial coronary arteries (B, D) after aldosterone infusion with or without additional 1% sodium chloride intake by masson's trichrome-stained method. Original magnifications: ×200. Collagen fibers were shown in blue and muscles were shown in red. Collagen volume fraction was determined by measuring the area of collagen within a given field. PVCA/VA, perivascular collagen area/vessel luminal area. CON, control rats; ALD, aldosterone alone-infused rats; HS-ALD, 1% NaCl in conjunction with aldosterone in rats. Mean±SD. $n=8$. $^{c}P<0.01$ *vs* CON; $^{f}P<0.01$ *vs* ALD.

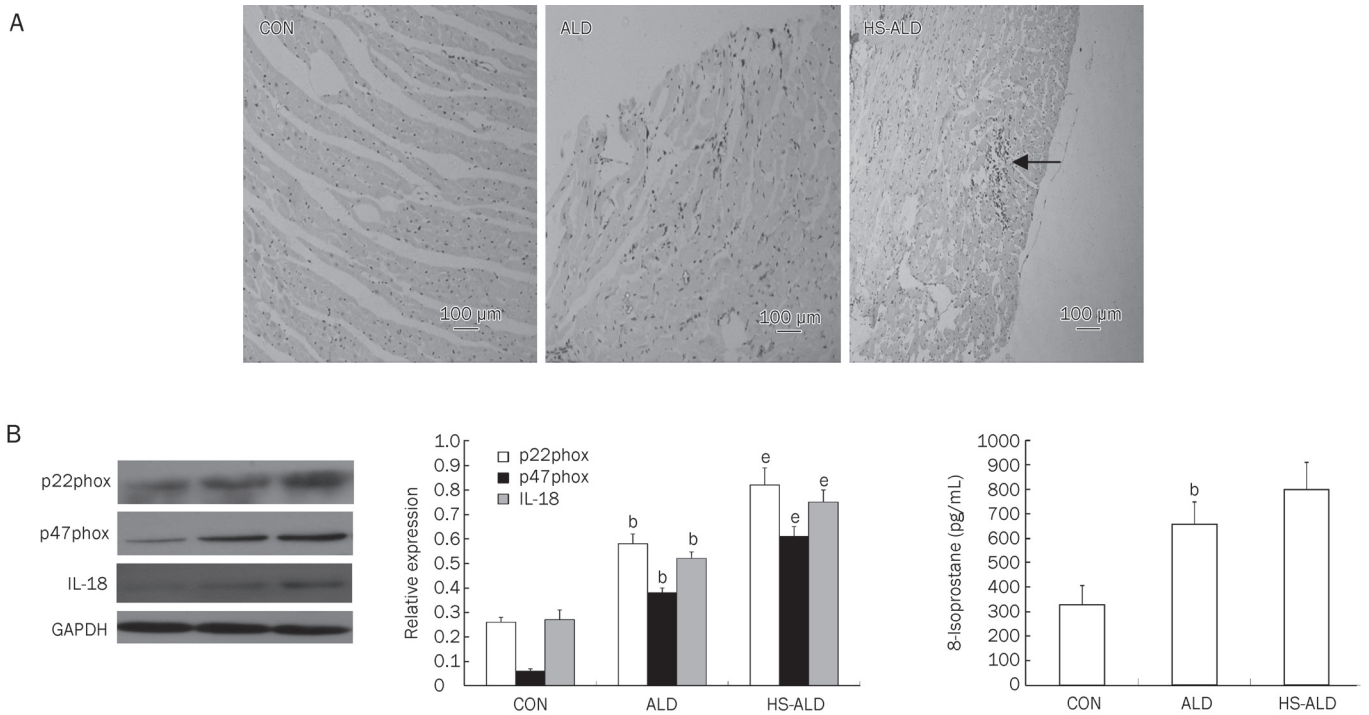

Figure 4. (A) Macrophage infiltration was presented at sites of myocardium induced by aldosterone infusion with or without additional 1% sodium chloride intake. Positive staining appeared as brown. Appearance of focal inflammatory infiltration in LV has been observed in ALD group. The focal inflammatory lesions were enlarged in HS-ALD group (the macrophage infiltration had been labeled). Original magnifications: ×100. (B) Effects of aldosterone infusion with or without additional 1% sodium chloride intake on the parameters about oxidative stress and IL-18 in LV myocardium. (C) Effects of aldosterone infusion with or without additional 1% sodium chloride intake on the serum 8-isoprostane levels. CON, control rats; ALD, aldosterone alone-infused rats; HS-ALD, 1% NaCl in conjunction with aldosterone in rats. Mean±SD. n=8. ^{b}P<0.05 *vs* CON; ^{e}P<0.05 *vs* ALD.

p22phox, p47phox, and IL-18 were up-regulated in the ALD group compared with those in the CON group (P<0.05). Furthermore, p22phox, p47phox, and IL-18 protein expressions in the HS-ALD group were up-regulated compared with those in the ALD group (P<0.05) (Figure 4B).

We found that serum 8-isoprostane levels, a marker for global oxidative stress, were significantly higher in the ALD group than those in the CON group (654.22±92.47 *vs* 326.96±79.65 pg/mL, P<0.05). There was also an increasing trend in serum 8-isoprostane levels in the HS-ALD group compared with those in the ALD group. However, serum 8-isoprostane levels were not significantly different between the HS-ALD group and the ALD group (797.50±111.33 pg/mL in the HS-ALD group, P>0.05) (Figure 4C).

Discussion

Aldosterone on a normal sodium diet could have a pivotal effect on cardiac injury. Some investigators have shown that aldosterone excess in the presence of salt loading and uninephrectomy is associated with cardiovascular remodeling[4, 5]. It has also been reported that other cofactors, such as low nitric oxide bioavailability, hypertension, or congestive heart failure must be present together with a high-sodium intake for damage to occur[6]. Due to the influence of high-sodium intake or other factors on myocardial injury, the actual effects of aldosterone on cardiac injury have remained poorly understood. Our study showed that chronic subcutaneous aldosterone infusion of 8 weeks' duration in the absence of sodium loading induced hypertension and LV hypertrophy, which was accompanied by an inflammatory response and collagen deposition in the myocardium.

Regarding the echocardiography observations, the present study showed that E/A was significantly lower in animals infused with aldosterone for 8 weeks compared with that in the CON group, indicating the impairment of diastolic function in the ALD group. Yoshida *et al* demonstrated that rats infused with aldosterone on a normal sodium diet for only 2 weeks showed cardiac hypertrophy. However, FS and EF were not significantly altered[10]. Unfortunately, they did not evaluate whether the LV diastolic function was altered. With prolonged infusion of aldosterone to 8 weeks, we observed that LVEDD, FS, and EF were not different compared with the control. Together, these studies indicated that more prolonged aldosterone exposure alone might lead to LV diastolic dysfunction and not influence LV systolic function. The possibility was also raised that diastolic dysfunction might occur earlier than systolic dysfunction in that condition.

Additional features of the myocardium following aldosterone alone treatment included cardiac interstitial fibrosis and perivascular fibrosis of the intramyocardial coronary arteries in ALD rats. LV hypertrophy was also observed following aldosterone infusion, as shown by increased LVMI and greater

LVAW and LVPW thickness. Moreover, the marked increase in swollen and denatured mitochondria observed by TEM in the ALD group pointed to remodeling of the myocardial structure and insufficient myocardium energy. Previous work has shown that diffuse accumulation of fibrosis tissue in the cardiac spaces contributes to increase ventricular diastolic stiffness and leads to, in severe cases, electrical conduction defects[11]. The resultant heterogeneity in myocardial structure, created by a disproportionate accumulation of collagen, may serve to explain the important clinical observations that patients with high-renin essential hypertension have a greater incidence of adverse cardiovascular events and impaired ventricular function, respectively[12, 13].

High-sodium intake could aggravate myocardial injuries induced by aldosterone, which was partly independent of blood pressure. The 8% sodium chloride alone or 8% sodium chloride administration in conjunction with exogenous aldosterone is usually used in experimental studies to detect the effects of high-sodium intake on the cardiac structure. In such situations, sodium intake levels are twenty times higher than that on a 0.3% normal sodium diet in rats. In our study urinary sodium of 24 h in the HS-ALD group was about six times higher than that in the CON group and the ALD group. We showed that SBP was not significantly different between the ALD group and the HS-ALD group. However, LV hypertrophy was more predominant in the HS-ALD group compared with that in the ALD group and was accompanied by significantly increased collagen deposition in the perivascular space of the coronary arteries and the breakdown of myocardial ultrastructure. This result suggested that moderate elevation of sodium chloride intake could aggravate myocardial injuries induced by aldosterone, which was partly independent of blood pressure. Regarding the synergistic action between aldosterone and sodium, fibroblast collagen synthesis may be involved in the regulation by aldosterone of Na^+/K^+-ATPase, and the expression of Na^+/K^+-ATPase is increased only in the presence of salt[14]. Moreover, a previous clinical study indicated that the association of serum aldosterone with both an increase in blood pressure and the later development of hypertension was seen only in the persons whose urine sodium index was at or above the median, but not in those whose urine sodium excretion was below the median[15]. Such an interaction between aldosterone and sodium is also supported by the observations made in Yanomamo Indians who consume a very low-salt diet. They exhibit markedly elevated serum aldosterone levels but little or no blood-pressure elevation[16]. In modern society, humans could easily increase sodium intake via food diversity. Therefore, lowering sodium intake can compensate for the risk of cardiac and vascular injury by aldosterone, especially in essential hypertension, primary and secondary aldosteronism.

The myocardial injury may be attributable to significantly up-regulated oxidative stress induced by aldosterone and high sodium intake. It is now established that the specificity of MR occupancy by aldosteone in epithelial tissues is determined by 11β-hydroxysteroid dehydrogenase type 2 (11β-HSD2)[17, 18], but the amount of 11β-HSD2 in non-epithelial tissues, such as heart, is at a negligible level[19]. MR in non-epithelial tissues should be exclusively occupied by glucocorticoids with very limited accessible aldosterone. The glucocorticoid-MR complex is inactive under the steady-state condition. Funder *et al* recently proposed a novel and intriguing hypothesis for MR activation in non-epithelial tissues, suggesting that the inactive glucocorticoid-MR may be activated by the generation of ROS[20]. With the possible positive feedback system triggered by inflammation and increased oxidative stress, further activation of the glucocorticoid-MR complex could occur, thus accounting for the vicious cycle of the aldosterone-induced cardiovascular injury. This postulated mechanism could well explain our study results, with high-sodium intake potentially aggravating myocardial injuries induced by aldosterone through up-regulated oxidative stress. The hypothesis has been supported by previous studies, which showed that the development of hypertension and the regression of cardiovascular remodeling were attenuated in mineralocorticoid treated animals after the treatment of antioxidant drugs, such as the superoxide dismutase mimetic Tempol[21, 22], the NADPH oxidase inhibitor apocynin[23, 24] or N-acetylcysteine[5].

Increased oxidative stress might also trigger and deteriorate inflammation. In the present study, noticeable inflammatory injury and significantly up-regulated IL-18 protein expression were observed in the ALD group compared with that in controls. Furthermore, the inflammatory injury was more serious and the IL-18 protein expression was up-regulated in the HS-ALD group compared with that in the ALD group. Previous experimental studies have indicated that aldosterone infusion alone for a shorter time may exclusively result in the infiltration of inflammation cells via oxidative stress[10]. Both of inflammation and increased oxidative stress may lead to the further activation of the glucocorticoid-MR complex, thus worsening myocardial inflammatory injuries induced by aldosterone[21]. It may be possible that aldosterone-induced oxidative stress stimulated a series of pro-inflammatory genes expression, such as IL-18, via a redox-sensitive mechanism, thereby leading to initiation of the cardiovascular inflammatory phenotype. Moreover, inflammation and, in particular, generation of free radicals may contribute to the activation of the fibrotic process and hypertrophy[25]. Cardiac fibrosis could be the reparative response to the inflammatory injury, although direct effects of aldosterone on fibrosis are possible[26, 27]. Furthermore, previous studies have indicated that adult cardiomyocytes express IL-18 and its receptors, and that proinflammatory cytokines and oxidative stress regulate their expression via activation of NF-κB[28–31]. In the present study, we found that IL-18, which was a predictor of cardiovascular events, might be involved in the cardiovascular injuries induced by aldosterone.

In summary, the present work provided evidence that long-term infusion of aldosterone on a normal sodium diet could result in hypertension, persistent inflammatory infiltration, cardiac fibrosis, LV hypertrophy and LV diastolic dysfunction. Moderate high-sodium intake could aggravate myocardial

injuries induced by aldosterone. These synergistic effects of sodium and aldosterone were mediated by oxidative stress via NADPH oxidase and IL-18. Our data could also underscore the potential benefits of lower sodium action in cardiac protection related to aldosterone. Further studies are needed to elucidate the detailed nature of the relationship between inflammation, oxidative stress, and activation of glucocorticoid/aldosterone-MR in the development of cardiovascular diseases.

Acknowledgements

This work was supported by grants from the State "15" Science and Technology Research Projects (2004BA720A29).

Author contribution

Hua CHENG designed research; Jing-yi LI performed research; Shao-ling ZHANG and Meng REN analyzed data; Yan-ling WEN and Li YAN contributed new analytical tools and reagents; Jing-yi LI and Hua CHENG wrote the paper.

References

1 Rossi GP, Di Bello V, Ganzaroli C, Sacchetto A, Cesari M, Bertini A, *et al*. Excess aldosterone is associated with alterations of myocardial texture in primary aldosteronism. Hypertension 2002; 40: 23–7.
2 Pitt B, Zannad F, Remme WJ, Cody R, Castaigne A, Perez A, *et al*. The effect of spironolactone on morbidity and mortality in patients with severe heart failure. Randomized Aldactone Evaluation Study Investigators. N Engl J Med 1999; 341: 709–17.
3 Pitt B, Remme W, Zannad F, Neaton J, Martinez F, Roniker B, *et al*. Eplerenone, a selective aldosterone blocker, in patients with left ventricular dysfunction after myocardial infarction. N Engl J Med 2003; 348: 1309–21.
4 Brilla CG, Weber KT. Mineralocorticoid excess, dietary sodium, and myocardial fibrosis. J Lab Clin Med 1992; 120: 893–901.
5 Sun Y, Zhang J, Lu L, Chen SS, Quinn MT, Weber KT. Aldosterone-induced inflammation in the rat heart : role of oxidative stress. Am J Pathol 2002; 161: 1773–81.
6 Martinez DV, Rocha R, Matsumura M, Oestreicher E, Ochoa-Maya M, Roubsanthisuk W, *et al*. Cardiac damage prevention by eplerenone: comparison with low sodium diet or potassium loading. Hypertension 2002; 39: 614–8.
7 Intersalt Cooperative Research Group. Intersalt: an international study of electrolyte excretion and blood pressure. Results for 24 hour urinary sodium and potassium excretion. BMJ 1988; 297: 319–28.
8 Paravicini TM, Touyz RM. Redox signaling in hypertension. Cardiovasc Res 2006; 71: 247–58.
9 Groemping Y, Rittinger K. Activation and assembly of the NADPH oxidase: a structural perspective. Biochem J 2005; 386: 401–16.
10 Yoshida K, Kim-Mitsuyama S, Wake R, Izumiya Y, Izumi Y, Yukimura T, *et al*. Excess aldosterone under normal salt diet induces cardiac hypertrophy and infiltration via oxidative stress. Hypertens Res 2005; 28: 447–55.
11 Weber KT, Sun Y, Tyagi SC, Cleutjens JP. Collagen network of the myocardium: function, structural remodeling and regulatory mechanisms. J Mol Cell Cardiol 1994; 26: 279–92.
12 Brunner HR, Laragh JH, Baer L, Newton MA, Goodwin FT, Krakoff LR, *et al*. Essential hypertension: renin and aldosterone, heart attack and stroke. N Engl J Med 1972; 286: 441–9.
13 Vensel LA, Devereux RB, Pickering TG, Herrold EM, Borer JS, Laragh JH. Cardiac structure and function in renovascular hypertension produced by unilateral and bilateral renal artery stenosis. Am J Cardiol 1986; 58: 575–82.
14 Horisberger JD, Rossier BC. Aldosterone regulation of gene transcription leading to control of ion transport. Hypertension 1992; 19: 221–7.
15 Vasan RS, Evans JC, Larson MG, Wilson PW, Meigs JB, Rifai N, *et al*. Serum aldosterone and the incidence of hypertension in nonhypertensive persons. N Engl J Med 2004; 351: 33–41.
16 Oliver WJ, Cohen EL, Neel JV. Blood pressure, sodium intake, and sodium related hormones in the Yanomamo Indians, a "no-salt" culture. Circulation 1975; 52: 146–51.
17 Funder JW. Mineralocorticoid receptors and hypertension. J Steroid Biochem Mol Biol 1995; 53: 53–5.
18 White PC, Mune T, Agarwal AK. 11 beta-Hydroxysteroid dehydrogenase and the syndrome of apparent mineralocorticoid excess. Endocr Rev 1997; 18: 135–56.
19 Fuller PJ, Young MJ. Mechanisms of mineralocorticoid action. Hypertension 2005; 46: 1227–35.
20 Funder JW. Aldosterone, mineralocorticoid receptors and vascular inflammation. Mol Cell Endocrinol 2004; 217: 263–9.
21 Shibata S, Nagase M, Yoshida S, Kawachi H, Fujita T. Podocyte as the target for aldosterone: roles of oxidative stress and Sgk1. Hypertension 2007; 49: 355–64.
22 Hirono Y, Yoshimoto T, Suzuki N, Sugiyama T, Sakurada M, Takai S, *et al*. Angiotensin II receptor type 1-mediated vascular oxidative stress and proinflammatory gene expression in aldosterone-induced hypertension: the possible role of local renin-angiotensin system. Endocrinology 2007; 148: 1688–96.
23 Park YM, Park MY, Suh YL, Park JB. NAD(P)H oxidase inhibitor prevents blood pressure elevation and cardiovascular hypertrophy in aldosterone-infused rats. Biochem Biophys Res Commun 2004; 313: 812–7.
24 Li L, Chu Y, Fink GD, Engelhardt JF, Heistad DD, Chen AF. Endothelin-1 stimulates arterial VCAM-1 expression via NADPH oxidase-derived superoxide in mineralocorticoid hypertension. Hypertension 2003; 42: 997–1003.
25 Nicoletti A, Michel JB. Cardiac fibrosis and inflammation: Interaction with hemodynamic and hormonal factors. Cardiovasc Res 1999; 41: 532–43.
26 Young M, Head G, Funder J. Determinants of cardiac fibrosis in experimental hypermineralocorticoid states. Am J Physiol 1995; 269: E657–62.
27 Weber KT, Brilla CG, Janicki JS. Myocardial fibrosis: functional significance and regulatory factors. Cardiovasc Res 1993; 27: 341–8.
28 Doi T, Sakoda T, Akagami T, Naka T, Mori Y, Tsujino T, *et al*. Aldosterone induces interleukin-18 through endothelin-1, angiotensin II, Rho/Rho-kinase, and PPARs in cardiomyocytes. Am J Physiol Heart Circ Physiol 2008; 295: H1279–87.
29 Chandrasekar B, Colston JT, de la Rosa SD, Rao PP, Freeman GL. TNF-alpha and H_2O_2 induce IL-18 and IL-18R beta expression in cardiomyocytes via NF-kappa B activation. Biochem Biophys Res Commun 2003; 303: 1152–8.
30 Rabkin SW. The role of interleukin 18 in the pathogenesis of hypertension-induced vascular disease. Nat Clin Pract Cardiovasc Med 2009; 6: 192–9.
31 Wang M, Markel TA, Meldrum DR. Interleukin 18 in the heart. Shock 2008; 30: 3–10.

Acta Pharmacologica Sinica (2012) 33: 401–406
 1671-4083/12 $32.00
www.nature.com/aps

Original Article

Heterogeneity of chemosensitivity in esophageal cancer using ATP-tumor chemosensitivity assay

Zhi-qiang LING[1], Chun-jian QI[2], Xiao-xiao LU[1], Li-juan QIAN[1], Lin-hui GU[1], Zhi-guo ZHENG[1], Qiang ZHAO[3], Shi WANG[4], Xian-hua FANG[5], Zhi-xing YANG[6], Jian YIN[7], Wei-min MAO[1, 3, *]

[1]Zhejiang Cancer Research Institute, [3]Department of Tumor Surgery, [4]Department of Endoscopy, [5]Department of Pathology, Zhejiang Province Cancer Hospital, Zhejiang Cancer Center, Hangzhou 310022, China; [2]Department of Oncology, the Changzhou No 2 People's Hospital, Affiliated to Nanjing Medical University, Changzhou 213003, China; [6]Institute for Nutritional Sciences, Shanghai Institute for Biological Sciences, Chinese Academy of Sciences, Shanghai 200031, China; [7]Huzhou Haichuang Biological Scientific Technology Co, Ltd, Huzhou 313000, China

Aim: Current chemotherapy for esophageal cancer is conducted on the basis of empirical information from clinical trials, which fails to take into account the known heterogeneity of chemosensitivity between patients. This study was aimed to demonstrate the degree of heterogeneity of chemosensitivity in esophageal cancers.
Methods: A total of 42 esophageal cancer specimens were collected. The heterogeneity of chemosensitivity in esophageal cancer specimens was examined using an *ex vivo* ATP-tumor chemosensitivity assay (ATP-TCA).
Results: Thirty eight specimens produced evaluable results (90.5%). The most active single agent tested was nedaplatin, to which 28.9% of samples were sensitive. Combinations of chemotherapy agents exhibited much higher sensitivity: cisplatin+paclitaxel was sensitive in 16 of 38 (42.1%) of samples, while nedaplatin+paclitaxel was more effective, which was sensitive in 20 of 38 cases (52.6%).
Conclusion: There was a marked heterogeneity of chemosensitivity in esophageal cancer. Chemosensitivity testing may provide a practical method for testing new regimens before clinical trials in esophageal cancer patients.

Keywords: esophageal cancer; chemotherapy; heterogeneity; nedaplatin; cisplatin; paclitaxel; ATP-tumor chemosensitivity assay

Acta Pharmacologica Sinica(2012) 33: 401–406; doi: 10.1038/aps.2011.195; published online 30 Jan 2012

Introduction

Esophageal cancer is a highly malignant gastrointestinal cancer that readily progresses to widespread metastasis to lymph nodes and easily infiltrates the trachea and great vessels[1]. Better treatment outcomes of esophageal cancer have been obtained by improved diagnostic technologies such as dye-spraying endoscopy[2], surgical skills such as three-field lymphadenectomy[3], and perioperative management[4]. Because esophageal cancer is generally more sensitive to anti-cancer drugs than other gastrointestinal carcinomas, various multidisciplinary treatments have been attempted and chemoradiation has long been established as a standard treatment for esophageal cancer because it is highly effective and can be performed relatively safely[5]. However, as in the case of surgery, chemoradiation mainly provides localized treatment, and treatment outcomes of cases for which radical surgery is impossible, such as cancer infiltrating into other organs, distant lymph node metastasis and metastasis to other organs, are still poor. In these cases, systemic chemotherapy is usually adopted, and many regimens have been used[5, 6].

Tumors show heterogeneity of genotype and phenotype, and such heterogeneity in esophageal cancer certainly affected response to cytotoxic agents[7-9]. Predictive assays based on thymidylate synthase levels show some promise, but cellular assays have largely been ignored due to low evaluability rates and technical problems which is common in tumor-derived tissue[10]. However, recent technical developments have produced assays, such as the ATP-tumor chemosensitivity assay (ATP-TCA), which has high availability rates with solid tumors and produces interpretable results in more than 90% of tumors tested[11, 12]. The results correlated well with outcome in patients with a sensitivity of 95% for predicting those who responded to primary treatment of stage III ovarian cancer[13]. The use of this assay was shown to double progression-free

* To whom correspondence should be addressed.
E-mail maowm1218@163.com
Received 2011-08-03 Accepted 2011-12-09

survival and overall survival in a case-control intervention study in recurrent ovarian carcinoma[14].

We performed this study to determine the degree of heterogeneity of chemosensitivity in esophageal cancer as a prelude to studies of the molecular basis of resistance in tumor-derived cells and the potential use of this assay to guide therapy. We also wanted to solve the ATP-TCA technical problems, particularly the use of tumor material from different origins.

Materials and methods

All procedures complied with the ethical guidelines for the collect of human tissue specimens and use of laboratory study at Zhejiang Province Cancer Hospital, Zhejiang Cancer Center, China.

Tumor specimens

A total of 42 specimens were studied and 38 of these produced evaluable results (90.5%). Thirty-five samples were from patients undergoing resection of their primary esophageal cancer (of all pathological stages) and three were pleural aspirates in patients with metastatic disease. The median age of the patients was 57 years (range 30–82). Local ethics committee approval was obtained and informed consent gained from all patients. Biopsies were taken from the luminal surface of resection specimens by a pathologist or surgeon, ensuring histopathological diagnosis and staging were not compromised.

ATP-tumor chemosensitivity assay (ATP-TCA)

Chemosensitivity was assessed in primary esophageal cancer tumor tissue samples using the ATP-TCA (TCA-100; DCS Innovative Diagnostik Systeme, Hamburg, Germany), which has been described in detail[15]. Briefly, surgical biopsies (1–2 cm^3) were obtained during primary surgery. Tumor cells were isolated by mechanical and enzymatic dissociation (TDE DCS) (Innovative Diagnostik Systeme; or collagenase, Sigma, St Louis, MO, USA). Approximately 2×10^4 cells were then seeded into each well of a 96-well polypropylene microplate. Test drug concentrations were used in triplicate at six different doses of 6.25%, 12.5%, 25%, 50%, 100%, and 200% of the test drug concentration (TDC). The TDCs were based on pharmacokinetic data for standard doses of the agents, adjusted to give good discrimination (Table 1). Two rows on each plate were reserved for controls, one row of maximum inhibitor (MI DCS) and one row of CAM only (MO-no drug control). Following preparation of the drug dilutions, 100 μL of the cell suspension was added to each well of the plate. The plate was incubated for 5–6 d at 37°C with high humidity and 5% CO_2. The cells were observed every 24 h microscopically to check for overgrowth or infection. At the end of the incubation period the cells were lysed by the addition of 50 μL of tumour cell extraction reagent (TCER DCS), and the ATP content of each well was assessed by the addition of 50 μL luciferin-luciferase reagent (DCS) to 50 μL of extracted cells. Luminescence measurements were made using Orion II luminometer (Berthold Diagnostic Systems).

Table 1. Drugs tested and their 100% TDC as used in the *ex vivo* ATP-TCA.

Drug/combination	100% TDC (μg/mL)
Paclitaxel (PTX)	13.8
Adriamycin (ADM)	1
5-Fluorouracil (5-Fu)	25
Nedaplatin (NDP)	18
Cisplatin (DDP)	6.3
DDP+PTX	6.3±13.8
NDP+PTX	18±13.8
DDP+5-Fu	6.3±25

Data analysis

Data was transferred directly from the luminometer to a spreadsheet (Excel 2003; Microsoft). A TCA index, or index of sensitivity, calculated as [600-sum (inhibition 6.25%-200%)] has been shown to allow simple comparison of results between drugs and tumors. In addition, IC_{50} and IC_{90} were determined by linear interpolation. Four categories of *ex vivo* sensitivity were defined as: (a) strong sensitivity, $IC_{90}\leq100\%$ TDC and $IC_{50}<25\%$ TDC; (b) partial sensitivity, $IC_{90}>100\%$ TDC and $IC_{50}\leq25\%$ TDC; (c) weak sensitivity, $IC_{90}\leq100\%$ TDC and $IC_{50}>25\%$ TDC; and (d) resistance, $IC_{90}>100\%$ TDC and $IC_{50}>25\%$ TDC.

All experiments were performed three times and judged acceptable if the results showed a coefficient of variation below 25%. The results of each experiment were entered into an access database for further analysis and compared with existing data for tumor-derived cells using descriptive statistics. Further statistical tests (SPSS Software, IL, USA) were performed when direct comparisons were necessary: the Wilcoxon rank-sum test was used to compare paired series. Combination effects were assessed using Chou's method[16], as previously used with the ATP-TCA[17]. The combination index (CI) was determined at 90% cell death, and was defined as follows: $CI_{A+B}=[(D_{A/A+B})/D_A]+[(D_{B/A+B})/D_B]+[\text{alpha}\ (D_{A/A+B}\times D_{B/A+B})/D_AD_B]$, where CI_{A+B}=CI for a fixed effect (F=90%) for the combination of cytotoxic A and cytotoxic B; $D_{A/A+B}$ or $D_{B/A+B}$=concentration of cytotoxic A or B in the combination A+B; D_A or D_B=concentration of cytotoxic A or B alone; alpha=parameter with value 0 when A and B are mutually exclusive, and 1 when A and B are mutually nonexclusive. The combination index indicated: synergism<0.8; additivity>0.8 and <1.2; antagonism>1.2; slight synergistic and additive cytotoxic activity for value of 0.8 and 1.2, respectively.

Results

For comparison between drugs and tumors, an Index <300, representing an average 50% inhibition across all concentrations tested was used indicate sensitivity, as previously published[12, 18]. The results showed considerable heterogeneity of chemosensitivity to single agents and drug combinations between the tumors tested (Figure 1 and Table 2). The most active single agent tested was NDP, to which 28.95% of samples were sensitive ($P<0.05$). Both drug combinations

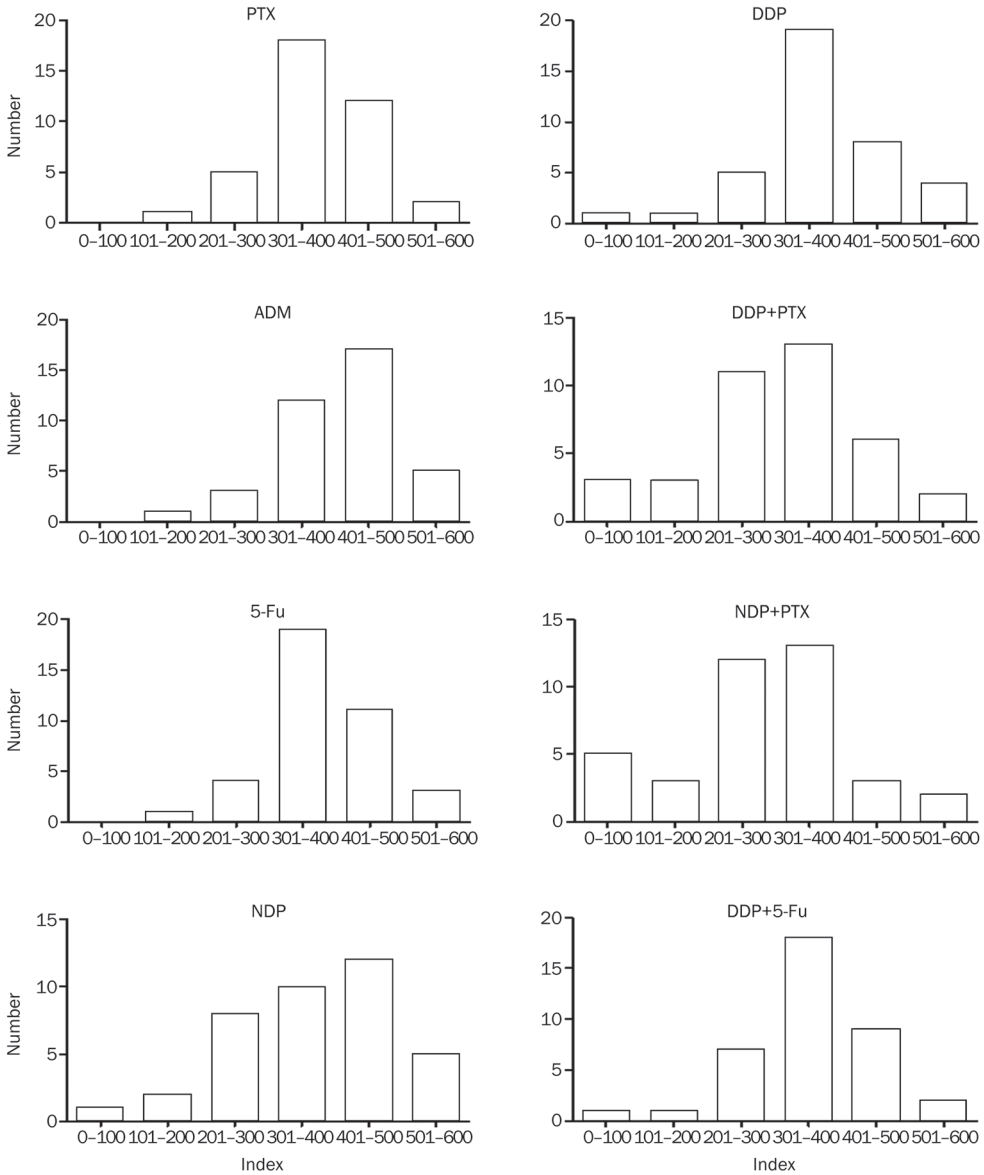

Figure 1. Frequency histograms show heterogeneity of the sensitivity index for each single agent and combination.

Table 2. Summary of sensitivity data (using an arbitrary threshold of sensitivity defined as a TCA index <300 for six concentrations use).

Drug/ combination	No sensitive	No in ATP-TCA	Sensitivity assessed (%)
PTX	6	38	15.8
ADM	4	38	10.5
5-Fu	5	38	13.2
NDP	11	38	29.0
DDP	7	38	18.4
DDP+PTX	16	38	42.1
NDP+PTX	20	38	52.6
DDP+5-Fu	9	38	23.7

achieved greater growth inhibition than drugs used alone (P<0.05), except for NDP. The correlation analysis was done using Pearson's rank correlation test among all 5 drugs tested. Results showed that there exist positive correlation among all 5 drugs tested (Figure 2 and Table 3).

Some tumors responded well to one drug or combination, while others showed no response to this and instead responded to an alternative regimen. For a limited panel of drugs and combinations, four cases were sensitive to only on drug/combination and resistant to all the others tested. Of these four, one was sensitive only to NDP, one to PTX, and two to NDP+PTX. One case was resistant to all drugs/combinations tested (2.6%).

Despite appearing sensitive to certain drugs using the Index threshold of <300, many tumors did not reach strong sensitivity level. Table 4 showed the patterns of chemosensitivity for different agents on tumors. Again, the most active single agent was NDP. NDP alone showed a strong sensitivity in 11 of 38 tumor samples tested, but ADM was 4 of 38 (29.0% *vs* 10.5%, P<0.01). Combinations of agents also showed more

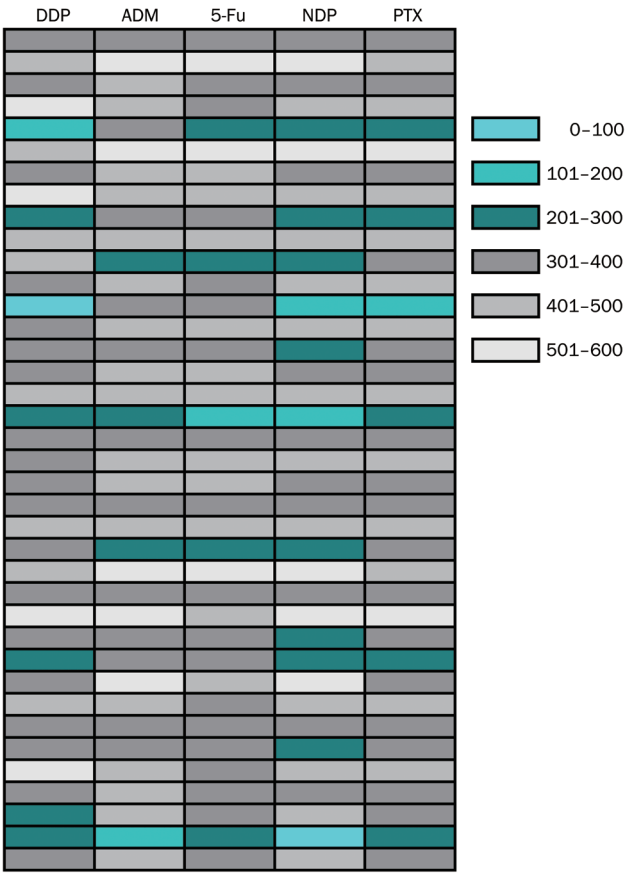

Figure 2. The ATP-TCA results of the 38 tumor specimens with five drugs were classified into 6 groups by different index values, and were marked with turquoise, cyan, dark cyan, dark grey, grey, and light grey which represent <100, 100–200, 200–300, 300–400, 400–500, and >500, respectively.

Table 4. Patterns of chemosensitivity exhibited by esophageal cancer specimens.

Drug/ combination	Strong sensitivity	Partial sensitivity	Weak sensitivity	Resis-tance
PTX	9	5	7	17
ADM	5	5	3	25
5-Fu	7	11	3	17
NDP	9	8	3	18
DDP	8	11	3	16
DDP+PTX	13	11	3	11
NDP+PTX	18	11	1	8
DDP+5-Fu	10	13	4	11

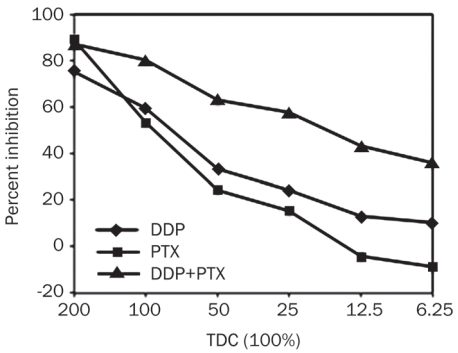

Figure 3. Results for DDP+PTX in one tumor, showing little activity of the DDP, but a synergistic increase in activity of the combination compared with PTX.

strong sensitivity cases. The DDP+PTX demonstrated a strong sensitivity in 16 of 38 of samples. The NDP+PTX was more effective, with strong sensitivity in 20 of 38 cases tested (42.1% *vs* 52.6%, $P<0.05$).

Figure 3 showed the results of testing DDP and PTX, alone and in combination, on esophageal cancer cells. DDP demonstrated partial sensitivity on its own, but when combined with the relatively resistance PTX the sensitivity was greatly improved. DDP and PTX combination had synergistic effect (IC_{90}=0.75), while NDP and PTX had additive effect (IC_{90}=0.93) (Figure 4).

Discussion

It would be of major importance to determine appropriate drugs to be used for treatment in patients with advanced can-

Table 3. The correlation analysis using Pearson's rank correlation test among all drugs tested.

		Pearson correlation				
		DDP	ADM	5-Fu	NDP	PTX
DDP	Pearson correlation	1	0.569	0.494	0.745	0.862
	P (2-tailed)		0.000	0.002	0.000	0.000
ADM	Pearson correlation	0.569	1	0.871	0.889	0.712
	P (2-tailed)	0.000		0.000	0.000	0.000
5-Fu	Pearson correlation	0.494	0.871	1	0.793	0.632
	P (2-tailed)	0.002	0.000		0.000	0.000
NDP	Pearson correlation	0.745	0.889	0.793	1	0.858
	P (2-tailed)	0.000	0.000	0.000		0.000
PTX	Pearson correlation	0.862	0.712	0.632	0.858	1
	P (2-tailed)	0.000	0.000	0.000	0.000	

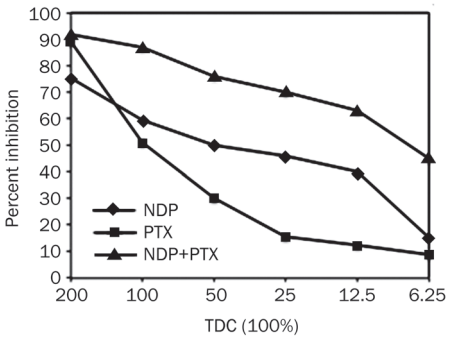

Figure 4. Results for NDP+PTX in one tumor, showing activity of the NDP, but an additive in activity of the combination compared with PTX.

cer. A number of chemosensitivity assays were developed over the last decades to predict the responsiveness of tumors to chemotherapy[19–21]. In recent years, the ATP-TCA method is a novel approach to test chemosensitivity in solid tumors[22–26].

In present study, the availability of esophageal cancer samples using the ATP-TCA was 90.5%, which is similar to the evaluability rates achieved in other 'cleaner' tumor types using this assay[27, 28]. Other *in vitro* studies of esophageal cancer cells, including the use of the MTT assay and histoculture drug response assay, have produced similar evaluability rates[29, 30]. The ATP-TCA has been shown to be more sensitive than these assays, and to have technical advantages over the MTT and clonogenic assays[27–30] . Previous studies with the ATP-TCA suggested that the assay was a good model for the investigation of tumor chemosensitivity and the results so far showed good correlation with clinical trial results in ovarian cancer[18, 31]. The chemosensitivity index has been used in previous studies to differentiate between sensitive and resistant tumors. The IC_{50} and IC_{90} were particularly useful measure of the efficacy of a drug. In this study we used chemotherapeutic agents at level related to their peak plasma concentrations, taking into account their degree of protein binding. We demonstrated that 29% of tumors were sensitive to NDP with Index <300, and 44.7% partial sensitive, which correlated well with the clinical response rate seen in patients. The results show considerable heterogeneity of chemosensitivity between patients to single agents and to drug combinations (Figure 1). Some tumor cells responded well to particular drugs or combinations, while other tumor cells showed no response to these, but instead responded to an alternative regimen. The histograms in Figure 1 all show a bell-shaped (Gaussian-like) distribution. Other distributions, ie with 2 peaks (one peak with sensitive and a second peak with resistant tumors) or an equal distribution without peak did not occur. Hence, bell-shaped distributions seem to be a general feature for all drugs tested. In principle, 2 peaks or an equal distribution without peak, whatever is, is right. But, fundamentally, the peak characteristic depends on the degree of heterogeneity and the purity of tumor cells in ATP-TCA analysis. The correlation analysis was performed using Pearson's rank correlation test among all five drugs tested. It was found that there exist positive correlation among all five drugs tested, suggesting the tumors are cross-resistant to all drugs. These also reflect the clinical reality that tumors are frequently rather cross-resistant.

Advanced esophageal cancer with widespread metastasis to lymph nodes or other organs is difficult to treat and has an extremely poor prognosis. In China, the most common chemotherapy single agent used in esophageal cancer was platinum compounds. The efficacy of platinum agents against cancer cells could be related to inhibition of DNA synthesis or to saturation of the cellular capacity to repair platinum adducts of DNA. Paclitaxel binds to tubulin and inhibits the disassembly of microtubules, thereby resulting in the inhibition of cell division[32]. Clinical studies demonstrated a range of response rates to this regimen, most of them between 25% and 50%. We tested the combinations containing NDP, which was effective to 29% tumors as a single agent. The combined treatment with NDP and PTX was the most effective group. 52.6% of samples were sensitive to adriamycin+paclitaxel using the Index <300 threshold and this was the most sensitive regimen (47.3%). The adriamycin was commonly used and its clinical activity against numerous solid malignancies make it an attractive drug for use in combination therapy[33].

In conclusion, there was a marked heterogeneity of chemosensitivity in esophageal cancer. Chemosensitivity testing might provide a practical method of testing new regimens before clinical trials in esophageal cancer patients. We believe that the ability to predict those patients who will respond well to chemotherapy will be a major step forward.

Acknowledgements

The authors wish to thank Dr Li-li ZHANG of the Huzhou Haichuang Biological Scientific Technology Co, Ltd, China for her excellent technical assistance. This work was supported in part by a grant from the Science and Technology General Project of Zhejiang Province, China (No 2009C33143).

Author contribution

Zhi-qiang LING performed research and participated in the preparation of manuscript; Chun-jian QI contributed new analytical tools and the preparation of manuscript; Li-juan QIAN and Lin-hui GU took part in tissue culture; Xiao-xiao LU and Zhi-guo ZHENG participated in statistical analysis; Qiang ZHAO and Shi WANG collected tissue specimens; Xian-hua FANG performed pathologic diagnosis; Zhi-xing YANG analyzed the data; Jian YIN gave technical support and reagents; and Wei-min MAO designed the research.

References

1 Parkin DM, Bray F, Ferlay J, Pisani P. Estimating the world cancer burden: Globocan 2000. Int J Cancer 2001; 94: 153–6.

2 Pohl J, May A, Rabenstein T, Pech O, Nguyen-Tat M, Fissler-Eckhoff A, *et al*. Comparison of computed virtual chromoendoscopy and conventional chromoendoscopy with acetic acid for detection of neoplasia in Barrett's esophagus. Endoscopy 2007; 39: 594–8.

3 Gockel I, Sgourakis G, Lyros O, Hansen T, Lang H. Dissection of lymph node metastases in esophageal cancer. Expert Rev Anticancer Ther

2011; 11: 571–8.
4 Buscaglia JM, Jayaraman V, Nagula S. Temporary use of a new fully-covered self-expanding metal stent for the management of post-esophagectomy strictures. Dig Endosc 2011; 23: 187–9.
5 Osaka Y, Shinohara M, Hoshino S, Ogata T, Takagi Y, Tsuchida A, *et al*. Phase II study of combined chemotherapy with docetaxel, CDDP and 5-FU for highly advanced esophageal cancer. Anticancer Res 2011; 31: 633–8.
6 Spigel DR, Greco FA, Meluch AA, Lane CM, Farley C, Gray JR, *et al*. Phase I/II trial of preoperative oxaliplatin, docetaxel, and capecitabine with concurrent radiation therapy in localized carcinoma of the esophagus or gastroesophageal junction. J Clin Oncol 2010; 28: 2213–9.
7 Ma Y, Ding Z, Qian Y, Wan YW, Tosun K, Shi X, *et al*. An integrative genomic and proteomic approach to chemosensitivity prediction. Int J Oncol 2009; 34: 107–15.
8 Marusyk A, Polyak K. Tumor heterogeneity: causes and consequences. Biochim Biophys Acta 2010; 1805: 105–17.
9 Watkins JM, Zauls AJ, Kearney PL, Shirai K, Ruppert BN, Harper JL, *et al*. Toxicity, response rates and survival outcomes of induction cisplatin and irinotecan followed by concurrent cisplatin, irinotecan and radiotherapy for locally advanced esophageal cancer. Jpn J Clin Oncol 2011; 41: 334–42.
10 Brown E, Markman M. Tumor chemosensitivity and chemoresistance assays. Cancer 1996; 77: 1020–5.
11 Kurbacher CM, Cree IA. Chemosensitivity testing using microplate adenosine triphosphate-based luminescence measurements. Methods Mol Med 2005; 110: 101–20.
12 Qi CJ, Ning YL, Zhu YL, Min HY, Ye H, Qian KQ. *In vitro* chemosensitivity in breast cancer using ATP-tumor chemosensitivity assay. Arch Pharm Res 2009; 32: 1737–42.
13 Konecny G, Crohns C, Pegram M, Felber M, Lude S, Kurbacher C, *et al*. Correlation of drug response with the ATP tumorchemosensitivity assay in primary FIGO stage III ovarian cancer. Gynecol Oncol 2000; 77: 258–63.
14 Sharma S, Neale MH, Di Nicolantonio F, Knight LA, Whitehouse PA, Mercer SJ, *et al*. Outcome of ATP-based tumor chemosensitivity assay directed chemotherapy in heavily pre-treated recurrent ovarian carcinoma. BMC Cancer 2003; 3: 19.
15 Whitehouse PA, Knight LA, Di Nicolantonio F, Mercer SJ, Sharma S, Cree IA, *et al*. Heterogeneity of chemosensitivity of colorectal adenocarcinoma determined by a modified *ex vivo* ATP-tumor chemosensitivity assay (ATP-TCA). Anticancer Drugs 2003; 14: 369–75.
16 Chou TC, Talalay P. Quantitative analysis of dose-effect relationships: the combined effects of multiple drugs or enzyme inhibitors. Adv Enzyme Regul 1984; 22: 27–55.
17 Whitehouse PA, Mercer SJ, Knight LA, Di Nicolantonio F, O'Callaghan A, Cree IA, *et al*. Combination chemotherapy in advanced gastrointestinal cancers: *ex vivo* sensitivity to gemcitabine and mitomycin C. Br J Cancer 2003; 89: 2299–304.
18 Kurbacher CM, Bruckner HW, Cree IA, Kurbacher JA, Wilhelm L, Pöch G, *et al*. Mitoxantrone combined with paclitaxel as salvage therapy for platinum-refractory ovarian cancer: laboratory study and clinical pilot trial. Clin Cancer Res 1997; 3: 1527–33.
19 Sumantran VN. Cellular chemosensitivity assays: an overview. Methods Mol Biol 2011; 731: 219–36.
20 Glaysher S, Cree IA. Cell sensitivity assays: the ATP-based tumor chemosensitivity assay. Methods Mol Biol 2011; 731: 247–57.
21 von Bueren AO, Oehler C, Shalaby T, von Hoff K, Pruschy M, Seifert B, *et al*. c-MYC expression sensitizes medulloblastoma cells to radio- and chemotherapy and has no impact on response in medulloblastoma patients. BMC Cancer 2011; 11: 74.
22 Wang X, Yan SK, Dai WX, Liu XR, Zhang WD, Wang JJ. A metabonomic approach to chemosensitivity prediction of cisplatin plus 5-fluorouracil in a human xenograft model of gastric cancer. Int J Cancer 2010; 127: 2841–50.
23 Di Nicolantonio F, Knight LA, Di Palma S, Sharma S, Whitehouse PA, Mercer SJ, *et al*. *Ex vivo* characterization of XR11576 (MLN576) against ovarian cancer and other solid tumors. Anticancer Drugs 2004; 15: 849–60.
24 Doerler M, Hyun J, Venten I, Potthoff A, Bartke U, Serova K, *et al*. Does chemosensitivity-assay-directed therapy have an influence on the prognosis of patients with malignant melanoma stage IV? A retrospective study of 14 patients with malignant melanoma stage IV. Eur J Med Res 2007; 12: 497–502.
25 Mercer SJ, Somers SS, Knight LA, Whitehouse PA, Sharma S, Di Nicolantonio F, *et al*. Heterogeneity of chemosensitivity of esophageal and gastric carcinoma. Anticancer Drugs 2003; 14: 397–403.
26 Michalski CW, Erkan M, Sauliunaite D, Giese T, Stratmann R, Sartori C, *et al*. *Ex vivo* chemosensitivity testing and gene expression profiling predict response towards adjuvant gemcitabine treatment in pancreatic cancer. Br J Cancer 2008; 99: 760–7.
27 Parker KA, Glaysher S, Polak M, Gabriel FG, Johnson P, Knight LA, *et al*. The molecular basis of the chemosensitivity of metastatic cutaneous melanoma to chemotherapy. J Clin Pathol 2010; 63: 1012–20.
28 Glaysher S, Yiannakis D, Gabriel FG, Johnson P, Polak ME, Knight LA, *et al*. Resistance gene expression determines the *in vitro* chemosensitivity of non-small cell lung cancer (NSCLC). BMC Cancer 2009; 9: 300.
29 Tanaka N, Kimura H, Faried A, Sakai M, Sano A, Inose T, *et al*. Quantitative analysis of cisplatin sensitivity of human esophageal squamous cancer cell lines using in-air micro-PIXE. Cancer Sci 2010; 101: 1487–92.
30 Fujita Y, Hiramatsu M, Kawai M, Nishimura H, Miyamoto A, Tanigawa N. Histoculture drug response assay predicts the postoperative prognosis of patients with esophageal cancer. Oncol Rep 2009; 21: 499–505.
31 Kurbacher CM, Cree IA, Bruckner HW, Brenne U, Kurbacher JA, Müller K, *et al*. Use of an *ex vivo* ATP luminescence assay to direct chemotherapy for recurrent ovarian cancer. Anticancer Drugs 1998; 9: 51–7.
32 Bhalla KN. Microtubule-targeted anticancer agents and apoptosis. Oncogene 2003; 22: 9075–86.
33 Bull JM, Tormey DC, Li SH, Carbone PP, Falkson G, Blom J, *et al*. A randomized comparative trial of adriamycin *versus* methotrexate in combination drug therapy. Cancer 1978; 41: 1649–57.

Acta Pharmacologica Sinica (2012) 33: 407–417

www.nature.com/aps

Original Article

Novel microtubule-targeted agent 6-chloro-4-(methoxyphenyl) coumarin induces G_2-M arrest and apoptosis in HeLa cells

Yi-ming MA, Yu-bo ZHOU*, Chuan-ming XIE, Dong-mei CHEN, Jia LI*

National Center for Drug Screening, State Key Laboratory of Drug Research, Shanghai Institute of Materia Medica, Chinese Academy of Sciences, Shanghai 201203, China

Aim: To identify a novel coumarin analogue with the highest anticancer activity and to further investigate its anticancer mechanisms.
Methods: The viability of cancer cells was investigated using the MTT assay. The cell cycle progression was evaluated using both flow cytometric and Western blotting analysis. Microtubule depolymerization was observed with immunocytochemistry *in vivo* and a tubulin depolymerization assay *in vitro*. Apoptosis was demonstrated using Annexin V/Propidium Iodide (PI) double-staining and sub-G_1 analysis.
Results: Among 36 analogues of coumarin, 6-chloro-4-(methoxyphenyl) coumarin showed the best anticancer activity (IC_{50} value about 200 nmol/L) in HCT116 cells. The compound had a broad spectrum of anticancer activity against 9 cancer cell lines derived from colon cancer, breast cancer, liver cancer, cervical cancer, leukemia, epidermoid cancer with IC_{50} value of 75 nmol/L–1.57 μmol/L but with low cytotocitity against WI-38 human lung fibroblasts (IC_{50} value of 12.128 μmol/L). The compound (0.04–10 μmol/L) induced G_2-M phase arrest in HeLa cells in a dose-dependent manner, which was reversible after the compound was removed. The compound (10–300 μmol/L) induced the depolymerization of purified porcine tubulin *in vitro*. Finally, the compound (0.04–2.5 μmol/L) induced apoptosis of HeLa cells in dose- and time-dependent manners.
Conclusion: 6-Chloro-4-(methoxyphenyl) coumarin is a novel microtubule-targeting agent that induces G_2–M arrest and apoptosis in HeLa cells.

Keywords: anticancer drug; 6-chloro-4-(methoxyphenyl) coumarin; cell cycle arrest; microtubule depolymerization; apoptosis

Acta Pharmacologica Sinica (2012) 33: 407–417; doi: 10.1038/aps.2011.176; published online 23 Jan 2012

Introduction

Coumarins are natural products widely abundant in natural sources, especially green plants. Coumarins have multiple biological activities[1], including anticoagulant[2–4], anti-inflammatory[5, 6], antimicrobial[7–12], antioxidant[13–16], antiallergic[17–20], anti-HIV[21], anticancer[22–28] and antiviral activities[29–32]. It has been suggested that alterations in the chemical structure of coumarins could change their cytotoxic properties. It has also been known for many years that coumarins have significant therapeutic potential[33–35] and are present in many natural therapeutic products[36–40]. Due to their attractive properties and potential clinical utility, we synthesized a series of coumarin analogues and evaluated their anticancer properties to find a novel coumarin analogue with good anticancer activity.

In the present study, we show that 6-chloro-4-(methoxyphenyl) coumarin (CMC) has the best anticancer activity among 36 different coumarin analogues. CMC had broad-spectrum anticancer activities in 9 cancer cell lines derived from 6 different tissues. Further analysis showed that CMC caused G_2-M arrest and apoptosis in HeLa cells via microtubule depolymerization.

Materials and methods

Cell culture

The colon cancer cell line LS-174t was cultured in MEM medium with 10% fetal bovine serum (Hyclone, Thermo Scientific, Logan, UT, USA). The colon cancer cell line HCT-116 was cultured in McCoy's 5A modified medium with 10% fetal bovine serum. The colon cancer cell lines Colo-205 and HCT-15, the breast cancer cell line MDA-MB-435S, and the leukemia cell line HL-60 were cultured in RPMI-1640 with 10% fetal bovine serum. The liver cancer cell line HepG2, the

* To whom correspondence should be addressed.
E-mail jli@mail.shcnc.ac.cn (Jia LI);
ybzhou@mail.shcnc.ac.cn (Yu-bo ZHOU)
Received 2011-09-24 Accepted 2011-11-18

epidermoid cancer cell line A431 and the cervical cancer cell line HeLa were cultured in DMEM (high glucose) with 10% fetal bovine serum. All cell lines mentioned above were purchased from the Cell Bank (Chinese Academy of Sciences, Shanghai, China). A human fetal lung fibroblast cell line (WI-38) was kindly provided by Dr Mei-yu GENG (Shanghai Institute of Materia Medica) and was cultured in MEM with 10% fetal bovine serum (Gibco, Invitrogen, USA). All cells were kept in a humidified atmosphere of 5% CO_2 and 95% air at 37 °C.

Reagents

Coumarin analogues were synthesized and provided by Prof Jie WU from Fudan University. The analogues were dissolved in 100% DMSO with a 5 g/L stock solution. The working solution was prepared by dilution of the stock solution with the culture medium.

An anti-phospho-Ser/Thr-Pro MPM-2 (Cat #05-368) antibody was purchased from Millipore Corporation (Boston, MA, USA). Anti-CDC25C (Cat #4688) antibody was from Cell Signal Technology (Boston, MA, USA). Peroxidase-affiniPure goat anti-rabbit IgG (Code: 112-035-175) and goat anti-mouse IgG (Code: 115-035-174) were purchased from Jackson ImmunoResearch Laboratories, Inc (Baltimore, MD, USA). Hoechst 33342 dye (Cat #H3570) and Alexa Fluor 488 dye-labeled donkey anti-mouse IgG (Cat #A-21202) were purchased from Invitrogen Corporation (Carlsbad, CA, USA).

Cell proliferation assay

The inhibitory effects of synthesized coumarin analogues on the growth of cancer cell lines were evaluated using the MTT viability assay as described previously[41]. Briefly, cells (3000 cells/well) were seeded onto plastic 96-well cell culture plates and cultured at 37 °C. After 24 h, compounds with doses ranging from 10 μmol/L to 10 nmol/L at a dilution ratio of 1:4 were added, and the cells were further incubated for 72 h. MTT was then added to each well at a final concentration of 1 g/L. After a 3 h incubation at 37 °C, the medium was gently discarded and DMSO (100 μL/well) was added to dissolve the formazan product. The optical density was determined at 550 nm/690 nm using a VersaMax Microplate Reader (Molecular Devices). Experiments were performed in four replicates. IC_{50} values were derived from a nonlinear regression model (curvefit) based on a sigmoidal dose response curve (variable slope) and computed using Graphpad Software (Graphpad Prism version 5.02). Data were expressed as the mean±SEM.

Cell cycle analysis

As described previously[42], both synchronized and asynchronized HeLa cells were treated with either DMSO (negative control), nocodazole (positive control), or CMC at 37 °C for the indicated time. The cells were then digested with 0.5 g/L trypsin, collected, washed twice with cold 1×PBS and fixed in 1 mL of 70% ethanol at 4 °C overnight. The next day, cells were washed twice with cold 1×PBS and incubated with 20 μg/mL RNase at 37 °C for 15 min. Cells were then stained with 20 mg/L PI for 30 min at 4 °C. Cell cycle distribution was determined using a BD FACSCalibur Flow Cytometer.

Cell synchronization

HeLa cells were synchronized using a double thymidine block as described previously[43]. Briefly, 1.5×10^5 cells were seeded in each well of a 6-well cell culture plate. The next day, a double thymidine block was performed with an initial block for 17 h and a 10 h release and was followed by a second block for 16 h. The final concentration of thymidine used in the block medium was 2 mmol/L. Following release from the second block, synchronized cells were treated with either DMSO (negative control), nocodazole (positive control) or CMC for the indicated times, and samples were collected for flow cytometry analysis.

Western analysis of G_2-M regulatory proteins

HeLa cells were treated with varying doses of CMC for 24 h. Cells were then lysed with cell lysis buffer [1% NP-40, 150 mmol/L NaCl, 20 mmol/L Tris-HCl, 1 mmol/L EDTA, 1 mmol/L EGTA and complete protease inhibitor cocktail (Cat #11697498001, Roche)]. Equal amounts of protein were resolved by SDS-polyacrylamide gel electrophoresis, transferred onto Hybond-C nitrocellulose membranes (GE Life Sciences) and immunoblotted as described previously[44]. Immunoreactive bands were detected with the enhanced chemiluminescence (ECL) system (GE Life Sciences).

Immunocytochemistry assay

Microtubules were observed using an immunocytochemistry assay[45, 46]. Briefly, HeLa cells were grown on glass coverslips for 24 h and then treated with varying doses of CMC for 8 h. Cells were then fixed with cold methanol (4 °C) for 5 min, blocked for 1 h with 5% BSA in 1×PBS at room temperature and incubated with monoclonal β-tubulin antibody (T-4026; Sigma, St Louis, MO, USA) overnight at 4 °C. Cells were then washed three times with 1×PBS and incubated with Alexa Fluor 488-labeled donkey anti-mouse IgG (Invitrogen) at room temperature for 1 h. The coverslips were washed, stained with 5 mg/L Hoechst 33342 dye (Molecular Probes, Invitrogen) and photographed using an Olympus confocal microscope (Olympus, Tokyo, Japan).

In vitro tubulin polymerization assay

An *in vitro* fluorescence-based tubulin polymerization assay kit (BK011, Cytoskeleton, Inc) was used according to the manufacturer's protocol for monitoring the time-dependent polymerization of tubulin to microtubules. The reaction mixture had a final volume of 50 μL in PEM buffer (80 mmol/L PIPES, 0.5 mmol/L EGTA, 2 mmol/L $MgCl_2$, pH 6.9) and contained 2 g/L bovine brain tubulin, 10 μmol/L fluorescent reporter and 1 mmol/L GTP in either the presence or absence of test compounds at 37 °C. Tubulin polymerization was followed by monitoring fluorescence enhancement due to the incorporation of a fluorescent reporter into microtubules as polymerization proceeded. Fluorescence emission at 450 nm

(excitation wavelength of 360 nm) was measured for 1 h at 0.5 min intervals in a FlexStation 3 Microplate Reader (Molecular Devices). Nocodazole was used as positive control.

Apoptosis detection assay

The quantitative assessment of apoptosis was determined using Annexin V-FITC and PI double staining. Annexin V binds to phosphatidylserine (PS) and other negatively charged phospholipids, thereby producing fluorescence primarily indicative of PS translocation from the inner to the outer cell membrane leaflet. This change reflects aminophospholipid translocase activity in apoptotic cells[47]. PI is a nucleic acid dye that penetrates the nuclear envelope of necrotic cells and was used here as a counterstain to differentiate between live, apoptotic, late-stage apoptotic/early stage necrotic and necrotic cells. Briefly, HeLa cells were treated with varying doses of either CMC or 1 μmol/L stauporine for the indicated times and were then stained with an Annexin V-FITC/PI double staining kit (KGA108, Kaiji Bio Co, Nanjing, China). After washing twice with cold 1×PBS, 5×10^5 cells were collected, resuspended in 500 μL binding buffer with 0.1 g/L Annexin V-FITC and 0.05 g/L PI, and then incubated for 15 min in the dark at room temperature. Finally, the percent of apoptotic cells was immediately measured with a BD FACS Calibur Flow Cytometer and analyzed with CellQuest software (BD Biosciences).

Results

CMC (compound 8) showed the best anticancer activity *in vitro* among the synthesized coumarin analogues

The anticancer activities of different synthesized coumarin analogues were evaluated in HCT116 colon cancer cells using the MTT viability assay. The corresponding chemical structures are shown in Figure 1, and the anticancer activities against HCT116 cells are shown in Table 1. Among the coumarin analogues, CMC (compound **8**) had the best anticancer activity with an IC_{50} value of approximately 200 nmol/L and was selected for further mechanistic study.

Table 1. The *in vitro* anti-proliferation activities of 36 coumarin analogues in HCT116 colorectal carcinoma cells.

Compound ID	IC_{50} (μmol/L)*
1	28.153±2.130
2	1.237±0.159
3	7.809±0.492
4	21.307±1.736
5	33.893±2.764
6	1.661±0.266
7	0.248±0.049
8	0.202±0.038
9	16.297±1.087
10	23.211±1.236
11	28.678±3.109
12	29.303±2.622
13	10.133±1.041
14	34.203±3.131
15	31.893±3.503
16	14.806±1.500
17	10.130±1.120
18	27.552±2.772
19	34.145±3.894
20	3.177±0.200
21	40.520±6.534
22	31.859±3.403
23	16.720±1.653
24	13.440±1.112
25	17.468±0.753
26	13.892±0.576
27	13.897±0.623
28	12.273±0.713
29	12.535±0.631
30	11.548±0.909
31	14.906±0.592
32	9.579±0.441
33	6.896±0.416
34	21.314±0.779
35	22.095±1.536
36	8.183±0.704
doxorubicin	0.061±0.006

*Cell proliferation assay was done according to the method mentioned in the Materials and methods section. The IC_{50} values represent the mean±SEM of quadruplicate determinations.

CMC exhibited very potent anticancer activity against different cancer cell lines

The effect of CMC on the viability of 9 human cancer cell lines derived from 6 different tissues was evaluated using an MTT assay. As shown in Figure 2, CMC exhibited very potent anticancer activity. The IC_{50} values for CMC ranged from 75 nmol/L to 1.57 μmol/L, and the average IC_{50} value was approximately 0.53 μmol/L. Then the selective cytotoxicity of CMC was further evaluated using human normal fetal fibroblast cell line WI-38. CMC exerted markedly weaker cytotoxicity against WI-38 cells with an IC_{50} value of approximately 12.128 μmol/L than against other 9 cancer cell lines.

CMC specifically and reversibly induced G_2-M phase arrest in HeLa cells

Using brightfield microscopy, we found that treatment with CMC caused detachment of adherent cancer cells. The cells became round (data not shown), a phenomenon that occurs during mitosis. To test the possibility that CMC affects mitosis, the effect of CMC on cell cycle progression in HeLa cells was examined. First, HeLa cells were treated with CMC at different concentrations for 24 h. As shown in Figure 3A, CMC treatment resulted in a dose-dependent accumulation of HeLa cells in G_2-M phase with concomitant losses from G_0-G_1 phase. No change in S-phase was observed.

To examine the specificity of the CMC-elicited mitotic arrest, HeLa cells were synchronized at the G_1/S boundary by double thymidine block and were then treated with either 0.63 μmol/L CMC or 0.33 μmol/L nocodazole (positive

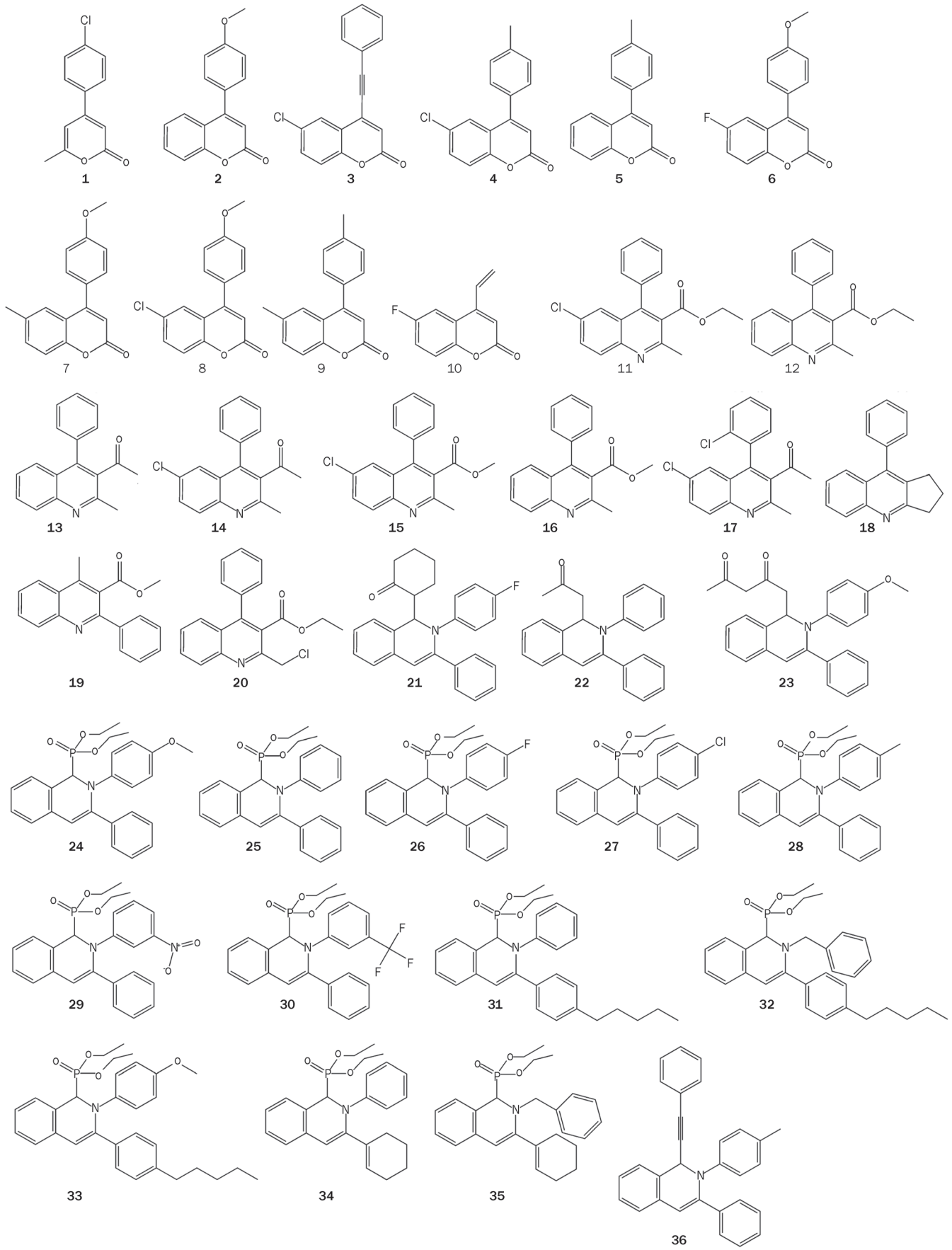

Figure 1. The chemical structures of synthesized coumarin analogues.

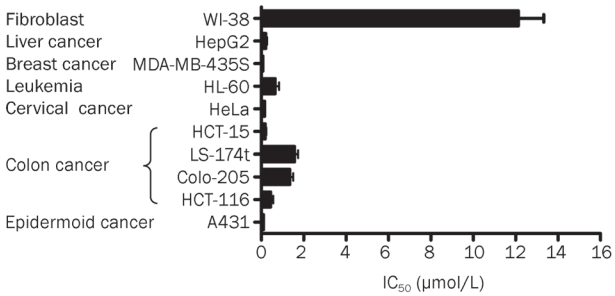

Figure 2. CMC had good anticancer activity in 9 different cancer cell lines. The viability of 9 cancer cell lines and 1 human fetal lung fibroblast cell line was assessed by MTT assay after 72 h of treatment with CMC. All results are expressed as the mean±SEM of four independent experiments.

control) immediately following their release from the block. Flow cytometry analysis was conducted to examine cell cycle progression of CMC-treated cells. Within 6 h and 9 h post-release, CMC-treated cells entered S phase and G_2 phase, respectively, just as did the control cells. However, at the 12 h time point after release, CMC-treated cells were arrested at mitosis in striking contrast to the entrance of control cells into the next cell cycle (Figure 3B). These data indicated that CMC induced an accumulation of cells specifically at G_2-M phase without affecting other cell cycle phases.

Finally, the reversibility of CMC-induced mitotic arrest was assessed by withdrawing CMC immediately after 12 h of treatment. Following CMC withdrawal, arrested cells began to exit from mitosis within 3 h, and 6 h later, most cells entered the next G_1 phase. This result indicated that CMC-induced mitotic arrest is reversible (Figure 3C).

CMC changed the phosphorylation state of G_2-M regulators in HeLa cells

As expected from the previous results, alterations in mitosis-specific protein expression were also detected. Briefly, HeLa cells were treated with CMC at different concentrations for 24 h and then samples were prepared. The levels of MPM-2, CDC25C and β-actin were measured using Western blot analysis. MPM-2 commonly reflects the phosphorylation level of mitosis-specific proteins. As shown in Figure 4, MPM-2 was

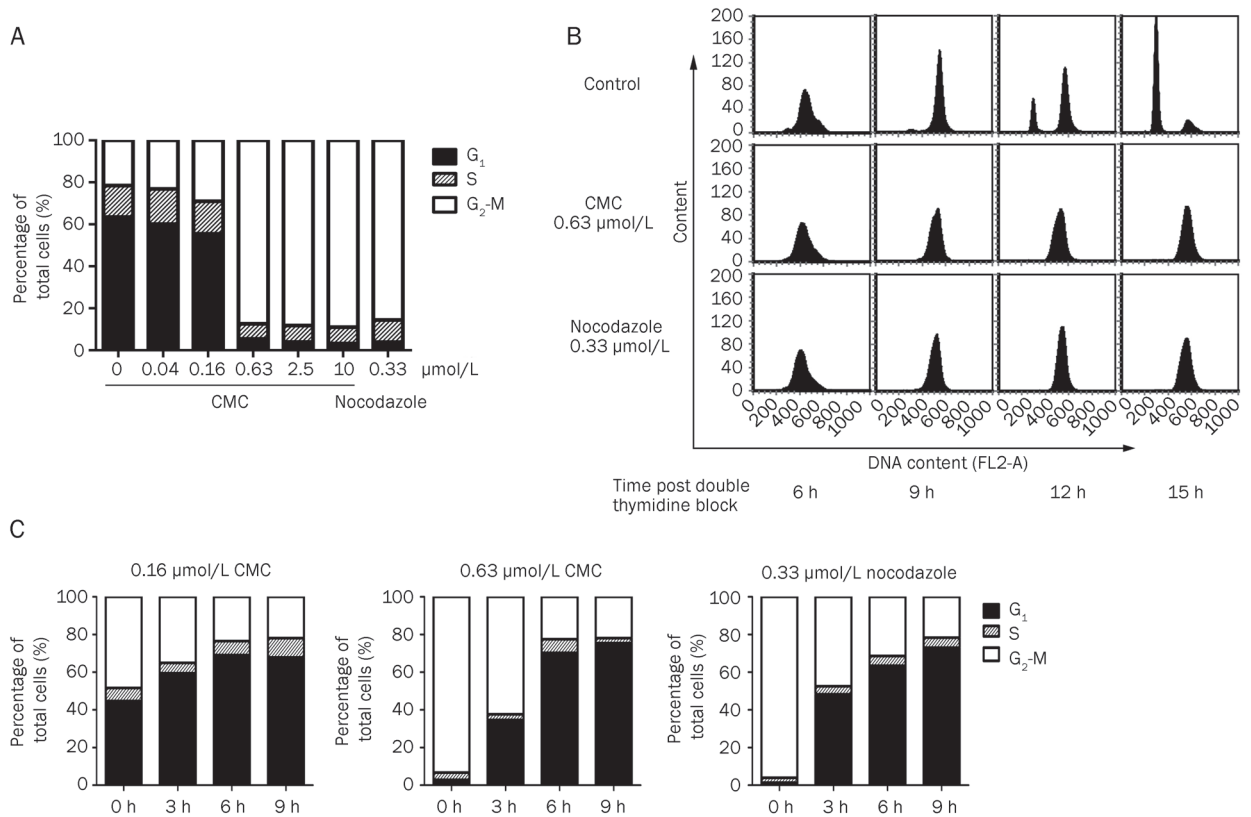

Figure 3. CMC-treated HeLa cells specifically and reversibly arrested in G_2-M phase. (A) HeLa cells arrested in G_2-M phase in a dose-dependent manner. HeLa cells were treated with CMC at doses ranging from 10 μmol/L to 0.04 μmol/L for 24 h. 0.33 μmol/L nocodazole was used as a positive control. The samples were fixed, stained with PI, and analyzed using flow cytometry. (B) HeLa cells were specifically arrested in G_2-M phase. To evaluate if CMC only induced G_2-M arrest, HeLa cells were synchronized at the G_1/S border using a thymidine-thymidine block. The cells were then released and treated with 0.63 μmol/L CMC. Samples were collected at 6 h, 9 h, 12 h, and 15 h and then subjected to flow cytometry analysis. (C) HeLa cells could re-enter the cell cycle following deprivation of CMC. HeLa cells were treated with either CMC or nocodazole (positive control) for 12 h. The medium containing CMC was then removed and fresh medium was added. Samples were collected at 0 h, 3 h, 6 h, and 9 h after deprivation of CMC and then subjected to flow cytometry analysis. All of the data shown are representative of three independent experiments with similar results.

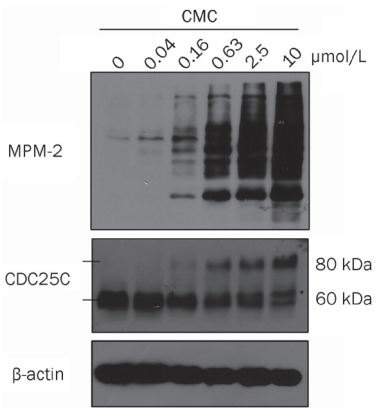

Figure 4. CMC changed the phosphorylation state of G_2-M regulators. HeLa cells were treated with CMC at doses ranging from 10 μmol/L to 0.04 μmol/L for 24 h. 0.1% DMSO was used as a negative control. Phosphorylation of a G_2-M-specific protein (MPM-2) and CDC25C were detected using western blot analysis. β-actin was used as an internal control. MPM-2 and CDC25C antibodies were diluted at 1:1000 in 1×TBST. β-actin antibody was diluted at 1:10000 in 1×TBST. A non-specific band that cross-reacted with the CDC25C antibody is marked with an asterisk.

slightly increased when cells were treated with 0.16 μmol/L CMC but was significantly increased when cells were treated with 0.63 μmol/L CMC. Consistent with this result, there was a shift to a slower migrating form of CDC25C that increased in a dose-dependent manner, which is indicative of changes in the phosphorylation state of the protein. These changes in protein phosphorylation are consistent with cell cycle arrest in mitosis as has been shown previously[48].

CMC induces G_2-M arrest through the depolymerization of microtubules in a direct manner

Cellular microtubules are important components of spindles, which play an important role in mitosis. After sister chromatids are pulled apart by spindles, a single mitotic cell can divide into two cells. To investigate whether CMC affected tubulin polymerization, the microtubule status of CMC-treated HeLa cells was detected by immunocytochemistry. Briefly, cells were exposed to either CMC or a reference drug (nocodazole) for 8 h, fixed and then incubated with β-tubulin antibody at 4 °C overnight. The next day, cells were incubated with Alexa Fluor® 488-labeled donkey anti-mouse IgG, stained with Hoechst 33342 and observed with confocal microscopy.

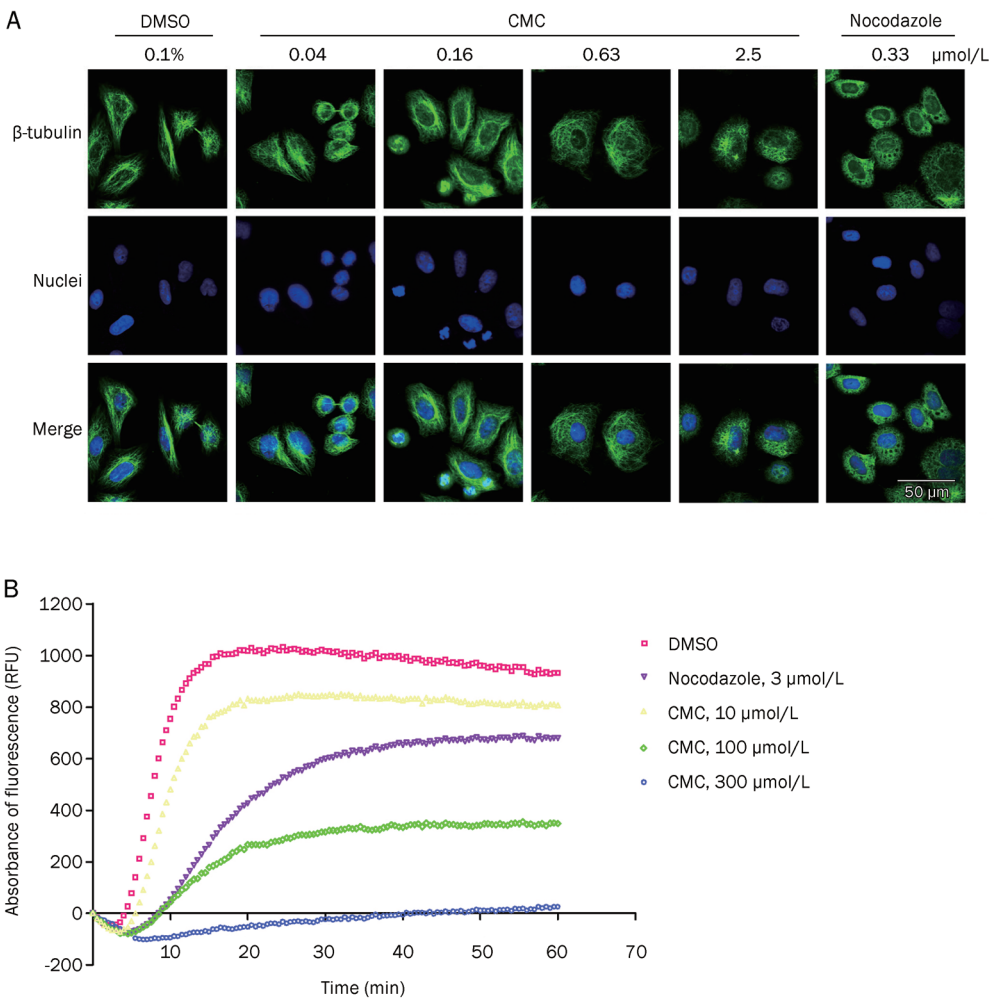

Figure 5. CMC inhibited the polymerization of microtubules. (A) CMC depolymerized microtubules *in vivo*. HeLa cells were treated with CMC at doses ranging from 2.5 μmol/L to 0.04 μmol/L for 8 h. 0.1% DMSO was used as a negative control, and 0.33 μmol/L nocodazole was used as a positive control. Samples were then prepared as mentioned in the "Materials and methods" section, and the status of microtubules was observed using an Olympus confocal microscope (Olym pus, Tokyo, Japan). (B) CMC depolymerized purified tubulin *in vitro*. CMC was added to fluorescently labeled bovine tubulin at 37 °C for 1 h, and its effect on tubulin polymerization was detected with a FlexStation 3 Microplate Reader (Molecular Devices). Nocodazole (3 μmol/L) was used as a positive control, and DMSO was used as a negative control.

CMC depolymerized microtubules in a dose-dependent manner (Figure 5A). When treated with 0.16 μmol/L CMC, the polymerization status of microtubules was only slightly changed; however, when cells were treated with 0.63 μmol/L CMC, almost all microtubules were depolymerized compared with the control group. This phenomenon was consistent with the aforementioned results of the cell cycle and Western blot analyses.

To deduce the mode of CMC-mediated microtubule depolymerization, we used a fluorescence-based tubulin polymerization assay. Nocodazole was used as the positive control. As shown in Figure 5B, CMC inhibited tubulin polymerization in a dose-dependent manner, thereby indicating that CMC inhibited the polymerization of tubulin in a direct manner.

CMC induced apoptosis in a time- and dose-dependent manner

It has been reported that G_2-M arrest caused by microtubule depolymerization is followed by apoptosis[49–51]; therefore, we chose to further investigate the apoptosis induced by CMC.

As shown in Figures 6A and 6B, persistent treatment with CMC led to a progressive increase in apoptosis in a time-dependent manner. Apoptosis of CMC-treated cells increased within 24 h (58.66% viable, 22.09% in early apoptosis and 16.59% cells in late apoptosis). Most cells were apoptotic at 48 h (56.58% in early apoptosis and 29.93% in late apoptosis). At 72 h, most cells were in late apoptosis (17.24% in early apoptosis and 77.87% in late apoptosis).

HeLa cells were then treated with varying doses of CMC for 48 h. As shown in Figures 6C and 6D, the levels of apoptosis in cells treated with 0.04 μmol/L CMC (a dose without induction of G_2-M arrest as shown in Figure 3A) was the same as the negative control. The levels of apoptosis increased in a dose-dependent manner when the cells were treated with G_2-M-arrest-inducing doses (doses greater than 0.16 μmol/L as shown in Figure 3A).

The three-dimensional profile of cell cycle progression *versus* time of CMC treatment shown in Figure 6E demonstrated that G_2-M arrest was maximal (~76.43%) at 12 h of treatment. After this point, the G_2-M population disappeared concomitant with the emergence of a characteristic hypodiploid (<2N DNA) sub-G_1 peak, which indicates apoptotic cells (Figures 6E and 6F). This apoptotic population peaked at 72 h (~59.33%) posttreatment. The *in vitro* findings strongly therefore indicate that CMC-treated cells arrest in G_2-M phase before beginning to apoptose.

Discussion

Coumarins are a hot topic of research due to their diverse pharmaceutical activities and wide distribution in nature. To find a coumarin analogue with good anticancer activity, we synthesized a series of coumarin analogues (Figure 1) and evaluated their effects on the viability of HCT116 cells (Table 1). CMC had the best anticancer activity and was thus selected for further mechanistic study. Nine cancer cell lines derived from 6 different tissues and the WI-38 cell line derived from normal embryonic (3 month gestation) lung tissue were used to evaluate the anticancer effects of CMC. We found that CMC had a high level of anticancer activity *in vitro*, with an IC_{50} value ranging from 75 nmol/L to 1.57 μmol/L. The cytotoxic effect of CMC on WI-38 cells was less potent, with an IC_{50} value of 12.128 μmol/L (Figure 2), which implies that CMC has relative selectivity for cancer cells versus normal cells. CMC also had the best anticancer activity and similar IC_{50} values against the HeLa, MDA-MB-435S, HCT-15, and A431 cell lines. The HeLa cell line was subsequently used for further anticancer mechanism study.

During the above experiments, it came to our attention that CMC caused the evident detachment of HeLa cells that became round (data not shown), a phenomenon frequently observed during the mitotic process. The effect of CMC on cell cycle progression was therefore evaluated to see if CMC affected cellular mitosis. After 24 h of treatment, CMC induced G_2-M arrest in a dose-dependent manner. The minimal dose that caused nearly complete arrest in G_2-M phase was approximately 0.63 μmol/L (Figure 3A); importantly, no concurrent change in S-phase was observed. To determine whether CMC only induced G_2-M arrest, we treated synchronized HeLa cells and found that CMC only influenced G_2-M phase without affecting other cell cycle phases (Figure 3B). G_2-M arrest caused by CMC could be reversed by deprivation of CMC (Figure 3C). Western blot analysis showed that increasing doses of CMC induced increased levels of phosphorylation of G_2-M phase-specific proteins, which provided proof of G_2-M arrest (Figure 4).

When cells were treated with CMC, the cell shape became round with an increased disorder of M-phase-condensed chromosome alignment in a dose-dependent manner (data not shown), which is reported to be induced by alterations to the microtubular cytoskeleton[52]. The microtubule state of CMC-treated cells was therefore tested by ICC. ICC analysis showed that CMC induced microtubule depolymerization after an eight-hour treatment (Figure 5A). Furthermore, CMC effects on tubulin polymerization were tested. These results showed that CMC could inhibit tubulin polymerization directly (Figure 5B). Many articles have reported that G_2-M arrest induced by tubulin-targeting agents is caused by their microtubule depolymerization effects[53–58]. The results shown in Figures 3–5 indicate that CMC caused G_2-M arrest by directly mediating depolymerization of microtubules.

Replicated chromosomes must be accurately segregated into each daughter cell during mitosis, and the spindle checkpoint is a surveillance mechanism that delays anaphase onset until all chromosomes are correctly attached in a bipolar fashion to the mitotic spindle[59]. Chemical inhibition of spindle dynamics, which relieves tension but does not destroy kinetochore-microtubule attachments, activates the spindle checkpoint[60, 61]. From the results shown in Figures 3 and 5, CMC depolymerized microtubules and induced G_2-M arrest in a dose-dependent manner. The dose of CMC needed to depolymerize microtubules is the same as the dose of CMC needed to induce G_2-M arrest, implying that the G_2-M arrest induced by CMC is via microtubule depolymerization.

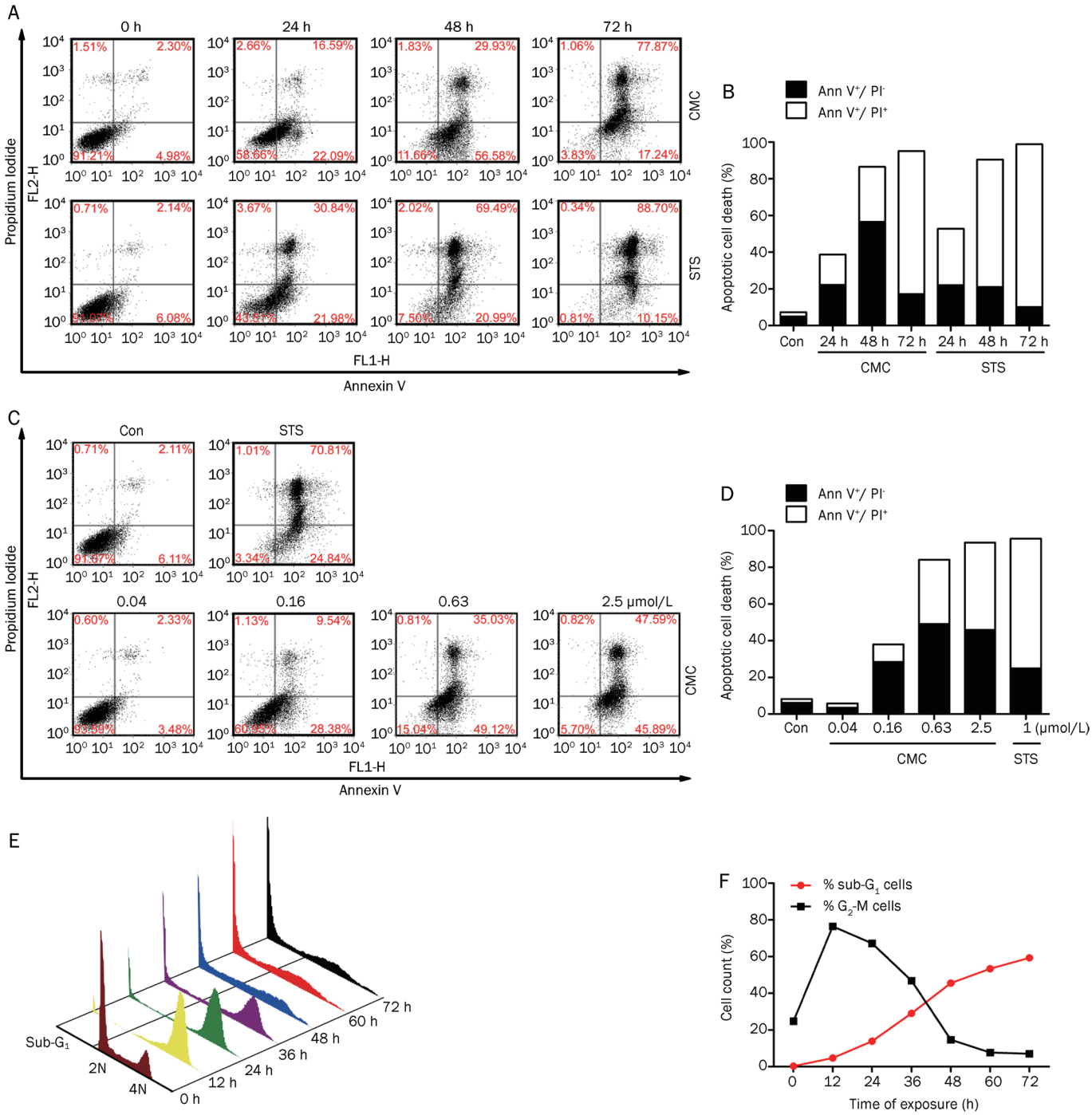

Figure 6. CMC induced apoptosis in a time- and dose-dependent manner. (A) (B) HeLa cells were treated with 0.63 μmol/L CMC. Samples were then collected at 24 h, 48 h, and 72 h followed by staining with Annexin V-FITC/PI. The level of apoptosis was detected using flow cytometry. (C) (D) HeLa cells were treated with CMC at doses ranging from 2.5 μmol/L to 0.04 μmol/L for 48 h. Samples were then stained with Annexin V-FITC/PI. Apoptosis was detected using flow cytometry. (E) (F) HeLa cells were treated with 0.63 μmol/L CMC for 12 h-72 h, and the percentage of sub-G_1 cells and G_2-M cells was analyzed using the ModFit software provided with the FACSCalibur flow cytometer.

It has been reported that microtubule-targeting agents can induce apoptosis via activation of the spindle checkpoint[62]; thus, apoptosis induced by CMC was evaluated using Annexin V/PI double staining. As shown in Figures 6A and 6B, 0.63 μmol/L CMC triggered apoptosis at 24 h and induced apoptosis in a time-dependent manner (Figures 6A and 6B). CMC also caused a significant increase in apoptosis at 48 h in a dose-dependent manner (Figures 6C and 6D), and G_2-M arrest induced by CMC occurs before the commencement of apoptosis (Figures 6E and 6F).

As mentioned, the importance of microtubules in mitosis makes them a superb target for a group of highly successful, chemically diverse anticancer drugs[63–65]. In view of the success of this class of drugs, it has been argued that microtubules represent the best cancer target to be identified so far, and it seems likely that drugs of this class will continue to be important chemotherapeutic agents even as more selective approaches are developed[63–65]. Relatively weak microtubule-targeting coumarins could also be used as adjuvants in chemotherapy to attain increased efficacy with decreased toxicity[63–65]. The maintenance of low concentrations of microtubule-targeted drugs in tumor tissue for long durations could be more efficacious in killing tumor cells than the rapidly rising and falling drug concentrations associated with bolus administration at maximum tolerated doses[63–65]. These advantages make coumarins a hot area for further study.

Still elusive is the fact that different anticancer coumarins with different substitutions can have different mechanisms. It is reported that coumarin can reduce the expression of Ras and Myc, and it can also induce G_0/G_1 arrest and apoptosis via ROS[66]. Another coumarin analogue, decursin, inhibits the proliferation of the advanced human prostate carcinoma cell lines DU145, PC-3 and LNCaP by causing G_1 arrest via an induction of Cip1/p21 and Kip1/p27[22]. Ferulenol and dicoumarol stimulate tubulin assembly[67, 68], and geiparvarin is able to inhibit GTP-induced polymerization[69]. Here, we report on a novel microtubule-targeting coumarin analogue with high anticancer activity. Our results provide clues for structure-activity relationship studies and for further structural design of novel microtubule-targeting coumarin analogues.

Acknowledgements

The authors thank Prof Jie WU from Fudan University for the synthesis of coumarin analogues and Prof Yi CHEN from the Shanghai Institute of Materia Medica for her helpful comments on this work. This work was supported by grants from the National Natural Science Foundation of China (No 30801405 and 81072667).

Author contribution

Yi-ming MA, Yu-bo ZHOU and Jia LI designed the research; Yi-ming MA, Chuan-ming XIE, and Dong-mei CHEN performed the research; Yi-ming MA, Yu-bo ZHOU, and Jia LI analyzed the data; and Yi-ming MA and Yu-bo ZHOU wrote the paper.

References

1 Kumar V, Tomar S, Patel R, Yousaf A, Parmar VS, Malhotra SV. $FeCl_3$-catalyzed Pechmann synthesis of coumarins in Ionic liquids. Synthetic Commun 2008; 38: 2646–54.
2 Mousa SA. Anticoagulants in thrombosis and cancer: the missing link. Expert Rev Anticancer Ther 2002; 2: 227–33.
3 Lowenthal J, Birnbaum H. Vitamin K and coumarin anticoagulants: dependence of anticoagulant effect on inhibition of vitamin K transport. Science 1969; 164: 181–3.
4 Bobek V, Boubelik M, Kovarik J, Taltynov O. Inhibition of adhesion breast cancer cells by anticoagulant drugs and cimetidine. Neoplasma 2003; 50: 148–51.
5 Fylaktakidou KC, Hadjipavlou-Litina DJ, Litinas KE, Nicolaides DN. Natural and synthetic coumarin derivatives with anti-inflammatory/antioxidant activities. Curr Pharm Design 2004; 10: 3813–33.
6 Hadjipavlou-Litina DJ, Litinas KE, Kontogiorgis C. The anti-inflammatory effect of coumarin and its derivatives. Curr Med Chem - Anti-Inflam Anti-Aller Agents 2007; 6: 293–306.
7 Ouahouo BM, Azebaze AG, Meyer M, Bodo B, Fomum ZT, Nkengfack AE. Cytotoxic and antimicrobial coumarins from *Mammea africana*. Ann Trop Med Parasit 2004; 98: 733–9.
8 Creaven BS, Egan DA, Kavanagh K, McCann M, Noble A, Thati B, *et al*. Synthesis, characterization and antimicrobial activity of a series of substituted coumarin-3-carboxylatosilver(I) complexes. Inorg Chim Acta 2006; 359: 3976–84.
9 Widelski J, Popova M, Graikou K, Glowniak K, Chinou I. Coumarins from *Angelica lucida* L–antibacterial activities. Molecules 2009; 14: 2729–34.
10 Vyasa KB, Nimavat KS, Jani GR, Hathi MV. Synthesis and antimicrobial activity of coumarin derivatives metal complexes: an *in vitro* evaluation. Orbital 2009; 1: 183–92.
11 Hishmat OH, Miky JAA, Farrag AA, Fadl-Allah EM. Synthesis of some coumarin derivatives and their antimicrobial activity. Arch Pharm Res 1989; 12: 181–5.
12 Ojala T, Remes S, Haansuu P, Vuorela H, Hiltunen R, Haahtela K, *et al*. Antimicrobial activity of some coumarin containing herbal plants growing in Finland. J Ethnopharmacol 2000; 73: 299–305.
13 Orlov YE. Chemical structure and antioxidant activity among natural coumarins. Chem Nat Comp 1986; 22: 340.
14 Thuong PT, Hung TM, Ngoc TM, Ha DT, Min BS, Kwack SJ, *et al*. Antioxidant activities of coumarins from Korean medicinal plants and their structure-activity relationships. Phytother Res 2010; 24: 101–6.
15 Torres R, Faini F, Modak B, Urbina F, Labbe C, Guerrero J. Antioxidant activity of coumarins and flavonols from the resinous exudate of *Haplopappus multifolius*. Phytochemistry 2006; 67: 984–7.
16 Yu W, Liu ZQ, Liu ZL. Antioxidant effect of coumarin derivatives on free radical initiated and photosensitized peroxidation of linoleic acid in micelles. J Chem Soc, Perkin Trans 1999; 2: 969–74.
17 Simonyan AV, Vlasenko SP, Dimoglo AS. Electron topological study of the link between antiallergic activity and structure for chalcone, coumarin and cinnamic acid derivatives. Pharm Chem J 1993; 27: 490–4.
18 Nugroho AE, Riyanto S, Sukari MA, Maeyama K. Anti-allergic effects of Marmin, a coumarine isolated from *Aegle marmelos* Correa: *In vitro* study. Int J Phytomed 2011; 3: 84–97.
19 Gonsior E, Schultze-Werninghaus G, Wuthrich B. Protective anti-allergic effects of a new coumarin compound (BM 15.100) in experimental asthma. Int J Clin Pharmacol Biopharm 1979; 17: 283–9.
20 Matsuda H, Tomohiro N, Ido Y, Kubo M. Anti-allergic effects of cnidii monnieri fructus (dried fruits of *Cnidium monnieri*) and its major component, osthol. Biol Pharmaceut Bull 2002; 25: 809–12.
21 Buckle DR, Outred DJ, Smith H, Spicer BA. N-benzylpiperazino derivatives of 3-nitro-4-hydroxycoumarin with H1 antihistamine and mast cell stabilizing properties. J Med Chem 1984; 27: 1452–7.
22 Yim D, Singh RP, Agarwal C, Lee S, Chi H, Agarwal R. A novel anticancer agent, decursin, induces G_1 arrest and apoptosis in human prostate carcinoma cells. Cancer Res 2005; 65: 1035–44.
23 Belluti F, Fontana G, Dal Bo L, Carenini N, Giommarelli C, Zunino F. Design, synthesis and anticancer activities of stilbene-coumarin hybrid compounds: Identification of novel proapoptotic agents. Bioorg Med Chem 2010; 18: 3543–50.
24 Kamal A, Adil SF, Tamboli, Jaki R, Siddardha B, Murthy USN. Synthesis

of coumarin linked naphthalimide conjugates as potential anticancer and antimicrobial agents. Lett Drug Design Disc 2009; 6: 201–9.
25 Kawase M, Sakagami H, Motohashi N, Hauer H, Chatterjee SS, Spengler G, *et al*. Coumarin derivatives with tumor-specific cytotoxicity and multidrug resistance reversal activity. *In Vivo* 2005; 19: 705–11.
26 Reddy NS, Mallireddigari MR, Cosenza S, Gumireddy K, Bell SC, Reddy EP, *et al*. Synthesis of new coumarin 3-(N-aryl) sulfonamides and their anticancer activity. Bioorg Med Chem Lett 2004; 14: 4093–7.
27 Bhattacharyya SS, Paul S, Mandal SK, Banerjee A, Boujedaini N, Khuda-Bukhsh AR. A synthetic coumarin (4-methyl-7 hydroxy coumarin) has anti-cancer potentials against DMBA-induced skin cancer in mice. Eur J Pharm 2009; 614: 128–36.
28 Devji T, Reddy C, Woo C, Awale S, Kadota S, Carrico-Moniz D. Pancreatic anticancer activity of a novel geranylgeranylated coumarin derivative. Bioorg Med Chem Lett 2011; 21: 5770–3.
29 Ishikawa T, Kotake K, Ishii H. Synthesis of toddacoumaquinone, a coumarin-naphthoquinone dimer, and its antiviral activities. Chem Pharm Bull 1995; 43: 1039–41.
30 Hwu JR, Singha R, Hong SC, Chang YH, Das AR, Vliegen I, *et al*. Synthesis of new benzimidazole-coumarin conjugates as anti-hepatitis C virus agents. Antiviral Res 2008; 77: 157–62.
31 Yang Z, Xiao H, Liu Y, Liu J, Wen L. Antiviral effect of coumarin analogue against respiratory syncytical virus infection *in vitro* and *in vivo*. Antiviral Res 1995; 26: 350–350.
32 Curini M, Epifano F, Maltese F, Marcotullio MC, Gonzales SP, Rodriguez JC. Synthesis of collinin, an antiviral coumarin. Aust J Chem 2003; 56: 59–60.
33 Hoult JR, Payá M. Pharmacological and biochemical actions of simple coumarins: natural products with therapeutic potential. Gen Pharmacol 1996; 27: 713–22.
34 Oldenburg J, Seidel H, Potzsch B, Watzka M. New insight in therapeutic anticoagulation by Coumarin derivatives. Hamostaseologie 2008; 28: 44–50.
35 Riveiro ME, De Kimpe N, Moglioni A, Vázquez R, Monczor F, Shayo C, *et al*. Coumarins: old compounds with novel promising therapeutic perspectives. Curr Med Chem 2010; 17: 1325–38.
36 Enderle C, Müller W, Grass U. Drug interaction: omeprazole and phenprocoumon. BMC Gastroenterol 2001; 1: 2.
37 Holbrook AM, Pereira JA, Labiris R, McDonald H, Douketis JD, Crowther M, *et al*. Systematic overview of warfarin and its drug and food interactions. Arch Intern Med 2005; 165: 1095–106.
38 Irena K. Studying plant-derived coumarins for their pharmacological and therapeutic properties as potential anticancer drugs. Expert Opin Drug Disc 2007; 2: 1605–18.
39 Montes R, Ruiz de Gaona E, Martinez-González MA, Alberca I, Hermida J. The c.-1639G > A polymorphism of the VKORC1 gene is a major determinant of the response to acenocoumarol in anticoagulated patients. Br J Haematol 2006; 133: 183–7.
40 Thornes RD, Lynch G, Sheehan MV. Cimetidine and coumarin therapy of melanoma. Lancet 1982; 2: 328.
41 Zang Y, Yu LF, Pang T, Fang LP, Feng X, Wen TQ, *et al*. AICAR induces astroglial differentiation of neural stem cells via activating the JAK/STAT3 pathway independently of AMP-activated protein kinase. J Biol Chem 2008; 283: 6201–8.
42 Zang Y, Yu LF, Nan FJ, Feng LY, Li J. AMP-activated protein kinase is involved in neural stem cell growth suppression and cell cycle arrest by 5-aminoimidazole-4-carboxamide-1-beta-D-ribofuranoside and glucose deprivation by down-regulating phospho-retinoblastoma protein and cyclin D. J Biol Chem 2009; 284: 6175–84.
43 Bengoechea-Alonso MT, Punga T, Ericsson J. Hyperphosphorylation regulates the activity of SREBP1 during mitosis. Proc natl Acad Sci U S A 2005; 102: 11681–6.
44 Zhou YB, Feng X, Wang LN, Du JQ, Zhou YY, Yu HP, *et al*. LGH00031, a novel ortho-quinonoid inhibitor of cell division cycle 25B, inhibits human cancer cells via ROS generation. Acta Pharmacol Sin 2009; 30: 1359–68.
45 Mooberry SL, Tien G, Hernandez AH, Plubrukarn A, Davidson BS. Laulimalide and isolaulimalide, new paclitaxel-like microtubule-stabilizing agents. Cancer Res 1999; 59: 653–60.
46 Sherr CJ. Cancer cell cycles. Science 1996; 274: 1672–7.
47 Bratton DL, Fadok VA, Richter DA, Kailey JM, Guthrie LA, Henson PM. Appearance of phosphatidylserine on apoptotic cells requires calcium-mediated nonspecific flip-flop and is enhanced by loss of the aminophospholipid translocase. J Biol Chem 1997; 272: 26159–65.
48 Scatena CD, Stewart ZA, Mays D, Tang LJ, Keefer CJ, Leach SD, *et al*. Mitotic phosphorylation of Bcl-2 during normal cell cycle progression and Taxol-induced growth arrest. J Biol Chem 1998; 273: 30777–84.
49 Aneja R, Liu M, Yates C, Gao J, Dong X, Zhou B, *et al*. Multidrug resistance-associated protein-overexpressing teniposide-resistant human lymphomas undergo apoptosis by a tubulin-binding agent. Cancer Res 2008; 68: 1495–503.
50 Hwang JH, Takagi M, Murakami H, Sekido Y, Shin-ya K. Induction of tubulin polymerization and apoptosis in malignant mesothelioma cells by a new compound JBIR-23. Cancer Lett 2011; 300: 189–96.
51 Chakrabarty S, Das A, Bhattacharya A, Chakrabarti G. Theaflavins depolymerize microtubule network through tubulin binding and cause apoptosis of cervical carcinoma HeLa cells. J Agr Food Chem 2011; 59: 2040–8.
52 Eichenlaub-Ritter U, Chandley AC, Gosden RG. Alterations to the microtubular cytoskeleton and increased disorder of chromosome alignment in spontaneously ovulated mouse oocytes aged *in vivo*: an immunofluorescence study. Chromosoma 1986; 94: 337–45.
53 Loganzo F, Discafani CM, Annable T, Beyer C, Musto S, Hari M, *et al*. HTI-286, a synthetic analogue of the tripeptide hemiasterlin, is a potent antimicrotubule agent that circumvents P-glycoprotein-mediated resistance *in vitro* and *in vivo*. Cancer Res 2003; 63: 1838–45.
54 Bacher G, Nickel B, Emig P, Vanhoefer U, Seeber S, Shandra A, *et al*. D-24851, a novel synthetic microtubule inhibitor, exerts curative antitumoral activity *in vivo*, shows efficacy toward multidrug-resistant tumor cells, and lacks neurotoxicity. Cancer Res 2001; 61: 392–9.
55 Zhang LH, Wu L, Raymon HK, Chen RS, Corral L, Shirley MA, *et al*. The synthetic compound CC-5079 is a potent inhibitor of tubulin polymerization and tumor necrosis factor-alpha production with antitumor activity. Cancer Res 2006; 66: 951–9.
56 Towle MJ, Salvato KA, Budrow J, Wels BF, Kuznetsov G, Aalfs KK, *et al*. *In vitro* and *in vivo* anticancer activities of synthetic macrocyclic ketone analogues of halichondrin B. Cancer Res 2001; 61: 1013–21.
57 Kasibhatla S, Baichwal V, Cai SX, Roth B, Skvortsova I, Skvortsov S, *et al*. MPC-6827: a small-molecule inhibitor of microtubule formation that is not a substrate for multidrug resistance pumps. Cancer Res 2007; 67: 5865–71.
58 Tahir SK, Han EK, Credo B, Jae HS, Pietenpol JA, Scatena CD, *et al*. A-204197, a new tubulin-binding agent with antimitotic activity in tumor cell lines resistant to known microtubule inhibitors. Cancer Res 2001; 61: 5480–5.
59 May KM, Hardwick KG. The spindle checkpoint. J Cell Sci 2006; 119: 4139–42.
60 Clute P, Pines J. Temporal and spatial control of cyclin B1 destruction in metaphase. Nat Cell Biol 1999; 1: 82–7.
61 Nicklas RB, Waters JC, Salmon ED, Ward SC. Checkpoint signals in grasshopper meiosis are sensitive to microtubule attachment, but

tension is still essential. J Cell Sci 2001; 114: 4173–83.
62 Carré M, Braguer D. Microtubule damaging agents and apoptosis. In: Tito Fojo Editor. The role of microtubules in cell biology, neurobiology and oncology. Humana Press; 2008. p 479–518.
63 Jordan MA, Wilson L. Microtubules as a target for anticancer drugs. Nature Reviews 2004; 4: 253–65.
64 Hadfield JA, Ducki S, Hirst N, McGown AT. Tubulin and microtubules as targets for anticancer drugs. Prog Cell Cycle Res 2003; 5: 309–25.
65 Jordan MA, Kamath K. How do microtubule-targeted drugs work? An overview. Curr Cancer Drug Tar 2007; 7: 730–42.
66 Chuang JY, Huang YF, Lu HF, Ho HC, Yang JS, Li TM, *et al*. Coumarin induces cell cycle arrest and apoptosis in human cervical cancer HeLa cells through a mitochondria- and caspase-3 dependent mechanism and NF-kappaB down-regulation. *In Vivo* 2007; 21: 1003–9.
67 Bocca C, Gabriel L, Bozzo F, Miglietta A. Microtubule-interacting activity and cytotoxicity of the prenylated coumarin ferulenol. Planta Med 2002; 68: 1135–7.
68 Madari H, Panda D, Wilson L, Jacobs RS. Dicoumarol: a unique microtubule stabilizing natural product that is synergistic with Taxol. Cancer Res 2003; 63: 1214–20.
69 Miglietta A, Bocca C, Gabriel L, Rampa A, Bisi A, Valenti P. Anti-microtubular and cytotoxic activity of geiparvarin analogues, alone and in combination with paclitaxel. Cell Biochem Funct 2001; 19: 181–9.

Acta Pharmacologica Sinica (2012) 33: 418–425
 1671-4083/12 $32.00
www.nature.com/aps

Original Article

Thiazolidione derivatives targeting the histidine kinase YycG are effective against both planktonic and biofilm-associated *Staphylococcus epidermidis*

Ren-zheng HUANG[1, 3, #], Li-kang ZHENG[2, #], Hua-yong LIU[1, #], Bin PAN[2], Jian HU[1], Tao ZHU[1], Wei WANG[1], Dan-bin JIANG[3], Yang WU[1], You-cong WU[1], Shi-qing HAN[2, *], Di QU[1, *]

[1]*Key Laboratory of Medical Molecular Virology of Ministries of Education and Health, Institute of Medical Microbiology and Institutes of Biomedical Sciences, Shanghai Medical College of Fudan University, Shanghai 200032, China;* [2]*College of Biotechnology and Pharmaceutical Engineering, Nanjing University of Technology, Nanjing 210009, China;* [3]*Yancheng Third People's Hospital, the Affiliated Yancheng Hospital of Southeast University Medical College, Yancheng 224001, China*

Aim: To evaluate the efficacies of six derivatives of Compound **2**, a novel YycG histidine kinase inhibitor with the thiazolidione core structure in the treatment of medical device-related biofilm infections.
Methods: The minimal inhibitory concentration (MIC) of the derivatives was determined using the macrodilution broth method, and the minimal bactericidal concentration (MBC) was obtained via sub-culturing 100 μL from each negative tube from the MIC assay onto drug-free Mueller-Hinton agar plates. Biofilm-killing effect for immature (6 h-old) biofilms was examined using a semiquantitative plate assay, and the effect on mature (24 h-old) biofilms was observed under a confocal laser scanning microscope (CLSM).
Results: The derivatives potently suppressed the growth of *Staphylococcus epidermidis*. The MIC values of the derivatives H2-10, H2-12, H2-20, H2-29, H2-27, and H2-28 on *S epidermidis* ATCC 35984 were 24.3, 6.5, 6.2, 3.3, 3.1, and 1.5 μg/mL, respectively. The MBC values of these derivatives were 48.6, 52.2, 12.4, 52.6, 12.4, and 6.2 μg/mL, respectively. The derivatives killed all bacteria in immature (6 h-old) biofilms and eliminated the biofilm proliferation. The derivatives also displayed strong bactericidal activities toward cells in mature (24 h-old) biofilms, whereas they showed low cytotoxicity and hemolytic activity toward Vero cells and human erythrocytes.
Conclusion: The bactericidal and biofilm-killing activities of the new anti-YycG compounds were significantly better than the parent Compound **2**.

Keywords: *Staphylococcus epidermidis*; antibacterial agent; half maximal inhibitory concentration; minimal inhibitory concentration; biofilm-killing activity

Acta Pharmacologica Sinica (2012) 33: 418–425; doi: 10.1038/aps.2011.166; published online 9 Jan 2012

Introduction

Coagulase-negative *Staphylococcus epidermidis* (*S epidermidis*) is one of the most common opportunistic pathogens involved in implanted medical device-associated nosocomial infections[1–3]. With the increasing use of implanted medical devices, such as intravascular catheters, artificial pacemakers, cerebrospinal fluid shunts, and artificial organs, *S epidermidis* biofilm-associated infections have become a common problem. The ability to form biofilms on the surfaces of the implanted devices is the primary pathogenic trait of *S epidermidis*, and the bacteria in the biofilms are resistant to antimicrobial treatments and host immune defenses[4–6]. Because of the increasing emergence of multidrug-resistant strains, the discovery of novel antibiotics to combat staphylococcal biofilm infections is imperative[7]. Completion of the genome sequencing of *S epidermidis*[8, 9] makes it possible to discover potential antimicrobial agents using genomics-based drug discovery strategies.

The majority of bacteria use a phosphotransfer mechanism termed a two-component system (TCS), comprised of a histidine kinase (HK) and a response regulator (RR), to sense environmental conditions and bring about appropriate changes in cellular behavior[10–12]. TCSs are important in regulating the virulence and propagation of pathogenic bacteria[13–15], and they are considered attractive targets for the development of

# These authors contributed equally to this work.
* To whom correspondence should be addressed.
E-mail dqu@fudan.edu.cn (Di QU);
hanshiqing@njut.edu.cn (Shi-qing HAN)
Received 2011-05-07 Accepted 2011-10-27

novel anti-bacterial drugs. The two-component YycG/YycF system, originally identified in *Bacillus subtilis*[16, 17], is highly conserved and specific to low G+C gram-positive bacteria, including *S epidermidis*. YycG/YycF is essential for cell viability, cell wall metabolism, autolysin synthesis, and biofilm formation in staphylococcal species. Upon sensing a signal from the external milieu, YycG autophosphorylates by transferring a phosphate group from ATP to a histidine residue within the kinase and then transferring it to an aspartate residue within the conserved receiver domain of the response regulator YycF. Phosphorylation of YycF results in changes in its ability to bind gene promoters and regulate transcription[18–20].

Several inhibitors that target YycG in *B subtilis*, *Staphylococcus aureus* (*S aureus*), and *S epidermidis* have been documented to inhibit bacterial growth[21–23]. We previously described two inhibitors (Compounds **2** and **5**) that target the HK domain of *S epidermidis* YycG and have bactericidal and biofilm-killing activities[24]. To obtain more effective and less toxic inhibitors, the structure of Compound **2** was optimized, and a series of derivatives were designed and synthesized, some of which inhibit the growth of planktonic *S epidermidis* cells[25]. In the present study, we explored the characteristics of these derivatives, including their YycG phosphorylation-inhibiting activity, bactericidal activity, biofilm-killing activity, and cytotoxicity. The inhibitory and bactericidal activities of these derivatives against *S aureus* were also assessed.

Our study of structure-based modification of a leading anti-TCS compound may contribute to the discovery of new antibiotics to treat staphylococcal biofilm infections.

Materials and methods

Bacterial strains, media, and derivatives of Compound 2

The bacterial strains used in this study were *S epidermidis* ATCC 12228 (biofilm negative), *S epidermidis* ATCC 35984 (biofilm positive), *S aureus* ATCC 49230, *S aureus* ATCC 25923, and *E coli* ATCC 25922. *E coli* strains were grown in Luria-Bertani (LB) broth, and staphylococcal strains were cultivated in tryptic soy broth medium (TSB; Oxoid Ltd, Basingstoke, UK). The six derivatives of Compound **2** mentioned in this report (including five reported previously[26] and one newly synthesized) are H2-10, H2-12, H2-20, H2-27, H2-28, and H2-29. These compounds were synthesized by modifying the functional groups while keeping the thiazolidione core structure intact. The structural formulas of the derivatives are listed in Figure 1. To generate the derivative compounds, the terminal (2-methoxy-4-vinyl-phenoxy)-acetic acid functional group of Compound **2** was replaced by a (5-vinyl-furan-2-yl)-benzoic acid fragment with similar structure and by a shortened side alkyl chain, according to the principle of multi-target-directed ligands. The derivatives were dissolved in dimethyl sulfoxide (DMSO; AMRESCO, USA) to create 200 mmol/L stock solutions.

Expression and purification of the YycG HATPase_c and HisKA domains

The HisKA and HATPase_c domains (amino acids 370–610, NCBI accession number YP_190074) of YycG (termed YycG′) from *S epidermidis* ATCC 35984 were expressed as a fusion protein with an N-terminal maltose binding protein six-histidine (MBP-His) tag. The 720-bp *YycG* ORF was PCR-amplified from *S epidermidis* ATCC 35984 chromosomal DNA with the primers YycG For-*Bam*H I (5′-CGCGGATCCGAACAACAACAAGTCGAACGT-3′) and YycG Rev-*Xho* I (5′-CCGCTCGAGTTATTCATCCCAATCACCGTCT-3′). After digestion with *Bam*H I and *Xho* I, the PCR product was cloned into pET28a (Novagen). The resultant plasmid was trans-

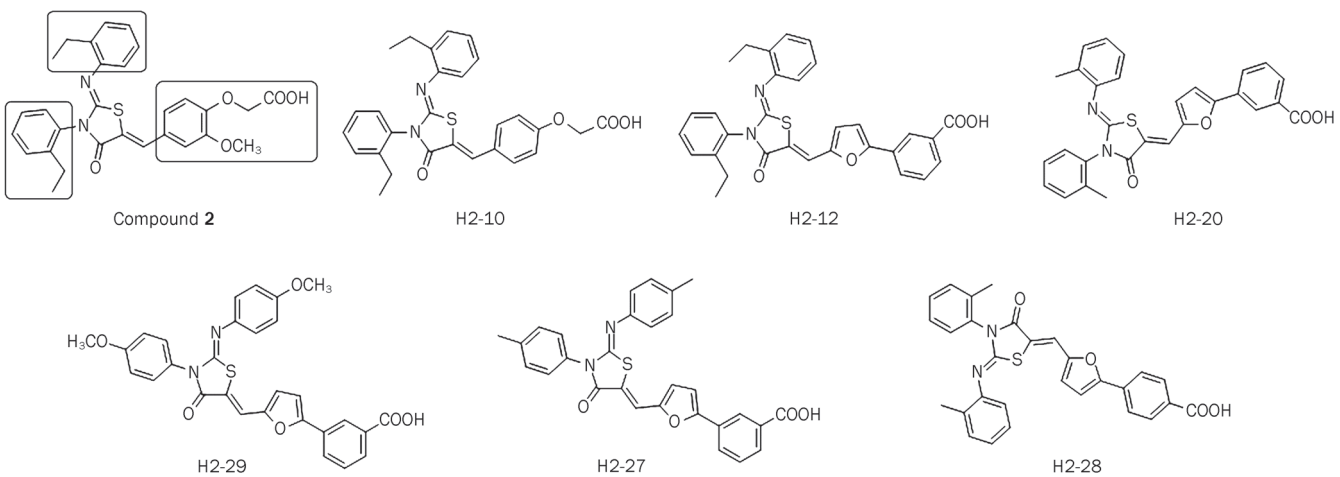

Figure 1. The structures of the thiazolidione derivatives. Based on the thiazolidione core structure of Compound **2** {2-{4-{3-(2-ethylphenyl)-2-[(2-ethylphenyl)imino]-4-oxothiazolidin-5-ylidene}methyl}-2-methoxyphenoxy}acetic acid, six derivatives were designed and synthesized by modifying the functional groups through cyclization, aldol condensation, substitution, and hydrolyzation reactions. H2-10, 2-{4-{[3-(2-ethylphenyl)-2-[(2-ethylphenyl)imino]-4-oxothiazolidin-5-ylidene}methyl}phenoxy}acetic acid; H2-12, 3-{5-{{3-(2-ethylphenyl)-2-[(2-ethylphenyl)imino]-4-oxothiazolidin-5-ylidene)methyl}furan-2-yl}benzoic acid; H2-20, 3-{5-{{4-oxo-3-(o-tolyl)-2-(o-tolylimino)thiazolidin-5-ylidene]methyl}furan-2-yl}benzoic acid; H2-27, 3-{5-{[4-oxo-3-(p-tolyl)-2-(p-tolylimino)thiazolidin-5-ylidene]methyl}furan-2-yl}benzoic acid; H2-29, 3-{5-{{3-(4-methoxyphenyl)-2-[(4-methoxyphenyl)imino]-4-oxothiazolidin-5-ylidene}methyl}furan-2-yl}benzoic acid; and H2-28, 4-{5-{[4-oxo-3-(o-tolyl)-2-(o-tolylimino)thiazolidin-5-ylidene]methyl}furan-2-yl}benzoic acid.

formed into *E coli* BL21 (DE3). The BL21 (DE3) strain carrying the plasmid was grown in LB to an optical density of 0.6 at 600 nm (OD_{600}), and then induced with 0.8 mmol/L isopropyl β-*D*-1-thiogalactopyranoside (IPTG). After 8 h induction at 25 °C, the cells were harvested, and recombinant YycG′ protein was purified by Ni^{2+} affinity chromatography using a Ni-NTA column (Qiagen, Germany). The MBP-His-tagged YycG′ was then cleaved with TEV protease, and the resultant un-tagged YycG′ was further purified by Ni-NTA and Superdex 75 gel filtration columns (GE Healthcare, USA).

Inhibition assay for YycG′ autophosphorylation activity

The Compound **2** derivatives were tested for inhibition of YycG′ autophosphorylation using the Kinase-Glo™ Luminescent Kinase Assay (Promega, Madison, WI, USA) in a solid black flat-bottomed 96-well plate[24]. Briefly, 0.13 μmol/L recombinant YycG′ was pre-incubated with serial dilutions of the derivatives in reaction buffer (40 mmol/L Tris pH 8.0, 20 mmol/L $MgCl_2$, and 0.1 mg/mL BSA) at 25 °C for 30 min. Then, 4 μmol/L ATP was added and the plates were incubated for 30 min at 25 °C, and Kinase-Glo™ Reagent was added to detect the remaining ATP, recorded by luminescence measurement (RLU). Recombinant YycG′ incubated with Compound **2** was used as a positive control, and recombinant protein with no derivative added was used as a negative control in these experiments. The rate of protein phosphorylation (Rp) inhibition by the derivatives was calculated using the equation (Eq 1).

The half maximal inhibitory concentration (IC_{50}, the concentration of the derivatives required to inhibit half of the autophosphorylation of the recombinant YycG′) was determined by Origin 8.0 software (OriginLab, Northampton, USA)[24].

Minimal inhibitory concentration (MIC) and minimal bactericidal concentration (MBC) assays

MIC assays for the antibacterial activities of the derivatives were performed according to the macrodilution (tube) broth method of the Clinical and Laboratory Standards Institute (CLSI) of America. Briefly, the derivatives were serially diluted twofold into eight tubes containing 4 mL Mueller-Hinton Broth (OXOID, UK), yielding final concentrations of 100 μg/mL to 0.78 μg/mL. The turbidity of cultures incubated for 6 h was adjusted to match that of a 0.5 McFarland standard (approximately 10^8 CFU/mL), and 0.02 mL of the bacterial inoculum was added to each tube. Inoculated broth containing no antibiotic was included as a bacterial growth control and a tube of un-inoculated broth was used as a sterility control. The bacteria were incubated at 37 °C for 12 h. The lowest concentration that completely inhibits visible growth of the organism as detected by the unaided eye was recorded as the MIC[27].

The MBC was obtained by sub-culturing 100 μL from each negative (no visible bacterial growth) tube from the MIC assay onto drug-free Mueller-Hinton agar plates. The plates were incubated at 37 °C for 24 h, and the MBC was defined as the lowest concentration of drug which produced subcultures growing no more than five colonies on each plate[27].

Biofilm-killing assays

Biofilm formation was detected using a semiquantitative plate assay[26]. An overnight culture of *S epidermidis* ATCC 35984 was diluted 1:200 into TSB medium, and incubated statically for 6 h in a polystyrene 96-well plate at 37 °C. Subsequent to the removal of planktonic cells, fresh TSB containing the serially diluted derivatives was added to each biofilm, and the plates were incubated for another 18 h at 37 °C. After incubation, the wells were washed gently three times with phosphate buffered saline (PBS), fixed with methanol, and stained with 2% (*w*/*v*) crystal violet[28]. The absorbance of the wells was determined at 570 nm using a spectrophotometer (DTX880, Beckman Coulter, USA).

To determine the effect of the derivatives on cell viability in mature biofilms, the Live-Dead Bacterial Viability method (Live-Dead BacLight, Molecular Probes, USA) was used. Overnight cultures of *S epidermidis* ATCC 35984 grown in TSB medium were subcultured for another 6 h. The turbidity of the culture was adjusted to match that of a 0.5 McFarland standard (approximately 10^8 CFU/mL) and inoculated (1:200) into cover-glass cell-culture dishes (WPI, USA), which were then incubated at 37 °C for 24 h. After removal of the planktonic cells, fresh TSB containing the derivatives at concentrations corresponding to 4×MIC was added, and the dishes were incubated at 37 °C for another 16 h. After incubation, the dishes were carefully washed three times with normal saline (NS), stained with Live-Dead reagents (containing SYTO 9 and PI) at room temperature for 15 min, and observed under a Leica TCS SP5 confocal laser scanning microscope (CLSM).

Cytotoxicity and erythrocyte hemolysis

The cytotoxicity of the derivatives to Vero cells (African green monkey kidney cells) was detected using the Cell Proliferation Kit I (Roche, Indianapolis, USA) in 96-well cell culture plates. After exposure of the cells (~10^4 cells per well) to the serially diluted derivatives for 48 h, relative cell numbers were assayed by co-incubation with 3-(4,5-dimethylthiazol-2-yl)-2,5-diphenyltetrazolium bromide (MTT) for 4 h at 37 °C in 5% CO_2. After incubation, the purple formazan salts were dissolved with DMSO, and the absorbance of each well was measured at 595 and 655 nm then converted to percentages of the control (cells treated with the solvent, 0.1% DMSO). The concentration of the derivatives with 50% cytotoxicity for Vero cells (CC_{50}) was calculated using the Origin 8.0 software (Origin Lab, Northampton, USA).

To determine the hemolytic activities of the derivatives on erythrocytes, 5% (*v*/*v*) healthy human erythrocytes re-suspended in NS were co-incubated with the derivatives at MIC,

$$Rp=\frac{RLU(YycG'+derivative+ATP+Kinase\text{-}Glo™)-RLU(YycG'+ATP+Kinase\text{-}Glo™)}{RLU\ (ATP+\ Kinase\text{-}Glo™)\ -RLU\ (YycG'+ATP+\ Kinase\text{-}Glo™)}\times 100\% \quad \text{(Eq 1)}$$

4×MIC, or 100 μg/mL for 1 h at 37 °C in 96-well microtiter plates. After the incubation, the suspensions were centrifuged at 350×*g* for 10 min, and the level of hemolysis was determined by measuring the absorbance of the supernatant at 570 nm[25]. Cells treated with DMSO (0.1%) and Triton-X100 (1%) were used as negative and positive controls, respectively.

Results

In our previous study, five derivatives were designed and synthesized based on the chemical structure of Compound **2**[24, 25]. The biological characteristics of the Compound **2** derivatives, including these five derivatives that were previously reported (H2-10, H2-12, H2-20, H2-29, and H2-27) and the newly synthesized H2-28, were further explored in the present investigation.

Inhibition of YycG′ enzyme activity by the derivatives

To detect the enzyme inhibiting activities of the derivatives on the YycG protein, recombinant YycG′ (~29 kDa) was expressed as a fusion protein with an N-terminal maltose binding protein tag and purified using the ProBond™ Purification System (protein purity >90%). The enzymatic activity of the recombinant YycG′ was measured using the Kinase-Glo™ Luminescent Kinase assay, and all 6 derivatives displayed dose-dependent inhibition of its autophosphorylation activity. At 100 μmol/L (50 μg/mL), H2-10, H2-12, H2-20, H2-29, H2-27, and H2-28 inhibited YycG′ (0.13 μmol/L) enzyme activity by 55.22%, 63.70%, 83.65%, 50.75%, 78.31%, and 58.59%, respectively. The IC_{50} values of the six derivatives were 88.35 μmol/L (42.9 μg/mL), 61.15 μmol/L (31.9 μg/mL), 34.83 μmol/L (17.2 μg/mL), 66.68 μmol/L (35.1 μg/mL), 22.15 μmol/L (10.9 μg/mL), and 82.51 μmol/L (40.7 μg/mL), respectively, and the IC_{50} of Compound **2** was 47.9 μmol/L (24.9 μg/mL) (Table 1).

Antimicrobial activity of the derivatives

The MIC values of the six derivatives for *S epidermidis* ATCC 35984 and 12228 were determined. All 6 derivatives were found to inhibit bacterial growth more effectively than Compound **2**. The MIC values of H2-10, H2-12, H2-20, H2-29, H2-27, and H2-28 on *S epidermidis* ATCC 35984 were 24.3, 6.5, 6.2, 3.3, 3.1, and 1.5 μg/mL, respectively; and the MBC values were 48.6, 52.2, 12.4, 52.6, 12.4, and 6.2 μg/mL, respectively (Table 1). Additionally, all derivatives inhibited the growth of *Sepidermidis* ATCC 12228 and *S aureus* (ATCC 49230 and ATCC 25923) (Table 2), whereas they had no effect on the growth of *E coli* strain ATCC 25922 at the highest tested concentration (100 μg/mL). The MIC/MBC values of these 6 derivatives ranged from 1/2 to 1/4, except for those of H2-12 and H2-29 (which had MIC/MBC values of 1/8 and 1/16, respectively).

Table 2. Anti-Staphylococcus activities of the derivatives.

Derivatives[a]	MIC[b] (mg/L)			
	S epidermidis ATCC 35984	*S epidermidis* ATCC 12228	*S aureus* ATCC 49230	*S aureus* ATCC 25923
Compound **2**[c]	26.0	26.0	51.9	51.9
H2-10	24.3	24.3	12.2	24.3
H2-12	6.5	6.5	6.5	6.5
H2-20	6.2	6.2	3.1	6.2
H2-29	3.3	3.3	6.6	6.6
H2-27	3.1	3.1	3.1	6.2
H2-28	1.5	1.5	3.1	3.1

[a] Stock solutions of the compounds were prepared in 0.1% (*v/v*) DMSO.
[b] MIC which represents minimal inhibitory concentration of the derivatives was determined by the broth microdilution (in tubes) method of the CLSI of America.
[c] MIC values for Compound **2** were determined in this work.

Effects of the derivatives on *S epidermidis* biofilm proliferation

Effects of the derivatives on the proliferation of 6-h-old *S epidermidis* ATCC 35984 biofilms were detected by a microtiter plate assay. All derivatives showed biofilm-killing effects on

Table 1. Biological effects of the six derivatives.

Derivatives[a]	Molecule weight	IC_{50}[b] (mg/L)	MIC[c] (mg/L)	MBC[c] (mg/L)	MBKC[c] (mg/L)	CC_{50}[d] (mg/L)	Hemolysis[e] (%)
Compound **2**[f]	519	24.9	26.0	51.9	51.9	50.0	2.31±0.35
H2-10	486	42.9	24.3	48.6	24.3	>100.0	0.36±0.11
H2-12	522	31.9	6.5	52.2	13.1	>100.0	0.16±0.03
H2-20	494	17.2	6.2	12.4	6.2	>100.0	0.29±0.12
H2-29	526	35.1	3.3	52.6	3.3	>100.0	0.59±0.32
H2-27	494	10.9	3.1	12.4	6.2	>100.0	0.15±0.10
H2-28	494	40.7	1.5	6.2	3.1	>100.0	0.12±0.06

[a] Stock solutions of the compounds were prepared in 0.1% (*v/v*) DMSO.
[b] IC_{50} represents half maximal inhibitory concentration of the derivatives, which inhibit half of the autophosphorylation of recombinant YycG′.
[c] MIC, MBC, and MBKC represent the minimal inhibitory concentration, minimal bactericidal concentration, and minimal biofilm-killing concentration of the derivatives against *S epidermidis* ATCC 35984.
[d] CC_{50} represents the derivative concentration that produces 50% cytotoxicity effects on Vero cells. The highest concentration tested in the experiment was 100 mg/L.
[e] Hemolytic activities of the derivatives on healthy human erythrocytes were shown at their MICs against *S epidermidis* ATCC 35984.
[f] All values for Compound **2** were determined in this work.

immature (6-h-old) *S epidermidis* ATCC 35984 biofilms (Figure 2), especially H2-28 and H2-29 [minimal biofilm-killing concentration (MBKC)=3.1 μg/mL and 3.3 μg/mL, respectively], which were stronger than Compound **2** (MBKC=51.9 μg/mL) (Table 1).

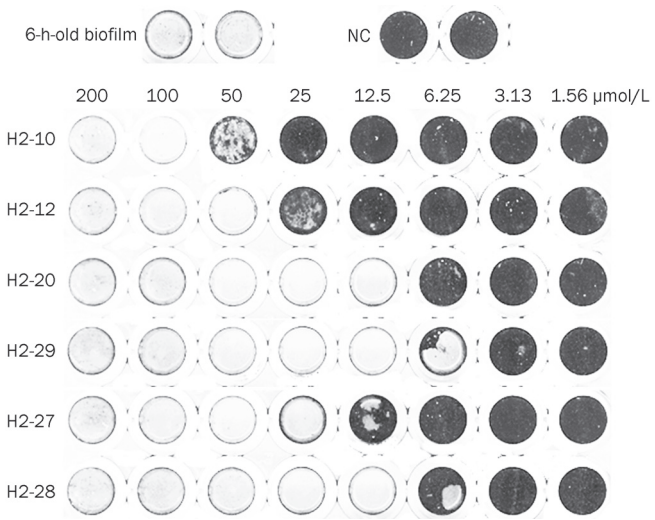

Figure 2. Macroscopic profiles of the biofilms co-cultured with the derivatives. *S epidermidis* strain ATCC 35984 was cultured in polystyrene microtiter plates at 37 °C for 6 h. After removal of planktonic cells, fresh medium containing serial dilutions of the derivatives was added to the 6-h-old biofilm, and then incubated at 37 °C for another 18 h. After incubation, the biofilms were visualized by crystal violet staining. The biofilm treated with 0.1% DMSO (NC) as well as the 6-h-old biofilm without further incubation served as controls. The images are representative of results from three independent experiments.

Bactericidal effects of the derivatives on mature *S epidermidis* biofilms

The bactericidal activities of the derivatives on mature (24-h-old) *S epidermidis* biofilms were detected by a confocal microscope; treatment with 0.1% DMSO or vancomycin (128 μg/mL) served as the controls. Each derivative was added individually to a mature biofilm at a concentration of 4×MIC, and incubated for 16 h. Significant reductions of viable cells in the mature biofilms were observed by CLSM with Live-Dead staining. All of the derivatives (24.3 μg/mL H2-10, 26.1 μg/mL H2-12, 24.7 μg/mL H2-20, 13.1 μg/mL H2-29, 12.4 μg/mL H2-27, and 12.4 μg/mL H2-28) showed bactericidal activity against bacteria in mature biofilms, especially H2-20, H2-27, and H2-29 (Figures 3). In contrast, DMSO (0.1%) and vancomycin (128 μg/mL, Bio Basic Inc, Canada) showed little effect on bacterial viability within a biofilm (Figure 3).

Cytotoxicity and hemolysis of the derivatives *in vitro*

The cytotoxicity of the derivatives to mammal cells was investigated using Vero cells and an MTT assay. Cells treated with 0.1% DMSO and untreated cells were used as controls. Compared with the control group, after treatment with the derivatives, no obvious cytotoxicity to Vero cells was detected. The CC_{50} values of all the derivatives were higher than 100 μg/mL, which was the highest concentration used in the present study (Table 1).

Hemolysis of healthy human erythrocytes induced by the derivatives was examined, with vancomycin treatment as a control. Erythrocytes treated with 1% Triton-X100 and untreated erythrocytes served as complete hemolysis (100%) and no hemolysis (0%) controls, respectively. At the MIC concentrations, none of the derivatives displayed obvious induction of hemolysis of healthy human erythrocytes (<1% compared to the control), even at the highest concentrations (100 μg/mL). Derivatives H2-20, H2-27, and H2-28 had the lowest hemolytic activities (Table 1).

Discussion

S epidermidis and *S aureus* biofilm formation have become two of the most prevalent causes of nosocomial infections, especially in patients with prosthetic medical devices such as indwelling catheters and implanted foreign polymer bodies[28, 29]. As biofilms render bacteria increasingly resistant to multiple antibiotics[30–32] and host defenses[33, 34], chronic biofilm infections persist in patients, and it often becomes necessary to remove the implanted devices[29]. New antimicrobial agents are thus urgently needed to combat biofilm-associated infections.

TCSs are composed of a sensor histidine kinase capable of autophosphorylation in response to an environmental signal and a response regulator that interacts with the phosphorylated HK and regulates the expression of specific genes[35]. The YycG/YycF TCS has been extensively studied in recent years because of its essential role in pathogenic bacteria[16, 18, 36]. YycG/YycF regulates bacterial murein biosynthesis[19, 37–42], cell division[16, 17, 39], lipid integrity[18, 37, 42, 43], virulence factor expression[19, 40, 42, 44–46], exopolysaccharide biosynthesis, and biofilm formation[19, 44, 46-48]. The YycG/YycF TCS is highly conserved in low G+C gram-positive bacteria but is absent in mammals and is thus considered a potential drug target in pathogenic bacteria[24, 27, 49–52]. We previously reported two newly discovered compounds targeting YycG[24] that clearly possess biofilm-killing activities against *S epidermidis*[31]. To improve the antibacterial activities of these compounds, a series of derivatives were designed and synthesized by modifying the functional groups of Compound **2** while keeping the thiazolidione core structure intact[25]. When the (5-vinyl-furan-2-yl)-benzoic acid fragment was incorporated into the thiazolidine-4-ones scaffold, the rigidity of the determined compound was enhanced. That change might stabilize the thiazolidiones in the bonding pocket. Six out of thirty-five derivatives were found to possess higher antibacterial activities than the compound they were derived from, and they inhibited autophosphorylation of YycG, suggesting that the bactericidal activity of these derivatives is based on inhibiting the enzyme activity of the YycG HK domain. However, the antibacterial activities of the derivatives did not always correlate with their IC_{50} values, as was the case with derivative H2-28 in the present

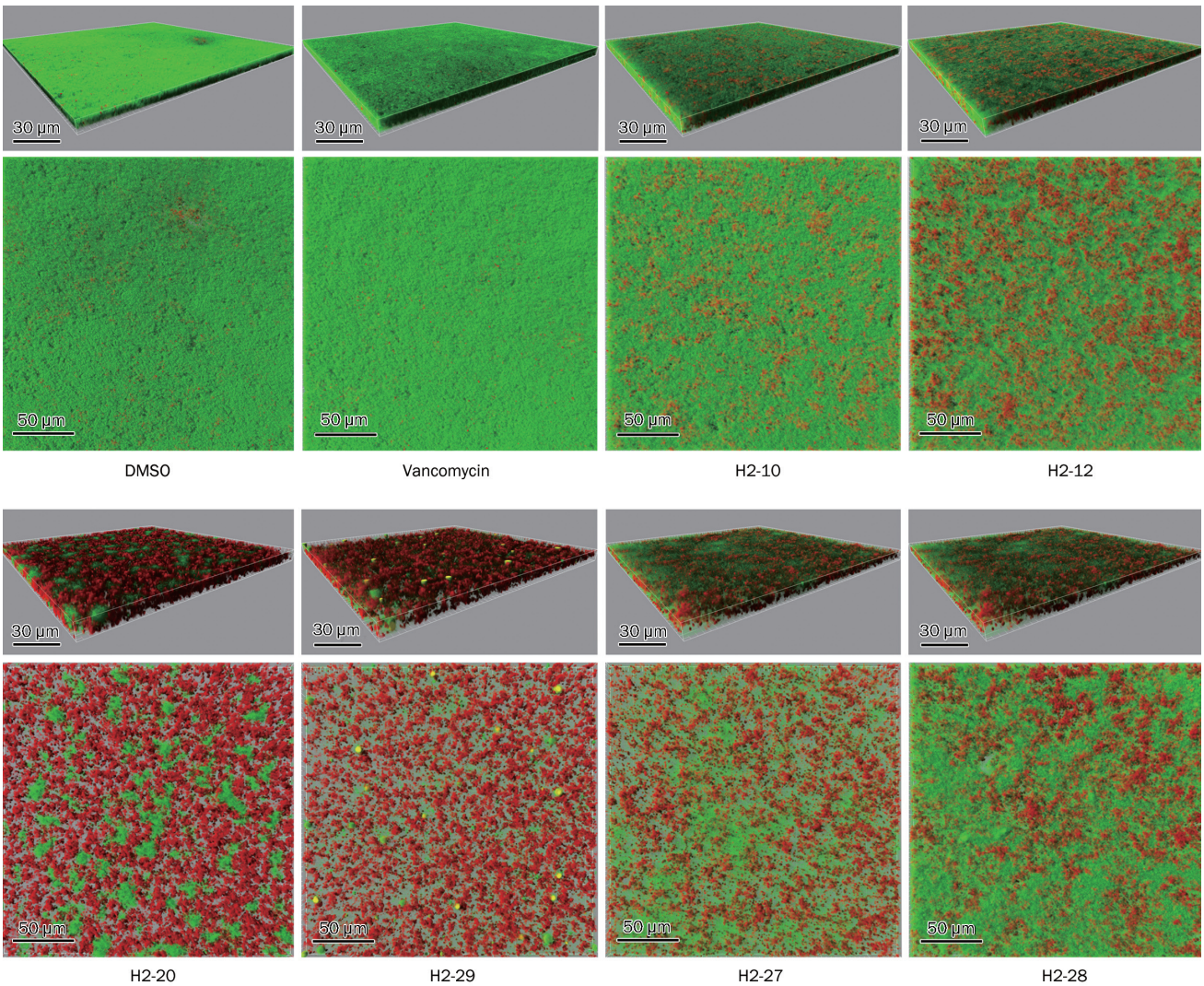

Figure 3. Bactericidal effects of the derivatives on mature *S epidermidis* biofilms. *S epidermidis* ATCC 35984 was grown in cover-glass cell-culture dishes at 37 °C for 24 h. Subsequent to the removal of planktonic cells, the 24-h-old biofilms were further incubated at 37 °C for another 16 h with fresh TSB containing the following substances: 0.1% DMSO, 128 μg/mL vancomycin, 24.3 μg/mL H2-10, 26.1 μg/mL H2-12, 24.7 μg/mL H2-20, 13.1 μg/mL H2-29, 12.4 μg/mL H2-27, or 12.4 μg/mL H2-28. After incubation, the biofilms on the dishes were washed with normal saline and stained with Live-Dead reagents (containing SYTO9 and PI), and observed under CLSM using a 63×objective lens. Images representative of the results from three independent experiments were three-dimensionally reconstructed using Imaris software based on CLSM data at approximately 0.5 μm increments. The green fluorescent cells are viable, while red fluorescent cells indicate dead bacteria.

study. This may be because the antibacterial activities of the derivatives may be affected by absorption by the bacterial cell, cell membrane permeability, or cellular metabolism, whereas the IC_{50} of the YycG inhibitors was determined by an autophosphorylation assay analyzing the direct interaction between the inhibitor and purified YycG′ protein *in vitro*. The YycG-targeting property of these derivatives accounts for their effectiveness against *S epidermidis* and *S aureus*, which are both low G+C gram-positive bacteria with highly conserved YycG/YycF TCSs; this is also consistent with the low cytotoxicity of these derivatives to mammalian cells and with the absence of inhibitory activity on the growth of *E coli* strain ATCC 25922, as mammalian and *E coli* cells do not have genes homologous to *yycG/yycF*.

Bacteria in biofilms are 100–1000 times more resistant to antibiotics than planktonic cells[30–32], and vancomycin has little effect on *S epidermidis* biofilms even at high concentrations[28, 53]. The anti-biofilm activities of the six derivatives described here toward *S epidermidis* ATCC 35984 were improved compared to Compound **2**. Lower concentrations of the derivatives compared with Compound **2** killed all bacteria in immature (6-h-old) biofilms and eliminated biofilm proliferation. More diluted derivatives did not eliminate biofilm formation but disrupted its structure so that it lost mechanical stability and could be washed away easily (Figure 2). The derivatives also displayed strong bactericidal activities toward cells in mature (24-h-old) biofilms, especially H2-20, H2-27, and H2-29, whereas Compound **2** mainly killed cells located at the bottom

of the biofilm[28].

In summary, six additional effective YycG inhibitors were designed and synthesized by modifying the chemical structure of the YycG inhibitor Compound **2**. Their bactericidal and biofilm-killing activities were significantly better than those of Compound **2**. The modification of anti-YycG leading compounds will help to discover new agents to combat biofilm infections and multidrug-resistant bacterial infections.

Acknowledgements

We would like to thank Prof Guo-qiang LIN, Shanghai Institute of Organic Chemistry, Chinese Academy of Sciences, for his invaluable advice. This work was supported by the Program of Ministry of Science and Technology of China (2012ZX09301002-005, 2012ZX10003008-010, and 2010DFA32100), the National Natural Science Foundation of China (30800036, 20942006, 21072095, and 81101214), the Scientific Technology Development Foundation of Shanghai (08JC1401600 and 10410700600), the High-Tech Research and Development Program of China (2006AA02A253), and the Specialized Research Fund for the Doctoral Program of Higher Education (SRFDP) (20100071120049).

Author contribution

Ren-zheng HUANG, Hua-yong LIU, Shi-qing HAN, and Di QU designed the research; Ren-zheng HUANG, Li-kang ZHENG, Hua-yong LIU, and Bin PAN performed most of the experiments; Tao ZHU, Dan-bin JIANG, and Wei WANG provided critical technical support; Jian HU and Yang WU analyzed the data; Ren-zheng HUANG, Hua-yong LIU, You-cong WU, Shi-qing HAN, and Di QU wrote the paper.

References

1 Rupp ME, Archer GL. Coagulase-negative staphylococci: pathogens associated with medical progress. Clin Infect Dis 1994; 19: 231–43; quiz 44–5.
2 Huebner J, Goldmann DA. Coagulase-negative staphylococci: role as pathogens. Annu Rev Med 1999; 50: 223–36.
3 Mermel LA, Farr BM, Sherertz RJ, Raad II, O'Grady N, Harris JS, *et al.* Guidelines for the management of intravascular catheter-related infections. Infect Control Hosp Epidemiol 2001; 22: 222–42.
4 Donlan RM, Costerton JW. Biofilms: survival mechanisms of clinically relevant microorganisms. Clin Microbiol Rev 2002; 15: 167–93.
5 Vandecasteele SJ, Peetermans WE, Merckx R, Van Eldere J. Expression of biofilm-associated genes in *Staphylococcus epidermidis* during *in vitro* and *in vivo* foreign body infections. J Infect Dis 2003; 188: 730–7.
6 Hoffman LR, D'Argenio DA, MacCoss MJ, Zhang Z, Jones RA, Miller SI. Aminoglycoside antibiotics induce bacterial biofilm formation. Nature 2005; 436: 1171–5.
7 Raad I, Alrahwan A, Rolston K. *Staphylococcus epidermidis*: emerging resistance and need for alternative agents. Clin Infect Dis 1998; 26: 1182–7.
8 Zhang YQ, Ren SX, Li HL, Wang YX, Fu G, Yang J, *et al.* Genome-based analysis of virulence genes in a non-biofilm-forming *Staphylococcus epidermidis* strain (ATCC 12228). Mol Microbiol 2003; 49: 1577–93.
9 Gill SR, Fouts DE, Archer GL, Mongodin EF, Deboy RT, Ravel J, *et al.* Insights on evolution of virulence and resistance from the complete genome analysis of an early methicillin-resistant *Staphylococcus aureus* strain and a biofilm-producing methicillin-resistant *Staphylococcus epidermidis* strain. J Bacteriol 2005; 187: 2426–38.
10 Stock AM, Wylie DC, Mottonen JM, Lupas AN, Ninfa EG, Ninfa AJ, *et al.* Phosphoproteins involved in bacterial signal transduction. Cold Spring Harb Symp Quant Biol 1988; 53: 49–57.
11 Stock AM, Robinson VL, Goudreau PN. Two-component signal transduction. Annu Rev Biochem 2000; 69: 183–215.
12 West AH, Stock AM. Histidine kinases and response regulator proteins in two-component signaling systems. Trends Biochem Sci 2001; 26: 369–76.
13 Barrett JF, Hoch JA. Two-component signal transduction as a target for microbial anti-infective therapy. Antimicrob Agents Chemother 1998; 42: 1529–36.
14 Stephenson K, Hoch JA. Two-component and phosphorelay signal-transduction systems as therapeutic targets. Curr Opin Pharmacol 2002; 2: 507–12.
15 Stephenson K, Hoch JA. Virulence- and antibiotic resistance-associated two-component signal transduction systems of Gram-positive pathogenic bacteria as targets for antimicrobial therapy. Pharmacol Ther 2002; 93: 293–305.
16 Fabret C, Hoch JA. A two-component signal transduction system essential for growth of *Bacillus subtilis*: implications for anti-infective therapy. J Bacteriol 1998; 180: 6375–83.
17 Fukuchi K, Kasahara Y, Asai K, Kobayashi K, Moriya S, Ogasawara N. The essential two-component regulatory system encoded by yycF and yycG modulates expression of the ftsAZ operon in *Bacillus subtilis*. Microbiology 2000; 146: 1573–83.
18 Martin PK, Li T, Sun D, Biek DP, Schmid MB. Role in cell permeability of an essential two-component system in *Staphylococcus aureus*. J Bacteriol 1999; 181: 3666–73.
19 Dubrac S, Boneca IG, Poupel O, Msadek T. New insights into the WalK/WalR (YycG/YycF) essential signal transduction pathway reveal a major role in controlling cell wall metabolism and biofilm formation in *Staphylococcus aureus*. J Bacteriol 2007; 189: 8257–69.
20 Dubrac S, Msadek T. Tearing down the wall: peptidoglycan metabolism and the WalK/WalR (YycG/YycF) essential two-component system. Adv Exp Med Biol 2008; 631: 214–28.
21 Okada A, Igarashi M, Okajima T, Kinoshita N, Umekita M, Sawa R, *et al.* Walkmycin B targets WalK (YycG), a histidine kinase essential for bacterial cell growth. J Antibiot (Tokyo) 2010; 63: 89–94.
22 Watanabe T, Hashimoto Y, Yamamoto K, Hirao K, Ishihama A, Hino M, *et al.* Isolation and characterization of inhibitors of the essential histidine kinase, YycG in *Bacillus subtilis* and *Staphylococcus aureus*. J Antibiot (Tokyo) 2003; 56: 1045–52.
23 Yamamoto K, Kitayama T, Minagawa S, Watanabe T, Sawada S, Okamoto T, *et al.* Antibacterial agents that inhibit histidine protein kinase YycG of *Bacillus subtilis*. Biosci Biotechnol Biochem 2001; 65: 2306–10.
24 Qin Z, Zhang J, Xu B, Chen L, Wu Y, Yang X, *et al.* Structure-based discovery of inhibitors of the YycG histidine kinase: new chemical leads to combat *Staphylococcus epidermidis* infections. BMC Microbiol 2006; 6: 96.
25 Qin Z, Lee B, Yang L, Zhang J, Yang X, Qu D, *et al.* Antimicrobial activities of YycG histidine kinase inhibitors against *Staphylococcus epidermidis* biofilms. FEMS Microbiol Lett 2007; 273: 149–56.
26 Pan B, Huang RZ, Han SQ, Qu D, Zhu ML, Wei P, *et al.* Design, synthesis, and antibiofilm activity of 2-arylimino-3-aryl-thiazolidine-4-ones. Bioorg Med Chem Lett 2010; 20: 2461–4.
27 Clinical and Laboratory Standards Institute: Methods for dilution antimicrobial susceptibility tests for bacteria that grow aerobically, 7th

ed. In Approved standard M7-A7 Clinical and Laboratory Standards Institute, Villanova, PA, USA; 2006.
28 Christensen GD, Simpson WA, Younger JJ, Baddour LM, Barrett FF, Melton DM, *et al*. Adherence of coagulase-negative staphylococci to plastic tissue culture plates: a quantitative model for the adherence of staphylococci to medical devices. J Clin Microbiol 1985; 22: 996–1006.
29 Mack D, Davies AP, Harris LG, Rohde H, Horstkotte MA, Knobloch JK. Microbial interactions in *Staphylococcus epidermidis* biofilms. Anal Bioanal Chem 2007; 387: 399–408.
30 Evans RC, Holmes CJ. Effect of vancomycin hydrochloride on *Staphylococcus epidermidis* biofilm associated with silicone elastomer. Antimicrob Agents Chemother 1987; 31: 889–94.
31 Baddour LM, Bettmann MA, Bolger AF, Epstein AE, Ferrieri P, Gerber MA*, et al.* Nonvalvular cardiovascular device-related infections. Clin Infect Dis 2004; 38: 1128–30.
32 Ceri H, Olson ME, Stremick C, Read RR, Morck D, Buret A. The Calgary Biofilm Device: new technology for rapid determination of antibiotic susceptibilities of bacterial biofilms. J Clin Microbiol 1999; 37: 1771–6.
33 Presterl E, Suchomel M, Eder M, Reichmann S, Lassnigg A, Graninger W*, et al.* Effects of alcohols, povidone-iodine and hydrogen peroxide on biofilms of *Staphylococcus epidermidis*. J Antimicrob Chemother 2007; 60: 417–20.
34 Mulcahy H, Charron-Mazenod L, Lewenza S. Extracellular DNA chelates cations and induces antibiotic resistance in *Pseudomonas aeruginosa* biofilms. PLoS Pathog 2008; 4: e1000213.
35 Gao R, Stock AM. Biological insights from structures of two-component proteins. Annu Rev Microbiol 2009; 63: 133–54.
36 Wagner C, Saizieu Ad A, Schonfeld HJ, Kamber M, Lange R, Thompson CJ*, et al*. Genetic analysis and functional characterization of the *Streptococcus pneumoniae* vic operon. Infect Immun 2002; 70: 6121–8.
37 Bisicchia P, Noone D, Lioliou E, Howell A, Quigley S, Jensen T*, et al*. The essential YycFG two-component system controls cell wall metabolism in *Bacillus subtilis*. Mol Microbiol 2007; 65: 180–200.
38 Dubrac S, Msadek T. Identification of genes controlled by the essential YycG/YycF two-component system of *Staphylococcus aureus*. J Bacteriol 2004; 186: 1175–81.
39 Howell A, Dubrac S, Andersen KK, Noone D, Fert J, Msadek T*, et al.* Genes controlled by the essential YycG/YycF two-component system of *Bacillus subtilis* revealed through a novel hybrid regulator approach. Mol Microbiol 2003; 49: 1639–55.
40 Liu M, Hanks TS, Zhang J, McClure MJ, Siemsen DW, Elser JL*, et al*. Defects in *ex vivo* and *in vivo* growth and sensitivity to osmotic stress of group A Streptococcus caused by interruption of response regulator gene vicR. Microbiology 2006; 152: 967–78.
41 Ng WL, Robertson GT, Kazmierczak KM, Zhao J, Gilmour R, Winkler ME. Constitutive expression of PcsB suppresses the requirement for the essential VicR (YycF) response regulator in *Streptococcus pneumoniae* R6. Mol Microbiol 2003; 50: 1647–63.
42 Ng WL, Tsui HC, Winkler ME. Regulation of the pspA virulence factor and essential pcsB murein biosynthetic genes by the phosphorylated VicR (YycF) response regulator in *Streptococcus pneumoniae*. J Bacteriol 2005; 187: 7444–59.
43 Mohedano ML, Overweg K, de la Fuente A, Reuter M, Altabe S, Mulholland F*, et al.* Evidence that the essential response regulator YycF in *Streptococcus pneumoniae* modulates expression of fatty acid biosynthesis genes and alters membrane composition. J Bacteriol 2005; 187: 2357–67.
44 Ahn SJ, Wen ZT, Burne RA. Effects of oxygen on virulence traits of Streptococcus mutans. J Bacteriol 2007; 189: 8519–27.
45 Kadioglu A, Echenique J, Manco S, Trombe MC, Andrew PW. The MicAB two-component signaling system is involved in virulence of *Streptococcus pneumoniae*. Infect Immun 2003; 71: 6676–9.
46 Senadheera MD, Guggenheim B, Spatafora GA, Huang YC, Choi J, Hung DC*, et al.* A VicRK signal transduction system in Streptococcus mutans affects gtfBCD, gbpB, and ftf expression, biofilm formation, and genetic competence development. J Bacteriol 2005; 187: 4064–76.
47 Ahn SJ, Burne RA. Effects of oxygen on biofilm formation and the AtlA autolysin of Streptococcus mutans. J Bacteriol 2007; 189: 6293–302.
48 Shemesh M, Tam A, Feldman M, Steinberg D. Differential expression profiles of Streptococcus mutans ftf, gtf and vicR genes in the presence of dietary carbohydrates at early and late exponential growth phases. Carbohydr Res 2006; 341: 2090–7.
49 Gilmour R, Foster JE, Sheng Q, McClain JR, Riley A, Sun PM*, et al.* New class of competitive inhibitor of bacterial histidine kinases. J Bacteriol 2005; 187: 8196–200.
50 Kitayama T, Iwabuchi R, Minagawa S, Sawada S, Okumura R, Hoshino K*, et al.* Synthesis of a novel inhibitor against MRSA and VRE: preparation from zerumbone ring opening material showing histidine-kinase inhibition. Bioorg Med Chem Lett 2007; 17: 1098–101.
51 Okada A, Gotoh Y, Watanabe T, Furuta E, Yamamoto K, Utsumi R. Targeting two-component signal transduction: a novel drug discovery system. Methods Enzymol 2007; 422: 386–95.
52 Stephenson K, Hoch JA. Developing inhibitors to selectively target two-component and phosphorelay signal transduction systems of pathogenic microorganisms. Curr Med Chem 2004; 11: 765–73.
53 Khardori N, Yassien M, Wilson K. Tolerance of *Staphylococcus epidermidis* grown from indwelling vascular catheters to antimicrobial agents. J Ind Microbiol 1995; 15: 148–51.

Acta Pharmacologica Sinica (2012) 33: 426–428
 1671-4083/12 $32.00
www.nature.com/aps

Letter

Differential sensitivity of RIP3-proficient and deficient murine fibroblasts to camptothecin anticancer drugs

Jin-xue HE#, Ying-qing WANG#, Jian-ming FENG, Jia-xin LI, Lei XU, Xiao-hua LI, Wei WANG, Xia-juan HUAN, Yi JIANG, Bing YU, Guang CHEN, Ze-hong MIAO*

Division of Anti-Tumor Pharmacology, State Key Laboratory of Drug Research, Shanghai Institute of Materia Medica, Chinese Academy of Sciences, Shanghai 201203, China

Acta Pharmacologica Sinica (2012) 33: 426–428; doi: 10.1038/aps.2012.1; published online 23 Jan 2012

Dear Editor,

Receptor-interacting protein 3 (RIP3) is a serine/threonine protein kinase, which has extensive substrates including its cognate kinase RIP1 and multiple metabolic enzymes involving oxidative phosphorylation[1, 2]. RIP3 has been shown to be essential for development, immunity and some physiological or pathophysiological responses to exogenous and endogenous stimuli[3–5]. In 2009, three groups independently reported that RIP3 acted as a molecular switch between apoptosis and necrosis (also called as necroptosis)[6–8]. Specifically, RIP3 could turn tumor necrosis factor (TNF)-induced cell death from apoptosis to necrosis[6]. Most of small-molecule anticancer drugs elicit their anticancer effects *via* apoptotic induction[9]. However, it is unclear whether RIP3 affects the cellular sensitivity to small-molecule anticancer drugs.

We treated A cells (NIH 3T3 cells, murine fibroblasts, $RIP3^{-/-}$; typically undergoing apoptosis in response to TNF stimulation) and N cells (NIH 3T3 cells, murine fibroblasts, $RIP3^{+/+}$; undergoing necroptosis in response to TNF stimulation)[6] with small-molecule anticancer drugs of different mechanisms of action. Detection by sulforhodamine B assays showed that A cells and N cells displayed differential sensitivity only to the examined topoisomerase I (Top1) inhibitors camptothecins. RIP3-deficient A cells revealed 32.6- and 40.2-fold higher sensitivity than RIP3-proficient N cells to SN38 and chimmitecan[10], respectively (Figure 1A). Such differential sensitivity was reflected as higher apoptosis rates (Figure 1B) and more rapid G_2/M arrest (Figure 1C) in A cells than in N cells treated with chimmitecan. Consistently, exposure to chimmitecan caused faster reduction of the target protein Top1 in A cells than in N cells (Figure 1D); and the treatment with chimmitecan or SN38 drove more γ-H2AX formation (a molecular marker for DNA double-strand breaks; Figure 1E) and produced more foci of phosphorylated ataxia telangiectasia mutated kinase (p-ATM) at Ser 1981 (sensing DNA double-strand breaks; Figures 1F and 1G) in A cells than in N cells. These results collectively indicate that the differential sensitivity of the RIP3-deficient A cells and the RIP3-proficient N cells to the examined Top1 inhibitors in all the tested events from inducing DNA double-strand breaks through sensing the damage signals to eliciting the final biological effects including cell cycle arrest, apoptosis and proliferation/growth inhibition.

Both A cells and N cells were kindly gifted from Prof Jiahuai HAN, who used them to successfully demonstrate the role of RIP3 in regulating TNF-inducing cell death[6]. The differential sensitivity of the RIP3-deficient and proficient murine fibroblasts to the Top1 inhibitors suggests a role of RIP3 in determining the cellular sensitivity to those agents. In this case, however, RIP3 does not seem to directly affect the choice of cell death between apoptosis and necrosis, because no significant difference of the cellular sensitivity to the other examined anticancer drugs except camptothecins was detectable (data not shown) and because RIP3-based differential responses of A cells and N cells to the Top1 inhibitors took place actually at the levels of the target protein Top1 and DNA double-strand breaks, not only at the level of cell death. In contrast, our data seem to imply that RIP3 is involved in the DNA damage

# These authors contributed equally to this work.
* To whom correspondence should be addressed.
E-mail zhmiao@mail.shcnc.ac.cn
Received 2011-12-31 Accepted 2012-01-05

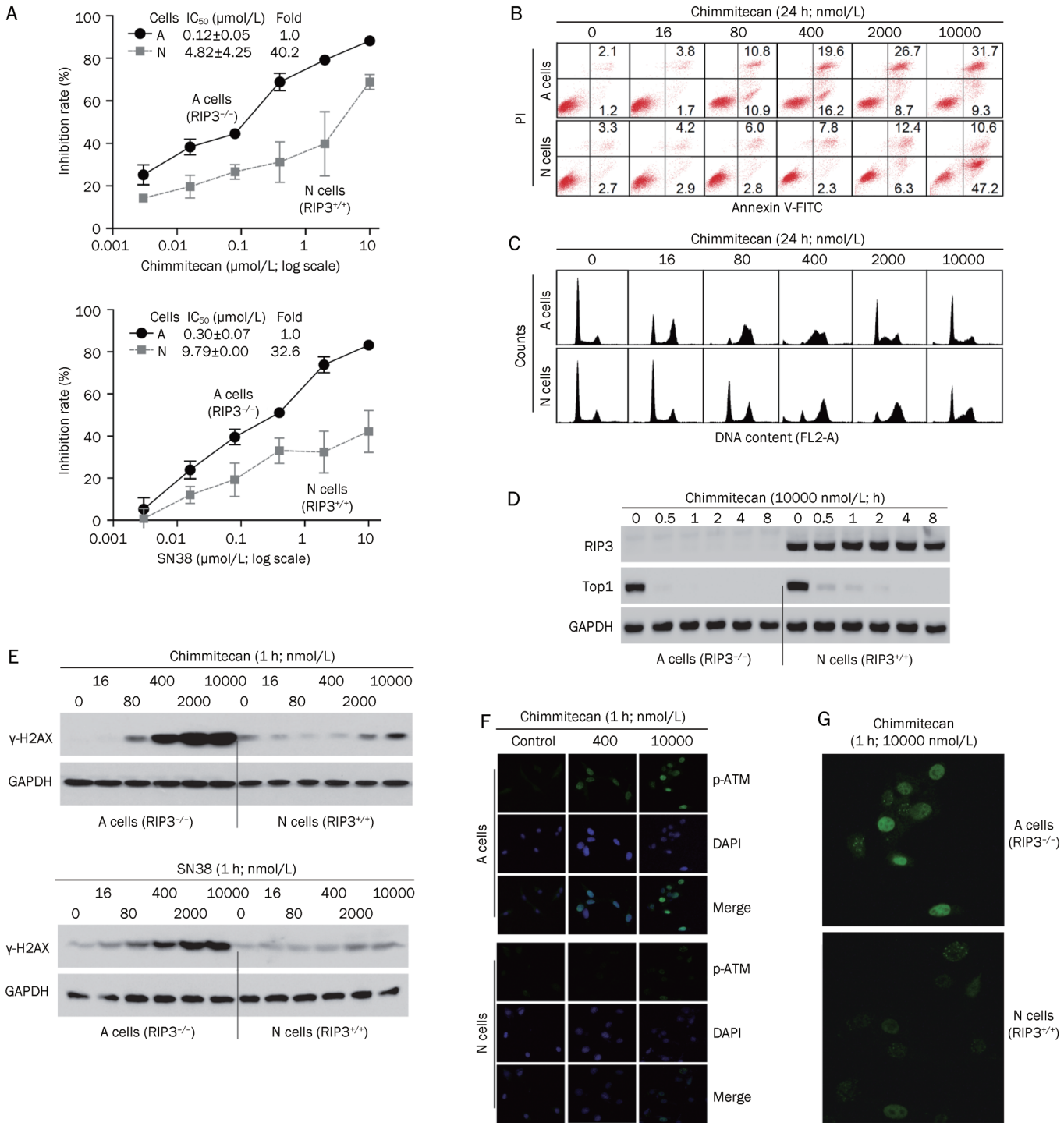

Figure 1. Differential sensitivity of RIP3-deficient A cells and RIP3-proficient N cells to camptothecins. (A) A cells and N cells displayed differential sensitivity to camptothecins. A cells (RIP3$^{-/-}$) and N cells (RIP3$^{+/+}$) were treated with gradient concentrations of chimmitecan or SN38 (10, 2, 0.4, 0.08, 0.016, and 0.0032 μmol/L) for 72 h. Cell viability was then determined by sulforhodamine B assays. The IC_{50} value was calculated by SoftMax® Pro Software and the data from three independent experiments were presented as mean±SD. (B) Exposure to chimmitecan for 24 h resulted in higher apoptosis rates in A cells. Both A cells and N cells were treated with the indicated concentrations of chimmitecan or vehicle for 24 h, then stained with an annexin V antibody and propidium iodide (PI), and analyzed by flow cytometry. The numbers represent apoptotic percentages. (C) Exposure of A cells and N cells to chimmitecan for 24 h induced G_2/M arrest. Both cells were treated with chimmitecan or vehicle for 24 h, fixed, stained with PI, and analyzed by flow cytometry. (D) Faster reduction of Top1 protein in A cells. Cells were treated with 10 000 nmol/L chimmitecan for the indicated times. Total cell lysates were collected and subjected to SDS-PAGE gels for Western blotting analyses. The protein levels of RIP3, Top1, and GAPDH were determined. (E) Faster formation of γ-H2AX in A cells. The levels of γ-H2AX were detected by Western blotting at 1 h after the treatment with camptothecins. (F) Higher levels of p-ATM at Ser1981 in A cells in responding to the treatment with chimmitecan. Cells were treated with chimmitecan (400 nmol/L and 10 000 nmol/L) or vehicle for 1 h, fixed and stained with a specific antibody against the phosphorylated ATM at Ser1981 of (p-ATM, green foci) for fluorescence microscopy analyses. Nuclei were identified by DAPI (4,6 diamidino-2-phenylindole) counterstaining (blue). (G) Enlarged images of p-ATM at 10 000 nmol/L chimmitecan in Figure 1F.

induced by the Top1 inhibitors and/or subsequent repair. As a clinically important class of anticancer drugs, Top1 inhibitors are extensively used to treat various solid tumors such as colon and lung cancers. Occurrence of drug resistance to those inhibitors is a serious obstacle to successful therapy in the clinic[11]. The differential sensitivity of A cells and N cells to SN38 and chimmitecan also suggests that RIP3 could contribute to cellular resistance to Top1 inhibitors. Actually, we detected and found that RIP3 was expressed at high levels in cancer cells originated from different human tissues including blood (K562), liver (SMMC-7402 and SMMC-7721), colon (HCT116), stomach (MKN45), lung (A549), breast (MDA-MB-468, MDA-MB-231, T47D, and BT549), cervix (HeLa) and bone (Rh30) (data not shown). Inhibition of RIP3 might be an alternative approach to circumventing drug resistance. However, the exact molecular mechanisms remain to be further clarified.

Taken together, our results demonstrate for the first time the differential sensitivity of the RIP3-deficient A cells and the RIP3-proficient N cells to Top1 inhibitors, suggesting a potential new role of RIP3 in Top1 inhibitor-induced DNA damage/repair and cellular resistance to Top1 inhibitors, probably independently of its regulation in the choice of cell death modes.

Acknowledgements

We thank Prof Jia-huai HAN (Xiamen University, China) for his kind gifts of RIP3-deficient A cells and RIP3-proficient N cells. This work was supported by grants from the National Natural Science Foundation of China (No 81025020 and No 81021062), the National Basic Research Program of China (No 2012CB932502), the National Science & Technology Major Project of China (No 2012ZX09301-001-002) and the State Key Laboratory of Drug Research of China (No SIMM1105KF-02).

References

1 Vandenabeele P, Galluzzi L, Vanden Berghe T, Kroemer G. Molecular mechanisms of necroptosis: an ordered cellular explosion. Nat Rev Mol Cell Biol 2010; 11: 700–14.

2 Zhang DW, Zheng M, Zhao J, Li YY, Huang Z, Li Z, *et al*. Multiple death pathways in TNF-treated fibroblasts: RIP3- and RIP1-dependent and independent routes. Cell Res 2011; 21: 368–71.

3 Oberst A, Dillon CP, Weinlich R, McCormick LL, Fitzgerald P, Pop C, *et al*. Catalytic activity of the caspase-8-FLIP(L) complex inhibits RIPK3-dependent necrosis. Nature 2011; 471: 363–7.

4 Kaiser WJ, Upton JW, Long AB, Livingston-Rosanoff D, Daley-Bauer LP, Hakem R, *et al*. RIP3 mediates the embryonic lethality of caspase-8-deficient mice. Nature 2011; 471: 368–72.

5 Lu JV, Weist BM, van Raam BJ, Marro BS, Nguyen LV, Srinivas P, *et al*. Complementary roles of Fas-associated death domain (FADD) and receptor interacting protein kinase-3 (RIPK3) in T-cell homeostasis and antiviral immunity. Proc Natl Acad Sci U S A 2011; 108: 15312–17.

6 Zhang DW, Shao J, Lin J, Zhang N, Lu BJ, Lin SC, *et al*. RIP3, an energy metabolism regulator that switches TNF-induced cell death from apoptosis to necrosis. Science 2009; 325: 332–6.

7 He S, Wang L, Miao L, Wang T, Du F, Zhao L, *et al*. Receptor interacting protein kinase-3 determines cellular necrotic response to TNF-alpha. Cell 2009; 137: 1100–11.

8 Cho YS, Challa S, Moquin D, Genga R, Ray TD, Guildford M, *et al*. Phosphorylation-driven assembly of the RIP1-RIP3 complex regulates programmed necrosis and virus-induced inflammation. Cell 2009; 137: 1112–23.

9 Fulda S, Debatin KM. Extrinsic versus intrinsic apoptosis pathways in anticancer chemotherapy. Oncogene 2006; 25: 4798-811.

10 Huang M, Miao ZH, Zhu H, Cai YJ, Lu W, Ding J. Chk1 and Chk2 are differentially involved in homologous recombination repair and cell cycle arrest in response to DNA double-strand breaks induced by camptothecins. Mol Cancer Ther 2008; 7: 1440–49.

11 Rasheed ZA, Rubin EH. Mechanisms of resistance to topoisomerase I-targeting drugs. Oncogene 2003; 22: 7296–304.